

# BROMOFORM-ASSISTED FREE RADICAL POLYMERISATION: A SIMPLE, INEXPENSIVE ROUTE FOR THE PREPARATION OF BLOCK COPOLYMERS

Helena Jayne Hutchins

Doctor of Philosophy

Aston University

June 2021

© Helena Jayne Hutchins, 2021

Helena Jayne Hutchins asserts her moral right to be identified as the author of this thesis.

This copy of this thesis has been supplied on the condition that anyone who consults it is understood to recognise that its copyrights rest with its author and that no quotation from the thesis and no information derived from it may be published without appropriate permission or acknowledgement.

**Aston University**  
**Bromoform-assisted free radical polymerisation: A simple, inexpensive route for the  
preparation of block copolymers**  
**Helena Jayne Hutchins**

**Doctor of Philosophy**

**2021**

The last three decades have marked unprecedented advances in polymer chemistry enabling the production of a wide range of well-defined block copolymers. Such macromolecules are crucial for structure-property relationship studies, bulk block copolymer self-assembly and in the pursuit of sequence-controlled macromolecules for biomimicry. However, in most cases the conventional RDRP (reversible-deactivation radical polymerisation) techniques, used to synthesise such materials, rely on toxic transition metals, sulfur or unstable compounds to provide control and often produce inherently coloured polymers [e.g. in the case of reversible addition-fragmentation chain transfer (RAFT)]. This highlights one of the key challenges in polymer chemistry; the need to produce block copolymers without the use of sulfur or transition metals.

In the quest for commercially relevant block copolymer materials, for which overall average molecular composition is key but molar mass distribution is of little importance, a straightforward, sulfur- and metal-free aqueous route to block copolymers using commercially available starting materials is described. Based on synthetic techniques first described in the 1950s for hydrophobic monomers in organic solvents, the alkyl halide bromoform ( $\text{CHBr}_3$ ) has been used to synthesise block copolymers. Unlike common bromine-containing chain transfer agents such as carbon tetrabromide ( $\text{CBr}_4$ ), bromoform is partially water-miscible and relatively inexpensive. In addition, bromoform is readily available, stable (easily stored) and can be used directly at low and ambient temperatures. Interestingly, bromoform has been reported to photodissociate under UV light and as a result of this the reactions described in this thesis are conducted under UV conditions.

Herein, this new aqueous-based technology has been studied using *N,N*-dimethylacrylamide (DMA) and *N*-isopropylacrylamide (NIPAM) as exemplar monomers to synthesise poly(*N,N*-dimethylacrylamide)-*block*-poly(*N*-isopropylacrylamide) [PDMA-*b*-PNIPAM] block copolymers of varying composition directly in water. Detailed kinetic studies, using this bromoform-assisted polymerisation technique were conducted to identify the optimal conditions for synthesising potentially bromine-terminated PDMA and PNIPAM macro-initiators for subsequent chain extension.

Following these kinetic studies, PDMA (made using 2 mol % bromoform, relative to monomer) was used as a macro-initiator for subsequent PDMA-*b*-PNIPAM copolymer synthesis. Both one-pot and two-step studies were conducted to identify potential routes to block copolymer synthesis. The one-pot study was completed as the simplest, cheapest route to forming the PDMA-*b*-PNIPAM copolymers. However, due to unwanted impurities formed during the one-step synthesis, alongside the need to understand the process in unprecedented detail, a two-step synthetic route was explored. The two-step synthetic route was completed using PDMA macro-initiators (using PDMA synthesised to both 91 and 70 % conversion) in order to further optimise the methodology.

Finally, a series of control reactions were conducted to provide further evidence that bromoform was required to impart the reversibly-cleavable chain end functionality under UV-irradiation, for block copolymers to be formed. Additionally, control reactions were undertaken to further indicate that block copolymers were formed in this study; demonstrating the potential of this technique as a simple, inexpensive route for the creation of functional block copolymers.

**Key words:** Bromoform, poly(*N,N*-dimethylacrylamide), poly(*N*-isopropylacrylamide), block copolymer, macro-initiator, commercially-relevant, photodissociation, reversibly-cleavable.

## Publications

G. E. Parkes, **H. J. Hutchins-Crawford**, C. Bourdin, S. Reynolds, L. J. Leslie, M. J. Derry, J. L. Harries and P. D. Topham, Thermally triggerable, anchoring block copolymers for use in aqueous inkjet printing, *Polym. Chem.*, 2020, **11**, 2869–2882.

Y. Jia, C. Yang, X. Chen, W. Xue, **H. J. Hutchins-Crawford**, Q. Yu, P. D. Topham and L. Wang, A review on electrospun magnetic nanomaterials: methods, properties and application, *J. Mater. Chem. C*, 2021, **9**, 9042-9082.

**H. J. Hutchins-Crawford**, P. Ninjiaranai, M. J. Derry, R. Molloy, B. J. Tighe and P. D. Topham, Bromoform-assisted free radical polymerisation: A simple, inexpensive route for the preparation of block copolymers, *Polym. Chem.*, 2021, **12**, 4317-4325.

P. D. Topham, R. Boucher, T. Chang, M. Dušková Smrčková, W. S. Farrell, J. He, M. Hess, W. Hu, **H. J. Hutchins-Crawford**, D. J. Keddie, P. E. Mallon, J. Merna, N. Stingelin, A. Sturcova and J. Vohlidal, A Brief Guide to Polymer Characterisation, *Pure Appl. Chem.*, *Manuscript under review*.

M. Bramham, **H. J. Hutchins-Crawford**, P. D. Topham, L. J. Leslie, The Effects of Repeated Autoclave Sterilisation on Silicone Materials for Biomedical Applications, *Manuscript in preparation*.

## Acknowledgements

I would like to start off by thanking my supervisor and mentor Professor Paul Topham for facilitating my come back to Aston to complete my PhD and for simply believing in me. The support, advice and encouragement you have given me over the past three years is one of the main reasons I have made it this far and I appreciate everything you have done to set me up for the next stage of my career. I would also like to thank my co-supervisor Professor Brian Tighe. Thank you for welcoming me to your research team, for supporting me and for all of your wonderful words of advice throughout my project. Thank you Paul and Brian, you pair of absolute jokers!

Additionally, I would like to thank Dr Matthew Derry for all of the papers, posters and thesis chapters you have supported with and proofread. I appreciate all of the time and effort you have put in to help me throughout my project. A special thanks also goes to Dr Val Franklin for our lunch time chats, for answering all my questions about everything lab related and arranging for endless engineers to come and fix equipment; without you my project wouldn't have been as successful.

Of course, I would like to thank all of the past and present members of the Topham, Tighe and Derry research groups as well as all of my friends in the PhD office, MB111. To all of you, for the support, advice and sometimes the distraction that I needed to get me through. I will miss you all and wish everyone the very best for the future.

Most importantly, I would like to thank my family; Mom, Dad, Zoe and Ross for your unconditional love, constant encouragement and support. For always asking about my work and letting me ramble on even if it sounded like I was talking in code and for all of the dinners, drinks and quality time you each made for me; this is truly what has kept me going. I would also like to thank my best friend, Mariska, for literally checking in on me daily to ask how things are going.

Last but certainly not least, to my partner Daniel, for supporting my career change, telling me over and over that I can do this and for always making me smile. I cannot wait to start the next chapter of my life with you by my side.



## Abbreviations

$^1\text{H}$ NMR	proton nuclear magnetic resonance
ACPA	4,4-azobiscyanovaleric acid
AIBN	2,2'-azobis(isobutyronitrile)
AMPS	2-acrylamido-2-methylpropane sulfonic acid
ATRP	atom transfer radical polymerisation
$\text{CDCl}_3$	deuterated chloroform
$\text{CHBr}_3$	bromoform
CTA	chain transfer agent
$\bar{D}$	molar mass dispersity
$\text{D}_2\text{O}$	deuterium oxide
DEE	diethyl ether
DLS	dynamic light scattering
DMA	<i>N,N</i> -dimethylacrylamide
DMF	dimethylformamide
DOSY	diffusion-ordered spectroscopy
DP	degree of polymerisation
DSC	differential scanning calorimetry
GPC	gel permeation chromatography
GTP	group transfer polymerisation
HPLC	high performance liquid chromatography
ITP	iodine transfer polymerisation
$k_p$	rate of propagation
LCST	lower critical solution temperature
MeOH	methanol
$M_n$	number-average molar mass

$M_w$	weight-average molar mass
NIPAM	<i>N</i> -isopropylacrylamide
NMP	nitroxide mediated polymerisation
PAM	polyacrylamide
PDMA	poly( <i>N,N</i> -dimethylacrylamide)
PDMA- <i>b</i> -PNIPAM	poly( <i>N,N</i> -dimethylacrylamide)- <i>block</i> -poly( <i>N</i> -isopropylacrylamide)
PDMA- <i>st</i> -PNIPAM	poly( <i>N,N</i> -dimethylacrylamide- <i>stat</i> - <i>N</i> -isopropylacrylamide)
PEG	poly(ethylene glycol)
PMMA	poly(methyl methacrylate)
PNIPAM	poly( <i>N</i> -isopropylacrylamide)
PNIPAM- <i>b</i> -PDMA	poly( <i>N</i> -isopropylacrylamide)- <i>block</i> -poly( <i>N,N</i> -dimethylacrylamide)
PS	polystyrene
PS- <i>b</i> -PMMA	poly(styrene)- <i>block</i> -poly(methyl methacrylate)
RAFT	reversible addition-fragmentation chain transfer
RDRP	reversible-deactivation radical polymerisation
RITP	reversible iodine transfer polymerisation
SEC	size exclusion chromatography
$T_g$	glass transition temperature
TGA	thermal gravimetric analysis
THF	tetrahydrofuran
UV	ultraviolet

# Contents

Thesis summary .....	2
Publications.....	3
Acknowledgements .....	4
Abbreviations .....	5
List of Tables.....	10
List of Figures.....	12
List of Schemes.....	21
List of Equations.....	23
Chapter 1. Introduction .....	24
1.1 Introduction to Thesis .....	25
1.2 Polymers .....	26
1.3 Polymer synthesis .....	26
1.3.1 Step polymerisation.....	27
1.3.2 Chain polymerisation.....	28
1.3.3 Living polymerisation.....	31
1.3.4 Reversible-deactivation radical polymerisation.....	33
1.4 Chain transfer .....	36
1.4.1 Chain transfer to monomer.....	36
1.4.2 Chain transfer to initiator .....	37
1.4.3 Chain transfer to polymer .....	37
1.4.4 Chain transfer to solvent .....	38
1.4.5 Chain transfer to RAFT CTA .....	39
1.5 Halogenated compounds .....	42
1.5.1 Halogens in controlled radical polymerisation.....	42
1.5.2 Halogens as leaving groups .....	44
1.5.3 Other uses of halogens in polymerisation reactions .....	46
1.5.4 Bromoform .....	47
1.6 Initiators .....	51
1.7 Monomers .....	52
1.8 Block copolymers .....	54
1.8.1 Block sequence.....	54
1.8.2 Photoiniferter polymerisation .....	56
1.9 Aims.....	58
Chapter 2. Materials and Experimental Methods .....	61
2.1 Materials .....	62

2.2	UV source .....	62
2.3	Experimental Methods.....	62
2.3.1	Bromoform-assisted polymerisation of <i>N,N</i> -dimethylacrylamide .....	62
2.3.2	Bromoform-assisted polymerisation of <i>N</i> -isopropylacrylamide .....	66
2.3.3	Synthesis of amphiphilic poly( <i>N,N</i> -dimethylacrylamide)- <i>block</i> -poly( <i>N</i> -isopropylacrylamide) via bromoform-assisted polymerisation .....	69
2.4	Characterisation Methods .....	76
2.4.1	<sup>1</sup> H Nuclear Magnetic Resonance Spectroscopy .....	76
2.4.2	Gel Permeation Chromatography .....	79
2.4.3	Differential Scanning Calorimetry .....	80
2.4.4	Thermal Gravimetric Analysis.....	80
2.4.5	Dynamic Light Scattering .....	80
Chapter 3.	Bromoform-assisted polymerisation of <i>N,N</i> -dimethylacrylamide .....	82
3.1	Homopolymerisation of <i>N,N</i> -dimethylacrylamide .....	83
3.2	Development of the <i>N,N</i> -dimethylacrylamide polymerisation procedure .....	84
3.3	Bromoform-assisted synthesis of poly( <i>N,N</i> -dimethylacrylamide) in HPLC-grade water .....	86
3.3.1	Thermal properties .....	93
3.4	Bromoform-assisted synthesis of poly( <i>N,N</i> -dimethylacrylamide) in DMF .....	95
3.4.1	Thermal properties .....	104
3.5	Polymerisations conducted in the absence of photoinitiator (ACPA).....	107
3.6	Synthesis of PDMA in the presence of air .....	110
3.7	Reaction scale-up .....	116
3.8	Conclusions .....	119
Chapter 4.	Bromoform-assisted polymerisation of <i>N</i> -isopropylacrylamide.....	123
4.1	Homopolymerisation of <i>N</i> -isopropylacrylamide.....	124
4.2	Development of the <i>N</i> -isopropylacrylamide polymerisation procedure.....	125
4.3	Bromoform-assisted synthesis of poly( <i>N</i> -isopropylacrylamide) in HPLC-grade water .....	126
4.3.1	Thermal properties .....	134
4.4	Bromoform-assisted synthesis of poly( <i>N</i> -isopropylacrylamide) in DMF .....	137
4.4.1	Thermal properties .....	146
4.5	Polymerisations conducted in the absence of photoinitiator (ACPA).....	148
4.6	Synthesis of PNIPAM in the presence of air .....	150
4.7	Reaction scale-up .....	153
4.8	Conclusions .....	156
Chapter 5.	Synthesis of poly( <i>N,N</i> -dimethylacrylamide)- <i>block</i> -poly( <i>N</i> -isopropylacrylamide) copolymers .....	160
5.1	One-pot method .....	162

5.1.1	Thermal properties .....	166
5.2	Two-step method .....	171
5.2.1	Macro-initiator at high conversion.....	172
5.2.2	Macro-initiator at 70 % conversion .....	182
5.3	Control experiments .....	190
5.4	Conclusion .....	193
Chapter 6.	Conclusions and Future Work .....	197
6.1	Conclusions .....	198
6.2	Future Work .....	203
References	.....	207
Appendix	.....	248

## List of Tables

Table 1.1. Summary of mean bond enthalpies for various C-X bonds where X is a carbon, hydrogen or halogen atom. Modified from Burrows <i>et al.</i> <sup>195</sup> .....	45
Table 1.2. Summary of the chain transfer constants of halogenated substances investigated in the polymerisation of styrene. Modified from Flory <sup>201</sup> .....	46
Table 3.1. Summary of final conversion, molar mass, molar mass dispersity and apparent rate constant data for the polymerisation of <i>N,N</i> -dimethylacrylamide at varied bromoform concentrations in water. ....	89
Table 3.2. Summary of the glass transition temperatures of PDMA (synthesised in water) at varying bromoform concentration (0, 0.5, 1.0 and 2.0 mol % relative to monomer).....	94
Table 3.3. Summary of final conversion, molar mass, molar mass dispersity and apparent rate constant data for the polymerisation of <i>N,N</i> -dimethylacrylamide at varying bromoform concentrations in DMF. ....	98
Table 3.4. Summary of the glass transition temperatures of PDMA (synthesised in DMF) at varying bromoform concentrations (0, 0.5, 1.0 and 2.0 mol % relative to monomer).....	106
Table 3.5. Apparent rate constant data at varying bromoform concentrations under inert atmosphere (i.e. oxygen-free) <i>versus</i> in the presence of air (not degassed but sealed prior to UV irradiation) for the homopolymerisation of <i>N,N</i> -dimethylacrylamide. ....	114
Table 3.6. Summary of final monomer conversion, molar mass and molar mass dispersity data for the polymerisation of <i>N,N</i> -dimethylacrylamide using 2 mol % bromoform targeting 20 g of macro-initiator (synthesised in water). ....	117
Table 3.7. Summary of the glass transition temperatures for the PDMA macro-initiators synthesised at larger scale (water syntheses). ....	118
Table 4.1. Summary of final conversion, molar mass, molar mass dispersity and apparent rate constant data for the polymerisation of <i>N</i> -isopropylacrylamide at varied bromoform concentrations in water. ....	129

Table 4.2. Summary of the glass transition temperatures of PNIPAM (synthesised in water) at varying bromoform concentration (0, 0.5, 1.0 and 2.0 mol % relative to monomer).....	134
Table 4.3. Summary of final conversion, molar mass, molar mass dispersity and apparent rate constant data for the polymerisation of <i>N</i> -isopropylacrylamide at varied bromoform concentrations in DMF. ....	141
Table 4.4. Summary of the glass transition temperatures of PNIPAM (synthesised in DMF) at varying bromoform concentrations (0, 0.5, 1.0 and 2.0 mol % relative to monomer).....	146
Table 4.5. Summary of final monomer conversion, molar mass and molar mass dispersity data for the polymerisation of <i>N</i> -isopropylacrylamide using 2 mol % bromoform targeting 20 g of macro-initiator (in water).....	153
Table 4.6. Summary of the glass transition temperature for the PNIPAM macro-initiator synthesised at larger scale (water synthesis). ....	154
Table 5.1. Summary of $M_n$ , $\bar{D}$ and the target and achieved PNIPAM DPs in PDMA- <i>b</i> -PNIPAM copolymers synthesised via the one-pot method, using 2 mol % bromoform and 1.0 mol % ACPA (relative to DMA monomer).....	163
Table 5.2. Summary of the glass transition temperatures for the PDMA macro-initiator, PDMA- <i>b</i> -PNIPAM copolymers (one-pot) and PNIPAM homopolymer synthesised using 2 mol % bromoform (relative to monomer). ....	167
Table 5.3. Summary of $M_n$ , $\bar{D}$ and the target and achieved PNIPAM DPs in PDMA- <i>b</i> -PNIPAM copolymers synthesised via the two-step method using PDMA that achieved high monomer conversion (91 %) in step one. ....	173
Table 5.4. Glass transition temperatures for PDMA macro-initiator, subsequent PDMA- <i>b</i> -PNIPAM block copolymers synthesised via the two-step method [using a macro-initiator synthesised to high conversion (91 %)] and a PNIPAM homopolymer (2 mol % bromoform). ....	178
Table 5.5. Summary of $M_n$ , $\bar{D}$ and the target and achieved PNIPAM DP in PDMA- <i>b</i> -PNIPAM copolymers synthesised via the two-step method using PDMA that was stopped at 70 % conversion.....	184

## List of Figures

Figure 1.1. Trend of molar mass with extent of reaction for chain and step growth and living polymerisation reactions. Modified from Cowie <sup>5</sup> . .....	30
Figure 1.2. Generic RAFT CTA structure showing the positions of the reactive double bond, stabilising group, weak single bond and leaving group. ....	39
Figure 1.3. Structures of commonly used CTAs in RAFT polymerisation including; dithioesters, dithiocarbamates, trithiocarbonates and xanthates. ....	41
Figure 1.4. Chemical structures of bromotrichloromethane (left) and carbon tetrabromide (right). ....	48
Figure 1.5. General structure of acrylamide monomers showing the vinyl ( $\text{CH}_2\text{CH}-$ ), carbonyl ( $\text{C}=\text{O}$ ) and nitrogen ( $\text{NR}_2$ ) functionalities. ....	52
Figure 1.6. Chemical structures of <i>N</i> -isopropylacrylamide (left) and poly( <i>N</i> -isopropylacrylamide) (right); where <i>n</i> represents the number of repeat units of NIPAM within the polymer chain. ....	53
Figure 1.7. Chemical structures of <i>N,N</i> -dimethylacrylamide (left) and poly( <i>N,N</i> -dimethylacrylamide) [PDMA] (right); where <i>n</i> represents the number of repeat units of DMA in the polymer chain. ....	54
Figure 2.1. $^1\text{H}$ NMR spectra (in $\text{D}_2\text{O}$ ) showing the progress of the DMA polymerisation through the disappearance of the monomer vinylic groups (5.6, 6.0 and 6.6 ppm) and the broadening of the polymer methyl groups (2.9 ppm) from PDMA. ....	77
Figure 2.2. $^1\text{H}$ NMR spectra (in $\text{CDCl}_3$ ) showing the progress of the DMA polymerisation through the disappearance of the monomer vinylic groups (5.6, 6.0 and 6.6 ppm) and the broadening of the polymer vinyl peaks (1.24 and 1.55 ppm) from PDMA. Also highlighting the overlap of the DMF and PDMA methyl group protons. ....	78
Figure 2.3. $^1\text{H}$ NMR spectra (in $\text{D}_2\text{O}$ ) showing the progress of the NIPAM polymerisation (in HPLC-grade water) through the disappearance of the monomer vinylic groups (5.6 and 6.1 ppm) and the broadening of the polymer methyl groups (1.0 ppm) from PNIPAM. ....	79



Figure 3.1. UV lamp and metal box set up showing UV irradiation from above. (a) Side view and (b) front facing. ....	84
Figure 3.2. Birds eye view of the stirrer plate, ice bath and reaction vessel for a typical polymerisation. ....	85
Figure 3.3. Temperature <i>versus</i> time plot for the trial synthesis of PDMA using an ice bath to provide temperature control.....	86
Figure 3.4. Exemplar $^1\text{H}$ NMR kinetic overlay for the synthesis of PDMA in water at 2.0 mol % bromoform showing the disappearance of monomer and broadening of polymer peaks throughout the course of the reaction. ....	87
Figure 3.5. Kinetic GPC traces for the synthesis of PDMA in water at a) 0, b) 0.5, c) 1.0 and d) 2.0 mol % bromoform concentrations (relative to monomer). ....	88
Figure 3.6. Comparative $^1\text{H}$ NMR spectra (in $\text{D}_2\text{O}$ ) showing the disappearance of the monomer vinyl protons (5.7, 6.0 and 6.6 ppm) between crude and precipitated PDMA (2 mol % bromoform, relative to monomer). ....	89
Figure 3.7. GPC traces of PDMA final precipitates at a) 0, b) 0.5, c) 1.0 and d) 2.0 mol % bromoform (relative to monomer, synthesised in water) demonstrating good reproducibility between runs and e) near-identical GPC traces of the final precipitate at each bromoform concentration.....	90
Figure 3.8. Monomer conversion <i>versus</i> time for the synthesis of PDMA at varying bromoform concentrations in water. ....	92
Figure 3.9. Semi-logarithmic plot for the synthesis of PDMA at varying bromoform concentration in water. ....	92
Figure 3.10. Molar mass <i>versus</i> conversion for the synthesis of PDMA at varying bromoform concentrations in water (error bars represent the standard deviation of the triplicate data)..	93
Figure 3.11. DSC thermograms (second heating cycle) for PDMA (synthesised in water) at varying bromoform concentration, highlighting the feature corresponding to the glass transition temperature for each sample.....	94

Figure 3.12. TGA degradation profiles for PDMA (synthesised in water) at varying bromoform concentration.....	95
Figure 3.13. Exemplar $^1\text{H}$ NMR kinetic overlay for the synthesis of PDMA in DMF at 2.0 mol % bromoform showing the disappearance of monomer and broadening of polymer peaks throughout the course of the reaction. ....	96
Figure 3.14. Kinetic GPC traces for the synthesis of PDMA in DMF at a) 0, b) 0.5, c) 1.0 and d) 2.0 mol % bromoform concentrations (relative to monomer). ....	97
Figure 3.15. Comparative $^1\text{H}$ NMR spectra (in $\text{CDCl}_3$ ) showing the disappearance of the monomer vinyl protons (5.7, 6.0 and 6.6 ppm) between crude and precipitated PDMA (2 mol % bromoform, relative to monomer). ....	99
Figure 3.16. $^1\text{H}$ NMR spectrum (in $\text{D}_2\text{O}$ ) of PDMA synthesised in water highlighting the presence of a low intensity methyl group peak at approximately 1.0 ppm [labelled with an asterix (*)].....	99
Figure 3.17. GPC traces of PDMA final precipitates at a) 0, b) 0.5, c) 1.0 and d) 2.0 mol % bromoform (relative to monomer, synthesised in DMF) demonstrating good reproducibility between runs and e) near-identical GPC traces of the final precipitate at each bromoform concentration.....	100
Figure 3.18. Monomer conversion <i>versus</i> time for the synthesis of PDMA at varying bromoform concentrations in DMF. ....	102
Figure 3.19. Semi-logarithmic plot for the synthesis of PDMA at varying bromoform concentration in DMF. ....	102
Figure 3.20. $M_n$ <i>versus</i> monomer conversion for the synthesis of PDMA at varied bromoform concentrations in DMF (error bars represent the standard deviation of the triplicate data). ....	103
Figure 3.21. DSC thermograms (second heating cycle) for PDMA (synthesised in DMF) at varying bromoform concentrations highlighting the glass transition temperature for each sample. ....	105
Figure 3.22. TGA degradation profile for PDMA (synthesised in DMF) at varying bromoform concentrations.....	106

Figure 3.23. Final $^1\text{H}$ NMR spectra for the attempted synthesis of PDMA in the absence of ACPA photoinitiator at varying bromoform concentrations (0, 0.5, 1.0 and 2.0 mol % relative to monomer) in water. ....	109
Figure 3.24. Example of the GPC traces obtained for the synthesis of PDMA with ACPA (black) and in the absence of ACPA (red) both at 2 mol % bromoform (relative to monomer). ....	110
Figure 3.25. Monomer conversion <i>versus</i> time for the synthesis of PDMA at varying bromoform concentrations in the presence of air. ....	111
Figure 3.26. Semi-logarithmic plot used to demonstrate the relationship, or lack thereof, between bromoform concentration and the rate of the reaction in the presence of air. ....	113
Figure 3.27. $M_n$ <i>versus</i> monomer conversion for the synthesis of PDMA at varying bromoform concentrations in the presence of air. ....	115
Figure 3.28. Molar mass <i>versus</i> monomer conversion for the synthesis of PDMA at varying bromoform concentrations a) 0, b) 0.5, c) 1.0 and d) 2.0 mol % bromoform (relative to monomer) under inert atmosphere (black squares - error bars represent the standard deviation of the triplicate data) and in the presence of air (red circles).....	115
Figure 3.29. DSC thermogram of PDMA macro-initiators (synthesised in water) to be used in block copolymer reactions. ....	118
Figure 3.30. TGA degradation profile for PDMA macro-initiators (synthesised in water at larger scale) to be used in block copolymer reactions. ....	119
Figure 4.1. Temperature <i>versus</i> time plot for the trial synthesis of PNIPAM using an ice bath to provide temperature control.....	126
Figure 4.2. Exemplar $^1\text{H}$ NMR kinetic overlay for the synthesis of PNIPAM in water at 2.0 mol % bromoform showing the disappearance of monomer and broadening of polymer peaks throughout the course of the reaction. ....	127
Figure 4.3. Kinetic GPC traces for the synthesis of PNIPAM in water at a) 0, b) 0.5, c) 1.0 and d) 2.0 mol % bromoform concentrations (relative to monomer). ....	128

Figure 4.4. Comparative $^1\text{H}$ NMR spectra (in $\text{D}_2\text{O}$ ) showing the disappearance of the monomer vinyl protons (5.6 and 6.1 ppm) between crude (bottom) and precipitated (top) PNIPAM (2 mol % bromoform, relative to monomer). .....	129
Figure 4.5. GPC traces of PNIPAM final precipitates at a) 0, b) 0.5, c) 1.0 and d) 2.0 mol % bromoform (relative to monomer, synthesised in water) demonstrating good reproducibility between runs and e) near-identical GPC traces of the final precipitate at each bromoform concentration.....	130
Figure 4.6. Monomer conversion <i>versus</i> time for the synthesis of PNIPAM at varying bromoform concentrations in water. ....	132
Figure 4.7. Semi-logarithmic plot for the synthesis of PNIPAM at varying bromoform concentration in water. ....	133
Figure 4.8. Molar mass <i>versus</i> monomer conversion for the synthesis of PNIPAM at varying bromoform concentrations in water (error bars represent the standard deviation of the triplicate data).....	133
Figure 4.9. DSC thermograms (second heating cycle) for PNIPAM (synthesised in water) at varying bromoform concentration, highlighting the feature corresponding to the glass transition temperature for each sample.....	135
Figure 4.10. TGA degradation profiles of PNIPAM (synthesised in water) at varying bromoform concentration.....	135
Figure 4.11. Size <i>versus</i> temperature of PNIPAM (synthesised in water) at varying bromoform concentrations highlighting the LCST (or coil-to-globule transition). ....	137
Figure 4.12. Exemplar $^1\text{H}$ NMR kinetic overlay for the synthesis of PNIPAM in DMF at 2.0 mol % bromoform showing the disappearance of monomer and broadening of polymer peaks throughout the course of the reaction. ....	138
Figure 4.13. Kinetic GPC traces for the synthesis of PNIPAM in DMF at a) 0, b) 0.5, c) 1.0 and d) 2.0 mol % bromoform concentrations (relative to monomer). ....	139

Figure 4.14. Comparative $^1\text{H}$ NMR spectra (in $\text{CDCl}_3$ ) showing the disappearance of the monomer vinyl protons (5.3 and 5.9 ppm) between crude (bottom) and precipitated (top) PNIPAM (2 mol % bromoform, relative to monomer). .....	140
Figure 4.15. PNIPAM synthesised in HPLC-grade water highlighting the presence of a low intensity methyl group peak at approximately 0.8 ppm [labelled with an asterix (*)]. .....	141
Figure 4.16. GPC traces of PNIPAM final precipitates at a) 0, b) 0.5, c) 1.0 and d) 2.0 mol % bromoform (relative to monomer, synthesised in DMF) demonstrating good reproducibility between runs and e) near-identical GPC traces of the final precipitate at each bromoform concentration.....	142
Figure 4.17. Monomer conversion <i>versus</i> time for the synthesis of PNIPAM at varying bromoform concentrations in DMF. ....	144
Figure 4.18. Semi-logarithmic plot for the synthesis of PNIPAM at varying bromoform concentration in DMF. ....	144
Figure 4.19. $M_n$ <i>versus</i> monomer conversion for the synthesis of PNIPAM at varied bromoform concentrations in DMF (error bars represent the standard deviation of the triplicate data). ....	145
Figure 4.20. DSC thermograms (second heating cycle) for PNIPAM (synthesised in DMF) at varying bromoform concentrations; highlighting the feature corresponding to the glass transition temperature for each sample. ....	147
Figure 4.21. TGA degradation profile for PNIPAM (synthesised in DMF) at varying bromoform concentrations.....	147
Figure 4.22. Final $^1\text{H}$ NMR spectra for the attempted synthesis of PNIPAM in the absence of ACPA photoinitiator at varying bromoform concentrations (0, 0.5, 1.0 and 2.0 mol % relative to monomer) in water. ....	149
Figure 4.23. Final $^1\text{H}$ NMR spectra for the attempted synthesis of PNIPAM in the presence of oxygen at varying bromoform concentrations (0, 0.5, 1.0 and 2.0 mol % relative to monomer) in water. ....	151
Figure 4.24. DSC thermograms of the PNIPAM macro-initiator (synthesised in water) to be used in future block copolymer reactions.....	154

Figure 4.25. TGA degradation profile for the PNIPAM macro-initiator (synthesised in water at larger scale) to be used in block copolymer reactions. ....	155
Figure 4.26. Size <i>versus</i> temperature of PNIPAM macro-initiator (synthesised in water) at varying bromoform concentrations highlighting the LCST (or coil-to-globule transition). ....	156
Figure 5.1. GPC traces of PDMA macro-initiator and PDMA- <i>b</i> -PNIPAM copolymers (one-pot) with target PNIPAM DPs ranging from 160 to 5800 (a) before precipitation and (b) after precipitation.....	165
Figure 5.2. Achieved molar mass of the copolymer <i>versus</i> average experimental degree of polymerisation (determined using $^1\text{H}$ NMR spectroscopy and Equation 5.3.) of the PNIPAM block in the PDMA- <i>b</i> -PNIPAM block copolymers synthesised during the one-pot synthesis. ....	166
Figure 5.3. DSC thermograms of the PDMA macro-initiator, PDMA- <i>b</i> -PNIPAM copolymers (one-pot) and PNIPAM homopolymer synthesised using 2 mol % bromoform (relative to monomer).....	168
Figure 5.4. TGA degradation profiles for PDMA macro-initiator, PDMA- <i>b</i> -PNIPAM copolymers (one-pot) and PNIPAM homopolymer synthesised using 2 mol % bromoform (relative to monomer).....	169
Figure 5.5. Size <i>versus</i> temperature of PNIPAM homopolymer (2 mol % bromoform relative to monomer) and PDMA- <i>b</i> -PNIPAM copolymers (one-pot) highlighting the LCST (or coil-to-globule transition). ....	170
Figure 5.6. $^1\text{H}$ NMR spectrum of precipitated PDMA macro-initiator (synthesised to 91 % conversion) showing no residual monomer peaks present in the sample at 5.6, 6.0 and 6.6 ppm. ....	172
Figure 5.7. GPC traces of PDMA macro-initiator and PDMA- <i>b</i> -PNIPAM copolymers (two-step, PDMA macro-initiator 91 % conversion) with target PNIPAM DPs ranging from 170 to 6000 (a) before precipitation and (b) after precipitation. ....	176
Figure 5.8. Achieved molar mass <i>versus</i> average experimental degree of polymerisation (determined using $^1\text{H}$ NMR spectroscopy and Equation 5.3.) of the PNIPAM block in the	

PDMA- <i>b</i> -PNIPAM block copolymers synthesised during the two-step synthesis (using PDMA synthesised to 91 % conversion).....	177
Figure 5.9. <sup>1</sup> H NMR spectra showing (a) PDMA macro-initiator (91 % conversion), (b) PDMA <sub>1500</sub> - <i>b</i> -PNIPAM <sub>170</sub> and (c) PDMA <sub>1500</sub> - <i>b</i> -PNIPAM <sub>380</sub> all after precipitation; indicating the presence of PNIPAM in the block copolymers. ....	177
Figure 5.10. DSC thermograms of the PDMA macro-initiator (91 % conversion), subsequent PDMA- <i>b</i> -PNIPAM block copolymers (synthesised via the two-step route) and a PNIPAM homopolymer (2 mol % bromoform). ....	179
Figure 5.11. TGA degradation profile for the PDMA macro-initiator (91 % conversion), subsequent PDMA- <i>b</i> -PNIPAM block copolymers (synthesised via the two-step route) and a PNIPAM homopolymer (2.0 mol % bromoform). ....	180
Figure 5.12. Size <i>versus</i> temperature of PNIPAM homopolymer (2 mol % bromoform relative to monomer) and PDMA- <i>b</i> -PNIPAM copolymers synthesised via the two-step method [using a PDMA macro-initiator synthesised to high conversion (91 %)] highlighting the LCST (or coil-to-globule transition). ....	181
Figure 5.13. <sup>1</sup> H NMR spectrum of precipitated PDMA macro-initiator (synthesised to 70 % conversion) showing no residual monomer peaks present in the sample at 5.6, 6.0 and 6.6 ppm. ....	183
Figure 5.14. GPC traces of PDMA macro-initiator and PDMA- <i>b</i> -PNIPAM copolymers (two-step, PDMA macro-initiator 70 % conversion) with target PNIPAM DPs ranging from 300 to 13,120 (a) before precipitation and (b) after precipitation. ....	186
Figure 5.15. Achieved molar mass <i>versus</i> average experimental DP (determined via <sup>1</sup> H NMR spectroscopy and Equation 5.3.) of the PNIPAM block in the PDMA- <i>b</i> -PNIPAM block copolymers in the two-step synthesis (PDMA synthesised to 70 % conversion). ....	187
Figure 5.16. <sup>1</sup> H NMR spectra showing (a) PDMA macro-initiator (70 % conversion), (b) PDMA <sub>3280</sub> - <i>b</i> -PNIPAM <sub>300</sub> , (c) PDMA <sub>3280</sub> - <i>b</i> -PNIPAM <sub>720</sub> , (d) PDMA <sub>3280</sub> - <i>b</i> -PNIPAM <sub>1180</sub> and (e) PDMA <sub>3280</sub> - <i>b</i> -PNIPAM <sub>1950</sub> all after precipitation; indicating the presence of PNIPAM in the block copolymers. ....	188

Figure 5.17.  $^1\text{H}$  NMR spectra showing only monomer peaks present for the attempted synthesis of PNIPAM in the absence of photoinitiator (namely ACPA) at varied bromoform (0, 0.5, 1.0 and 2.0 mol % relative to monomer) concentrations. All experiments were completed in 25 mL deionised water for 7 hours of UV irradiation (starting temperature 0 °C, ice bath replenished every 1 hour to maintain temperature control). ..... 191

Figure 5.18.  $^1\text{H}$  NMR spectra showing (a) PDMA after precipitation, (b) PDMA<sub>1500</sub>-*b*-PNIPAM<sub>3330</sub> (using 2 mol % bromoform in step 1) after precipitation and (c) only NIPAM monomer peaks present for the attempted synthesis of PDMA-*b*-PNIPAM from PDMA (0 mol % bromoform). ..... 192



## List of Schemes

Scheme 1.1. Chain polymerisation mechanism showing a) initiation, b) propagation and c) termination. ....	29
Scheme 1.2. RAFT reaction mechanism showing a) initiation, b) chain transfer to CTA, c) reinitiation, d) chain equilibrium and e) termination. Modified from Moad <i>et al.</i> <sup>115</sup> . ....	35
Scheme 1.3. Chain transfer to monomer. ....	36
Scheme 1.4. Chain transfer to initiator (A <sub>2</sub> ). ....	37
Scheme 1.5. Chain transfer to polymer a) intermolecular chain transfer and b) intramolecular transfer. ....	38
Scheme 1.6. Chain transfer to the solvent molecule carbon tetrachloride (CCl <sub>4</sub> ). ....	39
Scheme 1.7. ITP reaction mechanism showing a) initiation, b) chain transfer, c) reinitiation, d) chain equilibrium and e) termination. Modified from Boyer <i>et al.</i> <sup>185</sup> . ....	43
Scheme 1.8. RITP mechanism to show how the chain transfer agents can be generated <i>in situ</i> using molecular iodine. Modified from Patra <i>et al.</i> <sup>173</sup> . ....	44
Scheme 1.9. <i>In situ</i> generation of alkyl iodide species in BIT-RDRP. ....	44
Scheme 1.10. Mechanism showing the formation of two initiating radicals and nitrogen from ACPA using UV irradiation. ....	51
Scheme 2.1. Synthesis of poly( <i>N,N</i> -dimethylacrylamide) via bromoform-assisted polymerisation. ....	62
Scheme 2.2. Synthesis of poly( <i>N</i> -isopropylacrylamide) via bromoform-assisted polymerisation. ....	66
Scheme 2.3. Synthesis of poly( <i>N,N</i> -dimethylacrylamide)- <i>block</i> -poly( <i>N</i> -isopropylacrylamide) via bromoform-assisted polymerisation using poly( <i>N,N</i> -dimethylacrylamide) as a macro-initiator. ....	69
Scheme 3.1. Synthesis of PDMA via bromoform-assisted polymerisation at varied bromoform concentrations. ....	83

Scheme 4.1. Synthesis of PNIPAM via bromoform-assisted polymerisation at varied bromoform concentrations.....	124
Scheme 5.1. Synthesis of poly( <i>N,N</i> -dimethylacrylamide)- <i>block</i> -poly( <i>N</i> -isopropylacrylamide) (PDMA- <i>b</i> -PNIPAM) using bromine-terminated <i>N,N</i> -dimethylacrylamide (PDMA).....	161
Scheme 5.2. (a) Attempted synthesis of NIPAM homopolymer in the absence of ACPA photoinitiator. (b) Attempted synthesis of NIPAM homopolymer in the absence of bromoform and ACPA photoinitiator. (c). Attempted synthesis of PDMA- <i>b</i> -PNIPAM copolymers without bromoform in step 1. (d) Successful two-step synthesis of PDMA- <i>b</i> -PNIPAM copolymers using PDMA prepared using bromoform in step 1.....	193

## List of Equations

Equation 1.1. Number average molar mass ( $M_n$ ) .....	27
Equation 1.2. Weight-average molar mass ( $M_w$ ) .....	27
Equation 1.3. Molar mass dispersity ( $\mathcal{D}$ ) .....	27
Equation 1.4. Carothers equation .....	28
Equation 1.5. Extent of reaction ( $p$ ) [step-growth polymerisation] .....	28
Equation 2.1. PDMA (in water) and PNIPAM (in water and DMF) monomer conversion calculation .....	76
Equation 2.2. PDMA (in DMF) monomer conversion calculation.....	78
Equation 5.1. Target PNIPAM degree of polymerisation.....	163
Equation 5.2. Average experimental PNIPAM degree of polymerisation (determined using GPC data).....	164
Equation 5.3. Average experimental PNIPAM degree of polymerisation (determined using $^1\text{H}$ NMR data).....	164

# **Chapter 1. Introduction**

## 1.1 Introduction to Thesis

This thesis is concerned with the development of a bromoform-assisted free radical synthesis route to produce block copolymers. Polymerisations in the presence of bromoform were investigated using hydrophilic *N,N*-dimethylacrylamide (DMA), and temperature-responsive *N*-isopropylacrylamide (NIPAM). DMA and NIPAM were selected for this study as exemplar monomers due to their highly desirable water solubility [poly(*N*-isopropylacrylamide) (PNIPAM) is soluble in water below 32 °C<sup>1</sup>]; allowing the reactions to be conducted in aqueous media. Additionally, incorporating NIPAM within the copolymer allows block copolymer self-assembly to be explored. Bromoform is used under UV conditions to equip the poly(*N,N*-dimethylacrylamide) (PDMA) and PNIPAM chains with a reversibly cleavable bromine chain end. Refinement of the homopolymerisation studies led to an optimal route for the synthesis of the bromine-terminated PDMA and PNIPAM, now referred to as macro-initiators. A further in-depth investigation was then undertaken to determine the potential of these polymer chains to reinitiate under further UV irradiation and for subsequent block copolymer synthesis to occur. The copolymer synthetic routes included both one and two-step investigations in an attempt to understand the system in more detail to synthesise poly(*N,N*-dimethylacrylamide)-*block*-poly(*N*-isopropylacrylamide) (PDMA-*b*-PNIPAM).

Bromoform has been selected for use in this study as it is partially water-miscible (3.0 g/L at 20 °C<sup>2,3</sup>, 3.0 g/L at 25 °C<sup>3,4</sup> and 3.2 g/L at 30 °C<sup>2,3</sup>), readily available, inexpensive, stable (easily stored) and can be used directly at low and ambient temperatures, in contrast to other mediating agents (e.g. alkyl iodides or CTAs). This leads to the exploration of a new aqueous-based synthetic route for the production of commercially-relevant block copolymers.

Overall, this thesis is comprised of six chapters, including an introduction that sets the scene for the project. The remainder of the thesis consists of; Materials and Experimental Methods (Chapter 2), followed by three results and discussion chapters: Bromoform-assisted polymerisation of *N,N*-dimethylacrylamide (Chapter 3), Bromoform-assisted polymerisation of *N*-isopropylacrylamide (Chapter 4), Synthesis of poly(*N,N*-dimethylacrylamide)-*block*-poly(*N*-

isopropylacrylamide) copolymers (Chapter 5) and finally a Conclusions and Future Work (Chapter 6) section.

## **1.2 Polymers**

According to Cowie,<sup>5</sup> polymers are universally accepted by scientists simply as 'giant molecules', however, in more detail they are considered substances with molecular structures built up of many covalently bonded repeating units known as monomers<sup>6</sup>. Polymeric materials are recognised globally for their diverse and wide range of applications such as; packaging<sup>7,8</sup>, drug delivery systems<sup>9,10</sup>, tissue regeneration<sup>11–13</sup>, wound dressings<sup>14,15</sup> and contact lenses<sup>16,17</sup>. Modern medicine is becoming increasingly dependent on polymer research and its advances; of particular interest are what are sometimes referred to as 'smart'<sup>18–25</sup> or 'designer' polymers<sup>26</sup>. These materials are polymers which have been constructed from carefully selected monomers to result in specific desirable physical, chemical and even biological properties<sup>27,28</sup>. With the ability to control properties such as; biocompatibility<sup>29</sup>, biodegradability<sup>30–33</sup> and stimuli-responsiveness<sup>34,35</sup>, the final polymeric material can be tuned to meet the need of the given application. For example, progressions in biodegradable polymer technology has resulted in the production of biomedical scaffolds that support tissue growth and degrade once they have served their purpose in the body<sup>36</sup>. Such developments have only been possible with the continued research into polymer synthesis routes.

## **1.3 Polymer synthesis**

The purpose of polymer synthesis is to efficiently create macromolecules (large molecules) with controlled structures for desired applications. While there is a wide variety of existing polymerisation methods, no single technique is appropriate for all of the monomer species available. In many cases, a given polymerisation method is more suited to certain monomer species; dependent on the overall chemical composition of the monomer molecule and its associated properties (such as reactivity and solubility). Some methods, however, do provide a greater tolerance of monomer species resulting in a set of reactions that can all proceed via the same simple mechanism. It is important to consider the effect that the polymerisation

method has on the final composition of the polymer produced; specifically, the polymer number-average molar mass [ $M_n$  (kg mol<sup>-1</sup>)], weight-average molar mass [ $M_w$  (kg mol<sup>-1</sup>)] and molar mass dispersity ( $\mathcal{D}$ ). In a uniform system, each polymer chain produced would be the same length (monodisperse), however, this is unachievable in laboratory-based synthesis. Instead, for any given polymerisation reaction, a range of chain lengths will be produced. The  $M_n$  of the final polymer is a statistical average molar mass of all of the polymer chains in a sample<sup>37</sup> and is calculated from Equation 1.1<sup>5</sup>. Where  $M_i$  is the molar mass of a given polymer chain and  $N_i$  is the number of chains of that molar mass.

$$M_n = \frac{\sum N_i M_i}{\sum N_i} \quad \text{Equation 1.1.}$$

$M_w$  takes into account how much each chain length contributes to the molar mass average (Equation 1.2)<sup>5</sup>.  $\mathcal{D}$  then quantifies the distribution (or spread) of the respective molar masses for the varied chain lengths in a sample using  $M_n$  and  $M_w$ ; as seen in Equation 1.3<sup>38</sup>.

$$M_w = \frac{\sum N_i M_i^2}{\sum N_i M_i} \quad \text{Equation 1.2.}$$

$$\mathcal{D} = \frac{M_w}{M_n} \quad \text{Equation 1.3.}$$

The amount of control over the molar mass and molar mass dispersity is heavily dependent on the method of polymerisation that is used. Polymer synthesis can be broadly divided into two main categories; those of step and chain polymerisation.

### 1.3.1 Step polymerisation

Step polymerisation proceeds via a mechanism in which multi-functional ( $f \geq 2$ ) monomers react with one another via their end group functionality. Initially, they form dimers, then trimers, before eventually forming oligomers and long chain polymers<sup>39</sup>. In this technique there is no need for an initiator species (the interaction of reactive monomer molecules starts the reaction) as the reactive functions present on the monomer units allow for the growth of the polymer<sup>40</sup>.

Step polymerisation continues up until the point when there is no more (or a negligible amount) of monomer present in the system. There is no termination stage and the ends of the polymer chains remain active at the end of the polymerisation reaction. However, step polymerisations must be driven to extremely high monomer conversions in order to achieve high molar mass polymers as depicted by Carothers equation (Equation 1.4)<sup>40,41</sup>. Where DP refers to the degree of polymerisation and  $p$  is the extent of reaction. In more detail, Equation 1.5 shows that  $p$  is directly related to the number of monomer molecules initially present in the reaction,  $N_0$ , and the number of monomer molecules present at a given time,  $N$ .

$$DP = \frac{1}{1 - p} \quad \text{Equation 1.4.}$$

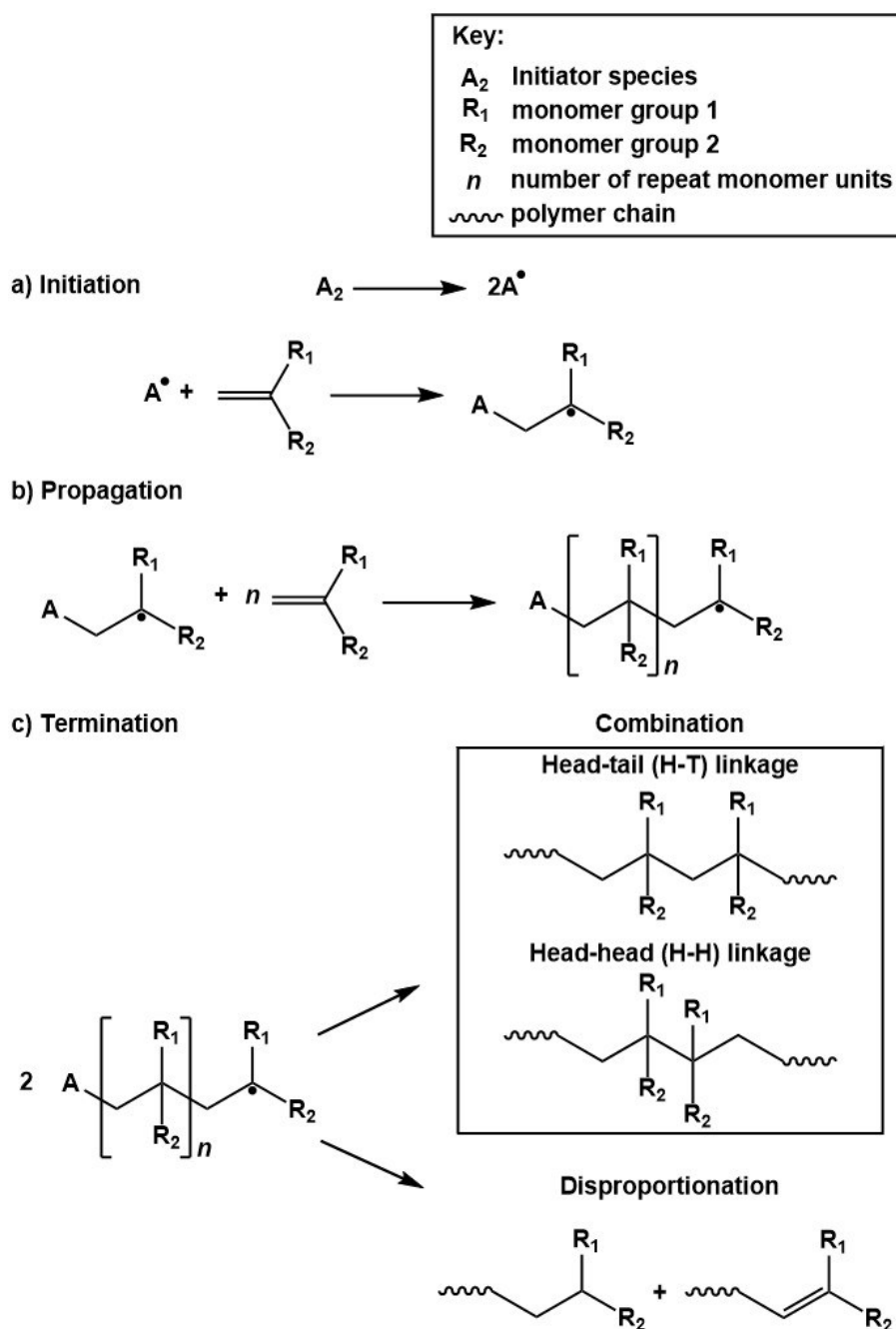
$$p = \frac{N_0 - N}{N_0} \quad \text{Equation 1.5.}$$

### 1.3.2 Chain polymerisation

Chain polymerisation proceeds via three steps; initiation, propagation, and termination<sup>42</sup> as seen in Scheme 1.1<sup>43</sup>. Polymer chains are typically generated by initiator species adding to monomer molecules<sup>44</sup>. The initiator used can be in a number of forms, such as free radical<sup>45</sup> (generated due to the decomposition of the initiator species often under mild conditions including UV light, heat<sup>46</sup> or gamma radiation<sup>47</sup>), organometallic complexes<sup>48</sup>, cations<sup>49</sup> and anions<sup>50</sup>. Each of these methods of chain polymerisation, using different initiator species, are referred to as free-radical<sup>45</sup>, coordination<sup>48</sup>, cationic<sup>49</sup> and anionic<sup>50</sup> polymerisation, respectively. In each case, once the first monomer species has bound to the initiator, propagation begins; this involves sequentially adding monomer units to the active species with the active site being gradually passed along the growing chain<sup>51</sup>. Termination can then occur via one of two processes<sup>52</sup>; combination or disproportionation (Scheme 1.1)<sup>43</sup>. Combination occurs when two polymer radicals meet to form a covalent bond. Combination can occur as



either a head-to-tail or head-to-head linkage. The most prevalent reaction depends on radical stability and steric hindrance<sup>53</sup>. On the other hand, disproportionation occurs when a hydrogen atom is abstracted from one polymer chain to another. This results in two dead polymer chains; one containing the abstracted hydrogen atom and the other with an unsaturated chain end.



Scheme 1.1. Chain polymerisation mechanism showing a) initiation, b) propagation and c) termination.

The molar mass of a polymer synthesised via chain polymerisations can be high when excessive amounts of monomer<sup>54</sup> are present in the reaction. For step polymerisation, an exact stoichiometric balance of monomers<sup>41</sup> and sufficiently long reaction times<sup>55</sup> are also required to synthesise high molar mass polymers (Figure 1.1<sup>5</sup>). High purity monomers should also be used in both cases to limit side reactions<sup>56</sup>; including unwanted termination. In the case of step polymerisation (more specifically condensation), it is also sometimes necessary to remove the small molecule, eliminated in the reaction, to promote the production of the polymer rather than the reverse reaction<sup>41</sup> (as seen in the synthesis of poly(ethylene terephthalate)<sup>57</sup>).

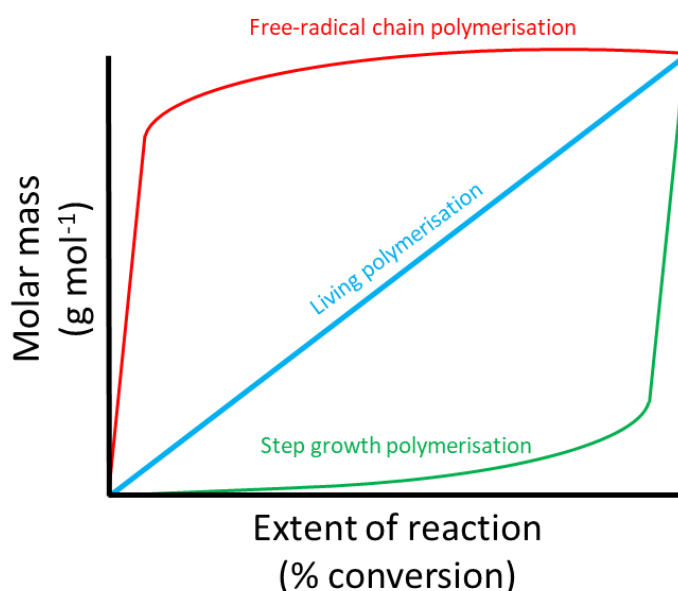


Figure 1.1. Trend of molar mass with extent of reaction for chain and step growth and living polymerisation reactions. Modified from Cowie<sup>5</sup>.

The molar mass of a polymer, produced via chain growth, is more heavily dependent on the monomer to initiator ratio. The molar mass dispersity achieved in conventional chain polymerisation (free radical polymerisation) can range between 2-5<sup>58,59</sup> when approaching 100 % monomer conversion. On the other hand, the molar mass dispersity achieved in step polymerisation is 2 when approaching 100 % monomer conversion and, as previously discussed, high molar masses are only achieved at significantly high monomer

conversions<sup>40,41</sup>. This demonstrates that both methods lack control over the final polymer produced and its corresponding mechanical (e.g. strength<sup>60</sup> and Young's modulus<sup>61</sup>) and physical (e.g. melting and boiling point<sup>62</sup> and glass transition temperature,  $T_g$ <sup>63</sup>) properties<sup>64</sup>. Typically, these traditional methods also limit control over the composition, chain architecture and possibility of introducing site-specific functionality within the polymer<sup>65</sup>. Further advancement in polymeric research has resulted in a series of synthetic pathways that can overcome such issues; the first, discovered in 1956 by Szwarc<sup>66</sup>, is known as living anionic polymerisation.

### 1.3.3 Living polymerisation

Living polymerisations are defined as a series of reactions in which irreversible chain transfer and chain termination are absent<sup>67</sup>. Herein the living polymerisation techniques known as anionic polymerisation, group transfer polymerisation (GTP) and cationic polymerisation will be discussed.

#### 1.3.3.1 Anionic polymerisation

Arguably one of the most successful living methods is anionic polymerisation, which offers the greatest degree of control; producing polymers with narrow molar mass distributions ( $\bar{D} < 1.1$ <sup>68–70</sup>). In the case of living anionic polymerisation no external energy source (such as light, heat or UV irradiation used in free radical polymerisation) is required to decompose the initiator and generate active radicals. Instead highly reactive initiators are selected (often alkyl lithium compounds<sup>71,72</sup>), relative to the monomer being polymerised, which go on to form relatively stable carbanions during initiation<sup>73,74</sup>. All chains are initiated at the start of the reaction providing each chain with equal probability to grow (Figure 1.1); leading to the narrow molar mass distributions previously mentioned<sup>68–70</sup>. The initiator selected must be more reactive than the resulting carbanion otherwise the polymerisation will not proceed, however, it should not be too reactive as this can lead to unwanted side reactions<sup>73</sup>. The nature of living anionic polymerisation leads to the elimination of termination events; there will be no chain-chain coupling due to the unfavourable electrostatic forces between the anionic charges present at

each chain end<sup>75</sup>. This then also provides the opportunity for further chain extension or chain end modification once the initial monomer has been completely consumed. Living anionic polymerisation has been used to produce polymers of high molar mass, through addition of more monomer, and highly valuable block copolymers; through the sequential addition of a second monomer<sup>23,76–78</sup>. In the case of block copolymer formation, the stability of the second monomer carbanion must be greater than that of the first monomer polymerised; restricting the sequence of monomer addition<sup>79</sup>.

Whilst living anionic polymerisation clearly has its advantages, this method is not without its drawbacks. The reagents, including initiator, monomer and solvent, must be rigorously purified to remove potential inhibitors such as oxygen, carbon dioxide and water<sup>80</sup>. If present in the system, these molecules can react irreversibly with the anionic chain end causing potentially unwanted termination<sup>75</sup>. However, in some cases highly selective reagents are added to produce polymers with desired chain end functionality for further reactions<sup>81</sup>. Additionally, the reaction vessel should be extremely dry, again to remove water, and often requires heating under vacuum overnight<sup>82</sup>. Most significantly, as the monomer must contain an anion stabilising group<sup>73,83</sup>, this limits the variety of monomer that can be polymerised via this method (styrene, 1,3-butadiene, isoprene, 2-vinylpyridine and ethylene oxide are some examples<sup>73,83</sup>).

#### **1.3.3.2 Other living techniques**

Other living polymerisation techniques include group transfer and cationic polymerisation. Similar to anionic living polymerisation, GTP is a living anionic chain growth process<sup>22,84</sup> and can be used to synthesise polymers with high molar mass and narrow molar mass dispersities<sup>85</sup>. Additionally, termination events are eliminated and further chain extension or chain end modification is possible once the initial monomer has been completely consumed<sup>86</sup>. However, in this case the reaction is initiated by silyl ketene acetals<sup>84,87</sup> and a co-catalyst (such as a Lewis acid (electron acceptor)<sup>84,86,87</sup>). One advantage of GTP is the ability to synthesise polymers from (meth)acrylic monomers at room temperature and above<sup>84,86</sup>. This unlike anionic living polymerisation, discussed previously, which has been shown to only produce

sufficient (meth)acrylic polymers at significantly low temperatures ( $-78\text{ }^{\circ}\text{C}$ <sup>88</sup>). The main drawback of GTP is the sensitivity of the catalysts to protic impurities<sup>89</sup>, such as the aforementioned water that must also be eliminated in anionic living polymerisation<sup>75</sup>.

Finally, in the case of cationic polymerisation Lewis<sup>90,91</sup> or protic acid initiators<sup>90,92</sup> and monomers with electron donating groups are required<sup>91,93</sup>. Reagents including solvent, initiator and in some cases a catalyst must be selected specifically for the monomer that is being polymerised.  $\text{H}^+$  and an anionic base ( $\text{B}^-$ ) species are generated from the initiator molecule, after which, a monomer unit will react with  $\text{H}^+$  to form a new cationic species. This cationic species can then continue to react with more monomer units during the propagation stage<sup>90,91</sup>. However, high molar mass polymers are difficult to achieve due to frequent side and chain transfer reactions that can occur in the cationic system<sup>91</sup>.

To overcome the strict reaction conditions and broaden the scope of polymers that can be synthesised in a controlled manner another series of synthetic routes, known as reversible-deactivation radical polymerisations, were developed.

#### **1.3.4 Reversible-deactivation radical polymerisation**

Reversible-deactivation radical polymerisation (RDRP) is a method of polymerisation where the active chain end is a free radical. This enables new polymeric materials to be designed to fit specific applications through the formation of polymers with complex architectures, compositions and functionalities<sup>65</sup>. However, unlike living polymerisation, termination is suppressed (relative to propagation) rather than eliminated and chain transfer is often a key process in many of the RDRP methods. Arguably, three of the most important and widely studied RDRP techniques are; nitroxide-mediated radical polymerisation<sup>43</sup> (NMP), atom transfer radical polymerisation<sup>94</sup> (ATRP) and reversible addition-fragmentation chain transfer<sup>95</sup> (RAFT) polymerisation. Each of these RDRP methods relies on forming a dynamic equilibrium between a limited number of propagating polymer chains and a predominant number of dormant chains<sup>97</sup>; due to either a persistent radical effect<sup>98</sup> or degenerative chain transfer<sup>99</sup>. This results in the aforementioned suppressed termination (relative to propagation)

and provides temporarily dormant chains that are capable of reactivation, functionalisation or chain extension<sup>100</sup>.

#### **1.3.4.1 Atom transfer radical polymerisation**

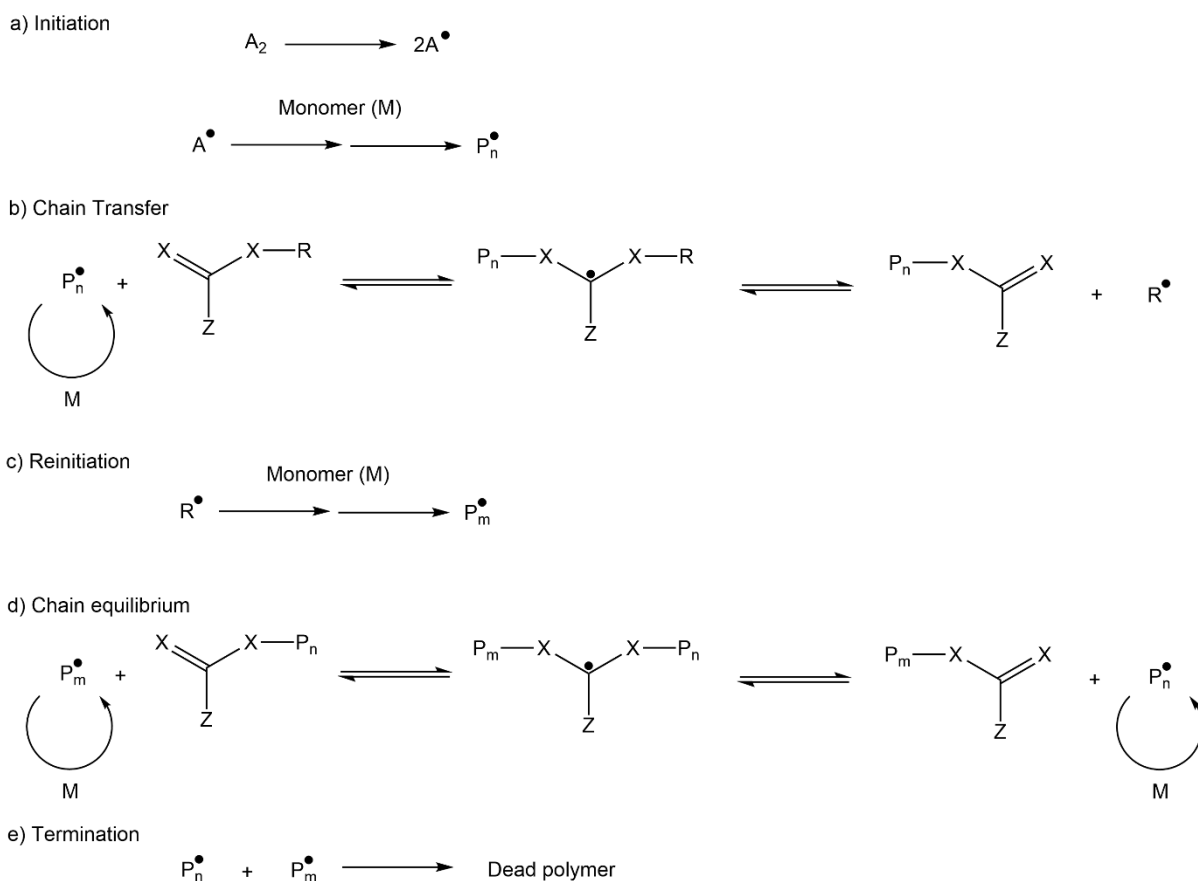
ATRP involves an alkyl halide initiator<sup>101,102</sup> and transition metal catalyst<sup>103</sup>. In the ATRP process the control arises from a reversible equilibrium generated between dormant and active radical species; with the equilibrium shifted to favour the side with low radical concentrations<sup>104</sup>. The dormant species is reactivated by the transition metal catalyst<sup>105</sup> and because of this intermittent reactivation/reversible dormancy the fraction of 'dead' terminated polymer chains that are formed is significantly reduced (<10%<sup>105</sup>), resulting in polymers with similar molar masses and  $\bar{D} < 1.2$ <sup>106,107</sup>.

#### **1.3.4.2 Nitroxide-mediated radical polymerisation**

NMP utilises an alkoxyamine<sup>108</sup> compound to generate highly stable nitroxide radicals capable of acting as persistent radicals during the polymerisation<sup>109</sup>. Initiating radicals react with the monomer species before propagation begins. After no more than a few propagation steps the growing chain is trapped by a nitroxide radical forming a temporarily dormant species<sup>110</sup>. This reversible termination and reactivation of the growing chains by nitroxyl radicals is what leads to a reduced formation of permanently unreactive (or 'dead') chains<sup>111</sup>. Overall, this results in the formation of polymers with controlled molar masses and  $\bar{D} < 1.2$ <sup>107</sup>.

#### **1.3.4.3 Reversible addition-fragmentation chain transfer**

Of all the RDRP methods, RAFT is recognised as the most versatile technique due to the applicability to the widest range of monomer structures<sup>112</sup>. In addition, RAFT permits a high degree of control over the molar mass and molar mass dispersity (often  $\bar{D} < 1.2$  for the latter)<sup>107,113</sup> whilst also having high tolerance over the reaction conditions; including the functionality of the reagents involved<sup>114</sup>. RAFT proceeds via a pathway that includes the traditional initiation and propagation steps with the addition of chain transfer and chain equilibration stages to limit termination to within less than 10 %<sup>115</sup> of the final polymer (Scheme 1.2<sup>115</sup>).



Scheme 1.2. RAFT reaction mechanism showing a) initiation, b) chain transfer to CTA, c) reinitiation, d) chain equilibrium and e) termination. Modified from Moad *et al.*<sup>115</sup>.

The control associated with RAFT polymerisations is heavily dependent on the chain transfer agent (CTA)<sup>116</sup>; sometimes referred to as a modifier<sup>5</sup> or RAFT-agent<sup>117</sup>. Chain transfer of the CTA between growing and dormant polymer chains regulates the molar mass of the polymer and limits termination reactions<sup>116</sup>; this stage is known as chain equilibrium.

RDRP techniques offer a series of reactions that are more tolerable to reaction conditions (e.g. in bulk, suspension, emulsion, protic organic/aqueous solvent)<sup>118,119</sup> whilst still providing good control to produce polymers with targeted molar masses and low dispersities<sup>106,107,113</sup>. The ability to synthesise polymers with control over the molar mass, molar mass dispersity and chain functionality, particularly in aqueous solvents<sup>119</sup>, is of great interest for developing greener synthetic routes to designer materials. Additionally, when compared to living anionic polymerisation, RDRP methods are often more inexpensive and robust<sup>120</sup>. RDRP techniques

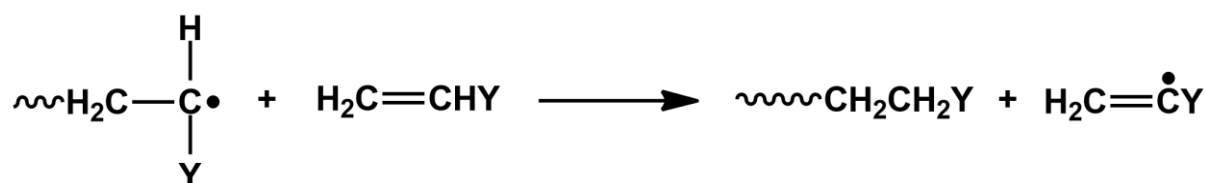
are also tolerable toward a wider scope of monomer species (e.g. (meth)acrylates, acrylonitriles and acrylamides<sup>21,121–133</sup>) including those that contain unprotected functionalities such as hydroxyl, amide and anhydride groups<sup>134</sup> and despite the drive for narrow molar mass distributions, this is not always necessary to prepare materials with desired characteristics and performance<sup>135–143</sup>.

## 1.4 Chain transfer

Chain transfer itself refers to the abstraction of an atom (or fragment of a molecule) from an inactive molecule (X-Y) by the polymer chain<sup>144</sup>. The proportion of chain transfer that may occur during a polymerisation reaction is heavily reliant on the strength of the X-Y bond in the inactive molecule<sup>145</sup> as well as the polymer structure and reaction conditions; such as the concentration of the reagents<sup>146</sup> and the temperature of the system<sup>44</sup>. Chain transfer can occur between a polymer chain and any of the following: monomer, initiator, polymer, solvent or CTA<sup>146</sup>, depending on the associated chain transfer constants.

### 1.4.1 Chain transfer to monomer

Transfer of the polymer radical to monomer involves hydrogen abstraction (Scheme 1.3)<sup>44</sup>. The new radical formed on the monomer molecule is often so stable that further propagation of that radical does not occur<sup>147</sup>. This results in rapid chain termination and is an example of degradative transfer, however, the probability of chain transfer to monomer is often incredibly low because of the energy that is required to break the strong carbon-hydrogen bond<sup>148</sup>.

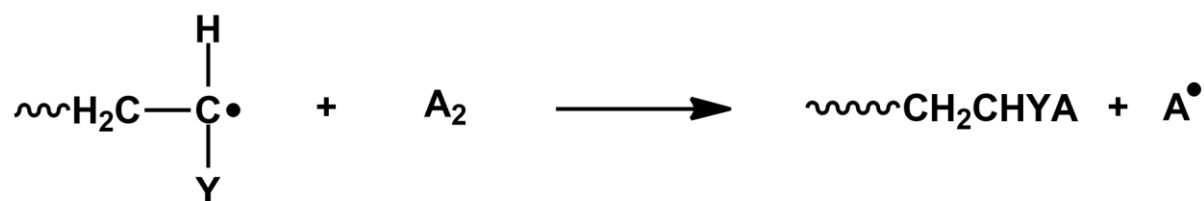


Scheme 1.3. Chain transfer to monomer.



### 1.4.2 Chain transfer to initiator

Chain transfer of the polymer radical to an initiator molecule results in the end-group functionality of both ends of the polymer chain being comprised of segments of initiator molecules (Scheme 1.4)<sup>44</sup>. The resultant radical that is then formed on the other portion of the initiator molecule can go on to produce a new growing polymer chain<sup>149</sup>. Control of initiator concentration is an important factor in limiting this method of chain transfer to result in the formation of high molar mass polymers<sup>150</sup>.

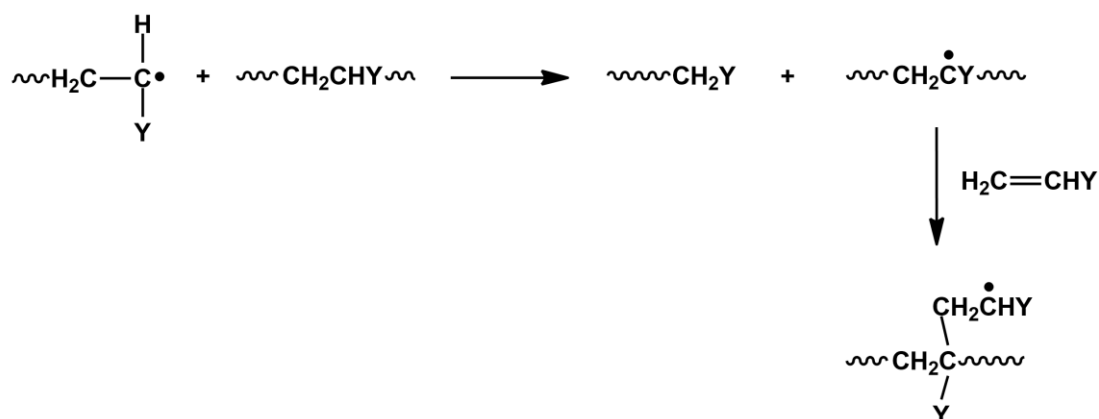


Scheme 1.4. Chain transfer to initiator (A<sub>2</sub>).

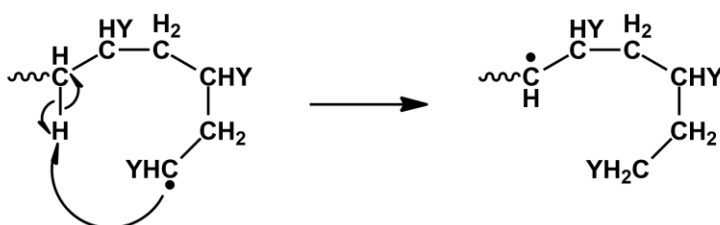
### 1.4.3 Chain transfer to polymer

Transfer of a polymer radical to a polymer chain results in short or long chain branching depending on the type of transfer; intra- or intermolecular (Scheme 1.5)<sup>44</sup>. Branching occurs due to the abstraction of an atom from a position within the polymer chain by a radical<sup>151</sup>. This mode of chain transfer can be intramolecular or intermolecular; where the initial radical was part of the same polymer chain in which the atom was extracted from (backbiting) or from a disparate polymer chain, respectively<sup>152</sup>. The rheological<sup>153</sup> and physical properties of the final polymer are directly related to the degree of branching<sup>154</sup>. Therefore, the potential for chain transfer to polymer must be considered when designing and conducting new polymer syntheses.

a) Intermolecular chain transfer



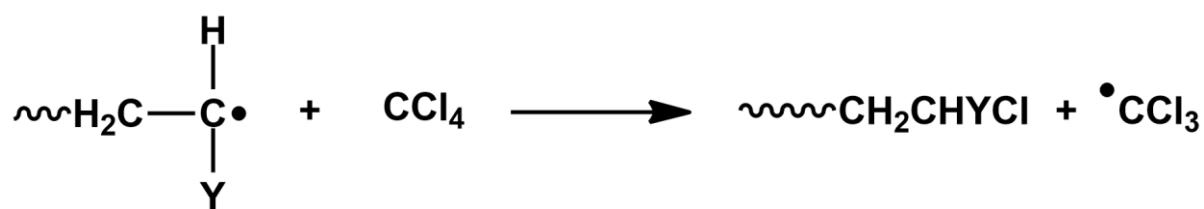
b) Intramolecular chain transfer



Scheme 1.5. Chain transfer to polymer a) intermolecular chain transfer and b) intramolecular transfer.

#### 1.4.4 Chain transfer to solvent

The ability of a solvent to take part in a chain transfer reaction is highly dependent on; the strength of the bond in which an atom would be extracted from the solvent molecule by the polymer chain<sup>155</sup>, the quantity of solvent present<sup>156</sup> and the stability of the solvent radical that is produced during the chain transfer<sup>157</sup>. Similar to chain transfer to monomer (Section 1.4.1), hydrogen abstraction can occur. In the case where hydrogen abstraction does not occur, as with solvent carbon tetrachloride ( $\text{CCl}_4$ ) (Scheme 1.6<sup>44,146</sup>), the solvent radical produced could also be capable of acting as an initiator fragment; forming a new growing polymer chain<sup>158</sup>.



Scheme 1.6. Chain transfer to the solvent molecule carbon tetrachloride (CCl<sub>4</sub>).

#### 1.4.5 Chain transfer to RAFT CTA

The transfer of a polymeric radical to a RAFT CTA occurs in a controlled manner due to the design of the CTA molecule (Figure 1.2); specifically the presence of a bond that is much weaker and susceptible to chain transfer than that of a carbon-hydrogen bond<sup>159</sup>. During the polymerisation there is an addition step between the propagating polymer chain (P<sub>n</sub>•) and RAFT CTA because of the weak bond present. This results in a temporarily dormant polymer chain and a new initiating radical (R•), which can then add to a monomer forming a new propagating species (P<sub>m</sub>•)<sup>160</sup>. A series of addition-fragmentation steps then produce an equilibrium between P<sub>n</sub>•, RAFT CTA and P<sub>m</sub>• via the path of an intermediate radical (Scheme 1.2<sup>115</sup>). It is this equilibrium between the growing chains that produces polymers with low molar mass dispersity while the ratio of monomer to RAFT CTA allows for control over the molar mass of the final polymer synthesised<sup>161</sup>. More specifically, the ratio of monomer to RAFT CTA depicts the number of polymer chains formed which is directly related to the molar mass of the final product.

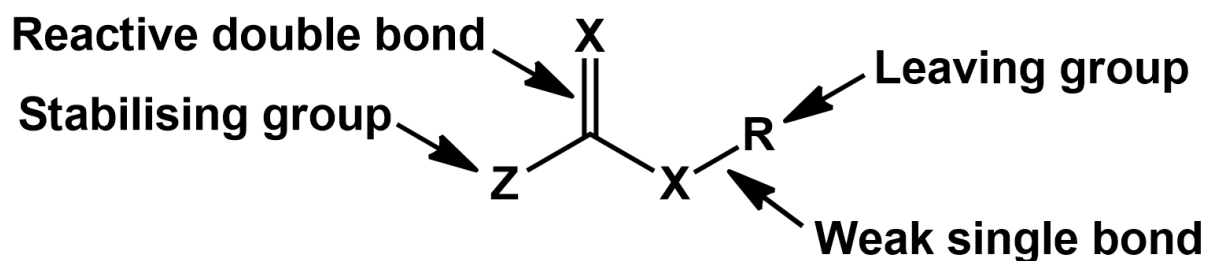


Figure 1.2. Generic RAFT CTA structure showing the positions of the reactive double bond, stabilising group, weak single bond and leaving group.

Additionally, specific functionality can be introduced through the design of the RAFT CTA molecule. The desired function is often introduced so that the product can act as a macroCTA<sup>161,162</sup> (a polymer with specific end group functionality) in a further reaction to create unique materials with particular compositions, architectures and properties. The ratio of RAFT CTA to initiator is an important factor when targeting a product which includes the end functionality of the RAFT CTA molecule. This ratio influences the functionality at both the  $\alpha$  and  $\omega$  polymer chain ends<sup>163</sup>. At the  $\alpha$  chain end, there is a competition between initiator and RAFT CTA-derived chains<sup>99</sup>. However, at the  $\omega$  chain end, this contest is between RAFT CTA-terminated chain ends, capable of further reaction, and dormant chains that have terminated<sup>164</sup>.

RAFT CTA compounds are selected due to their chain transfer constants<sup>165</sup>. The chain transfer constant is a measure of the reactivity of a CTA and is calculated from the ratio of the chain transfer and propagation rate coefficients of a particular polymerisation reaction<sup>144</sup>. The chain transfer constant can be tuned via the design of the RAFT CTA molecule through the choice of Z and R group (Figure 1.2)<sup>164,166</sup>. The Z group modifies the addition-fragmentation rate within the polymerisation by stabilising the dormant radical species while the R group is designed to be a good radical leaving group capable of reinitiating polymerisation<sup>164,167</sup>. Some of the most widely studied RAFT CTAs are dithioesters<sup>168,169</sup>, dithiocarbamates<sup>170</sup>, trithiocarbonates<sup>171</sup> and xanthates<sup>172</sup> (Figure 1.3) which contain carbon, nitrogen, sulfur or oxygen functionalities in the Z group position, respectively.

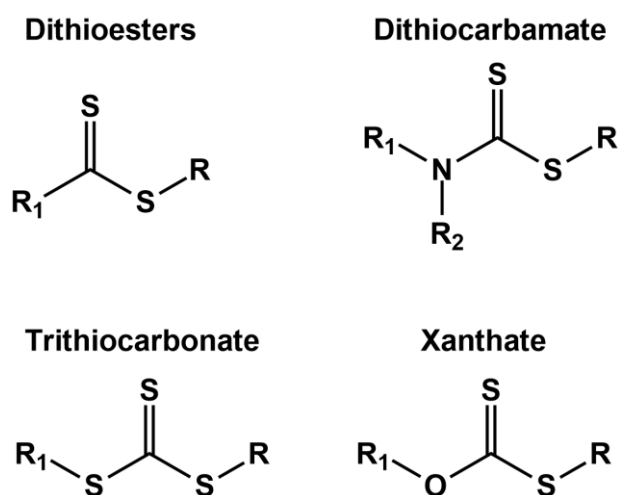


Figure 1.3. Structures of commonly used CTAs in RAFT polymerisation including; dithioesters, dithiocarbamates, trithiocarbonates and xanthates.

Whilst these RAFT CTAs are widely used in controlled radical polymerisations they are not without their disadvantages. These compounds can be difficult to synthesise, which results in increased cost<sup>173</sup>. RAFT CTAs, and in some cases the reagents required to synthesise them, are often not readily available to purchase and any residual RAFT CTA left in the final polymer can be highly toxic<sup>174</sup>. This hinders their potential to be used in the production of polymeric biomaterials, which, as previously discussed, is an ever-growing component of the polymer industry.

Another class of reagent that has effective chain transfer capabilities are certain halogenated compounds<sup>159</sup>. When compared with traditional RAFT agents, many halogenated compounds have the advantage of being readily available and inexpensive; reducing the need to synthesise these compounds. In addition, halogenated compounds have been used throughout the polymer industry as monomers, solvents and, in ATRP, as initiators<sup>175</sup> suggesting that they are versatile reagents. Even with the discussed versatility, the use of halogenated compounds to mediate polymerisation in the published literature is limited.

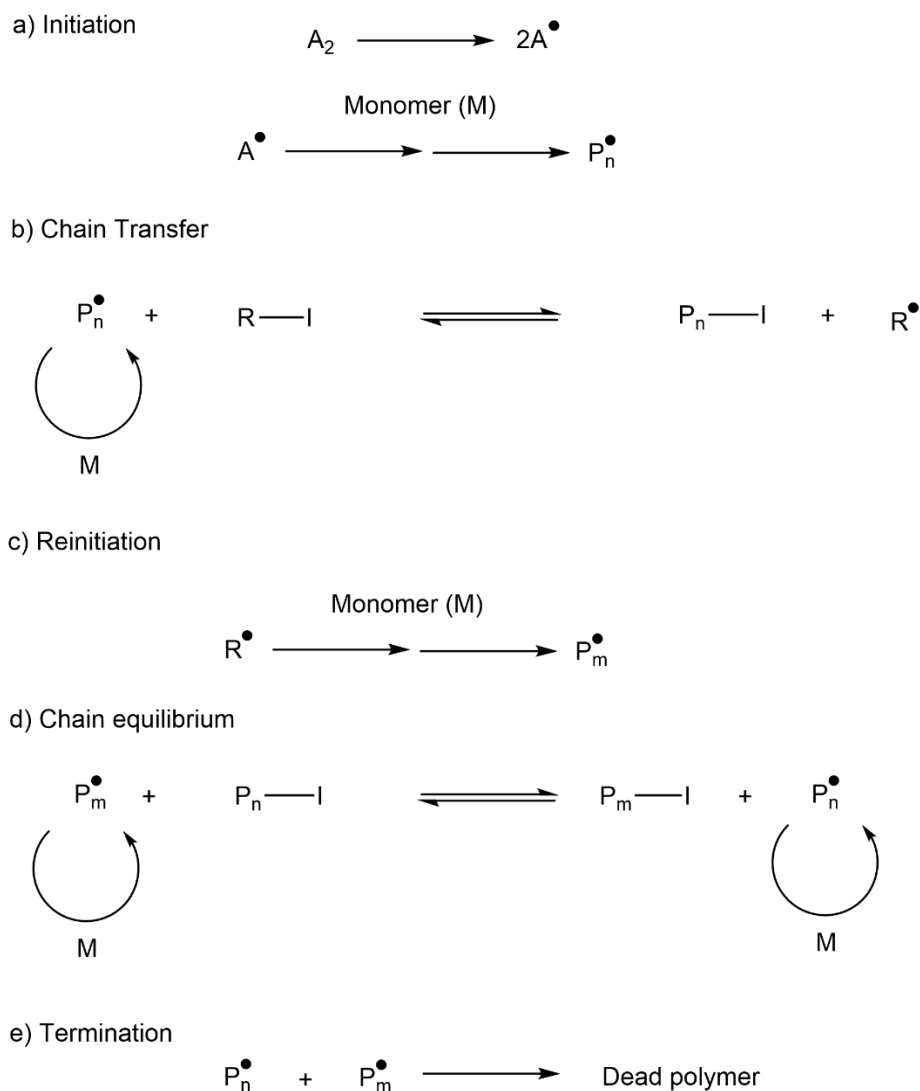
## 1.5 Halogenated compounds

Halogenated compounds are molecules that contain one or more of the group VII elements namely; fluorine, chlorine, bromine or iodine (*N.B.* astatine will not be discussed because of the negligible experimental data available due to its radioactive nature<sup>176</sup>).

### 1.5.1 Halogens in controlled radical polymerisation

An additional method of controlled radical polymerisation not yet mentioned is (reversible) iodine transfer polymerisation [(R)ITP]; whereby molecules that contain iodine are used as CTAs. Like RAFT, ITP and RITP offer the opportunity to control the molar mass and molar mass dispersity of the polymer produced whilst also providing desired chain end functionality. This can lead to the synthesis of polymers with specific compositions and architectures<sup>177</sup>, including the generation of amphiphilic (having both hydrophilic and hydrophobic components<sup>178</sup>) copolymers that are of growing interest. ITP and RITP have successfully been employed in the polymerisation reactions of many monomers, including styrene<sup>179</sup>, acrylates<sup>180</sup>, vinyl acetate<sup>181</sup>, fluorinated monomers (tetrafluoroethylene, butyl  $\alpha$ -fluoroacrylate, vinylidene fluoride, hexafluoropropene)<sup>182</sup> and chlorinated monomers (vinyl chloride and vinylidene chloride)<sup>183 184</sup>.

Similarly to RAFT, ITP proceeds via initiation, chain transfer, propagation and chain equilibration steps (Scheme 1.7<sup>185</sup>). The propagating radical,  $P_n^\bullet$ , is generated in the same manner as with conventional free radical polymerisation. The iodine-containing chain transfer agent then reacts with the propagating radical to form a polymeric chain transfer agent and a newly liberated radical. The radical ( $R^\bullet$ ) then reacts with a monomer molecule in a reinitiation step whereby a new propagating radical,  $P_m^\bullet$ , is formed. Continued propagation occurs through repetition of this process; transferring the iodine molecule between the active and dormant polymer chains. Termination can occur between polymer chain end radicals by the same mechanisms described in conventional free radical polymerisation, producing 'dead' polymer chains.




Scheme 1.7. ITP reaction mechanism showing a) initiation, b) chain transfer, c) reinitiation, d) chain equilibrium and e) termination. Modified from Boyer *et al.*<sup>185</sup>.

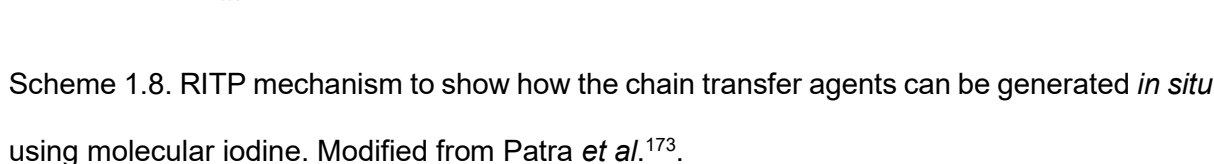
The iodine chain transfer agents explored in the literature are derivatives of alkyl iodides including; methyl-2-iodopropionate<sup>177</sup>, ethyl iodoacetate<sup>186</sup>, ethyl 2-iodopropionate<sup>183</sup> and iodoform<sup>187</sup>. As one of the simplest alkyl iodides, iodoform has been explored in more detail in ITP reactions<sup>188</sup>.

The difference between ITP and RITP is that RITP generates the iodine-containing transfer agent *in situ* (in the reaction mixture) through the use of molecular iodine (Scheme 1.8<sup>173</sup>). Molecular iodine reacts with the generated radicals to form initiator or polymer molecules with reversibly capped iodo chain ends that are capable of reversible chain transfer.<sup>189</sup> RITP, first

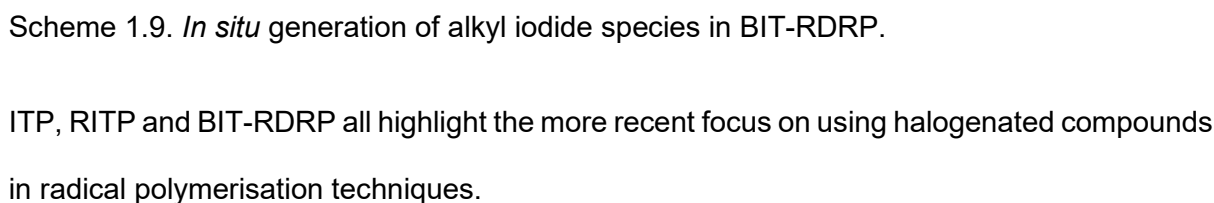
$$\begin{array}{c}
 \text{A}_2 \longrightarrow 2\text{A}^\bullet \\
 \text{Monomer (M)} \searrow \\
 \begin{array}{l}
 \xrightarrow{\text{I}_2} 2\text{A—I} \\
 \xrightarrow{\text{I}_2} 2\text{P}_n^\bullet \xrightarrow{\text{I}_2} 2\text{P}_n\text{—I}
 \end{array}
 \end{array}$$
  

$$\text{P}_n^\bullet + \text{A—I} \rightleftharpoons \text{P}_n\text{—I} + \text{A}^\bullet$$


  
 $\text{P}_n \rightarrow \text{M} \rightarrow \text{P}_n$



In a similar way, bromine-iodine transformation reversible-deactivation radical polymerisation (BIT-RDRP), an emerging technique that was first described in 2017<sup>191,192</sup>, also generates the alkyl iodine reagent *in situ* in the polymerisation system. However, in this case an alkyl bromide (commonly those used as ATRP initiators) undergoes a reaction with sodium iodide to form an alkyl iodide capable of reversibly capping the polymer chain end<sup>191–194</sup> (Scheme 1.9).

$$\text{R-Br} \xrightleftharpoons{\text{NaI}} \text{R-I} + \text{NaBr}$$


### 1.5.2 Halogens as leaving groups

The main reason for alkyl halides and their related compounds being of interest for their potential in chain transfer reactions is due to the carbon-halogen bond dissociation enthalpies

H.J.Hutchins, PhD Thesis, Aston University, 2021. 44



as seen in Table 1.1<sup>195</sup>. This property renders halogens as good leaving groups. Additionally, the halide radical stability increases in the following order  $F^{\bullet} < Cl^{\bullet} < Br^{\bullet} < I^{\bullet}$  due to the corresponding decrease in electronegativity of the atoms as group VII is descended<sup>195</sup>. The mean bond dissociation enthalpy of a carbon-iodine bond is the weakest of those described in Table 1.1, suggesting why ITP was a successful polymerisation route for study. However, typical carbon-chlorine and carbon-bromine bond dissociation enthalpies are also relatively weak; especially when compared to a carbon-hydrogen bond. This suggests that molecules containing carbon-chlorine and carbon-bromine bonds could also be tailored for polymerisation reactions, similar to the aforementioned RAFT CTAs (Section 1.4.5). On the other hand, carbon-fluorine bonds are stronger than carbon-hydrogen bonds (see Table 1.1) and will not be discussed further regarding potential chain transfer capabilities.

An additional benefit of using halogenated compounds (where the halogen is chlorine, bromine or iodine) is the fact that carbon-halogen bonds are known to be reversible; after initially reacting with a polymer radical, they can be cleaved from the polymer chain end to reproduce reactive radicals capable of reinitiating polymerisation reactions<sup>196</sup>. This is an ideal property in the synthesis of macro-initiators for block copolymer production; where a macro-initiator is a polymer that contains a functional group capable of initiating polymerisation<sup>197</sup>.

Table 1.1. Summary of mean bond enthalpies for various C-X bonds where X is a carbon, hydrogen or halogen atom. Modified from Burrows *et al.*<sup>195</sup>.

Bond	Mean bond enthalpy (kJ mol <sup>-1</sup> )
C-C	347
C-H	412
C-F	467
C-Cl	346
C-Br	290
C-I	228

### 1.5.3 Other uses of halogens in polymerisation reactions

As previously mentioned, alkyl halides are popularly employed as initiators in ATRP reactions<sup>174,198</sup>, with some also being able to act as a CTA; such as the aforementioned iodoform. In addition to this, both carbon tetrachloride and carbon tetrabromide have been utilised as CTAs in controlled radical polymerisations<sup>199,200</sup>. Flory states that both molecules have a greater susceptibility to act as CTAs in comparison to a variety of alkyl halides investigated. This is evidenced through the experimentally determined chain transfer constants of these compounds for the polymerisation of styrene, as seen in Table 1.2<sup>201</sup>. Flory<sup>201</sup> showed that carbon tetrabromide demonstrates the largest chain transfer constant of the compounds investigated in this study. In addition, iodoform has been utilised in ITP and chloroform, although used most frequently as a solvent, has demonstrated chain transfer capabilities (Table 1.2<sup>201</sup>). Therefore, a logical suggestion for another useful halogenated compound, with potentially useful chain transfer capabilities, is bromoform. Advantages of using bromoform in the synthesis of block copolymers are discussed in section 1.5.4.

Table 1.2. Summary of the chain transfer constants of halogenated substances investigated in the polymerisation of styrene. Modified from Flory<sup>201</sup>.

Chain transfer agent	Experimentally determined chain transfer constants ( $C_s \times 10^4$ )	
	At 60 °C	At 100 °C
carbon tetrachloride	90	180
carbon tetrabromide	13600	23500
tetrachloroethane	-	18
ethylene dichloride	0.32	-
ethylene dibromide	-	6.6
chloroform	0.5	-
methylene chloride	0.15	-
<i>n</i> -butyl chloride	0.04	0.37
<i>n</i> -butyl bromide	0.06	0.35
<i>n</i> -butyl iodide	1.85	5.5

## 1.5.4 Bromoform

### 1.5.4.1 Properties

As previously discussed, bromoform has been alluded to as a useful molecule to be exploited for potential chain transfer capabilities, valuable in radical polymerisation reactions. Bromoform itself contains desired reversibly cleavable C-Br bonds. Of particular interest is that the C-Br bonds in bromoform are known to undergo photodissociation upon exposure to UV light (photodissociation of bromoform has been discussed at 193<sup>202</sup>, 234<sup>203</sup>, 248<sup>204</sup>, 266<sup>205</sup>, 267<sup>203</sup> and between 266-324<sup>206</sup> nm); primarily (but not wholly) into  $\text{Br}_2\text{HC}^\bullet$  and  $\text{Br}^\bullet$  radicals. This could therefore be potentially useful for producing bromine-terminated polymers (referred to from this point forward as macro-initiators) that can be used in further reactions to form block copolymers. The other potential dissociation pathway of bromoform is hydrogen transfer whereby the hydrogen atom in bromoform is involved in a transfer reaction with a polymer which would inevitably result in the formation of dead polymer chains. The likelihood of bromine transfer occurring is dependent on two factors; the bond stability of C-Br *versus* C-H and the radical stability of  $\text{Br}_2\text{HC}^\bullet$  *versus*  $\text{Br}_3\text{C}^\bullet$  (where  $\text{Br}_3\text{C}^\bullet$  is the radical that would form should hydrogen transfer occur)<sup>204</sup>. As previously mentioned, the C-Br bond is weaker than the C-H bond (see Table 1.2) in bromoform, therefore the dissociation would favour Br over H transfer based on bond strength alone. However, H transfer could still be present due to the higher stability of  $\text{Br}_3\text{C}^\bullet$  over  $\text{Br}_2\text{HC}^\bullet$ . It is therefore reasonable to assume that both Br and H transfer will occur in a competitive manner; as discussed later (see Section 1.5.4.2).

Somewhat more importantly for the synthesis of biomedical materials, bromoform is partially water soluble; 3.0 g/L at 20 °C<sup>2,3</sup>, 3.0 g/L at 25 °C<sup>3,4</sup> and 3.2 g/L at 30 °C<sup>2,3</sup>. This opens the pathway for block copolymer synthesis in aqueous media. This has multiple benefits, not only for the synthesis of polymers that could be used in the body but also for the environmental impact; as water can replace the use of toxic organic solvents. Additionally, using water instead of organic solvents results in reduced costs for the overall process. However, it should

be noted that bromoform itself is acutely toxic<sup>2</sup> and any unreacted bromoform should be appropriately removed from any products before use.

Finally, when compared to available RAFT CTAs, bromoform is a more cost-effective alternative that could be used in the synthesis of block copolymers. This has been demonstrated in the success of iodoform, molecular iodine and alkyl bromides in the aforementioned ITP, RITP and BIT-RDRP reactions. Whilst iodoform has successfully demonstrated chain transfer capabilities it has not been considered for the study discussed herein due to its extremely limited water solubility; 0.12g/L at 25 °C<sup>3</sup>.

#### 1.5.4.2 Previous studies

Bromine-based transfer agents have been discussed in a small number of polymerisation reactions within the literature, dating back to the 1950s<sup>207–209</sup>. The initial work of Dunn *et al.*<sup>209</sup> discusses the use of bromotrichloromethane and carbon tetrabromide (Figure 1.4) in the preparation of poly(styrene)-*block*-poly(methyl methacrylate) [PS-*b*-PMMA] copolymers.

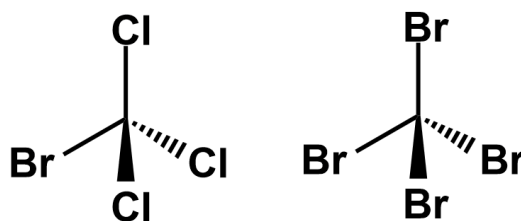


Figure 1.4. Chemical structures of bromotrichloromethane (left) and carbon tetrabromide (right).

Claims were made that a starting block of polystyrene (PS) with a terminal C-Br bond (a PS macro-initiator) was synthesised and used in a secondary reaction to produce the PS-*b*-PMMA copolymer. Both UV and thermal conditions were investigated to determine the effect of the brominated compounds on the rate of homopolymerisation of PS and ability to synthesise PS-*b*-PMMA. However, this is claimed only to have been investigated to 10% monomer conversion. Additionally, potential competing side reactions resulting in the formation of branched polymers, as well as block copolymers, are discussed. Whilst this investigation, for

its time, presented promising results, the discussion and conclusions drawn were limited by the available analytical techniques of the 1950s. Carbon tetrabromide has been further explored for its chain transfer capabilities and is known to have a high chain transfer constant in free radical polymerisations<sup>210</sup>. However, the pertinent limitation of carbon tetrabromide for the work herein is its restricted water solubility (0.24 g/L at 30 °C<sup>3</sup>); resulting in reactions that would have to be conducted in more harmful organic solvents.

Based on the work of Dunn *et al.*, Miller investigated graft<sup>207</sup> and block<sup>208</sup> polymers using acrylamide, acrylonitrile and acrylic acid monomers. In the graft polymerisation route, Miller reported the photopolymerisation of acrylamide and acrylonitrile in the presence of  $\alpha$ -chloroacrylonitrile for the purpose of synthesising a homopolymer with a labile C-Cl bond. Expanding on this, Miller reported the block copolymer synthesis of acrylonitrile and acrylic acid with acrylamide. Monobromoethane, dibromomethane and bromoform were investigated for their chain transfer capabilities, again, using photopolymerisation. Additionally, random copolymers of these monomer combinations were also synthesised to compare the properties with the block copolymers. It was concluded that monobromoethane and dibromomethane either did not show, or took extended periods of time to reveal, Br atom removal. In contrast, bromoform did present chain transfer capabilities; particularly when acrylamide was added as the second block. However, it is unclear from this work whether bromoform is behaving as a photoinitiator in the initial homopolymerisations of the acrylonitrile and acrylic acid. In each case, only bromoform and monomer (and in some cases a solvent) were added to the system before being subjected to UV irradiation. Another dispute in this work is that the precipitation methods for isolating the block copolymers appeared to yield the same block ratio no matter what the initial target ratio was, which is most likely due to fractionation in the precipitation stage. The intrinsic viscosity and softening points of the block and random copolymers were compared during this study to values for mixtures of the two homopolymers. Like the work of Dunn *et al.*, this study is limited by the access and availability of analytical techniques of that

time. Today, there is a broader range of conventional analytical techniques that can be exploited to better determine the success of block copolymer synthesis.

In 1983, a patent by Wu *et al.*<sup>211</sup> reported the use of this bromoform-assisted copolymerisation technique in the formation of 2-acrylamido-2-methylpropane sulfonic acid (AMPS) and acrylamide block copolymers for use in oil recovery from water. However, there is little discussion or clarity on the role of bromoform as a photoinitiator or chain transfer agent, and the process is only a minor part of the overall discussion.

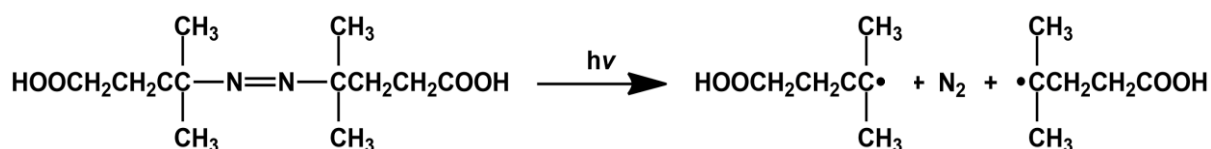
More recently, Thananukul *et al.*<sup>212</sup> reported the use of bromoform in the synthesis of polyacrylamide (PAM) homopolymer. In this investigation, the focus was on determining the role of bromoform; its ability to behave as a photoinitiator or chain transfer agent and the effect of bromoform concentration on the rate of reaction. In this work, UV radiation was used to dissociate bromoform and 4,4-azobiscyanovaleric acid (ACPA) photoinitiator. Additionally, control reactions were conducted with no ACPA present. The findings of this work concluded that under the described conditions, bromoform does not behave as a photoinitiator during the homopolymerisation; contradictory to some of the previous findings with other monomer systems that have been discussed. Multiple concentrations of bromoform were investigated and it was concluded that bromoform presents chain transfer capabilities without having a significant effect on the overall rate of the reaction. Instead, the existence of chain transfer is claimed due to the observed molar mass regulation of PAM at different bromoform concentrations (as measured by viscometry). It is implied from this research that although hydrogen transfer from bromoform to the polymer chain can occur it is likely that bromine transfer is more prevalent. Therefore, the possibility exists to use this method in the synthesis of block copolymers.

Whilst literature reports concerning bromoform, and its chain transfer ability, are limited, the foundation of this work appears promising. The work herein significantly advances this research, with the aim of aqueous-based block copolymer synthesis.

## 1.6 Initiators

A high proportion of the literature evaluated in this report has focused on the use of conventional redox<sup>213,214</sup> (a reduction-oxidation system used to generate radicals<sup>215,216</sup>) and thermal initiators, such as 2,2'-azobis(isobutyronitrile) (AIBN<sup>148</sup>), within the various polymerisation techniques<sup>43,96,100,187</sup>. However, the system discussed herein describes photopolymerisation and utilises a photoinitiator, namely ACPA. As aforementioned, Miller<sup>207</sup> suggested that bromoform itself can behave as a photoinitiator; as no other form of initiator are used in his series of reactions yet homopolymer and apparent block copolymer are formed. This is contradicted by the findings of Thananukul *et al.*<sup>212</sup> whereby homopolymerisation of acrylamide does not proceed without photoinitiator (ACPA) being present in the system. Therefore, as part of this investigation, whilst employing bromoform for the purpose of synthesising block copolymers, it is of interest to further evidence whether bromoform also has initiating capabilities.

ACPA has been selected as the photoinitiator for this investigation to enable direct comparison with the work of Thananukul *et al.*<sup>212</sup>. Additionally, ACPA has been successfully employed as a photoinitiator in controlled radical polymerisations with a wide variety of monomers; including, but not limited to, acrylamides<sup>212</sup>, acrylates<sup>217</sup>, methacrylates<sup>218</sup>, styrenes<sup>119,177</sup>, acrylic acids<sup>219</sup> and fluorinated<sup>220</sup> structures. ACPA breaks down under UV irradiation (at approximately 350 nm<sup>221</sup>) to form two radicals capable of initiating polymerisation (see Scheme 1.10). Crucial to this research, ACPA is water soluble and allows for aqueous-based polymerisation reactions to be conducted.



Scheme 1.10. Mechanism showing the formation of two initiating radicals and nitrogen from ACPA using UV irradiation.

As previously mentioned, acrylamide monomers have been investigated in controlled radical polymerisation reactions involving UV initiators in water<sup>212,222</sup>. Together with the broad scope of literature discussing the synthesis of acrylamide-based polymers with thermal<sup>223 224 225</sup> and redox<sup>226</sup> initiators this indicates that acrylamide monomers are a versatile class of reagents to study under these relatively unexplored conditions. Additionally, acrylamide monomers have been utilised in block copolymer synthesis for a range of applications including; poly(2-methoxyethylacrylate-co-dimethylacrylamide), poly(2-methoxyethylacrylate-co-acrylamide)<sup>227</sup> and polyacrylamide-grafted dextran polymer hydrogels (water swollen polymer networks) in targeted drug delivery<sup>228</sup> and crosslinked polyacrylamide/collagen networks as wound dressings<sup>229</sup>.

## 1.7 Monomers

As previously mentioned, acrylamide-based monomers are considered versatile reagents in the synthesis of polymeric materials. Acrylamides (Figure 1.5<sup>230</sup>) and their associated polymers are hydrophilic as they are able to interact with water molecules via hydrogen bonding<sup>231,232</sup>. This is a distinct trait of many polymeric hydrogels which have been used in the biomedical industry to produce useful products such as contact lenses, wound dressings and tissue engineering scaffolds<sup>233</sup>. Additionally, acrylamide monomers are known for their high initial rates of propagation ( $k_p$ )<sup>234–236</sup> which results in a series of reactions that can achieve high monomer conversions in a reasonable timeframe. For these reasons, acrylamides have been chosen as exemplar monomers to study the scope, potential and limitations of bromoform-assisted free-radical polymerisations.

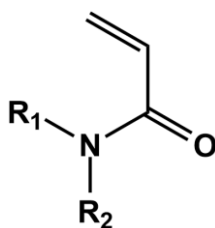


Figure 1.5. General structure of acrylamide monomers showing the vinyl ( $\text{CH}_2\text{CH}-$ ), carbonyl ( $\text{C}=\text{O}$ ) and nitrogen ( $\text{NR}_2$ ) functionalities.



*N*-Isopropylacrylamide (NIPAM) is of growing interest in the biomedical polymer industry, predominantly regarding the synthesis of block copolymers containing poly(*N*-isopropylacrylamide) [PNIPAM] (Figure 1.6<sup>237</sup>). A variety of synthetic routes for PNIPAM have been discussed in the literature including, but not being limited to, ATRP<sup>238,239</sup>, NMP<sup>240,241</sup>, RAFT<sup>238,242,243</sup> and RITP<sup>244</sup>. Various copolymers incorporating NIPAM have been synthesised using, for example, ethylene glycol<sup>245,246</sup>, methacrylic acid<sup>246</sup>,  $\epsilon$ -caprolactone<sup>245</sup>, ethylene oxide<sup>247,248</sup>, 2-(dimethylamino)ethyl methacrylate<sup>249</sup> and styrene<sup>250</sup>.

The key property of PNIPAM, of interest in biomedical applications, is its well-known reversible tuneable thermo-responsivity close to body temperature<sup>251,252</sup>. PNIPAM exhibits a lower critical solution temperature (LCST) whereby its properties change so that it becomes hydrophobic above 32 °C<sup>1</sup>. This transition is known to be sensitive, reversible and reproducible and is driven by the rearrangement of water molecules around the isopropyl group<sup>253</sup>. Below the LCST the water molecules are physically bound to the hydrophilic amide groups and arranged in such a way that they form a shield around the hydrophobic groups throughout the polymer<sup>254</sup>. This shield is often referred to as a hydrophobic hydration shell and is enthalpically favoured (whilst being entropically disfavoured) due to the water molecules forming stronger and longer-lived hydrogen bonds in this arrangement compared to the bulk<sup>255–258</sup>.



Figure 1.6. Chemical structures of *N*-isopropylacrylamide (left) and poly(*N*-isopropylacrylamide) (right); where *n* represents the number of repeat units of NIPAM within the polymer chain.

All of the reagents, described so far in this study, including; bromoform, ACPA and NIPAM, are soluble in water. Consequently, incorporating a hydrophobic comonomer would cause

constraints; resulting in an organic solvent being needed for the synthesis<sup>259</sup> unless emulsion conditions are used<sup>260–262</sup>. Therefore, in this study, a comonomer that incorporates hydrophilic character has been selected; more specifically *N,N*-dimethylacrylamide (DMA) (see Figure 1.7). Similarly to NIPAM, DMA has been investigated thoroughly with regards to controlled polymerisation methods. DMA is known to be versatile to both synthetic route and comonomer compatibility; with examples in the literature including ATRP<sup>263,264</sup>, NMP<sup>265</sup> and RAFT<sup>129</sup> copolymerisation of DMA with methyl methacrylate<sup>266–268</sup>, styrene<sup>269</sup>, butadiene<sup>269</sup>, ethylene oxide<sup>263</sup>, 2-hydroxyethyl methacrylate<sup>270</sup>, acrylic acid<sup>268</sup> and cellulose<sup>264</sup>. Additionally, DMA has successfully been incorporated into materials for use in cleaning of waste water<sup>271</sup>, shape memory hydrogels<sup>272</sup>, medicinal diagnostics<sup>273</sup> and pharmaceutical<sup>265</sup> applications, to name a few. Finally, DMA is known to be suitable for use in photoinitiated polymerisation reactions<sup>274,275</sup>. This information suggests that DMA exhibits the required properties to be incorporated into the aqueous-based bromoform-assisted block copolymer synthesis route, explored in this investigation, to produce commercially-relevant materials.

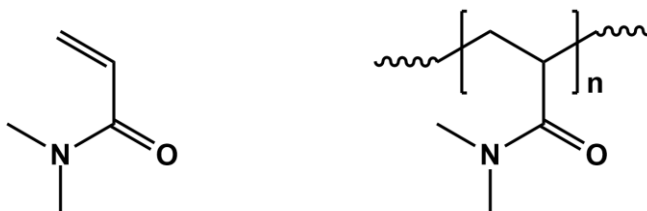


Figure 1.7. Chemical structures of *N,N*-dimethylacrylamide (left) and poly(*N,N*-dimethylacrylamide) [PDMA] (right); where *n* represents the number of repeat units of DMA in the polymer chain.

## 1.8 Block copolymers

### 1.8.1 Block sequence

Whilst controlled radical polymerisation methods have been praised for their suitability in the synthesis of designer polymers they are not without their inadequacies. Apparent in the literature is the discussion over the importance of monomer sequence in block copolymer

formation, particularly in RAFT. In simpler terms, the formation of block copolymers is a sequential process and the order in which the blocks are formed is important. The dependency of which block should be synthesised first is heavily reliant on the following factors; (1) the intermediate radical stability of the macroradical (or macro-CTA), (2) the relative radical leaving group ability and (3) the reactivity of the macroradical species towards the sequential monomer<sup>276</sup> (cross propagation<sup>174</sup>).

The fragmentation of the macroradical species favours the better leaving group<sup>164</sup>. For the described monomers leaving group ability decreases in the following order: methacrylates ~ methacrylamides >> styrenics ~ acrylates ~ acrylamides ~ *N*-vinylheteroaromatics > vinyl amides > vinyl esters<sup>277</sup>. This has been further evidenced in the formation of poly(methyl methacrylate)-*block*-poly(styrene) copolymers, as styrenics are poorer leaving groups than methacrylates and so poly(methyl methacrylate) (PMMA) must be synthesised first<sup>169,278</sup>.

Regarding the NIPAM and DMA block copolymers studied herein it is therefore useful to identify which monomer would form the more stable intermediate radical, provide the better leaving group and be more reactive. However, there is little available information in the literature. It is suggested that DMA is the more reactive monomer (in aqueous systems), therefore provides the better leaving group and would likely form the more stable intermediate radical<sup>279</sup>. Structurally, the key difference between DMA and NIPAM is that DMA is a tertiary amide whereas NIPAM is a secondary amide. When looking at the statistical copolymerisation of NIPAM and DMA, experimentally determined reactivity ratios, the preference of a chain end radical to react with monomer 1 (continuing homopolymerisation) or monomer 2 (forming a copolymer<sup>280</sup>) of the monomers is a prudent place to start. It was concluded that NIPAM has a reactivity ratio of 0.838 whereas DMA has a reactivity ratio of 1.105; this means that DMA will prefer to homopolymerise first before cross propagating with NIPAM suggesting gradient or block copolymers would be formed<sup>281</sup>. Whilst this information is appropriate for a statistical copolymer synthetic route, it could also be applicable to block copolymer synthesis. If radicals capable of initiating new polymer chains are present, during the addition of the second

monomer (as seen in RAFT<sup>115</sup>), this could produce a mixture of homopolymers rather than a block copolymer if the sequence of addition is not appropriate. For example, if DMA is added as the second block its preference to homopolymerise over cross propagation could result in PDMA homopolymers being formed over the desired block copolymers. On the other hand if the NIPAM is added in the second step its reactivity ratio suggests it will cross propagate with the PDMA macro-initiator resulting in block copolymers being successfully formed. However, this is not definitive evidence and does not eliminate the use of a PNIPAM macro-initiator for successful block copolymer syntheses. It could, however, relate to the overall reaction times or conditions required to successfully incorporate DMA as the second block in the copolymer; due to the implied lower reactivity of the PNIPAM macro-initiator. This is further backed up in the previous NIPAM and DMA block copolymer studies that have been conducted; where either a mono or difunctional DMA macroinitiator is used as the first block<sup>279</sup>.

Limitations of reactivity ratio data are currently debated with many arguments for and against their reliability. Many sources state that temperature, pressure and solvent have little to no effect on the determined reactivity ratios<sup>282</sup>. In contrast, other sources have determined that parameters such as solvent can result in changes of the reactivity ratios<sup>283</sup>. Additionally, experimental and analytical difficulties, estimation procedures and variability in mathematical models used to determine reactivity ratios makes it difficult to use these values as anything more than a relative estimation<sup>276</sup>. The reactivity ratios discussed for NIPAM and DMA presently are based on a RAFT copolymerisation study, using thermal initiator AIBN, a CTA and DMF as the solvent<sup>281</sup>, different to the conditions investigated herein.

### **1.8.2 Photoiniferter polymerisation**

To overcome monomer sequence selectivity, observed in controlled radical polymerisation methods (particularly RAFT) as discussed in Section 1.8.1, a concept known as initiator-transfer agent-terminator or 'iniferter' polymerisation has been employed<sup>149</sup>. Similarly to RAFT CTAs, iniferters are molecules that produce chain end functionalities capable of being reinitiated for the synthesis of polymers with varied architectures such as; block, star, graft

and crosslinked materials. The key difference to traditional RAFT polymerisation is that the iniferter behaves simultaneously as an initiator, transfer agent and terminator whereas in RAFT, a separate initiator is required.

Of interest to this research is photoiniferter polymerisation, which exploits the photodissociation of weak A-B bonds. Interestingly, key RAFT agents with thiocarbonylthio groups such as trithiocarbonate<sup>284,285</sup>, dithiocarbamate<sup>149,277,286</sup> and xanthate<sup>277</sup> structures, have been utilised as photoiniferters due to the C-S bond present being susceptible to dissociation upon UV irradiation. This is not dissimilar to the process discussed herein utilising the photodissociation of the C-Br bond in bromoform as a transfer agent. The added benefit of using traditional RAFT agents as photoiniferters is that the radicals produced, upon reinitiation by exposure to light, still allow for control over the reaction via degenerative chain transfer and reversible deactivation mechanisms<sup>286</sup>. This method of radical formation avoids generating low molar mass radicals that would usually occur from the free radical initiators traditionally used in RAFT. Eliminating these low molar mass radicals further prevents termination reactions by radical coupling.<sup>164</sup>

Further investigations have determined that monomer sequence in block copolymer formation can be inverted, during photoiniferter polymerisation, to produce polymers of reverse block order than those traditionally favoured in other RDRP techniques. This is due to the photolysis of C-S bonds forming leaving group radicals that are not produced by the traditional RAFT mechanism<sup>46,285,287,288</sup>. The photodissociation of the thiocarbonylthio function at the polymer chain end allows for efficient reinitiation of the species towards a usually unfavourable block sequence. This has successfully been observed for the formation of DMA and methyl methacrylate block copolymers. Typically, methyl methacrylate presents the better leaving group and it has been observed that in DMA copolymerisation PMMA should be synthesised as the first block producing the subsequent macro-CTA. The PMMA macro-CTA is the more stable radical former compared to the PDMA macro-CTA and goes on to produce poly(methyl methacrylate)-*block*-poly(*N,N*-dimethylacrylamide) copolymers sufficiently using RAFT. In the

case of PDMA macro-CTAs produced via RAFT, only a mixture of homopolymers or extremely slow chain extension of the PDMA macro-CTA with comonomer, at high conversion, can be achieved. However, utilising the photoiniferter method, successful inversion of the monomer sequence can be achieved; resulting more easily in the formation of poly(*N,N*-dimethylacrylamide)-*block*-poly(methyl methacrylate) from a variety of thiocarbonylthio iniferters<sup>277</sup>.

The literature discussed in this section has exposed the issue of the selectivity towards the sequence of monomer addition in controlled radical polymerisations. It has highlighted the fact that whilst reactivity ratios (discussed in Section 1.8.1) are available in the literature, there is little agreement on how the reaction conditions (such as temperature, solvent and pressure) affect them<sup>276,279,281–283</sup>. Furthermore, reactivity ratios are more widely studied regarding the formation of statistical copolymers as opposed to block copolymers. Existing literature leans towards the synthesis of NIPAM and DMA block copolymers using PDMA as the more favoured first block and consequent macro-initiator. The interest in photoiniferter polymerisation stems from the fact that bromoform is being investigated for its potential chain transfer ability under UV conditions in this study. This is an identical property found in photoiniferter polymerisation as the CTAs and consequent macro-CTAs previously discussed can dissociate using UV light to synthesise block copolymers irrespective of the monomer order selectivity. Hence, there is the possibility that by using bromoform, and its photodissociation, block copolymers can be formed regardless of the sequence in which the monomer is added.

## 1.9 Aims

Polymers are globally recognised as versatile materials used in a wide variety of applications from the formation of plastics to drug delivery systems. The polymer industry is becoming increasingly focused on research that enables the design of, and ability to fine-tune, polymer structures to have specific properties for targeted use. Advances in controlled radical polymerisation techniques have led to the synthesis of polymers with controllable molar

masses and dispersities as well as desirable chain compositions, functionalities and architectures. This is particularly useful for the synthesis of commercially-relevant block copolymers.

The overarching objective of this research is to develop a new, inexpensive, industrially viable polymerisation technique to synthesise block copolymers. This is achieved using bromoform as an inexpensive reagent to mediate chain growth and chain end functionality. To achieve this, the scope and limitations of a bromoform-assisted technique must be investigated before potentially useful materials can be produced. Contradictory reports in the literature imply that bromoform can behave as both an initiator and a chain transfer agent in polymerisations.<sup>207,208,212</sup> Therefore, investigation is required to further comment on the role of bromoform in these reactions; specifically to this project the homo- and co- polymerisations of *N*-isopropylacrylamide and *N,N*-dimethylacrylamide. These monomers have been chosen as exemplars due to their solubility in aqueous media and utility in a range of applications. One advantage of this method is the highly desirable partial water miscibility of bromoform; resulting in polymers that can be prepared in aqueous media. This removes the need for toxic or harmful organic solvents in the synthesis and is key to the development of greener block copolymer synthetic routes. Additionally, the reagents used in this investigation (including ACPA photoinitiator) are stable, inexpensive, commercially available and, importantly, contain no metal or sulfur. Moreover, the water soluble monomers *N*-isopropylacrylamide and *N,N*-dimethylacrylamide have already been used for the production of commercially-relevant materials. Therefore, this study demonstrates the potential for a simple, inexpensive route to functional block copolymers.

To summarise, the aims of this PhD project are:

- To determine a viable synthetic route to produce block copolymers via bromoform-assisted free radical polymerisation.
- To understand the scope and limitations of this new technique in the synthesis of macro-initiators and amphiphilic block copolymers.
- To use bromoform-assisted polymerisation to synthesise useful materials for targeted applications.



## **Chapter 2. Materials and Experimental Methods**

## 2.1 Materials

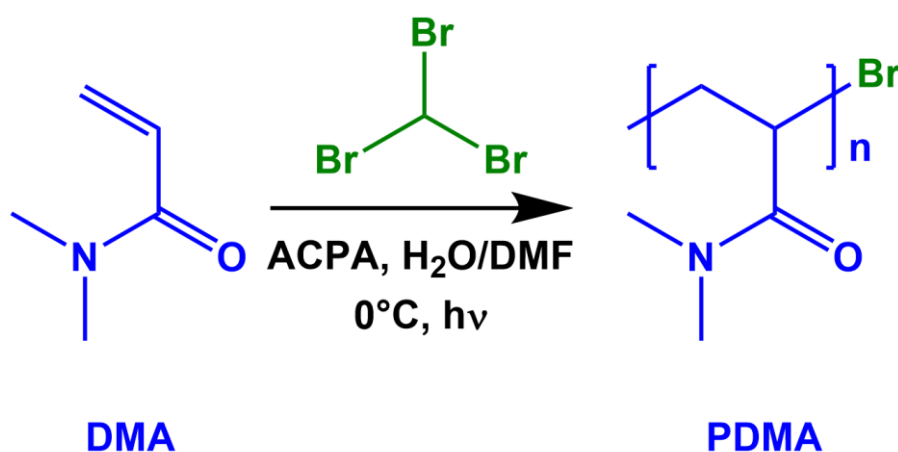
4,4-Azobiscyanovaleric acid (ACPA,  $\geq 98\%$ ), bromoform ( $\text{CHBr}_3$ , 96 % stabilised with ethanol), *N*-isopropylacrylamide (NIPAM, 97 %) and *N,N*-dimethylacrylamide (DMA, 99 %) were purchased from Sigma Aldrich and used without further purification. Chloroform-*d* ( $\text{CDCl}_3$ , 99 %) and deuterium oxide ( $\text{D}_2\text{O}$ , 99.9 %) were purchased from Goss Scientific and used as supplied. Diethyl ether (DEE, laboratory reagent grade), dimethyl formamide (DMF, high performance liquid chromatography (HPLC)-grade and laboratory reagent grade), methanol (MeOH, laboratory reagent grade), tetrahydrofuran (THF, laboratory reagent grade) and water ( $\text{H}_2\text{O}$ , HPLC-grade) were purchased from Fisher Scientific and used as supplied.

## 2.2 UV source

The ultraviolet (UV) light source was a Philips Solarium Model MD 1-15 lamp comprising four parallel 15 W fluorescent tubes that emitted UV light in the 315-400 nm wavelength range. The vertical distance between the UV light source and the surface of the solution was fixed at 10 cm.

## 2.3 Experimental Methods

### 2.3.1 Bromoform-assisted polymerisation of *N,N*-dimethylacrylamide



Scheme 2.1. Synthesis of poly(*N,N*-dimethylacrylamide) via bromoform-assisted polymerisation.

### 2.3.1.1 Bromoform-assisted synthesis of poly(*N,N*-dimethylacrylamide) [PDMA] in water

*N,N*-Dimethylacrylamide was polymerised via free radical photopolymerisation in deionised water using varying bromoform concentration (0.0, 0.5, 1.0 and 2.0 mol % with respect to *N,N*-dimethylacrylamide).

A typical experimental setup was as follows: A 50 mL round-bottomed flask was charged with 0.0565 g ACPA ( $2.02 \times 10^{-4}$  mol; 1.0 mol % relative to *N,N*-dimethylacrylamide monomer) and HPLC-grade water (25 mL) and stirred with heating (55 °C) for 1 hour to ensure full dissolution. After cooling to room temperature, bromoform ( $\text{CHBr}_3$ ;  $4.04 \times 10^{-4}$  mol; 2.0 mol % relative to *N,N*-dimethylacrylamide monomer) and 2.00 g DMA monomer (0.0202 mol) was added to the reaction flask which was then sealed with a rubber septum and parafilm. The clear solution was degassed via vacuum and nitrogen cycles over a period of 15 minutes before being placed into an ice bath for 20 minutes. The reaction flask and ice bath were then placed in an aluminium cabinet with magnetic stirring and irradiated with UV light from above for 60 minutes. An increase in solution viscosity was observed over the course of the reaction. For kinetic studies, 0.1 mL of the reaction solution was removed periodically prior to analysis via gel permeation chromatography (GPC) and  $^1\text{H}$  nuclear magnetic resonance (NMR) spectroscopy. The resulting PDMA was isolated by removing the water via lyophilisation and redissolving in methanol before dropwise precipitation into a five-fold excess of chilled diethyl ether. The supernatant was decanted and the PDMA was then washed with the same solvent. The homopolymer precipitate was then dried in a vacuum oven to remove excess solvent (175 mbar, 40 °C) until constant weight was achieved to produce the final white solid.

The reaction, using 2 mol% bromoform, was also scaled up to 20 g (DMA monomer) to synthesise the starting block for both the one-pot and two-step synthesis of PDMA-*b*-PNIPAM. In this case the reaction was irradiated with UV light for a period of 2 hours and 45 minutes to achieve monomer conversion of  $\geq 91\%$  as determined by  $^1\text{H}$  NMR (See Chapter 3).

**Poly(*N,N*-dimethylacrylamide) 0 mol % bromoform:**

$M_n = 246.7 \text{ kg mol}^{-1}$   $\bar{D} = 3.4$   $^1\text{H NMR}$  (300 MHz,  $\text{D}_2\text{O}$ ,  $\delta$  in ppm) 1.53 (br, 2H), 2.52 (br, 1H), 2.81 (br, 6H)

**Poly(*N,N*-dimethylacrylamide) 0.5 mol % bromoform:**

$M_n = 294.8 \text{ kg mol}^{-1}$   $\bar{D} = 2.8$   $^1\text{H NMR}$  (300 MHz,  $\text{D}_2\text{O}$ ,  $\delta$  in ppm) 1.53 (br, 2H), 2.51 (br, 1H), 2.81 (br, 6H)

**Poly(*N,N*-dimethylacrylamide) 1.0 mol % bromoform:**

$M_n = 271.2 \text{ kg mol}^{-1}$   $\bar{D} = 2.8$   $^1\text{H NMR}$  (300 MHz,  $\text{D}_2\text{O}$ ,  $\delta$  in ppm) 1.53 (br, 2H), 2.52 (br, 1H), 2.81 (br, 6H)

**Poly(*N,N*-dimethylacrylamide) 2.0 mol % bromoform:**

$M_n = 242.3 \text{ kg mol}^{-1}$   $\bar{D} = 3.5$   $^1\text{H NMR}$  (300 MHz,  $\text{D}_2\text{O}$ ,  $\delta$  in ppm) 1.54 (br, 2H), 2.51 (br, 1H), 2.81 (br, 6H)

**2.3.1.2 Bromoform-assisted synthesis of poly(*N,N*-dimethylacrylamide) in DMF**

*N,N*-Dimethylacrylamide was polymerised via radical photopolymerisation in DMF using varying bromoform concentration (0.0, 0.5, 1.0 and 2.0 mol % with respect to *N,N*-dimethylacrylamide).

A typical experimental setup was as follows: A 50 mL round-bottomed flask was charged with 0.0565 g ACPA ( $2.02 \times 10^{-4}$  mol; 1.0 mol % relative to *N,N*-dimethylacrylamide monomer), bromoform ( $\text{CHBr}_3$ ;  $4.04 \times 10^{-4}$  mol; 2.0 mol % relative to *N,N*-dimethylacrylamide monomer), 2.00 g DMA monomer (0.0202 mol) and DMF (25 mL) before being sealed with a rubber septum and parafilm. The clear solution was degassed via vacuum and nitrogen cycles over a period of 15 minutes before being placed into an ice bath for 20 minutes. The reaction flask and ice bath were then placed in an aluminium cabinet with magnetic stirring and irradiated

with UV light from above for 6 hours. The ice bath was replenished every 2 hours. For kinetic studies, 0.1 mL of the reaction solution was removed periodically prior to analysis via GPC and  $^1\text{H}$  NMR spectroscopy. The resulting PDMA was isolated by concentrating the DMF solution before dropwise precipitation into a five-fold excess of chilled diethyl ether. The supernatant was then decanted and the PDMA was then washed with the same solvent. The homopolymer precipitate was then dried in a vacuum oven to remove excess solvent (40 mbar, 40 °C) until constant weight was achieved to produce the final white solid.

**Poly(*N,N*-dimethylacrylamide) 0 mol % bromoform:**

$M_n = 22.3 \text{ kg mol}^{-1}$   $\bar{D} = 2.9$   $^1\text{H}$  NMR (300 MHz,  $\text{CDCl}_3$ ,  $\delta$  in ppm) 1.69 (br, 2H), 2.66 (br, 1H), 2.92 (br, 6H)

**Poly(*N,N*-dimethylacrylamide) 0.5 mol % bromoform:**

$M_n = 23.1 \text{ kg mol}^{-1}$   $\bar{D} = 2.7$   $^1\text{H}$  NMR (300 MHz,  $\text{CDCl}_3$ ,  $\delta$  in ppm) 1.68 (br, 2H), 2.44 (br, 1H), 2.96 (br, 6H)

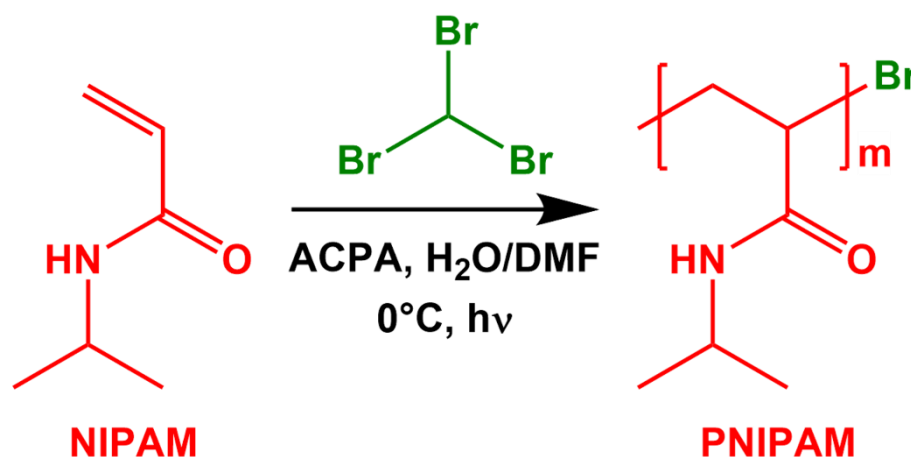
**Poly(*N,N*-dimethylacrylamide) 1.0 mol % bromoform:**

$M_n = 22.6 \text{ kg mol}^{-1}$   $\bar{D} = 2.8$   $^1\text{H}$  NMR (300 MHz,  $\text{CDCl}_3$ ,  $\delta$  in ppm) 1.68 (br, 2H), 2.71 (br, 1H), 2.95 (br, 6H)

**Poly(*N,N*-dimethylacrylamide) 2.0 mol % bromoform:**

$M_n = 22.2 \text{ kg mol}^{-1}$   $\bar{D} = 2.7$   $^1\text{H}$  NMR (300 MHz,  $\text{CDCl}_3$ ,  $\delta$  in ppm) 1.69 (br, 2H), 2.62 (br, 1H), 2.96 (br, 6H)

### 2.3.2 Bromoform-assisted polymerisation of *N*-isopropylacrylamide



Scheme 2.2. Synthesis of poly(*N*-isopropylacrylamide) via bromoform-assisted polymerisation.

#### 2.3.2.1 Bromoform-assisted synthesis of poly(*N*-isopropylacrylamide) [PNIPAM] in water

*N*-Isopropylacrylamide was polymerised via radical photopolymerisation in deionised water using varying bromoform concentration (0.0, 0.5, 1.0 and 2.0 mol % with respect to *N*-isopropylacrylamide).

A typical experimental setup was as follows: A 50 mL round-bottomed flask was charged with 0.0496 g ACPA ( $1.77 \times 10^{-4}$  mol; 1.0 mol % relative to *N*-isopropylacrylamide monomer) and HPLC-grade water (25 mL) and stirred with heating (55 °C) for 1 hour to ensure full dissolution. After cooling to room temperature, bromoform (CHBr<sub>3</sub>;  $3.53 \times 10^{-4}$  mol; 2.0 mol % relative to *N*-isopropylacrylamide monomer) and 2.00 g NIPAM monomer (0.0177 mol) was added to the reaction flask which was then sealed with a rubber septum and parafilm. The clear solution was degassed via vacuum and nitrogen cycles over a period of 15 minutes before being placed into an ice bath for 20 minutes. The reaction flask and ice bath was then placed in an aluminium cabinet with magnetic stirring and irradiated with UV light from above for 30 minutes. An increase in solution viscosity was observed over the course of the reaction. For kinetic studies, 0.1 mL of the reaction solution was removed periodically prior to analysis via

GPC and  $^1\text{H}$  NMR spectroscopy. The resulting PNIPAM was isolated by dropwise precipitation into a five-fold excess of warm (40 °C) HPLC-grade water. The supernatant was then decanted and the PNIPAM was then washed with the same solvent. Residual water was then removed using lyophilisation until constant weight was achieved to produce the final white solid.

**Poly(*N*-isopropylacrylamide) 0 mol % bromoform:**

$M_n = 521.1 \text{ kg mol}^{-1}$   $\bar{D} = 2.4$   $^1\text{H}$  NMR (300 MHz,  $\text{D}_2\text{O}$ ,  $\delta$  in ppm) 1.02 (br, 6H), 1.45 (br, 2H), 1.88 (br, 1H), 3.76 (br, 1H)

**Poly(*N*-isopropylacrylamide) 0.5 mol % bromoform:**

$M_n = 532.6 \text{ kg mol}^{-1}$   $\bar{D} = 2.2$   $^1\text{H}$  NMR (300 MHz,  $\text{D}_2\text{O}$ ,  $\delta$  in ppm) 1.02 (br, 6H), 1.46 (br, 2H), 1.88 (br, 1H), 3.76 (br, 1H)

**Poly(*N*-isopropylacrylamide) 1.0 mol % bromoform:**

$M_n = 535.2 \text{ kg mol}^{-1}$   $\bar{D} = 2.2$   $^1\text{H}$  NMR (300 MHz,  $\text{D}_2\text{O}$ ,  $\delta$  in ppm) 1.02 (br, 6H), 1.46 (br, 2H), 1.89 (br, 1H), 3.76 (br, 1H)

**Poly(*N*-isopropylacrylamide) 2.0 mol % bromoform:**

$M_n = 530.2 \text{ kg mol}^{-1}$   $\bar{D} = 2.2$   $^1\text{H}$  NMR (300 MHz,  $\text{D}_2\text{O}$ ,  $\delta$  in ppm) 1.02 (br, 6H), 1.45 (br, 2H), 1.89 (br, 1H), 3.78 (br, 1H)

**2.3.2.2 Bromoform-assisted synthesis of poly(*N*-isopropylacrylamide) in DMF**

*N*-Isopropylacrylamide was polymerised via radical photopolymerisation in DMF using varying bromoform concentration (0.0, 0.5, 1.0 and 2.0 mol % with respect to *N*-isopropylacrylamide).

A typical experimental setup was as follows: A 50 mL round-bottomed flask was charged with 0.0496 g ACPA ( $1.77 \times 10^{-4}$  mol; 1.0 mol % relative to *N*-isopropylacrylamide monomer) bromoform ( $\text{CHBr}_3$ ;  $3.53 \times 10^{-4}$  mol; 2.0 mol % relative to *N*-isopropylacrylamide monomer), 2.00 g NIPAM monomer (0.0177 mol) and DMF (25 mL) before being sealed with a rubber septum and parafilm. The clear solution was degassed via vacuum and nitrogen cycles over

a period of 15 minutes before being placed into an ice bath for 20 minutes. The reaction flask and ice bath was then placed in an aluminium cabinet with magnetic stirring and irradiated with UV light from above for 6 hours. The ice bath was replenished every 2 hours. For kinetic studies, 0.1 mL of the reaction solution was removed periodically prior to analysis via GPC and  $^1\text{H}$  NMR spectroscopy. The resulting PNIPAM was isolated by dropwise precipitation into a five-fold excess of warm (40 °C) HPLC-grade water. The supernatant was then decanted and the PNIPAM was then washed with the same solvent. The homopolymer precipitate was then dried in a vacuum oven to remove residual DMF solvent (40 mbar, 40 °C) and residual water was then removed using lyophilisation until constant weight was achieved to produce the final white solid.

**Poly(*N*-isopropylacrylamide) 0 mol % bromoform:**

$M_n = 27.2 \text{ kg mol}^{-1}$   $\bar{D} = 2.2$   $^1\text{H}$  NMR (300 MHz,  $\text{CDCl}_3$ ,  $\delta$  in ppm) 1.18 (br, 6H), 1.61 (br, 2H), 2.20 (br, 1H), 4.04 (br, 1H)

**Poly(*N*-isopropylacrylamide) 0.5 mol % bromoform:**

$M_n = 26.3 \text{ kg mol}^{-1}$   $\bar{D} = 2.2$   $^1\text{H}$  NMR (300 MHz,  $\text{CDCl}_3$ ,  $\delta$  in ppm) 1.17 (br, 6H), 1.67 (br, 2H), 2.18 (br, 1H), 4.04 (br, 1H)

**Poly(*N*-isopropylacrylamide) 1.0 mol % bromoform:**

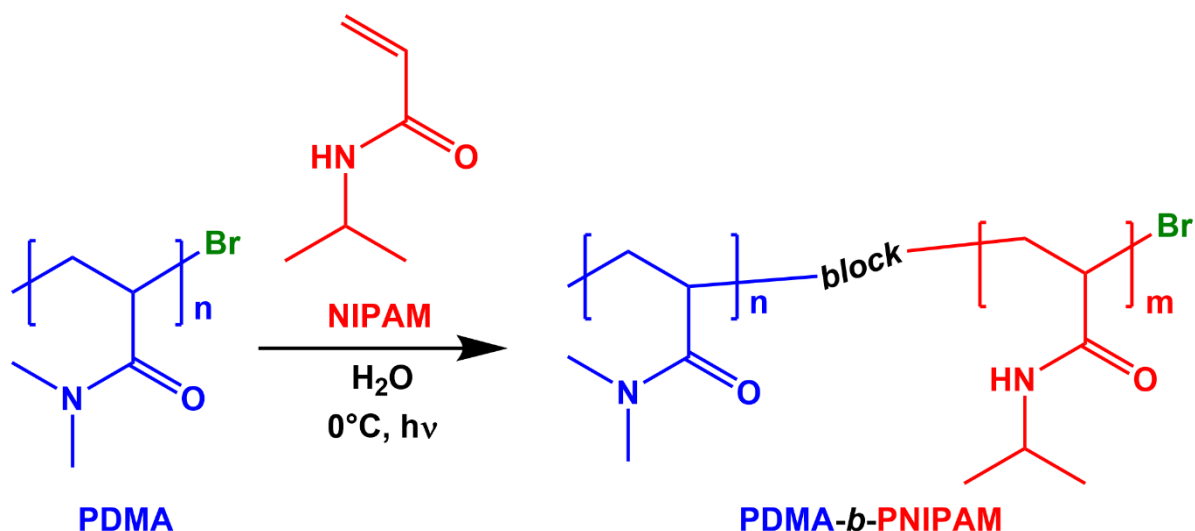
$M_n = 25.7 \text{ kg mol}^{-1}$   $\bar{D} = 2.2$   $^1\text{H}$  NMR (300 MHz,  $\text{CDCl}_3$ ,  $\delta$  in ppm) 1.18 (br, 6H), 1.60 (br, 2H), 1.96 (br, 1H), 4.04 (br, 1H)

**Poly(*N*-isopropylacrylamide) 2.0 mol % bromoform:**

$M_n = 23.8 \text{ kg mol}^{-1}$   $\bar{D} = 2.3$   $^1\text{H}$  NMR (300 MHz,  $\text{CDCl}_3$ ,  $\delta$  in ppm) 1.17 (br, 6H), 1.67 (br, 2H), 2.22 (br, 1H), 4.03 (br, 1H)



### 2.3.3 Synthesis of amphiphilic poly(*N,N*-dimethylacrylamide)-*block*-poly(*N*-isopropylacrylamide) via bromoform-assisted polymerisation



Scheme 2.3. Synthesis of poly(*N,N*-dimethylacrylamide)-*block*-poly(*N*-isopropylacrylamide) via bromoform-assisted polymerisation using poly(*N,N*-dimethylacrylamide) as a macro-initiator.

#### 2.3.3.1 One-pot synthesis of poly(*N,N*-dimethylacrylamide)-*block*-poly(*N*-isopropylacrylamide)

The synthesis of poly(*N,N*-dimethylacrylamide)-*block*-poly(*N*-isopropylacrylamide) (PDMA-*b*-PNIPAM) was conducted using a PDMA macro-initiator (synthesised using 2.0 mol % bromoform and 1.0 mol% ACPA). The portion of the crude PDMA solution was determined based on conversion data to ensure 1 g of the PDMA macro-initiator would be available for the copolymerisation reaction. Using the example where the final conversion was  $\geq 99.9\%$  the procedure was as follows: A 50 mL round-bottomed flask was charged with PDMA macro-initiator (1.00 g; 0.0101 mol; 12.5 mL of the crude solution from the bulk polymerisation), NIPAM monomer (at 90:10, 80:20, 70:30, 60:40, 50:50, 40:60, 30:70, 20:80 and 10:90 molar ratios of DMA:NIPAM) and HPLC-grade water (12.5 mL). The clear solution was sealed using a rubber septum and parafilm and degassed via vacuum and nitrogen cycles over a period of 15 minutes before being placed into an ice bath for 20 minutes. Finally, the reaction flask and

ice bath were placed in an aluminium cabinet with magnetic stirring and irradiated with UV light for 120 minutes.

The water was removed via lyophilisation, then the copolymer was dissolved in the minimum amount of THF prior to dropwise precipitation into five-fold excess of chilled diethyl ether. Residual solvent was removed *in vacuo* before redissolution in HPLC-grade water. Finally, the water was removed via lyophilisation until constant weight was achieved to produce the final white solid.

**Poly(*N,N*-dimethylacrylamide)<sub>1450</sub>-*block*-poly(*N*-isopropylacrylamide)<sub>100</sub> (PDMA<sub>1450</sub>-*b*-PNIPAM<sub>100</sub>)**

$M_n = 145.3 \text{ kg mol}^{-1}$   $\bar{D} = 4.2$   $^1\text{H NMR}$  (300 MHz, D<sub>2</sub>O,  $\delta$  in ppm) 1.04 (br, 6H), 1.23-1.51 (br, 4H), 2.50 (br, 2H), 2.79-3.01 (br, 6H), 3.75 (br, 1H)

**Poly(*N,N*-dimethylacrylamide)<sub>1450</sub>-*block*-poly(*N*-isopropylacrylamide)<sub>230</sub> (PDMA<sub>1450</sub>-*b*-PNIPAM<sub>230</sub>)**

$M_n = 148.1 \text{ kg mol}^{-1}$   $\bar{D} = 4.3$   $^1\text{H NMR}$  (300 MHz, D<sub>2</sub>O,  $\delta$  in ppm) 1.04 (br, 6H), 1.26-1.52 (br, 4H), 2.51 (br, 2H), 2.80-3.00 (br, 6H), 3.74 (br, 1H)

**Poly(*N,N*-dimethylacrylamide)<sub>1450</sub>-*block*-poly(*N*-isopropylacrylamide)<sub>550</sub> (PDMA<sub>1450</sub>-*b*-PNIPAM<sub>550</sub>)**

$M_n = 145.9 \text{ kg mol}^{-1}$   $\bar{D} = 3.4$   $^1\text{H NMR}$  (300 MHz, D<sub>2</sub>O,  $\delta$  in ppm) 1.01 (br, 6H), 1.29-1.56 (br, 4H), 2.49 (br, 2H), 2.80-3.00 (br, 6H), 3.76 (br, 1H)

**Poly(*N,N*-dimethylacrylamide)<sub>1450</sub>-*block*-poly(*N*-isopropylacrylamide)<sub>860</sub> (PDMA<sub>1450</sub>-*b*-PNIPAM<sub>860</sub>)**

$M_n = 184.4 \text{ kg mol}^{-1}$   $\bar{D} = 4.0$   $^1\text{H NMR}$  (300 MHz, D<sub>2</sub>O,  $\delta$  in ppm) 1.02 (br, 6H), 1.28-1.51 (br, 4H), 1.88 (br, 1H), 2.51 (br, 2H), 2.80-3.01 (br, 6H), 3.77 (br, 1H)

**Poly(*N,N*-dimethylacrylamide)<sub>1450</sub>-*block*-poly(*N*-isopropylacrylamide)<sub>1360</sub> (PDMA<sub>1450</sub>-*b*-PNIPAM<sub>1360</sub>)**

$M_n = 186.3 \text{ kg mol}^{-1}$   $\bar{D} = 5.0$   $^1\text{H NMR}$  (300 MHz, D<sub>2</sub>O,  $\delta$  in ppm) 1.02 (br, 6H), 1.25-1.50 (br, 4H), 1.88 (br, 1H), 2.49 (br, 2H), 2.80-3.01 (br, 6H), 3.78 (br, 1H)

**Poly(*N,N*-dimethylacrylamide)<sub>1450</sub>-*block*-poly(*N*-isopropylacrylamide)<sub>1960</sub> (PDMA<sub>1450</sub>-*b*-PNIPAM<sub>1960</sub>)**

$M_n = 259.1 \text{ kg mol}^{-1}$   $\bar{D} = 5.3$   $^1\text{H NMR}$  (300 MHz, D<sub>2</sub>O,  $\delta$  in ppm) 1.03 (br, 6H), 1.28-1.52 (br, 4H), 1.90 (br, 1H), 2.51 (br, 2H), 2.80-3.01 (br, 6H), 3.77 (br, 1H)

**Poly(*N,N*-dimethylacrylamide)<sub>1450</sub>-*block*-poly(*N*-isopropylacrylamide)<sub>3240</sub> (PDMA<sub>1450</sub>-*b*-PNIPAM<sub>3240</sub>)**

$M_n = 233.2 \text{ kg mol}^{-1}$   $\bar{D} = 6.4$   $^1\text{H NMR}$  (300 MHz, D<sub>2</sub>O,  $\delta$  in ppm) 1.01 (br, 6H), 1.28-1.52 (br, 4H), 1.88 (br, 1H), 2.50 (br, 2H), 2.80-3.00 (br, 6H), 3.77 (br, 1H)

**Poly(*N,N*-dimethylacrylamide)<sub>1450</sub>-*block*-poly(*N*-isopropylacrylamide)<sub>5220</sub> (PDMA<sub>1450</sub>-*b*-PNIPAM<sub>5220</sub>)**

$M_n = 216.2 \text{ kg mol}^{-1}$   $\bar{D} = 8.4$   $^1\text{H NMR}$  (300 MHz, D<sub>2</sub>O,  $\delta$  in ppm) 1.03 (br, 6H), 1.30-1.59 (br, 4H), 1.89 (br, 1H), 2.50 (br, 2H), 2.81-3.02 (br, 6H), 3.79 (br, 1H)

**Poly(*N,N*-dimethylacrylamide)-*block*-poly(*N*-isopropylacrylamide) (PDMA-*b*-PNIPAM)**

**Target molar ratio = 10:90**

Deemed unsuccessful due to insolubility of NIPAM monomer at this ratio under the described conditions.

### **2.3.3.2 Two-step synthesis of PDMA-*b*-PNIPAM**

The synthesis of PDMA-*b*-PNIPAM was conducted using a PDMA macro-initiator (synthesised using 2.0 mol % bromoform and 1.0 mol% ACPA, and purified as described previously) as follows: A 50 mL round-bottomed flask was charged with precipitated PDMA macro-initiator

(1.00 g; 0.0101 mol), NIPAM monomer (at 90:10, 80:20, 70:30, 60:40, 50:50, 40:60, 30:70, 20:80 and 10:90 molar ratios of DMA:NIPAM) and HPLC-grade water (25 mL). The clear solution was sealed using a rubber septum and parafilm and degassed via vacuum and nitrogen cycles over a period of 15 minutes before being placed into an ice bath for 20 minutes. Finally, the reaction flask and ice bath was placed in an aluminium cabinet with magnetic stirring and irradiated with UV light for 120 minutes.

The water was removed via lyophilisation, before the copolymer was dissolved in the minimum amount of THF prior to dropwise precipitation into five-fold excess of chilled diethyl ether. Residual solvent was removed *in vacuo* before redissolution in HPLC-grade water. Finally, the water was removed via lyophilisation until constant weight was achieved to produce the final white solid. These experiments were completed using bromine-terminated poly(*N,N*-dimethylacrylamide) [PDMA-Br] macro-initiators synthesised to 91 and 70 % conversion.

#### 2.3.3.2.1 Two-step synthesis using PDMA macro-initiator synthesised to 91 % conversion

**Poly(*N,N*-dimethylacrylamide)<sub>1500</sub>-*block*-poly(*N*-isopropylacrylamide)<sub>110</sub> (PDMA<sub>1500</sub>-*b*-PNIPAM<sub>110</sub>)**

$M_n = 163.6 \text{ kg mol}^{-1}$   $\bar{D} = 3.4$   $^1\text{H NMR}$  (300 MHz, D<sub>2</sub>O,  $\delta$  in ppm) 1.02 (br, 6H), 1.25-1.50 (br, 4H), 1.89 (br, 1H), 2.50 (br, 2H), 2.80-3.01 (br, 6H), 3.77 (br, 1H)

**Poly(*N,N*-dimethylacrylamide)<sub>1500</sub>-*block*-poly(*N*-isopropylacrylamide)<sub>270</sub> (PDMA<sub>1500</sub>-*b*-PNIPAM<sub>270</sub>)**

$M_n = 165.8 \text{ kg mol}^{-1}$   $\bar{D} = 3.4$   $^1\text{H NMR}$  (300 MHz, D<sub>2</sub>O,  $\delta$  in ppm) 1.03 (br, 6H), 1.26-1.52 (br, 4H), 1.90 (br, 1H), 2.52 (br, 2H), 2.81-3.02 (br, 6H), 3.79 (br, 1H)

**Poly(*N,N*-dimethylacrylamide)<sub>1500</sub>-*block*-poly(*N*-isopropylacrylamide)<sub>420</sub> (PDMA<sub>1500</sub>-*b*-PNIPAM<sub>420</sub>)**

$M_n = 196.3 \text{ kg mol}^{-1}$   $\bar{D} = 3.2$   $^1\text{H NMR}$  (300 MHz, D<sub>2</sub>O,  $\delta$  in ppm) 1.02 (br, 6H), 1.25-1.51 (br, 4H), 1.88 (br, 1H), 2.51 (br, 2H), 2.80-3.01 (br, 6H), 3.78 (br, 1H)

**Poly(*N,N*-dimethylacrylamide)<sub>1500</sub>-*block*-poly(*N*-isopropylacrylamide)<sub>750</sub> (PDMA<sub>1500</sub>-*b*-PNIPAM<sub>750</sub>)**

$M_n = 164.4 \text{ kg mol}^{-1}$   $\bar{D} = 5.3$   $^1\text{H NMR}$  (300 MHz, D<sub>2</sub>O,  $\delta$  in ppm) 1.02 (br, 6H), 1.25-1.50 (br, 4H), 1.88 (br, 1H), 2.50 (br, 2H), 2.80-3.01 (br, 6H), 3.77 (br, 1H)

**Poly(*N,N*-dimethylacrylamide)<sub>1500</sub>-*block*-poly(*N*-isopropylacrylamide)<sub>1310</sub> (PDMA<sub>1500</sub>-*b*-PNIPAM<sub>1310</sub>)**

$M_n = 264.8 \text{ kg mol}^{-1}$   $\bar{D} = 4.1$   $^1\text{H NMR}$  (300 MHz, D<sub>2</sub>O,  $\delta$  in ppm) 1.02 (br, 6H), 1.26-1.50 (br, 4H), 1.89 (br, 1H), 2.51 (br, 2H), 2.80-3.01 (br, 6H), 3.78 (br, 1H)

**Poly(*N,N*-dimethylacrylamide)<sub>1500</sub>-*block*-poly(*N*-isopropylacrylamide)<sub>2050</sub> (PDMA<sub>1500</sub>-*b*-PNIPAM<sub>2050</sub>)**

$M_n = 392.6 \text{ kg mol}^{-1}$   $\bar{D} = 4.1$   $^1\text{H NMR}$  (300 MHz, D<sub>2</sub>O,  $\delta$  in ppm) 1.02 (br, 6H), 1.27-1.48 (br, 4H), 1.88 (br, 1H), 2.50 (br, 2H), 2.80-3.01 (br, 6H), 3.78 (br, 1H)

**Poly(*N,N*-dimethylacrylamide)<sub>1500</sub>-*block*-poly(*N*-isopropylacrylamide)<sub>3330</sub> (PDMA<sub>1500</sub>-*b*-PNIPAM<sub>3330</sub>)**

$M_n = 463.6 \text{ kg mol}^{-1}$   $\bar{D} = 3.9$   $^1\text{H NMR}$  (300 MHz, D<sub>2</sub>O,  $\delta$  in ppm) 1.02 (br, 6H), 1.29-1.47 (br, 4H), 1.90 (br, 1H), 2.52 (br, 2H), 2.80-3.01 (br, 6H), 3.77 (br, 1H)

**Poly(*N,N*-dimethylacrylamide)<sub>1500</sub>-*block*-poly(*N*-isopropylacrylamide)<sub>5100</sub> (PDMA<sub>1500</sub>-*b*-PNIPAM<sub>5100</sub>)**

$M_n = 603.7 \text{ kg mol}^{-1}$   $\bar{D} = 3.4$   $^1\text{H NMR}$  (300 MHz, D<sub>2</sub>O,  $\delta$  in ppm) 1.02 (br, 6H), 1.29-1.47 (br, 4H), 1.88 (br, 1H), 2.50 (br, 2H), 2.80-3.01 (br, 6H), 3.78 (br, 1H)

**Poly(*N,N*-dimethylacrylamide)-*block*-poly(*N*-isopropylacrylamide) (PDMA-*b*-PNIPAM)**

**Target molar ratio = 10:90**

Deemed unsuccessful due to insolubility of NIPAM monomer at this ratio under the described conditions.

#### 2.3.3.2.2 Two-step synthesis using PDMA macro-initiator synthesised to 70 % conversion

**Poly(*N,N*-dimethylacrylamide)<sub>3280</sub>-*block*-poly(*N*-isopropylacrylamide)<sub>300</sub> (PDMA<sub>3280</sub>-*b*-PNIPAM<sub>300</sub>)**

$M_n = 259.1 \text{ kg mol}^{-1}$   $\bar{D} = 3.3$   $^1\text{H NMR}$  (300 MHz, D<sub>2</sub>O,  $\delta$  in ppm) 1.07 (br, 6H), 1.31-1.57 (br, 4H), 1.95 (br, 1H), 2.55 (br, 2H), 2.85-3.06 (br, 6H), 3.82 (br, 1H)

**Poly(*N,N*-dimethylacrylamide)<sub>3280</sub>-*block*-poly(*N*-isopropylacrylamide)<sub>720</sub> (PDMA<sub>3280</sub>-*b*-PNIPAM<sub>720</sub>)**

$M_n = 272.2 \text{ kg mol}^{-1}$   $\bar{D} = 3.1$   $^1\text{H NMR}$  (300 MHz, D<sub>2</sub>O,  $\delta$  in ppm) 1.07 (br, 6H), 1.30-1.56 (br, 4H), 1.94 (br, 1H), 2.56 (br, 2H), 2.85-3.06 (br, 6H), 3.82 (br, 1H)

**Poly(*N,N*-dimethylacrylamide)<sub>3280</sub>-*block*-poly(*N*-isopropylacrylamide)<sub>1180</sub> (PDMA<sub>3280</sub>-*b*-PNIPAM<sub>1180</sub>)**

$M_n = 301.5 \text{ kg mol}^{-1}$   $\bar{D} = 3.1$   $^1\text{H NMR}$  (300 MHz, D<sub>2</sub>O,  $\delta$  in ppm) 1.07 (br, 6H), 1.31-1.55 (br, 4H), 1.93 (br, 1H), 2.56 (br, 2H), 2.85-3.06 (br, 6H), 3.82 (br, 1H)

**Poly(*N,N*-dimethylacrylamide)<sub>3280</sub>-*block*-poly(*N*-isopropylacrylamide)<sub>1950</sub> (PDMA<sub>3280</sub>-*b*-PNIPAM<sub>1950</sub>)**

$M_n = 255.2 \text{ kg mol}^{-1}$   $\bar{D} = 4.2$   $^1\text{H NMR}$  (300 MHz, D<sub>2</sub>O,  $\delta$  in ppm) 1.07 (br, 6H), 1.30-1.55 (br, 4H), 1.94 (br, 1H), 2.55 (br, 2H), 2.85-3.06 (br, 6H), 3.82 (br, 1H)

**Poly(*N,N*-dimethylacrylamide)<sub>3280</sub>-*block*-poly(*N*-isopropylacrylamide)<sub>3120</sub> (PDMA<sub>3280</sub>-*b*-PNIPAM<sub>3120</sub>)**

$M_n = 369.1 \text{ kg mol}^{-1}$   $\bar{D} = 3.5$   $^1\text{H NMR}$  (300 MHz, D<sub>2</sub>O,  $\delta$  in ppm) 1.07 (br, 6H), 1.32-1.54 (br, 4H), 1.94 (br, 1H), 2.56 (br, 2H), 2.85-3.06 (br, 6H), 3.82 (br, 1H)

**Poly(*N,N*-dimethylacrylamide)<sub>3280</sub>-*block*-poly(*N*-isopropylacrylamide)<sub>4430</sub> (PDMA<sub>3280</sub>-*b*-PNIPAM<sub>4430</sub>)**

$M_n = 325.8 \text{ kg mol}^{-1}$   $\bar{D} = 5.1$   $^1\text{H}$  NMR (300 MHz,  $\text{D}_2\text{O}$ ,  $\delta$  in ppm) 1.07 (br, 6H), 1.33-1.52 (br, 4H), 1.94 (br, 1H), 2.56 (br, 2H), 2.85-3.06 (br, 6H), 3.83 (br, 1H)

**Poly(*N,N*-dimethylacrylamide)<sub>3280</sub>-*block*-poly(*N*-isopropylacrylamide)<sub>7040</sub> (PDMA<sub>3280</sub>-*b*-PNIPAM<sub>7040</sub>)**

$M_n = 409.2 \text{ kg mol}^{-1}$   $\bar{D} = 4.4$   $^1\text{H}$  NMR (300 MHz,  $\text{D}_2\text{O}$ ,  $\delta$  in ppm) 1.07 (br, 6H), 1.33-1.52 (br, 4H), 1.94 (br, 1H), 2.56 (br, 2H), 2.85-3.06 (br, 6H), 3.82 (br, 1H)

**Poly(*N,N*-dimethylacrylamide)<sub>3280</sub>-*block*-poly(*N*-isopropylacrylamide)<sub>12,600</sub> (PDMA<sub>3280</sub>-*b*-PNIPAM<sub>12,600</sub>)**

$M_n = 464.6 \text{ kg mol}^{-1}$   $\bar{D} = 4.4$   $^1\text{H}$  NMR (300 MHz,  $\text{D}_2\text{O}$ ,  $\delta$  in ppm) 1.07 (br, 6H), 1.29-1.51 (br, 4H), 1.94 (br, 1H), 2.56 (br, 2H), 2.85-3.05 (br, 6H), 3.82 (br, 1H)

**Poly(*N,N*-dimethylacrylamide)-*block*-poly(*N*-isopropylacrylamide) (PDMA-*b*-PNIPAM)**

**Target molar ratio = 10:90**

Deemed unsuccessful due to insolubility of NIPAM monomer at this ratio under the described conditions.

## 2.4 Characterisation Methods

This section describes the methods used to characterise the materials synthesised.

### 2.4.1 <sup>1</sup>H Nuclear Magnetic Resonance Spectroscopy

<sup>1</sup>H Nuclear Magnetic Resonance (NMR) spectroscopy was used to confirm the chemical structure of the samples along with monitoring the percentage monomer conversion with time during the kinetic studies of the homopolymerisation reactions (*vide infra*). Samples were prepared in deuterium oxide (D<sub>2</sub>O) or chloroform-d (CDCl<sub>3</sub>) to approximately 10 % (w/v) and spectra were recorded on a 300 MHz Bruker Avance spectrophotometer. Chemical shifts (δ, ppm) stated are referenced relative to the chemical shift of the residual solvent (H<sub>2</sub>O or CHCl<sub>3</sub>) resonances.

#### 2.4.1.1 Calculating monomer conversion

As aforementioned, the percentage conversion of monomer to polymer during the course of the polymerisation was monitored using <sup>1</sup>H NMR spectroscopy. Specifically, peaks present for the monomer and polymer were compared to one another.

For the synthesis of PDMA in HPLC-grade water, the integrals of the vinylic monomer protons (present at 5.6, 6.0 and 6.6 ppm) and the polymer methyl protons (present at 2.9 ppm) were used along with Equation 2.1 to determine the overall conversion. Figure 2.1 shows the spectra collected for a typical kinetic study for the synthesis of PDMA in this research.

$$\frac{\text{monomer}}{\text{monomer} + \text{polymer}} = \frac{1 - x}{6(1 - x) + 6x} \quad \text{Equation 2.1.}$$



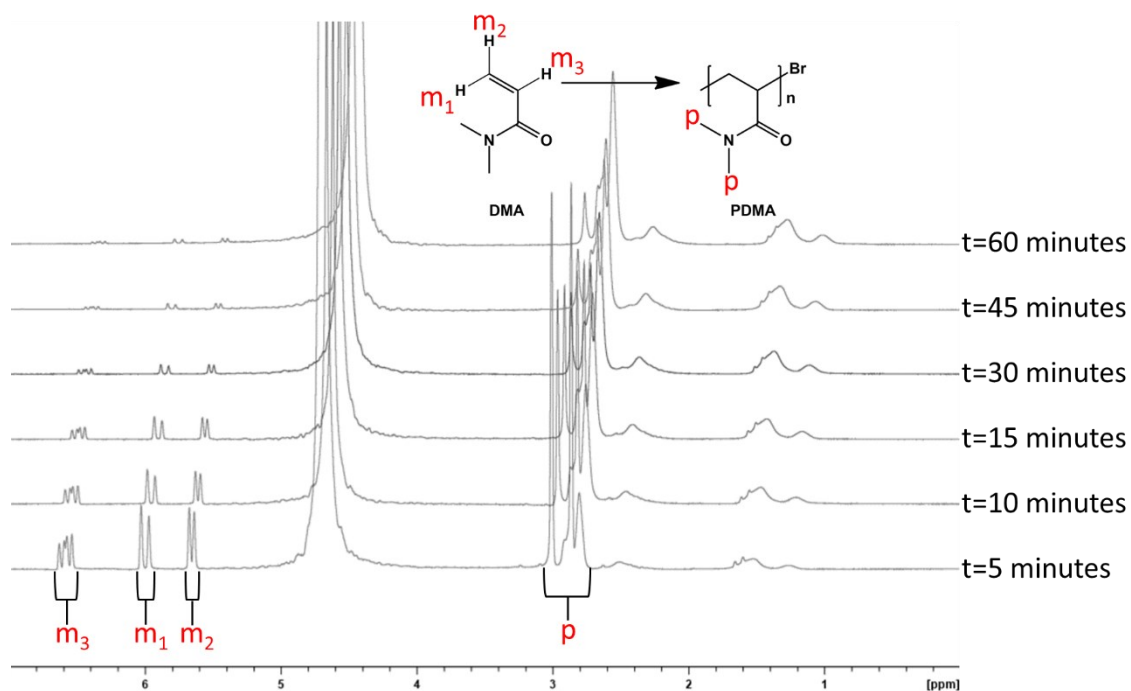


Figure 2.1.  $^1\text{H}$  NMR spectra (in  $\text{D}_2\text{O}$ ) showing the progress of the DMA polymerisation through the disappearance of the monomer vinylic groups (5.6, 6.0 and 6.6 ppm) and the broadening of the polymer methyl groups (2.9 ppm) from PDMA.

For the bromoform-assisted synthesis of PDMA in DMF the integral of the methyl group protons (as seen in Figure 2.1) could not be used to calculate the conversion. This was due to the overlap of the DMF methyl group protons at 2.88 and 2.96 ppm<sup>289</sup> (Figure 2.2). Instead the integral of the vinyl monomer protons present at 1.24 and 1.55 ppm (Figure 2.2) were used alongside Equation 2.2.

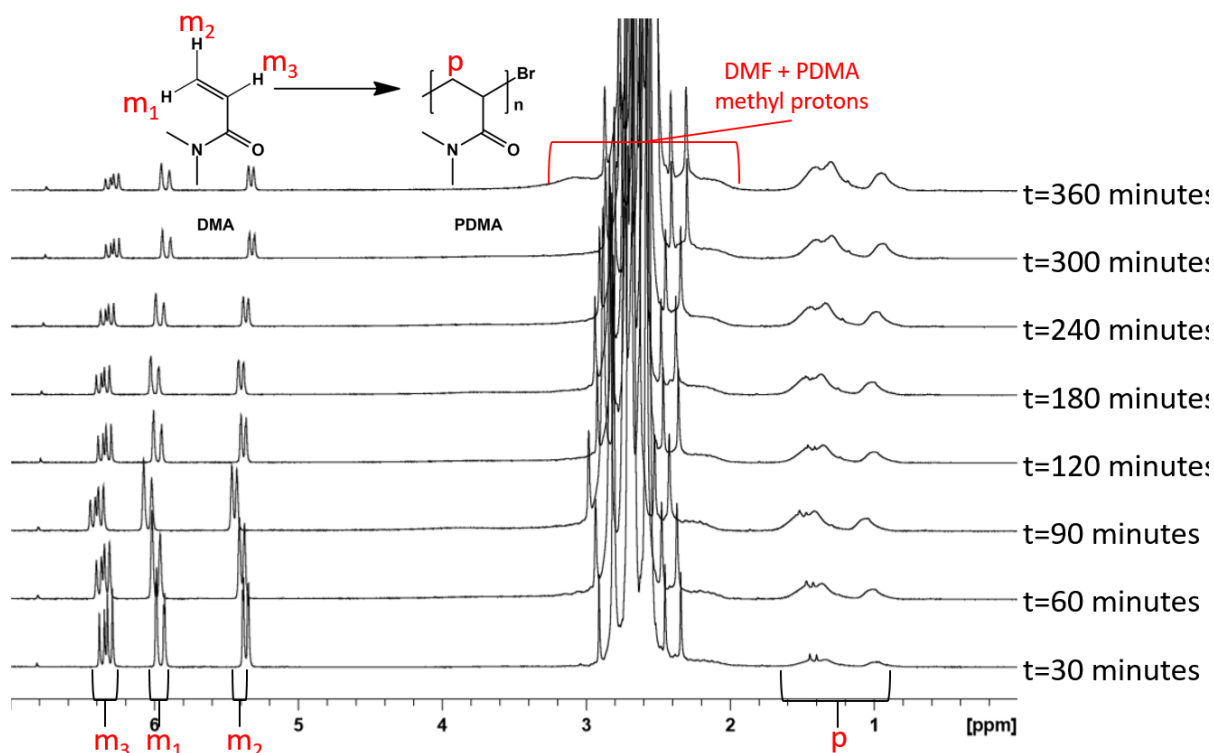


Figure 2.2.  $^1\text{H}$  NMR spectra (in  $\text{CDCl}_3$ ) showing the progress of the DMA polymerisation through the disappearance of the monomer vinylic groups (5.6, 6.0 and 6.6 ppm) and the broadening of the polymer vinyl peaks (1.24 and 1.55 ppm) from PDMA. Also highlighting the overlap of the DMF and PDMA methyl group protons.

$$\frac{\text{monomer}}{\text{monomer} + \text{polymer}} = \frac{1 - x}{2(1 - x) + 2x} \quad \text{Equation 2.2.}$$

Finally, for the synthesis of PNIPAM in both HPLC-grade water and DMF, the integrals of the vinylic monomer protons (present at 5.6 and 6.1 ppm) and the polymer methyl protons (present at 1.0 ppm) were used along with Equation 2.1 to determine the overall monomer conversion. Figure 2.3 shows the spectra collected for a typical kinetic study for the synthesis of PNIPAM in this research.

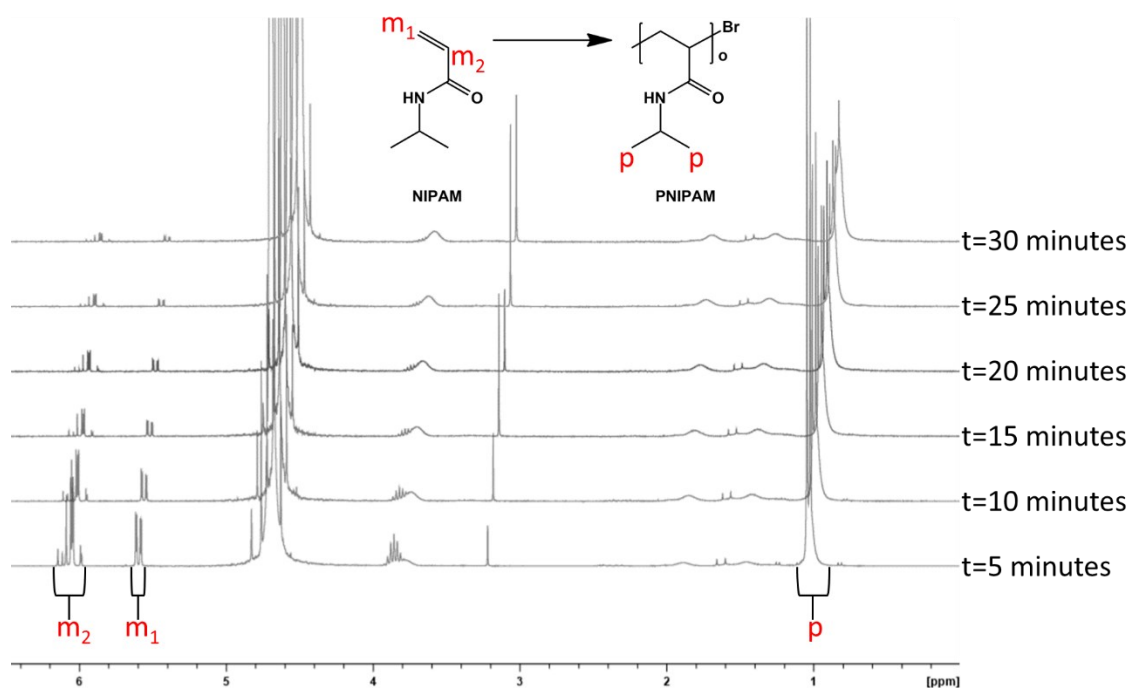


Figure 2.3.  $^1\text{H}$  NMR spectra (in  $\text{D}_2\text{O}$ ) showing the progress of the NIPAM polymerisation (in HPLC-grade water) through the disappearance of the monomer vinylic groups (5.6 and 6.1 ppm) and the broadening of the polymer methyl groups (1.0 ppm) from PNIPAM.

## 2.4.2 Gel Permeation Chromatography

Gel Permeation Chromatography (GPC), also referred to as Size Exclusion Chromatography (SEC) was used to determine the molar mass ( $M_n$ ) and dispersity ( $M_w/M_n$ ,  $\mathcal{D}$ ) for the homo- and co- polymers. GPC of PDMA and PNIPAM homopolymers (both at varied bromoform content), PDMA macro-initiator and the PDMA-*b*-PNIPAM copolymers were performed at 40 °C using an Agilent Infinity II multi-detector GPC comprising two PL gel Mixed-C columns and a guard column. The eluent solution consisted of HPLC-grade DMF containing 0.10% w/v lithium bromide (LiBr) and the flow rate was set to 1.0 mL min $^{-1}$ . Calibrations were generated using near monodispersed poly(methyl methacrylate) standards ( $M_p$  range = 550 to 2,210,000 g mol $^{-1}$ ) and experimental data were analysed using Agilent GPC/SEC software (Version A.02.01).

### 2.4.3 Differential Scanning Calorimetry

Differential Scanning Calorimetry (DSC) was used to study the thermal behaviour of the synthesised materials; particularly the shifts and/or changes between the glass transition temperatures ( $T_g$ ) of the homopolymers and resulting copolymers.

DSC measurements were performed using a Mettler Toledo DSC 1 system and STARe software (Version 12.0) for analysis. PNIPAM homopolymer samples were exposed to three cycles (heating, cooling and heating) between -20 and 250 °C. PDMA homopolymers samples were exposed to three cycles (heating, cooling and heating) between 0 and 150 °C. Finally, PDMA-*b*-PNIPAM copolymers were exposed to three cycles (heating, cooling and heating) between 0 and 200 °C.

### 2.4.4 Thermal Gravimetric Analysis

Thermal Gravimetric Analysis (TGA) was also used to study the thermal behaviour of the synthesised materials, focusing on the degradation patterns of the products by monitoring change in mass with increasing temperature. TGA was performed using a Pyris 1 thermogravimetric analyser under nitrogen atmosphere (flow rate 30 ml min<sup>-1</sup>). All samples were heated from 100-600 °C at a heating rate of 10 °C per minute.

### 2.4.5 Dynamic Light Scattering

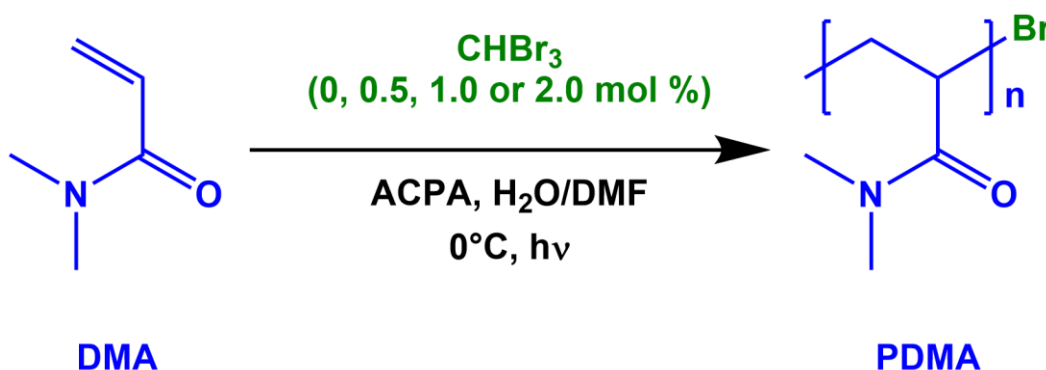
Dynamic Light Scattering (DLS) was employed to determine the lower critical solution temperature (LCST) of the PNIPAM homopolymers and all PDMA-*b*-PNIPAM copolymers. Specifically, the size (Z-average) of the polymer and copolymer samples (prepared in HPLC-grade H<sub>2</sub>O) were measured as a function of temperature, specifically between 25 - 50 with measurements at every 1 °C interval. DLS measurements were performed using a Malvern Zetasizer Nano ZS instrument. Z-average was measured for each sample at a solution concentration of 1 mg/mL in HPLC-grade water. Each sample was analysed three times at each temperature with the software determining the most appropriate number of scans (12 - 16) for each run. DLS was used to highlight the differences between the homopolymer and

block copolymers in terms of their observed size; due to self-assembly upon reaching the LCST. The instrument is verified monthly using an aqueous polystyrene latex (Z-average  $290 \pm 10$  nm) verification standard.

# **Chapter 3. Bromoform-assisted polymerisation of *N,N*- dimethylacrylamide**

### 3.1 Homopolymerisation of *N,N*-dimethylacrylamide

This chapter describes the synthesis of poly(*N,N*-dimethylacrylamide) [PDMA] via bromoform-assisted polymerisation (Scheme 3.1). Multiple investigations were undertaken to determine the most appropriate synthetic route to a PDMA macro-initiator for use in further polymerisation reactions; to form block copolymers. As demonstrated in Scheme 3.1, due to the primary dissociation pathway of bromoform, it is predicted that the polymerisations will produce PDMA with a reversibly capped bromine chain end.



Scheme 3.1. Synthesis of PDMA via bromoform-assisted polymerisation at varied bromoform concentrations.

The main part of this study focuses on the synthesis of PDMA with varied bromoform content to provide insight into the role of increasing bromoform concentration on the overall polymerisation and determine the optimum route to synthesis a PDMA macro-initiator for future block copolymer synthesis. Moreover, these reactions were conducted in both high performance liquid chromatography (HPLC)-grade water and dimethylformamide (DMF) to determine the effect of solvent on the production of PDMA using this bromoform-assisted synthetic route. In addition to this research, two supplementary studies were conducted; an investigation in the absence of photoinitiator [namely 4,4-azobiscyanovaleric acid (ACPA)], and a study to determine the role of oxygen in the polymerisation system. The investigation in the absence of ACPA was designed to highlight the potential of bromoform to behave as a photoinitiator as implied in the earlier work of Miller<sup>208</sup>, Dunn *et al.*<sup>209</sup> and Wu *et al.*<sup>211</sup> (during

the polymerisation of acrylonitrile and acrylic acid, styrene and methyl methacrylate, and acrylic acid and 2-acrylamido-2-methylpropanesulfonic acid (AMPS), respectively), in addition to its potential chain transfer agent (CTA) capabilities (as suggested by Thananukul *et al.*<sup>212</sup>). The final investigation, whereby oxygen was not removed from the reaction flask, was used to further develop the synthetic methodology; determining whether there was a need for a degassing stage for the reaction to be successful under the described conditions.

### 3.2 Development of the *N,N*-dimethylacrylamide polymerisation procedure

As discussed in Chapter 2, the UV light source used throughout this work was a Philips Solarium Model MD 1-15 lamp comprising four parallel 15 W fluorescent tubes that emitted UV light in the 315-400 nm wavelength range<sup>290</sup>. The UV lamp was placed face down on the opening of a metal box to irradiate the reaction mixture from above (Figure 3.1).

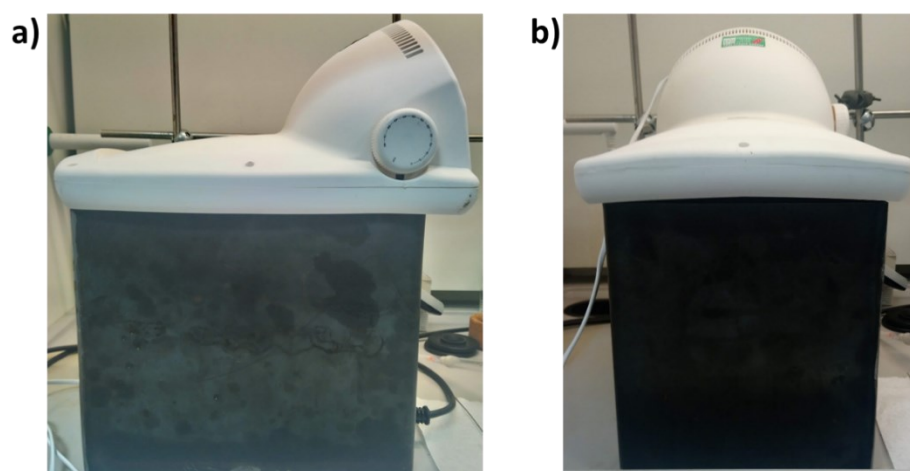


Figure 3.1. UV lamp and metal box set up showing UV irradiation from above. (a) Side view and (b) front facing.

Borosilicate round-bottomed flasks were used as the reaction vessel for all investigations and are known to significantly transmit UV light ( $> 200\text{ nm}$ <sup>291</sup>). The reaction vessel was equipped with a magnetic stirrer bar and placed on a magnetic stirring plate (set to 500 revolutions per minute) at a fixed distance (10 cm) from the UV lamp (Figure 3.2). ACPA was selected as a



suitable photoinitiator as it is known to photo-dissociate in the region of 200-402 nm<sup>292,293</sup>, which is ideal for both the lamp and borosilicate glass used in this study.

Trial reactions conducted identified that the heat produced from the UV light source and the reaction were significant enough to increase the reaction temperature from 25 °C up to 45 °C (after 2 hours of UV irradiation). Therefore, an ice bath was introduced to provide temperature control throughout the course of the reaction (Figure 3.2).



Figure 3.2. Birds eye view of the stirrer plate, ice bath and reaction vessel for a typical polymerisation.

The ice did not cover the top of the vessel to allow sufficient UV irradiation from above. The reaction solution was stirred in the ice bath for 20 minutes to allow a homogenous solution to be formed and the temperature to stabilise. A temperature *versus* time study of the reaction solution concluded that the temperature increased by a maximum of 4.9 °C over a 60 minute period of UV irradiation (Figure 3.3). The initial increase in temperature, observed in Figure 3.3, is attributed to the highly exothermic nature of the polymerisation during the early stages of propagation. After which, as the rate of reaction slows down, the ice bath is able to cool and maintain the temperature of the solution  $\leq 4.3$  °C. Overall, the ice bath provided control over

the temperature of the solution, significantly reducing potential thermal effects on the dissociation of ACPA or bromoform and the overall rate of the polymerisation.

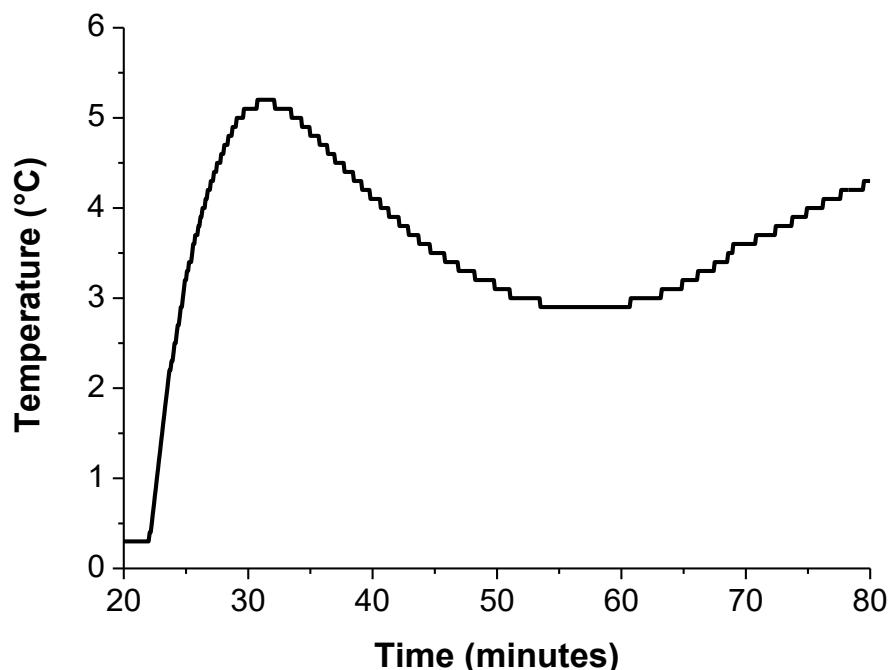


Figure 3.3. Temperature *versus* time plot for the trial synthesis of PDMA using an ice bath to provide temperature control.

### 3.3 Bromoform-assisted synthesis of poly(*N,N*-dimethylacrylamide) in HPLC-grade water

The focus of this research was to successfully synthesise block copolymers from macro-initiators containing a labile C-Br bond; formed from the use of bromoform in the homopolymerisation reaction. Therefore, a detailed study was required that focused on the synthesis of the macro-initiator. This section describes the synthesis of PDMA macro-initiators, formed at varied bromoform concentrations (0, 0.5, 1.0 and 2.0 mol % relative to monomer) and fixed ACPA concentration [1.0 mol% with respect to *N,N*-dimethylacrylamide (DMA)] in water. Experiments were conducted in an ice bath to provide control over the temperature of the system during the UV irradiation. In all cases, experiments were repeated

in triplicate to eliminate potential anomalies within the data and highlight patterns and processes that were occurring. The effect of the addition of bromoform on the DMA homopolymerisation was studied by monitoring monomer conversion and number-average molar mass ( $M_n$ ) using  $^1\text{H}$  nuclear magnetic resonance (NMR) spectroscopy (Figure 3.4 and Appendices 1 - 3) and gel permeation chromatography (GPC, using poly(methyl methacrylate) [PMMA] standards) (Figure 3.5), respectively.

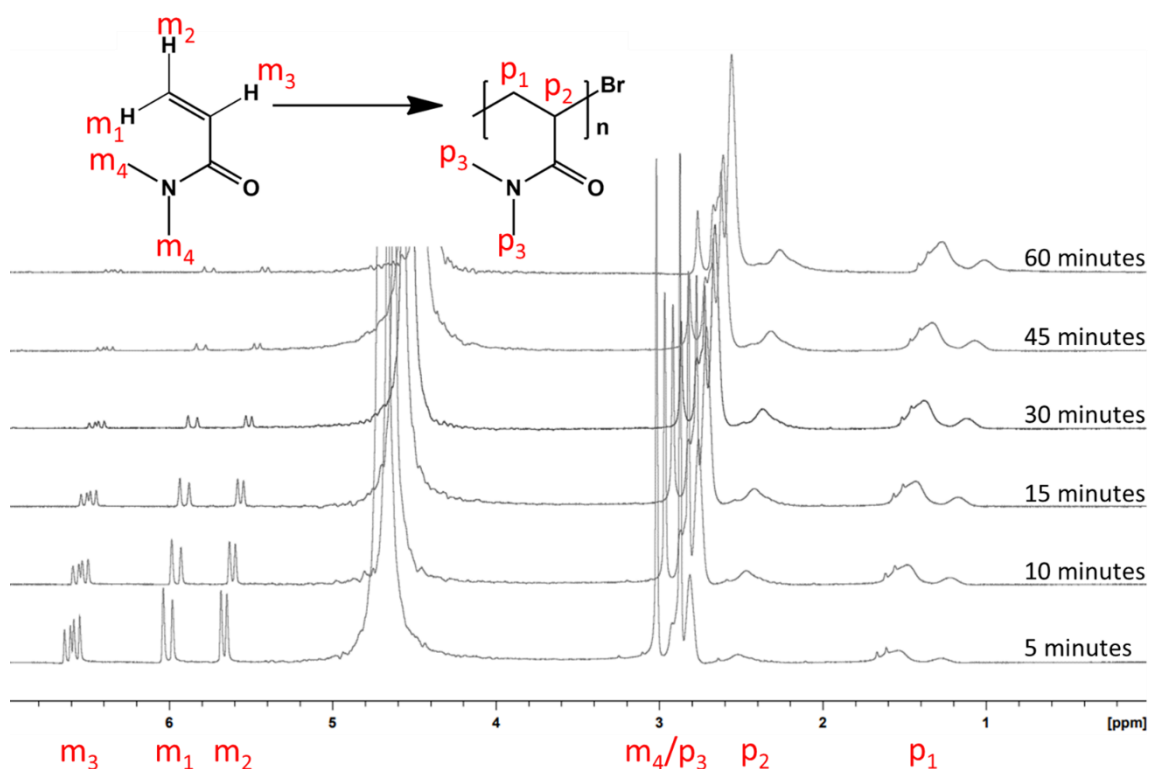


Figure 3.4. Exemplar  $^1\text{H}$  NMR kinetic overlay for the synthesis of PDMA in water at 2.0 mol % bromoform showing the disappearance of monomer and broadening of polymer peaks throughout the course of the reaction.

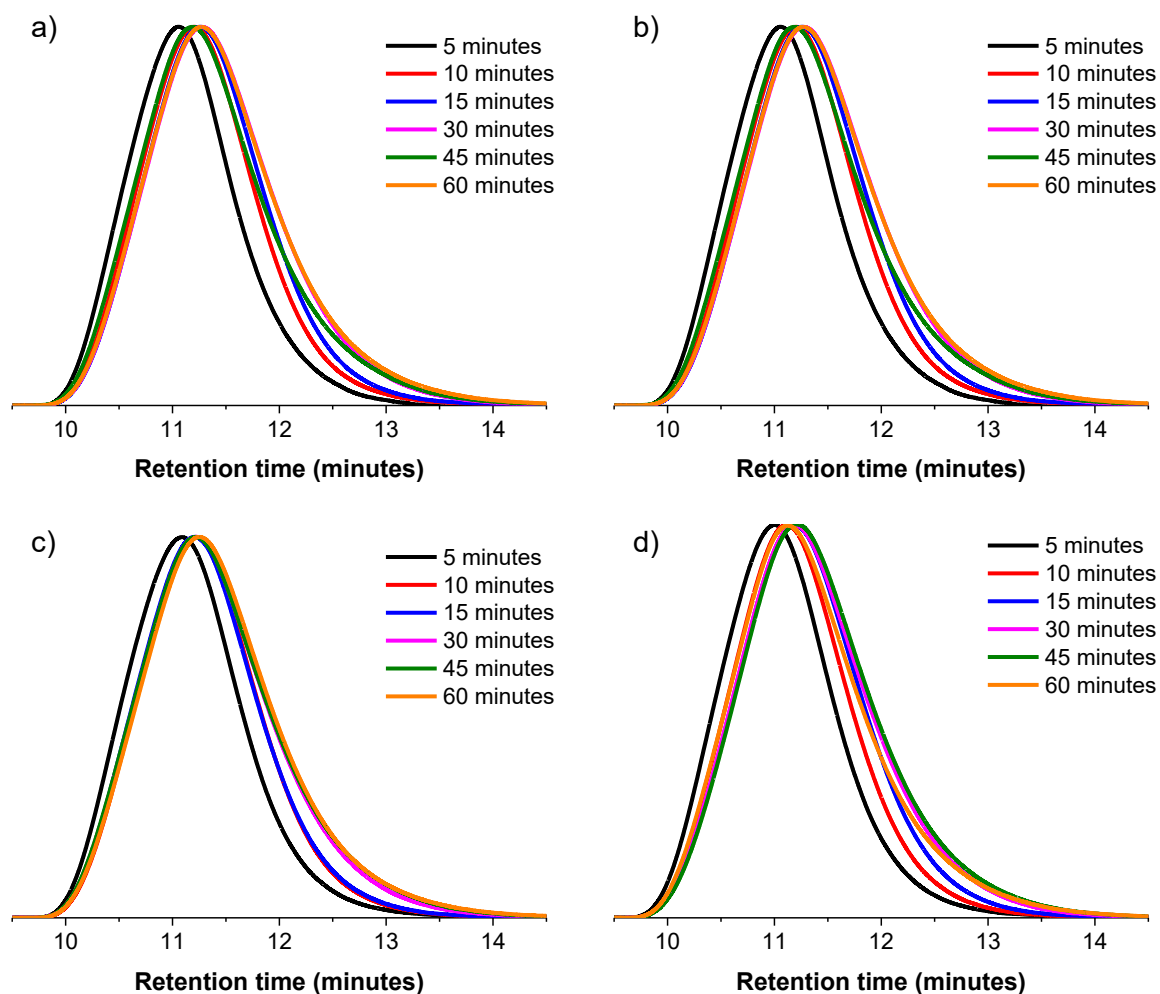


Figure 3.5. Kinetic GPC traces for the synthesis of PDMA in water at a) 0, b) 0.5, c) 1.0 and d) 2.0 mol % bromoform concentrations (relative to monomer).

High monomer conversions ( $\geq 93\%$ ) were achieved in each case, and the  $M_n$  of the resulting PDMA appears to increase upon addition of bromoform before then decreasing with increasing bromoform concentration present (see data summarised in Table 3.1). The resulting PDMA, in each case, was isolated by precipitation and dried in a vacuum oven until constant weight was achieved. Excess unreacted monomer was confirmed to be removed via  $^1\text{H}$  NMR spectroscopy (Figure 3.6). The GPC traces of the purified PDMA (purification via precipitation), synthesised using each bromoform concentration, demonstrate good reproducibility between the results (Figure 3.7).

Table 3.1. Summary of final conversion, molar mass, molar mass dispersity and apparent rate constant data for the polymerisation of *N,N*-dimethylacrylamide at varied bromoform concentrations in water.

Experiment series	Bromoform content (mol %) <sup>a</sup>	Final monomer conversion (%) <sup>b</sup>	$M_n$ (kg mol <sup>-1</sup> ) <sup>c</sup>	$\mathcal{D}$ ( $M_w/M_n$ ) <sup>c</sup>	$k_{app}$ (min <sup>-1</sup> )
HJH027	0	97	246.7	3.4	0.14
HJH028	0.5	95	294.8	2.8	0.12
HJH029	1.0	93	271.2	2.8	0.13
HJH030	2.0	96	242.3	3.5	0.12

a. Relative to monomer

b. Calculated using <sup>1</sup>H NMR spectroscopy and Equation 2.2

c. Determined using DMF GPC with PMMA standards

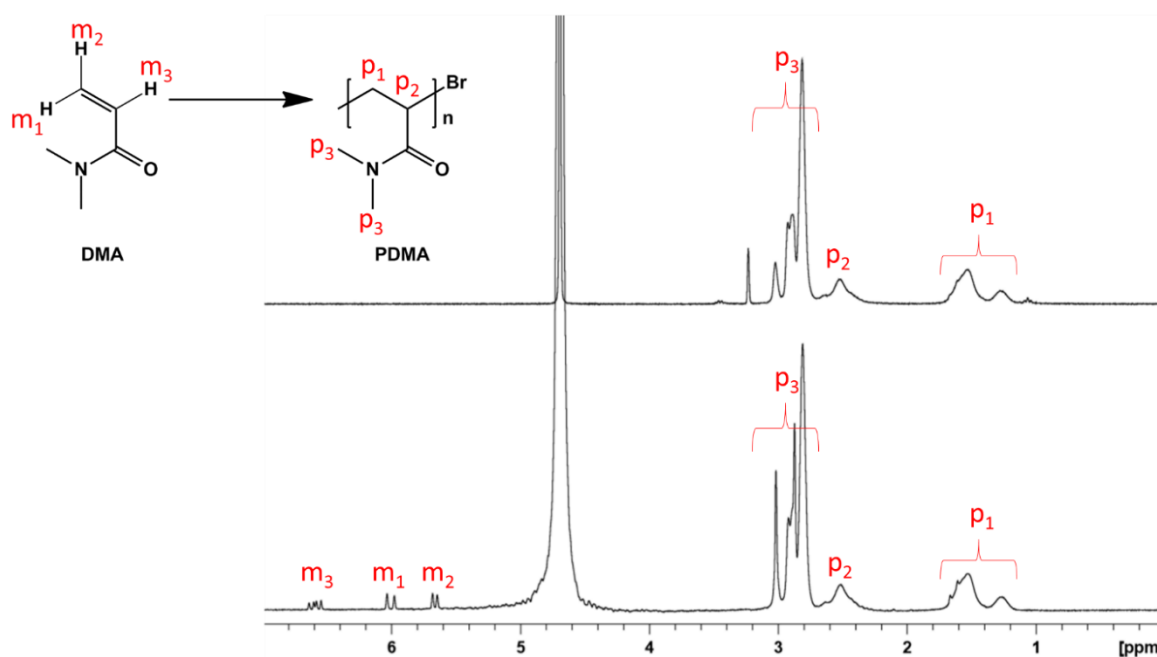


Figure 3.6. Comparative <sup>1</sup>H NMR spectra (in D<sub>2</sub>O) showing the disappearance of the monomer vinyl protons (5.7, 6.0 and 6.6 ppm) between crude and precipitated PDMA (2 mol % bromoform, relative to monomer).

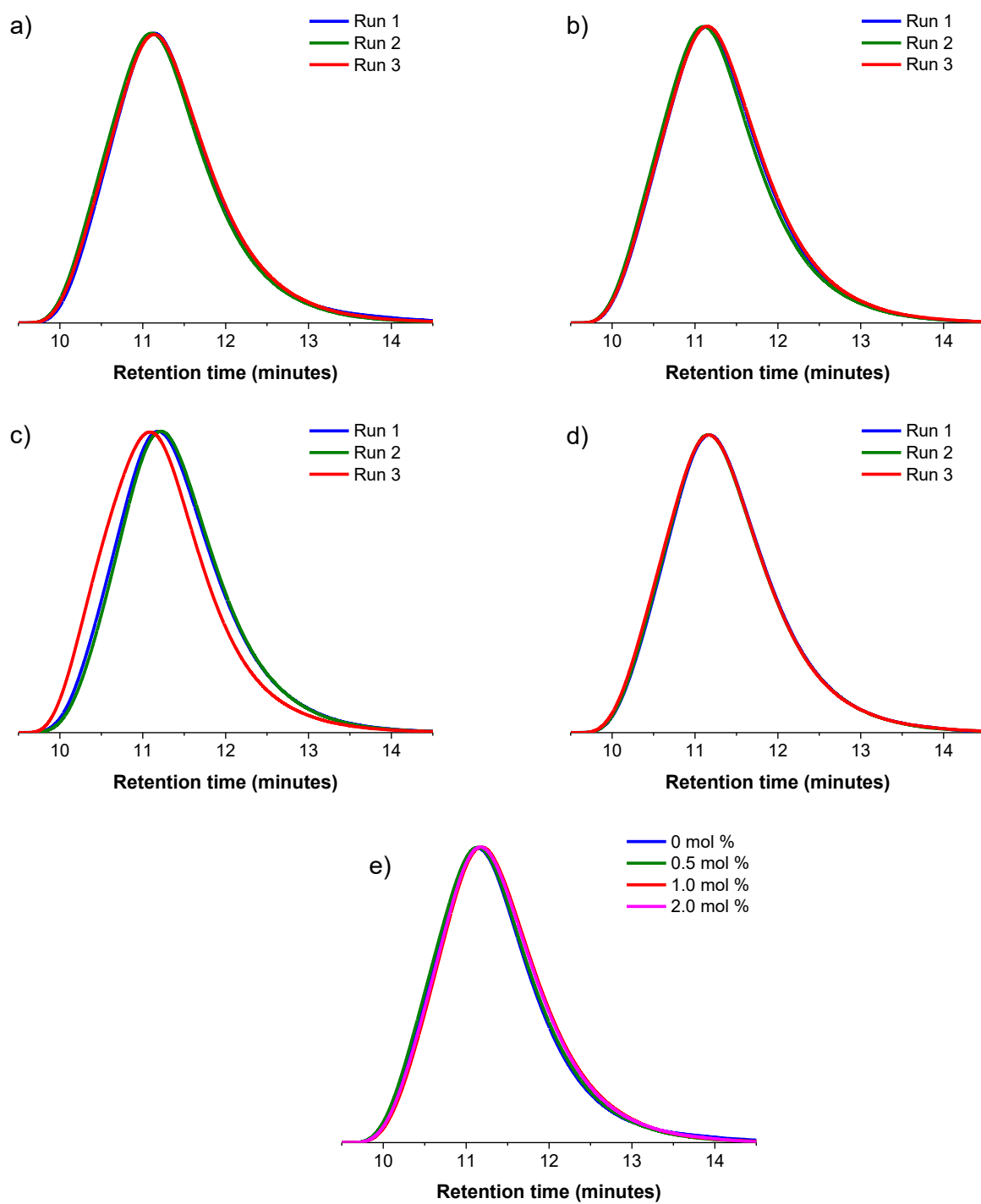


Figure 3.7. GPC traces of PDMA final precipitates at a) 0, b) 0.5, c) 1.0 and d) 2.0 mol % bromoform (relative to monomer, synthesised in water) demonstrating good reproducibility between runs and e) near-identical GPC traces of the final precipitate at each bromoform concentration.

The final molar mass of each sample (see Table 3.1) appears to increase on addition of 0.5 mol % bromoform, however, closer inspection of the broad GPC curves indicates that the molar mass profiles are near-identical in all cases (Figure 3.7). It should be noted that the molar mass profiles exceed the upper limit of the GPC calibration range, which will affect the  $M_n$  values obtained from seemingly identical broad curves. Therefore, it is reasonable to assume that bromoform is not behaving as a chain transfer agent under the described reaction conditions, as the molar mass would be expected to decrease when increasing the bromoform content. These observations disagree with those made in the previous work conducted by Thananukul *et al.*<sup>212</sup>, where it was demonstrated that bromoform exhibits successful chain transfer capabilities during the polymerisation of acrylamide, highlighted through the apparent regulation of molar mass with increasing bromoform content. However, the system discussed herein differs to the Thananukul *et al.* study as an ice bath has been used to provide control over the temperature of the reaction. In the Thananukul *et al.* study, temperatures of up to 50 °C are reported during the 60 minutes of UV irradiation that the reaction solutions are exposed to. Therefore significant thermal effects could be the reason that bromoform exhibited CTA capabilities in their work.

Further analysis of the kinetic data collected (Table 3.1, Figure 3.8 and Figure 3.9) demonstrate little to no difference in polymerisation rate observed for all bromoform concentrations studied. This is similar to the work of Thananukul *et al.*<sup>212</sup>, where it was reported that the addition of bromoform to the polymerisation system did not significantly affect the rate of polymerisation. Additionally, the molar mass dispersity,  $\bar{D}$ , of the final polymers was high (2.8 - 3.5), with no apparent relationship between molar mass dispersity and bromoform content.

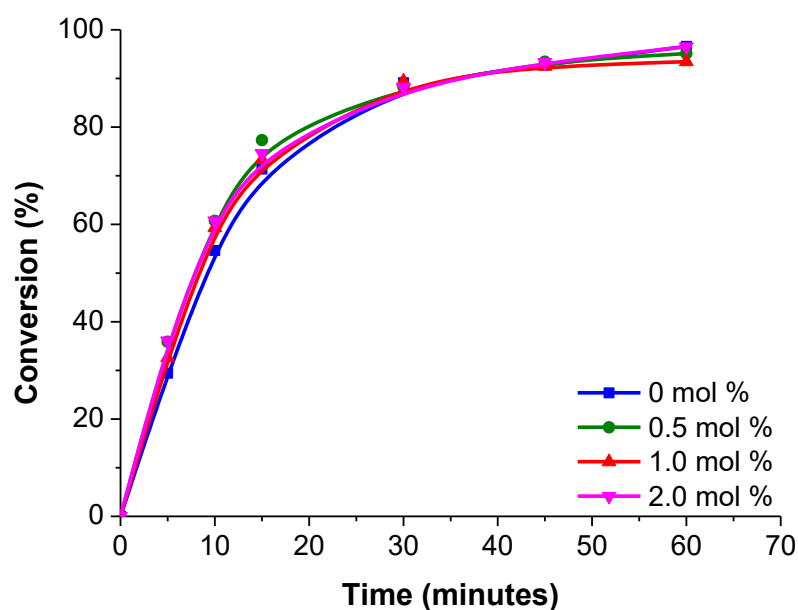


Figure 3.8. Monomer conversion *versus* time for the synthesis of PDMA at varying bromoform concentrations in water.

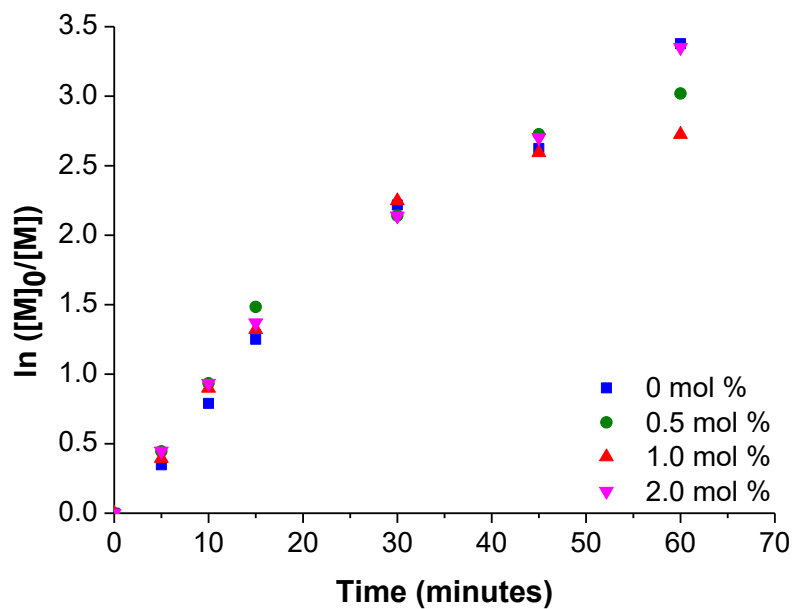


Figure 3.9. Semi-logarithmic plot for the synthesis of PDMA at varying bromoform concentration in water.



The kinetic study shows that the PDMA molar mass decreases as the polymerisation proceeds at all bromoform concentrations (Figure 3.10). This is a typical observation in free radical polymerisations due to high initial rates of propagation leading to the formation of high molar mass chains, before the monomer concentration is reduced and thus shorter polymer chains are synthesised, resulting in a reduction in the average molar mass in the system<sup>294–296</sup>.

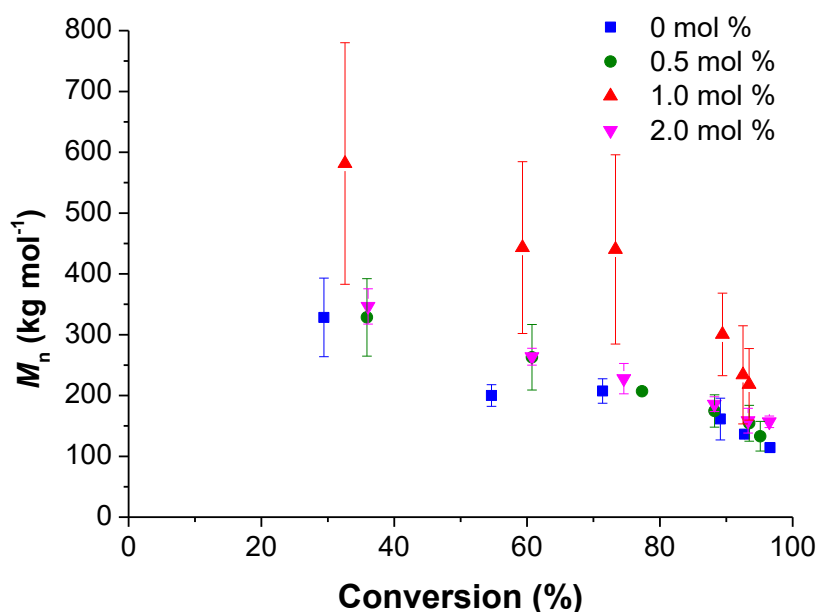


Figure 3.10. Molar mass *versus* conversion for the synthesis of PDMA at varying bromoform concentrations in water (error bars represent the standard deviation of the triplicate data).

### 3.3.1 Thermal properties

In preparation for the synthesis of block copolymers, the resulting PDMA was purified by precipitation and further characterised via differential scanning calorimetry (DSC) and thermal gravimetric analysis (TGA) to determine the glass transition temperature ( $T_g$ ) and degradation profile, respectively. These results were then collated for later comparison to identify any changes between the properties of the homopolymers and any subsequent block copolymers that may be synthesised.

For all samples, the  $T_g$  was determined to be between 110.0 - 114.5 °C (Figure 3.11 and Table 3.2) which is within the expected range according to the literature (89 - 130 °C<sup>297–302</sup>). Finally,

the available literature data indicate that PDMA degrades between 350-450 °C<sup>302</sup>, via a one-step degradation profile, forming volatile, small molecules. This is evidenced in Figure 3.12, which shows the degradation profile of PDMA at all bromoform concentrations.

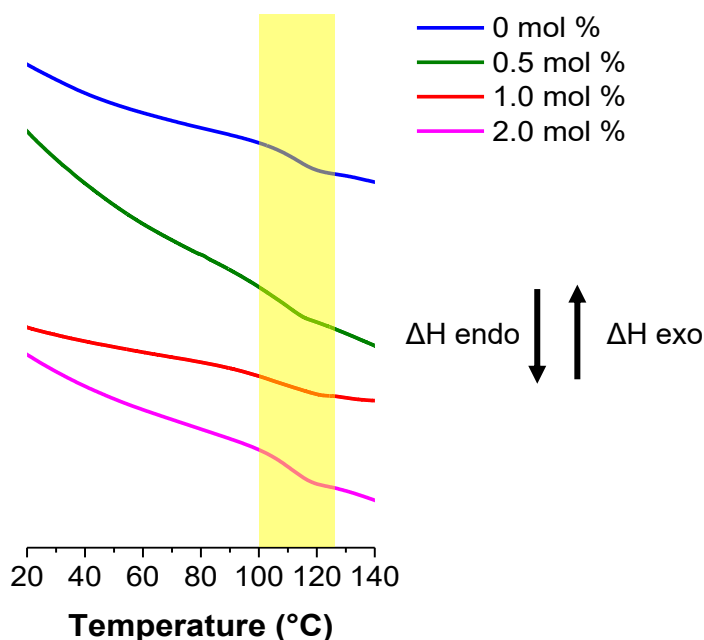


Figure 3.11. DSC thermograms (second heating cycle) for PDMA (synthesised in water) at varying bromoform concentration, highlighting the feature corresponding to the glass transition temperature for each sample.

Table 3.2. Summary of the glass transition temperatures of PDMA (synthesised in water) at varying bromoform concentration (0, 0.5, 1.0 and 2.0 mol % relative to monomer).

Experiment series	Bromoform (mol %) <sup>a</sup>	Onset of $T_g$ (°C)	Endset of $T_g$ (°C)	Midpoint of $T_g$ (°C)
HJH027	0	110	119	114.5
HJH028	0.5	106	114	110.0
HJH029	1.0	104	121	112.5
HJH030	2.0	107	118	112.5

a) Relative to monomer

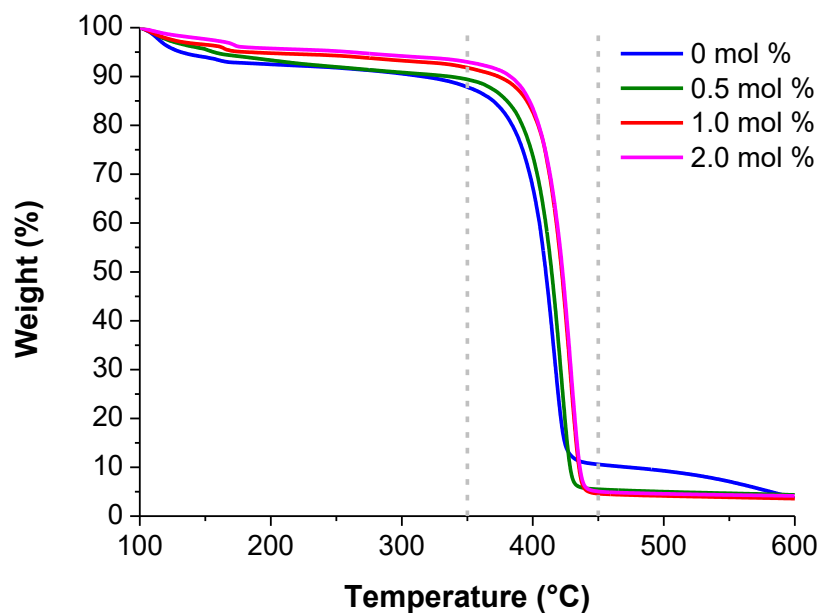


Figure 3.12. TGA degradation profiles for PDMA (synthesised in water) at varying bromoform concentration.

In this study, PDMA has been successfully synthesised at varying bromoform concentration in water. These results suggest that there is no control over the molar mass of the PDMA produced with increasing bromoform content (from 0 - 2.0 mol % relative to monomer). Eliminating the role of bromoform as a CTA for the synthesis of PDMA under the described conditions. Additionally, the rate of the polymerisation is changed negligibly at each bromoform concentration, with no apparent trend observed. The molar mass dispersities in the final samples are relatively high, but there is good reproducibility observed for syntheses conducted at each bromoform concentration.

### 3.4 Bromoform-assisted synthesis of poly(*N,N*-dimethylacrylamide) in DMF

To further build on the work conducted in Section 3.3, another series of PDMA syntheses were conducted at varying bromoform concentration (0, 0.5, 1.0 and 2.0 mol % relative to monomer) and fixed ACPA concentration (1.0 mol % with respect to *N,N*-dimethylacrylamide); this time in DMF. To allow for direct comparison, ACPA concentration, volume of solvent, initial

concentration of monomer and initial temperature (use of ice bath) were identical to those used in the investigation described in Section 3.3. In all cases, experiments were repeated in triplicate. The effect of bromoform on the homopolymerisation was studied by monitoring monomer conversion and molar mass using  $^1\text{H}$  NMR spectroscopy (Figure 3.13 and Appendices 4 - 6) and GPC (Figure 3.14), respectively.

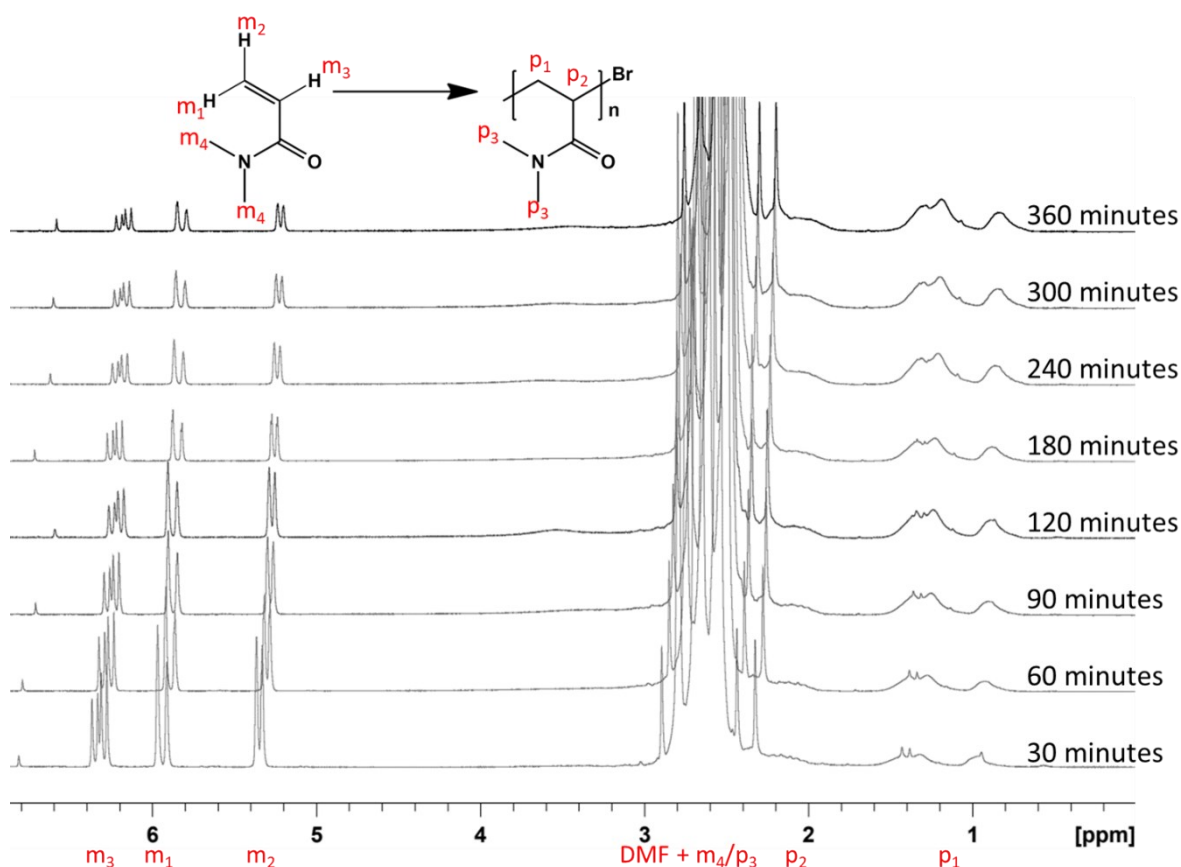


Figure 3.13. Exemplar  $^1\text{H}$  NMR kinetic overlay for the synthesis of PDMA in DMF at 2.0 mol % bromoform showing the disappearance of monomer and broadening of polymer peaks throughout the course of the reaction.

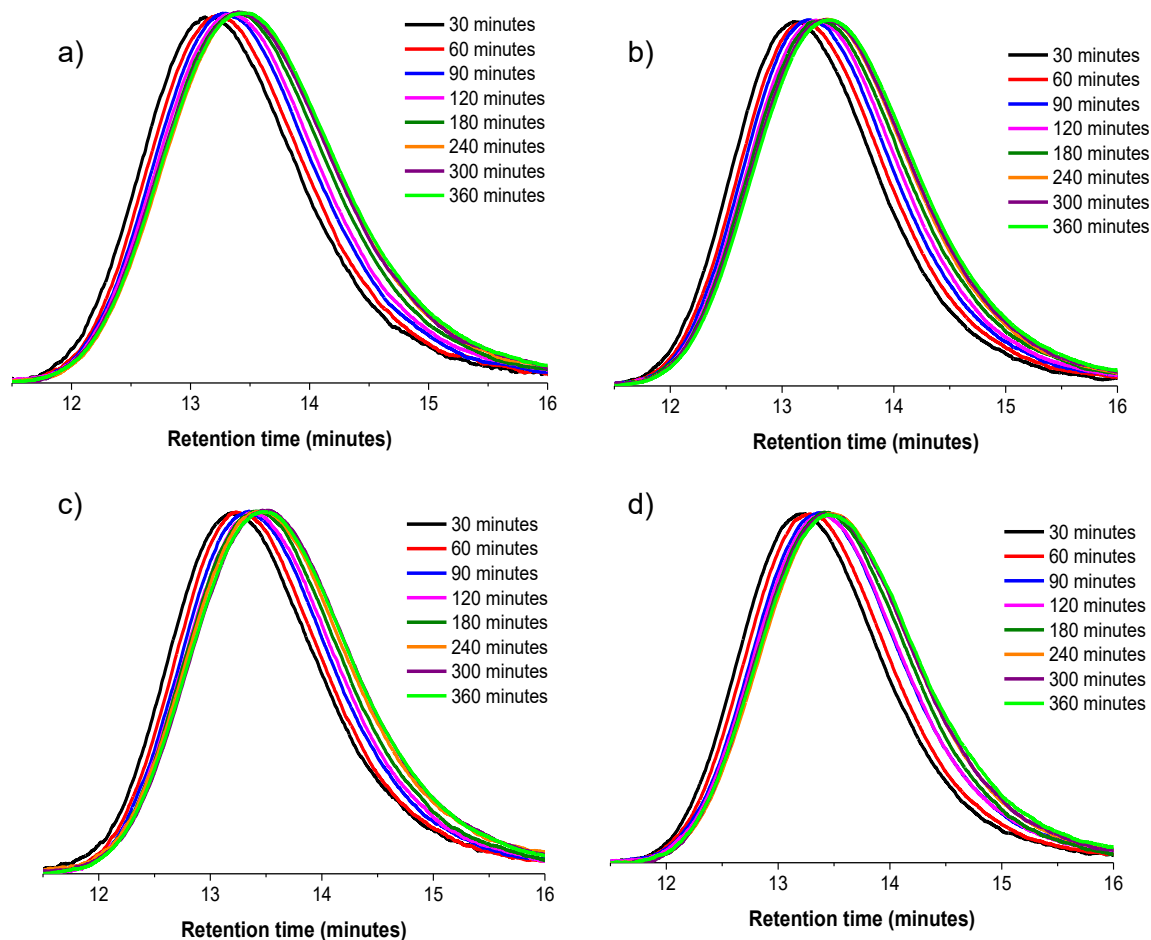


Figure 3.14. Kinetic GPC traces for the synthesis of PDMA in DMF at a) 0, b) 0.5, c) 1.0 and d) 2.0 mol % bromoform concentrations (relative to monomer).

Compared to the equivalent syntheses in water, lower final monomer conversions ( $\geq 77\%$ ) were achieved in each case, even with extended UV exposure times (from 60 to 360 minutes). Similarly, the  $M_n$  of the resulting PDMA appeared to increase upon addition of bromoform before then decreasing with increasing bromoform concentration (see data summarised in Table 3.3). The resulting PDMA, in each case, was isolated by precipitation and dried in a vacuum oven until constant weight was achieved. Excess unreacted monomer was successfully removed after precipitation, as confirmed via  $^1\text{H}$  NMR spectroscopy (Figure 3.15). The peak at 0.8 ppm [labelled with an asterisk (\*)] in the precipitated PDMA is thought to be contributed to by the methyl groups of the ACPA initiator fragment at the  $\alpha$  chain end, from the initiation step in the reaction. Upon further investigation of the PDMA samples produced in the

water studies, a similar peak was also identified (Figure 3.16). The intensity of this peak is reduced when compared to Figure 3.15 due to the significantly higher molar mass of the polymers produced in the water study. Finally, the GPC traces of the purified PDMA synthesised using each bromoform concentration demonstrate that there is good reproducibility between the results (Figure 3.17).

Table 3.3. Summary of final conversion, molar mass, molar mass dispersity and apparent rate constant data for the polymerisation of *N,N*-dimethylacrylamide at varying bromoform concentrations in DMF.

Experiment series	Bromoform content (mol %) <sup>a</sup>	Final monomer conversion (%) <sup>b</sup>	$M_n$ (kg mol <sup>-1</sup> ) <sup>c</sup>	$\bar{D}$ ( $M_w/M_n$ ) <sup>c</sup>	$k_{app}$ (min <sup>-1</sup> )
HJH043	0	77	22.3	2.9	0.0046
HJH044	0.5	80	23.1	2.7	0.0052
HJH045	1.0	81	22.6	2.8	0.0056
HJH046	2.0	83	22.2	2.7	0.0051

a) Relative to monomer

b) Calculated using <sup>1</sup>H NMR spectroscopy and Equation 2.2

c) Determined using DMF GPC with PMMA standards

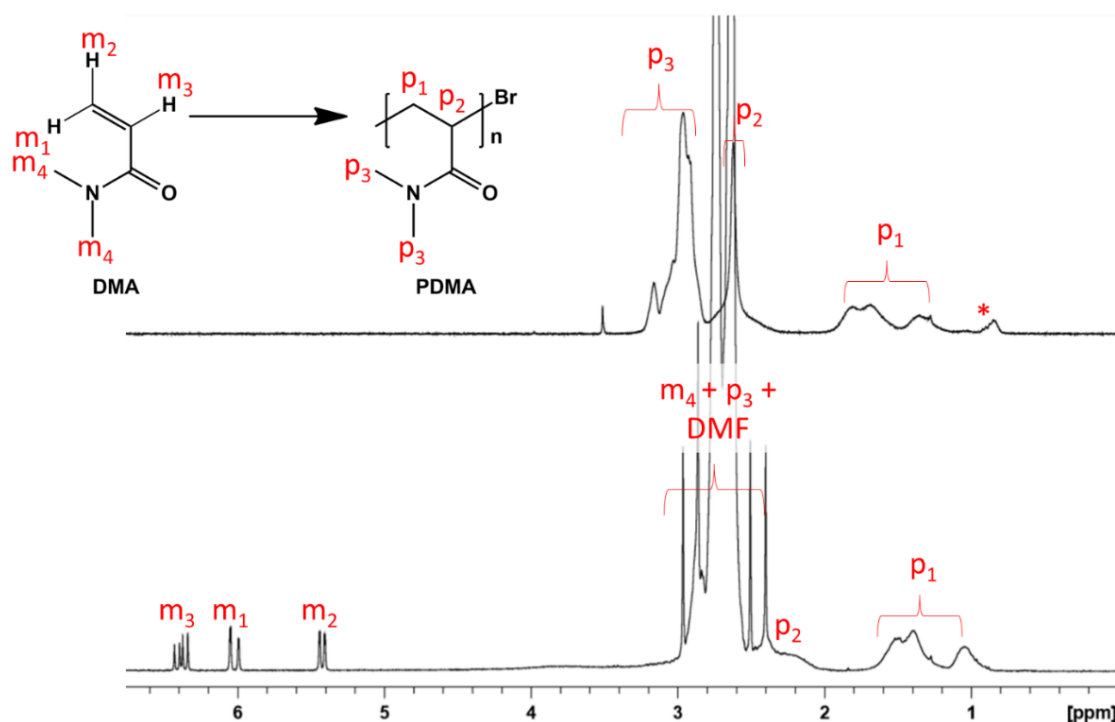


Figure 3.15. Comparative  $^1\text{H}$  NMR spectra (in  $\text{CDCl}_3$ ) showing the disappearance of the monomer vinyl protons (5.7, 6.0 and 6.6 ppm) between crude and precipitated PDMA (2 mol % bromoform, relative to monomer).

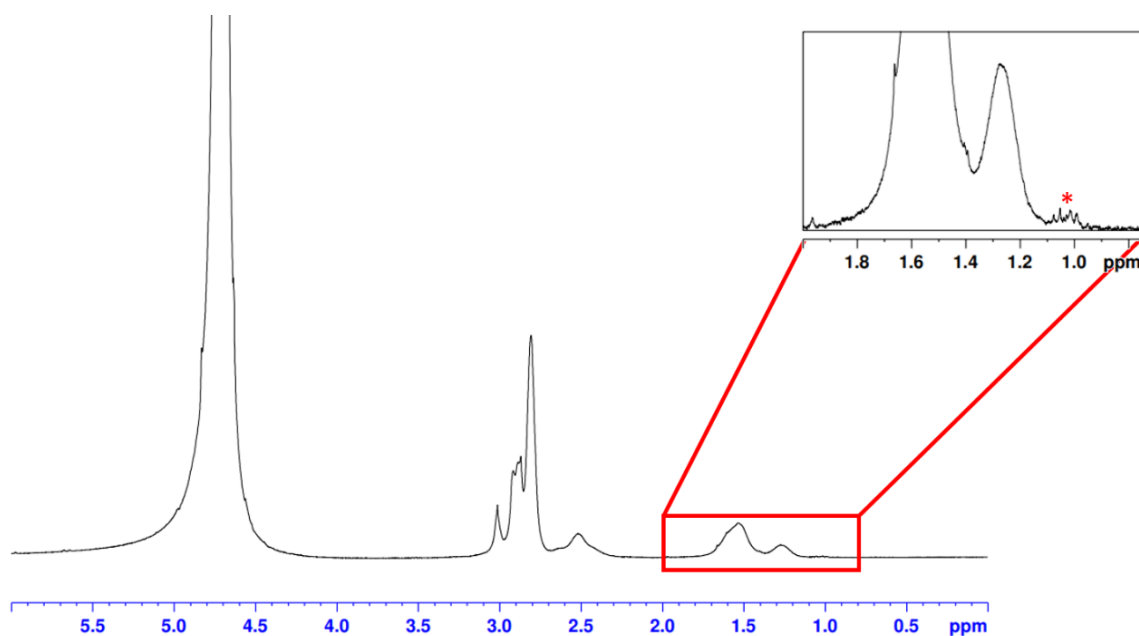


Figure 3.16.  $^1\text{H}$  NMR spectrum (in  $\text{D}_2\text{O}$ ) of PDMA synthesised in water highlighting the presence of a low intensity methyl group peak at approximately 1.0 ppm [labelled with an asterisk (\*)].

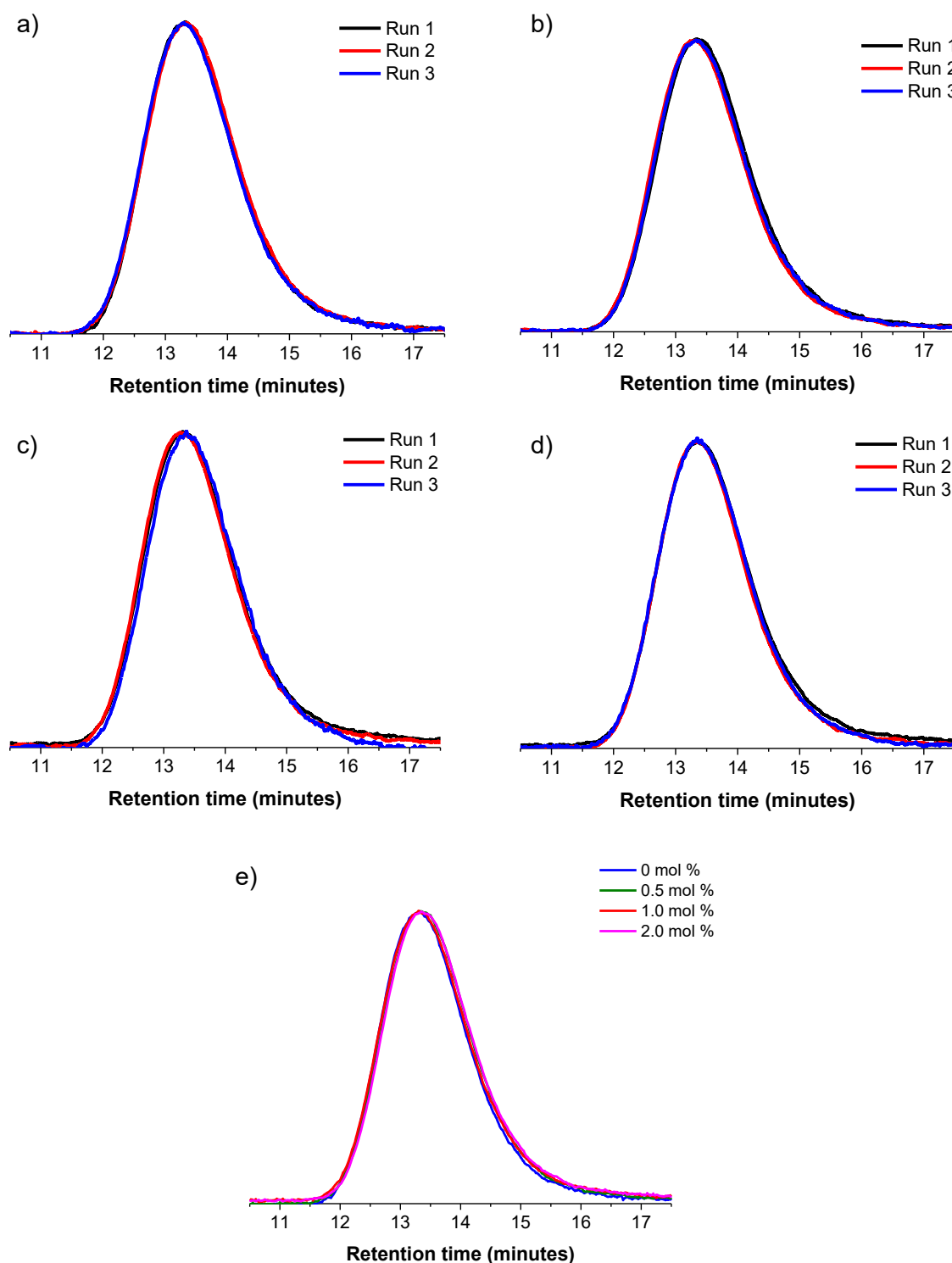


Figure 3.17. GPC traces of PDMA final precipitates at a) 0, b) 0.5, c) 1.0 and d) 2.0 mol % bromoform (relative to monomer, synthesised in DMF) demonstrating good reproducibility between runs and e) near-identical GPC traces of the final precipitate at each bromoform concentration.



The final molar mass of each sample (see Table 3.1) appears to increase on addition of 0.5 mol % bromoform, however, closer inspection of the broad GPC curves indicates that the molar mass profiles for the PDMA synthesised are near-identical in all cases (Figure 3.17). Therefore, it is reasonable to assume that bromoform is not behaving as a chain transfer agent in either the water or DMF studies, for the synthesis of PDMA under the conditions described. In the same way as the polymerisation studies in water, these observations disagree with the previous work conducted by Thananukul *et al.*<sup>212</sup>. In this case bromoform demonstrated successful chain transfer capabilities during the polymerisation of acrylamide; highlighted through the apparent regulation of molar mass with increasing bromoform content. However, as previously described the system discussed herein differs to the Thananukul *et al.* study as an ice bath has been used to provide control over the temperature of the reaction. In the Thananukul *et al.*<sup>212</sup> study, temperatures of up to 50 °C are reported during the 60 minutes of UV irradiation that the reaction solutions are exposed to. Therefore, significant thermal effects could be the reason that bromoform exhibited CTA capabilities in their work.

In the same way as the polymerisations in water, the kinetic studies in DMF (Table 3.3, Figure 3.18 and Figure 3.19) show that bromoform has little influence over the apparent rate constant for each reaction, as they are near-identical in all cases. Moreover, the molar mass dispersity,  $\bar{D}$ , of the final polymers remains high (2.7 - 2.9), with no suggested relationship between molar mass dispersity and bromoform content. Interestingly, this conversion data (determined from <sup>1</sup>H NMR and Equation 2.2) has identified the presence of an induction period of up to 60 minutes during the DMF reactions (Figure 3.18); regardless of whether bromoform is present or not.

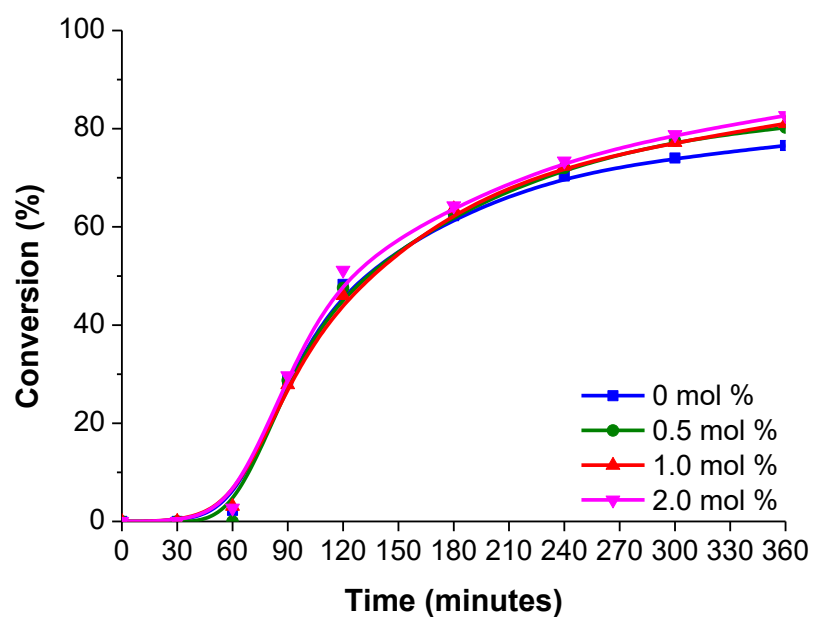


Figure 3.18. Monomer conversion *versus* time for the synthesis of PDMA at varying bromoform concentrations in DMF.

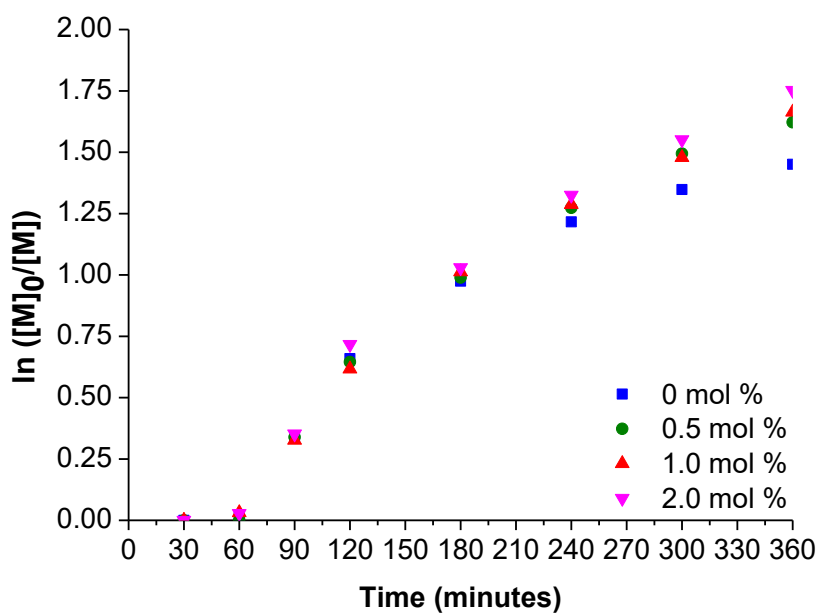


Figure 3.19. Semi-logarithmic plot for the synthesis of PDMA at varying bromoform concentration in DMF.

Figure 3.20 indicates that the molar mass of PDMA decreases as the polymerisation proceeds for all bromoform concentrations used. As previously discussed, this is a typical observation in free radical polymerisations<sup>294–296</sup>. In addition, the GPC data for the kinetic studies at 30 and 60 minutes show traces at low retention times for all bromoform concentrations (Figure 3.14). This indicates that high molar mass chains have been formed early on in the reactions and the induction periods observed in Figure 3.18 are present due to the limitations of the  $^1\text{H}$  NMR spectra at low monomer conversions ( $\leq 10\%$ ).

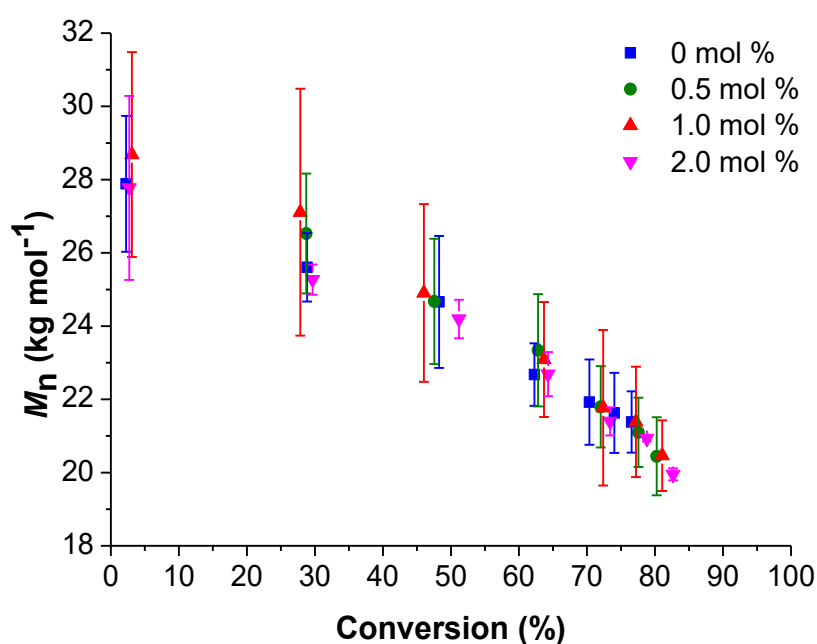


Figure 3.20.  $M_n$  versus monomer conversion for the synthesis of PDMA at varied bromoform concentrations in DMF (error bars represent the standard deviation of the triplicate data).

Notably, the final molar masses seen in the DMF formulation ( $22.2 - 23.1 \text{ kg mol}^{-1}$ ) were considerably lower than those achieved when using water as the solvent ( $242.3 - 294.8 \text{ kg mol}^{-1}$ ), even with the considerably extended UV irradiation period (increased from 60 to 360 minutes). Solvent effects on the rate of reaction and molar mass of radical polymerisations have been described in the literature. More specifically, solvent effects on the initiation stage has been described for acrylamide monomers; suggesting that more polar solvents accelerate the initiator decomposition which in turn triggers the propagation stage of the reaction.

Changes in the propagation rate ( $k_p$ ) have also been attributed to solvent effects due to hydrogen bonding<sup>273,303–307</sup>, electron interactions<sup>303,308</sup> and the stability of the growing radical<sup>309</sup>. Less prominent solvent interactions originating from solvent size, monomer concentration and steric effects have shown less pronounced variations in  $k_p$ <sup>310</sup>. Many studies have suggested that in more polar solvents (such as water) the rate of reaction is greater than in less polar solvents (such as DMF). A study specifically investigating the solvent effect on PDMA synthesis concluded that there is significant enhancement of the rate of reaction in water due to the increased reactivity of the monomer double bond. This is a result of hydrogen bonding present at the carbonyl group (on the amide) with water<sup>273</sup> which has been described for a variety of monomers with amide groups<sup>306</sup> including DMA<sup>307</sup> and NIPAM<sup>304,305</sup>. This effect, whilst still present in many organic solvents, is significantly reduced and results in a decrease in the rate of reaction. Additionally, the effect of solvent on a thiol chain transfer agent was also discussed in this study; describing an appreciable difference in the final molar mass of the PDMA when moving from less polar (organic) to polar (water) solvents<sup>273,311</sup>. The CTA is less efficient in water and therefore provides less control over the final molar mass of the polymer produced.

In the investigation described herein there is a clear solvent effect when moving from water to DMF. The shorter reaction time and faster rate of reaction observed, in water, is likely due to the increased reactivity of the monomer double bond due to the aforementioned hydrogen bonding at the carbonyl in the amide. With regards to the difference in the molar mass observed, this could be a result of a more significant interaction of bromoform with water, compared to DMF which ultimately results in less control during the reaction and polymers with greater molar masses being produced. Additionally, the lower final conversions achieved, in the DMF study, also contribute to the differences observed in the final molar masses.

### **3.4.1 Thermal properties**

As previously described, in preparation for the synthesis of PDMA-*b*-PNIPAM the resulting PDMA samples were purified by precipitation and further characterised via DSC and TGA to

determine the glass transition temperature and degradation profile, respectively. These results were then collated for later comparison to identify any changes between the properties of the homopolymers and any subsequent block copolymers that may be synthesised.

Like the polymerisations conducted in water, the  $T_g$  was determined to be within the known literature range (89 - 130 °C<sup>297–302</sup>); more specifically between 115.5 - 122.0 °C (Figure 3.21 and Table 3.4). Additionally, the degradation profiles, shown in Figure 3.22, are also near-identical to those produced in the water study; confirming that the samples degrade between 350 and 450 °C<sup>302</sup> as expected.

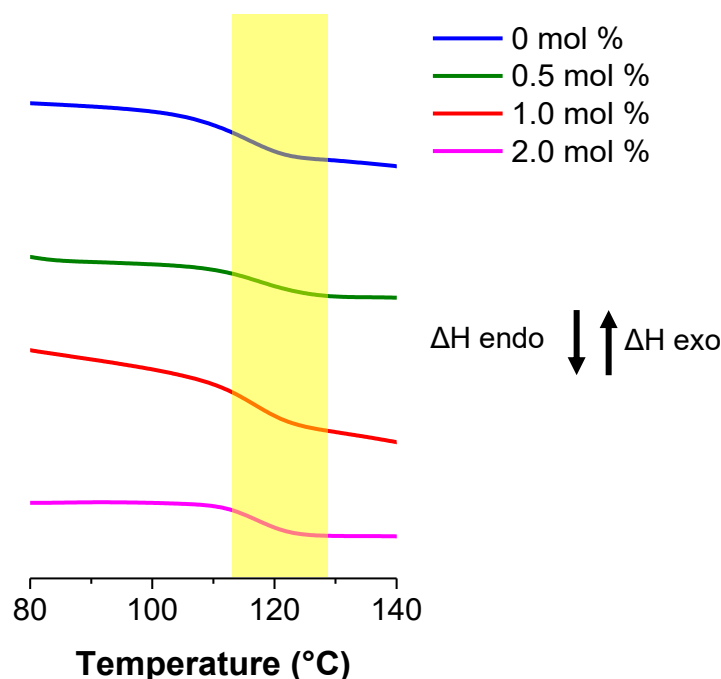


Figure 3.21. DSC thermograms (second heating cycle) for PDMA (synthesised in DMF) at varying bromoform concentrations highlighting the glass transition temperature for each sample.

Table 3.4. Summary of the glass transition temperatures of PDMA (synthesised in DMF) at varying bromoform concentrations (0, 0.5, 1.0 and 2.0 mol % relative to monomer).

Experiment series	Bromoform (mol %) <sup>a</sup>	Onset of $T_g$ (°C)	Endset of $T_g$ (°C)	Midpoint of $T_g$ (°C)
HJH043	0	112	119	115.5
HJH044	0.5	119	125	122.0
HJH045	1.0	115	123	119.0
HJH046	2.0	118	125	121.5

a) Relative to monomer

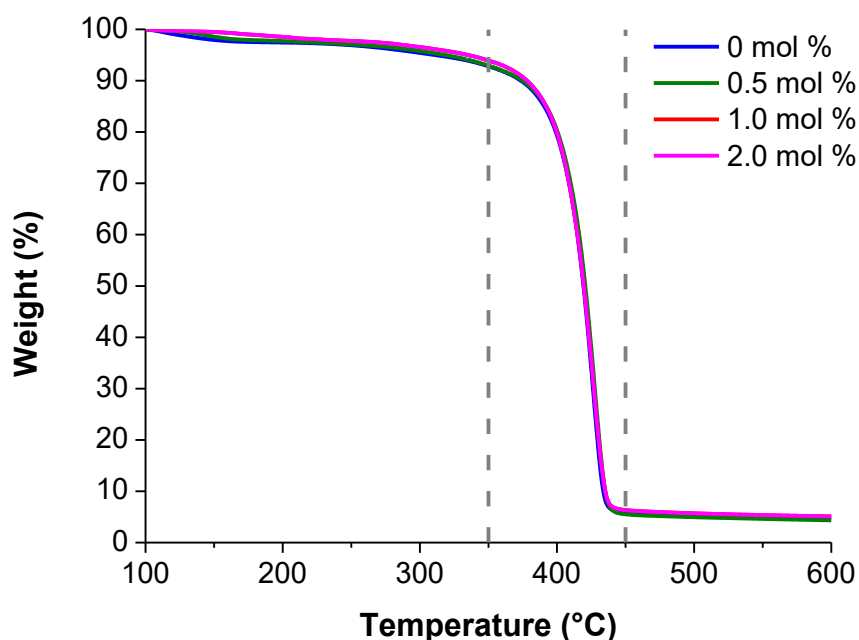


Figure 3.22. TGA degradation profile for PDMA (synthesised in DMF) at varying bromoform concentrations.

The DMA homopolymerisations at varying bromoform concentration described in this section uncover an apparent solvent effect, when moving from water to DMF. The rate of reaction was significantly decreased when using DMF and the reaction time had to be increased, from 60 to 360 minutes, in order to achieve significant monomer conversion ( $\geq 77\%$ ). Additionally, a significant decrease in molar mass was observed, even with the extended UV irradiation. The final molar masses suggest that bromoform is not behaving as a CTA for the reactions

described herein; as the molar mass would be expected to decrease with increasing bromoform content. However, the final GPC traces are near-identical at all bromoform concentrations.

### 3.5 Polymerisations conducted in the absence of photoinitiator (ACPA)

As described in Sections 3.3 and 3.4, PDMA can be synthesised at varying bromoform concentrations when the photoinitiator ACPA is also present in the system. The next stage of this investigation was to determine whether bromoform itself could also behave as a photoinitiator under these conditions. In the previous work of Miller<sup>208</sup>, Dunn *et al.*<sup>209</sup> and Wu *et al.*<sup>211</sup> bromoform (amongst other similar bromine-containing compounds) is described as a photoinitiator. In the case of work described by Miller<sup>208</sup>, it is claimed that bromoform, dibromomethane and monobromomethane are all sources of Br<sup>•</sup> radicals, upon irradiation with UV light, that can successfully initiate the homopolymerisations of acrylonitrile and acrylic acid. However, in a control experiment, acrylonitrile was shown to self-polymerise in the absence of a known radical source. This calls into question the claim that bromoform initiated these reactions rather than simply a self-polymerisation reaction occurring. Additionally, there is no indication that the temperature of the reaction is controlled in these experiments. Miller states that the UV lamp used can heat the reaction solution to up to 50 °C (over a 3 hour period)<sup>208</sup>. Heat contributions from the UV lamp cannot be assumed to be negligible, and could provide enough energy for initiation to occur using the bromine radicals produced. Moving onto the work of Dunn *et al.*<sup>209</sup>, the Br<sup>•</sup> radicals are generated from bromotrichloromethane or carbon tetrabromide. In both cases, Dunn *et al.* claim that the Br<sup>•</sup> radicals are capable of initiating the polymerisation of styrene, when the only other reagents present are monomer and solvent. Additionally, a control reaction conducted in this study suggests that styrene will not self-polymerise under the described conditions. Furthermore, Dunn *et al.* demonstrated that the rate of the reaction increases when the concentration of carbon tetrabromide is increased, providing further evidence that the bromine radicals are initiating this reaction. However, the temperature of the styrene polymerisation is not controlled and Dunn *et al.* commented on the

added complication of side reactions that could also be occurring. They suggest that hydrogen chloride or hydrogen bromide are produced which can result in the introduction of more halogen atoms into the polymer than would be expected; ultimately causing retardation of the reaction. Finally, in the case of Wu *et al.*<sup>211</sup>, acrylamide, AMPS and acrylic acid were copolymerised in the presence of bromoform and in some cases DMF solvent. In this case there was no discussion on whether the acrylamide, AMPS or acrylic acid were able to self-polymerise under the described conditions. As with the research of Miller and Dunn *et al.*, there was no attempt to control the temperature of the reaction solution under UV irradiation. It could therefore be assumed that the AMPS and acrylic acid could be initiated by the bromine radicals produced in addition to the thermal effects on the reaction over the 4.5 hours of UV irradiation to which they are subjected<sup>211</sup>. Notably, many of the reactions described in the preliminary literature involve more reactive monomers which could be a contributing factor to the apparent initiation using bromine-containing compounds.

A secondary study was therefore conducted whereby PDMA was targeted at varying bromoform concentrations (0, 0.5, 1.0 and 2.0 mol % relative to monomer) in the absence of ACPA photoinitiator. Water was used as the solvent and all other conditions, including volume of water, initial concentration of monomer, temperature (use of ice bath) and UV exposure time were identical to those used in the investigation described in Section 3.3.

Figure 3.23 depicts the final <sup>1</sup>H NMR spectrum for polymerisations conducted at each bromoform concentration and shows that the reaction solution does not contain polymer after 60 minutes of UV irradiation in each case. This is unlike the kinetic study shown in Figure 3.4, where the intensity of the monomer peaks reduces and the polymer peaks increases over time. To further confirm that these polymerisations were unsuccessful, GPC traces were obtained. Indeed, there was no peak present to indicate polymer formation had occurred (Figure 3.24). This evidence suggests that bromoform-derived radical species that are capable of initiating DMA polymerisation are not generated under the described conditions and thus the photopolymerisation of *N,N*-dimethylacrylamide cannot proceed. Additionally, the reaction



with no ACPA and 0 mol % bromoform indicates that *N,N*-dimethylacrylamide will not self-polymerise under the described conditions (Figure 3.23).

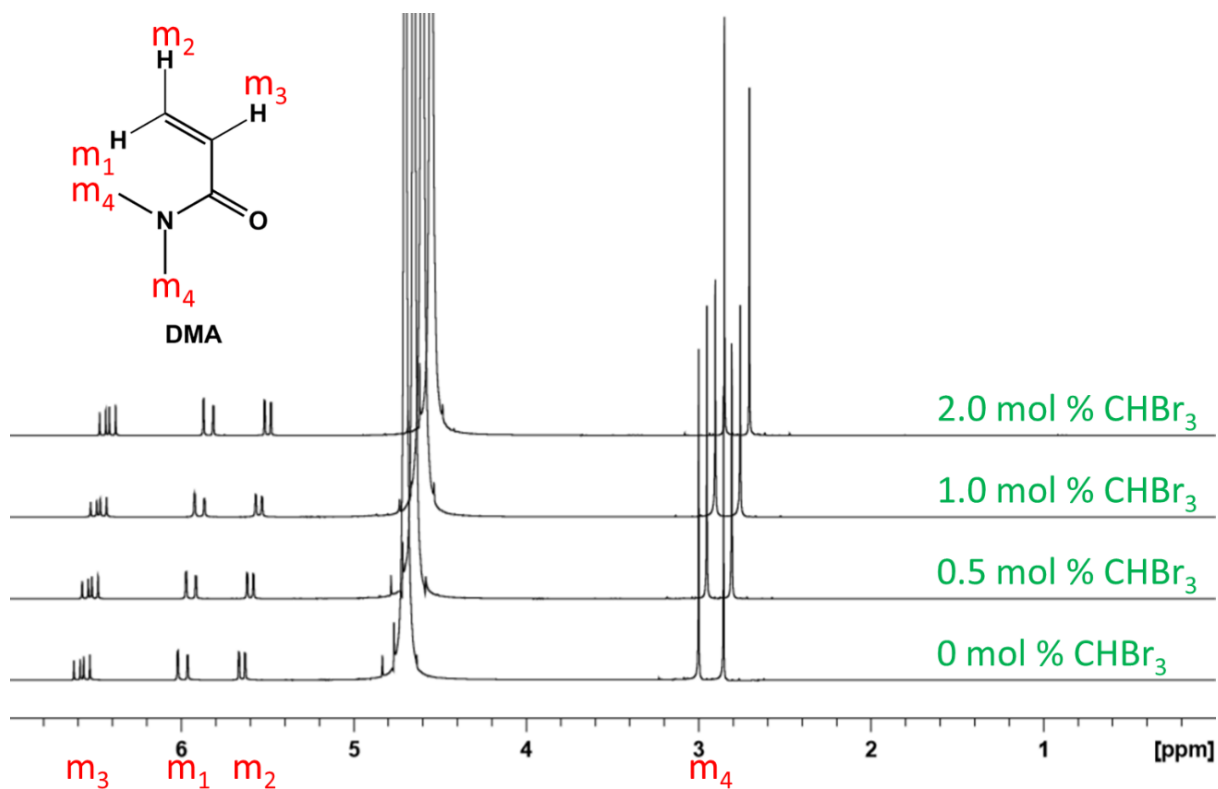


Figure 3.23. Final <sup>1</sup>H NMR spectra for the attempted synthesis of PDMA in the absence of ACPA photoinitiator at varying bromoform concentrations (0, 0.5, 1.0 and 2.0 mol % relative to monomer) in water.

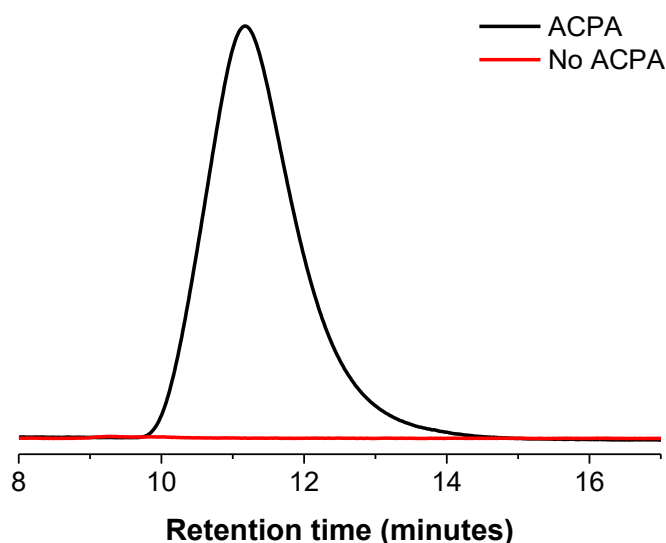


Figure 3.24. Example of the GPC traces obtained for the synthesis of PDMA with ACPA (black) and in the absence of ACPA (red) both at 2 mol % bromoform (relative to monomer).

Whilst the observation that bromoform is not capable of initiating the polymerisation of *N,N*-dimethylacrylamide is not in agreement with some findings in the literature, it does corroborate the more recent work of Thananukul *et al.*<sup>212</sup>. Similarly, bromoform is deemed incapable of acting as a photoinitiator in the homopolymerisation of acrylamide at varying bromoform concentrations. Interestingly, no evidence of temperature control is described in the Thananukul *et al.*<sup>212</sup> study.

### 3.6 Synthesis of PDMA in the presence of air

Upon determining that the polymerisation of *N,N*-dimethylacrylamide will not proceed in the absence of ACPA photoinitiator, under the conditions investigated herein, a final study was conducted to investigate the influence of oxygen on the polymerisations. The purpose of this investigation was to determine the need of running the reactions under an inert atmosphere; as it is more beneficial and cost effective for industrial scale-up if the reactions can be completed in the presence of air. Four reaction formulations were set up using 0, 0.5, 1.0 and 2.0 mol % bromoform (relative to monomer), and whilst the flasks were sealed with a rubber septum, they were not subjected to oxygen removal via vacuum-nitrogen cycles. Water was

used as the solvent and all other conditions, including ACPA concentration, volume of water, initial concentration of monomer, initial temperature (use of ice bath) and UV exposure time, were identical to those used in the investigations described in Section 3.3.

Figure 3.25 shows the percentage monomer conversion with time for each of the four bromoform concentrations investigated. This graph suggests that whilst there is now a significant induction period, polymerisation still proceeds. Notably, there does not appear to be a relationship between bromoform concentration and the length of the induction period, although there was a difference between reactions. Polymerisation was observed to begin between 15 and 30 minutes of UV exposure for formulations containing 0.5 and 2.0 mol % bromoform, whereas reactions containing 0 and 1.0 mol % bromoform begin to polymerise between 30 and 45 minutes of UV exposure.

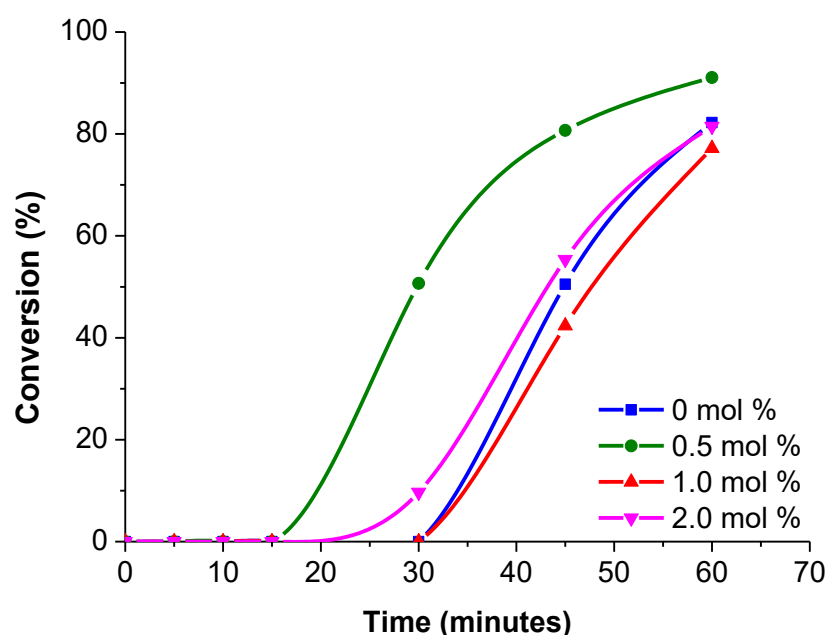


Figure 3.25. Monomer conversion *versus* time for the synthesis of PDMA at varying bromoform concentrations in the presence of air.

The effect of the presence of oxygen in free radical polymerisation formulations has been extensively discussed in the literature<sup>312–316</sup>. Oxygen is an excellent free radical scavenger<sup>266</sup> and can react with initiating or propagating radicals to form the typically unreactive peroxy

radical<sup>314,316</sup>. This results in extended induction periods, as demonstrated herein, or termination of growing polymer chains within a polymerisation reaction<sup>314,316</sup>. In this example, for the polymerisation of *N,N*-dimethylacrylamide, there is an observed induction period of  $\geq 15$  minutes upon UV exposure at each bromoform concentration (0, 0.5, 1.0, 2.0 mol % relative to monomer).

ACPA (or possibly bromoform-derived) radicals that are generated during the reaction may interact with the oxygen present in the reaction flask. Bromoform is known to react with oxygen via several different mechanisms under varying conditions. Of particular relevance, reactions of tribromomethyl ( $\text{Br}_3\text{C}^\bullet$ ) and dibromomethyl ( $\text{Br}_2\text{HC}^\bullet$ ) radicals can occur with molecular oxygen ( $\text{O}_2$ )<sup>317,318</sup>. As previously discussed, bromoform can undergo dissociation into  $\text{Br}_2\text{HC}^\bullet$  and  $\text{Br}^\bullet$  radicals upon UV irradiation, or hydrogen transfer, whereby  $\text{Br}_3\text{C}^\bullet$  and  $\text{H}^\bullet$  are produced. It was already determined in Section 3.5 that these radicals ( $\text{Br}_2\text{HC}^\bullet$ ,  $\text{Br}^\bullet$ ,  $\text{Br}_3\text{C}^\bullet$  and  $\text{H}^\bullet$ ) are not capable of initiating the polymerisation of *N,N*-dimethylacrylamide under the described conditions. However, the  $\text{Br}_3\text{C}^\bullet$  and  $\text{Br}_2\text{HC}^\bullet$  radicals produced are known to react rapidly with  $\text{O}_2$  to form tribromomethyl and dibromomethyl peroxy radicals, respectively. These radicals are then known to decompose in water to form a combination of  $\text{H}^+$ ,  $\text{Br}^-$ ,  $\text{CO}$  and  $\text{CO}_2$ . Additionally, ACPA is also known to react with  $\text{O}_2$  to form unreactive peroxide radicals which can self-terminate through combination<sup>319</sup>, either between two ACPA peroxide radicals or the ACPA peroxide radical and another radical in the system. This second radical could be an ACPA-derived radical not involved in a reaction with  $\text{O}_2$  or one of the many radicals formed from UV-induced bromoform dissociation as previously described.

As the flask was sealed with a rubber septum the polymerisation still proceeded once the oxygen that was present had been consumed. The difference in the time taken for the polymerisation to begin could be due to variations in the residual oxygen dissolved in the reaction solution, which has also been described elsewhere during the radical polymerisation of other acrylamide monomers<sup>212,312,315</sup>. Additionally, the quantity of oxygen present in the flask may exhibit some routine variation, resulting in the differing induction periods observed.

Using the available monomer conversion data, a semi-logarithmic plot (Figure 3.26) was produced to determine the rate of each reaction. As with the inert atmosphere, there appears to be no relationship between bromoform content and the resulting rate of polymerisation. However, when comparing the calculated values for  $k_{app}$  under the inert atmosphere and in the presence of air, the rate decreased by approximately half in all cases (Table 3.5).

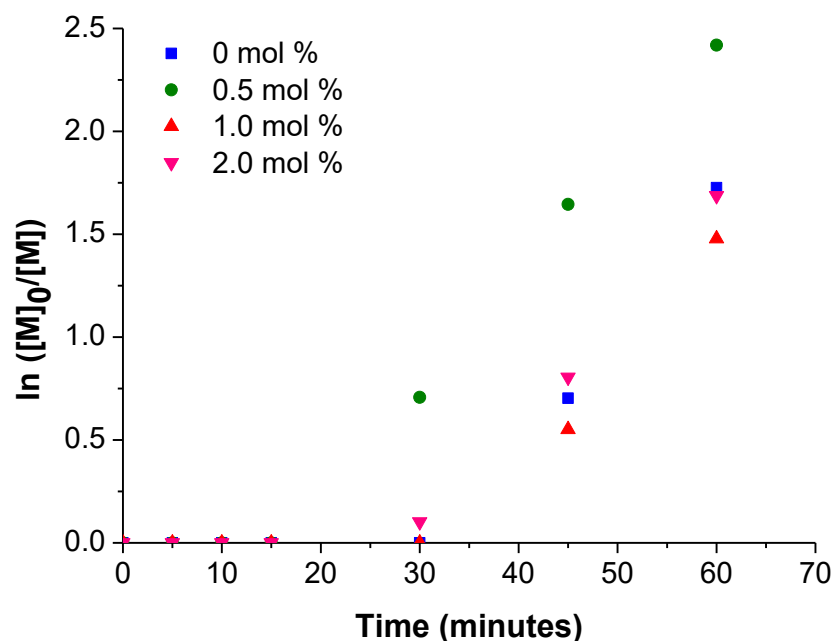


Figure 3.26. Semi-logarithmic plot used to demonstrate the relationship, or lack thereof, between bromoform concentration and the rate of the reaction in the presence of air.

The apparent decrease (by half) in  $k_{app}$  between the inert and air atmospheres further suggests that it is the ACPA-derived radicals that are interacting with oxygen in the flask. The decrease in active ACPA radicals would result in the observed decrease in polymerisation rate, since fewer initiating radicals will result in fewer polymer chains being initiated and thus propagating at any one time. In turn, this will also result in a slower rate of monomer consumption<sup>44</sup>, meaning that the molar mass of the final polymers synthesised in the presence of air should appear larger than those under the inert atmosphere at similar monomer conversions (%)<sup>320</sup>.

Table 3.5. Apparent rate constant data at varying bromoform concentrations under inert atmosphere (i.e. oxygen-free) *versus* in the presence of air (not degassed but sealed prior to UV irradiation) for the homopolymerisation of *N,N*-dimethylacrylamide.

Experiment series	Bromoform content (mol %) <sup>a</sup>	$k_{app}$ inert atmosphere (min <sup>-1</sup> )	$k_{app}$ in the presence of air (min <sup>-1</sup> ) <sup>b</sup>
HJH027	0	0.14	0.068
HJH028	0.5	0.12	0.057
HJH029	1.0	0.13	0.062
HJH030	2.0	0.12	0.053

a) Relative to initial monomer concentration

b) Flask sealed but oxygen not removed

For the system exposed to air, the GPC data indicate that once the induction period has passed, the molar mass of the polymers is initially high before decreasing over time (Figure 3.27). This phenomenon has previously been discussed and is a typical observation in free radical polymerisation systems<sup>294–296</sup>. As expected, the molar mass of the polymers synthesised in the systems where 0, 0.5 and 2.0 mol % bromoform was present appears to be larger than that observed at similar conversions (%) for the polymerisations conducted in the absence of air (Figure 3.28). It is only at the 1.0 mol % bromoform concentration reaction where the molar mass is lower than that observed when the polymerisation is conducted in the absence of air.

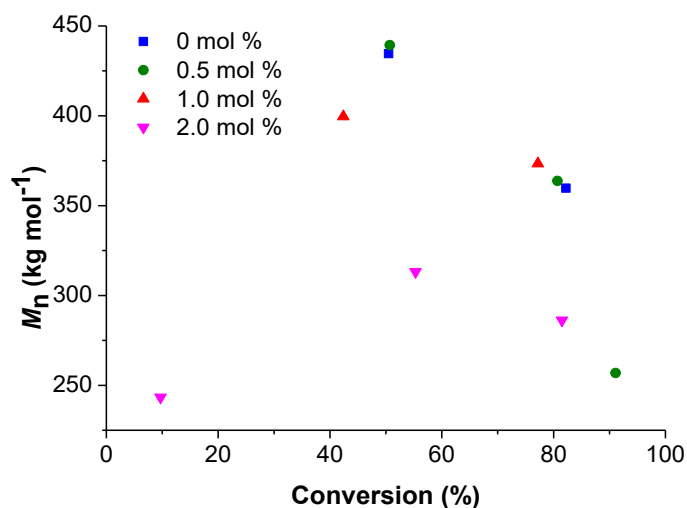


Figure 3.27.  $M_n$  versus monomer conversion for the synthesis of PDMA at varying bromoform concentrations in the presence of air.

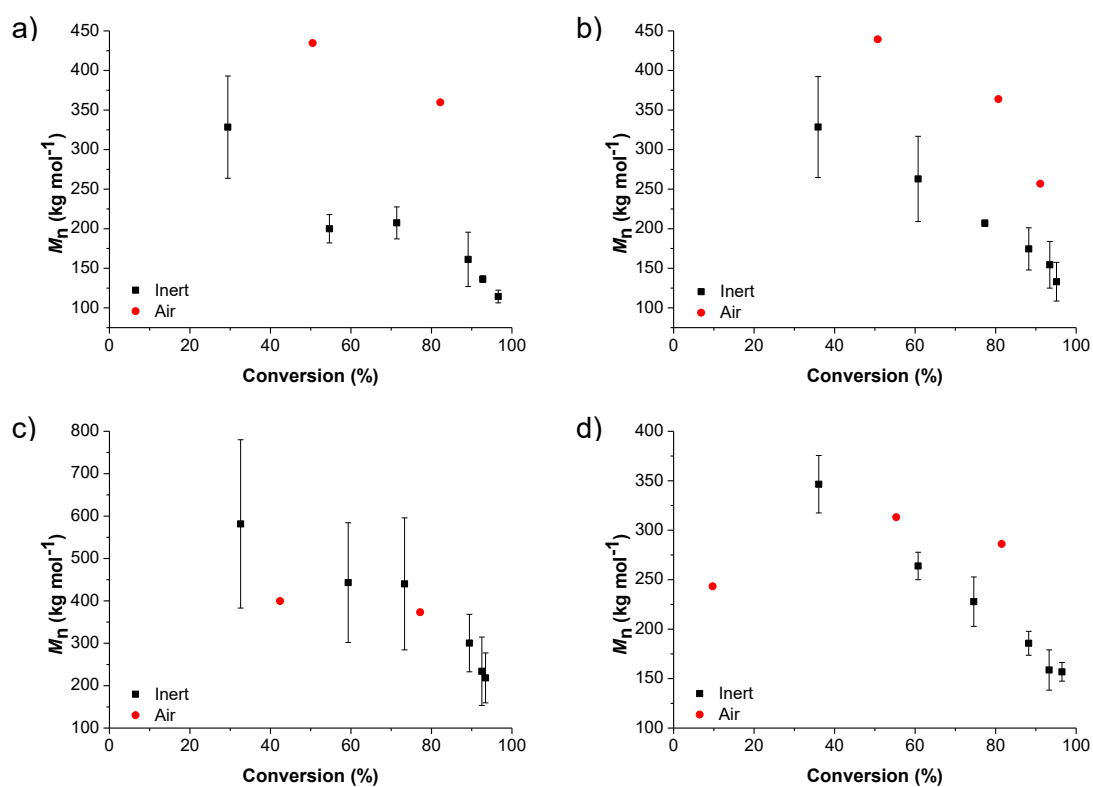


Figure 3.28. Molar mass versus monomer conversion for the synthesis of PDMA at varying bromoform concentrations a) 0, b) 0.5, c) 1.0 and d) 2.0 mol % bromoform (relative to monomer) under inert atmosphere (black squares - error bars represent the standard deviation of the triplicate data) and in the presence of air (red circles).

During this investigation, the effect of oxygen on the reaction system has been explored; significantly an induction period was identified ( $\geq 15$  minutes) for all reactions. The interactions of oxygen with bromoform and ACPA have been reviewed extensively and justify the need for degassing (via vacuum-nitrogen cycles) in order to eliminate oxygen from future syntheses of PDMA macro-initiators.

### 3.7 Reaction scale-up

In order to obtain enough PDMA macro-initiator for efficient block copolymer studies, the homopolymerisation reaction was scaled up by a factor of ten to produce 20 g of polymer. Using the results obtained in Section 3.3, it was determined that the reaction with 2 mol % bromoform offered the opportunity for the highest proportion of potentially bromine-terminated chains to be formed within the usable bromoform miscibility range. Therefore, 2 mol % bromoform was used during the synthesis of 20 g PDMA macro-initiator for the purpose of synthesising poly(*N,N*-dimethylacrylamide)-*block*-poly(*N*-isopropylacrylamide) [PDMA-*b*-PNIPAM] block copolymers (see Chapter 5).

In all cases,  $^1\text{H}$  NMR spectroscopy and GPC data were obtained for the PDMA macro-initiators used in subsequent block copolymer reactions and are summarised in Table 3.6. For experiments HJH031 (macro-initiator used in the one-pot investigation) and 36 (macro-initiator used in the two-step investigation), the reaction reached  $\geq 91$  % conversion. In experiment HJH038 (macro-initiator used in a secondary two-step investigation), the reaction was stopped at 70 % conversion in an attempt to increase the number of bromine-terminated polymer chains. This approach was informed by the literature related to controlled radical polymerisation methods [such as reversible addition-fragmentation chain transfer (RAFT) polymerisation, atom transfer radical polymerisation (ATRP) and nitroxide-mediated polymerisation (NMP)], during which chain ends are often lost under monomer starved conditions (at high conversions, i.e.  $\geq 90$  %) to side reactions<sup>321–325</sup>.



Table 3.6. Summary of final monomer conversion, molar mass and molar mass dispersity data for the polymerisation of *N,N*-dimethylacrylamide using 2 mol % bromoform targeting 20 g of macro-initiator (synthesised in water).

Experiment code	Final monomer conversion (%) <sup>a</sup>	$M_n$ (kg mol <sup>-1</sup> ) <sup>b</sup>	$\bar{D}$ <sup>b</sup>
HJH031	99	143.6	3.6
HJH036	91	148.4	3.9
HJH038	70	324.7	2.8

a) Calculated using <sup>1</sup>H NMR spectroscopy and Equation 2.1

b) Determined using DMF GPC with PMMA standards

The GPC data obtained shows that macro-initiators at  $\geq 91$  % conversion were synthesised in the molar mass region 143.6 - 148.4 kg mol<sup>-1</sup> with relatively high dispersities in the range of 3.6-3.9. This is not dissimilar to the molar mass and molar mass dispersity values obtained during the kinetic study (targeting 2 g of PDMA macro-initiator) described in Section 3.2. The macro-initiator at 70 % targeted monomer conversion had a significantly higher molar mass of 324.7 g mol<sup>-1</sup>. Figure 3.10 (see Section 3.2) suggests that the significantly larger molar mass, at 70 % conversion, is not dissimilar to that observed in the kinetic studies of the small scale (2 g) kinetic reactions that were previously conducted; where the  $M_n$  observed at 70 % conversion is approximately double that seen when the reaction reaches high (> 90 %) conversion.

The  $T_g$  of the PDMA samples synthesised at larger scale was determined using DSC (as described in Section 2.4.3). Figure 3.29 shows the DSC thermogram for each PDMA macro-initiator, identifying the region in which the glass transition occurs. Table 3.7 summarises all of the PDMA macro-initiators synthesised at the larger scale and demonstrates that the  $T_g$  is within the literature range (89 - 130 °C<sup>297-302</sup>). There is a small observed molar mass

dependence of  $T_g$  with the higher molar mass PDMA macro-initiators exhibiting higher  $T_g$  values.

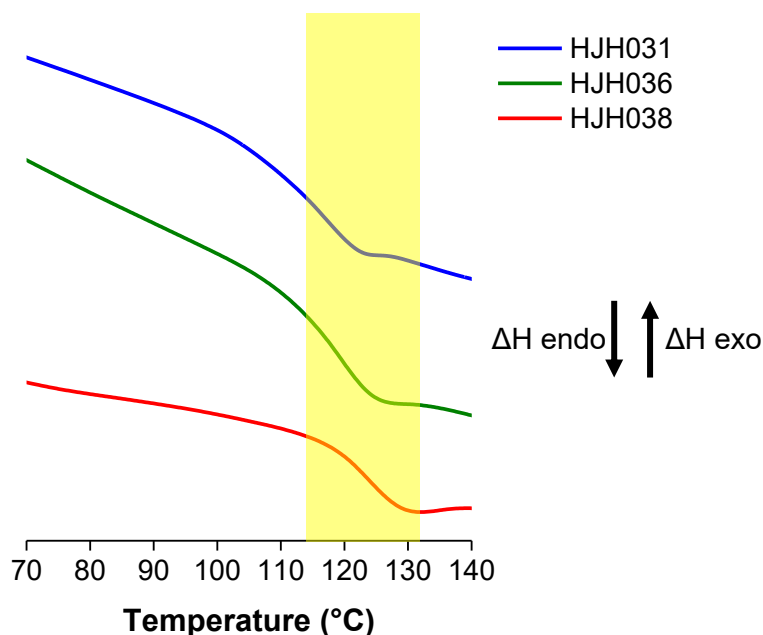


Figure 3.29. DSC thermogram of PDMA macro-initiators (synthesised in water) to be used in block copolymer reactions.

Table 3.7. Summary of the glass transition temperatures for the PDMA macro-initiators synthesised at larger scale (water syntheses).

Experiment series	Onset of $T_g$ (°C)	Endset of $T_g$ (°C)	Midpoint of $T_g$ (°C)
HJH031	110	122	116.0
HJH036	116	125	120.5
HJH038	121	128	124.5

Finally, the available literature data indicate that PDMA macro-initiators degrade between 350 and 450 °C<sup>302</sup> via a one-step degradation profile, forming volatile, small molecules. This is evidenced in Figure 3.30 which shows the degradation profile for all PDMA macro-initiators synthesised at the larger scale.

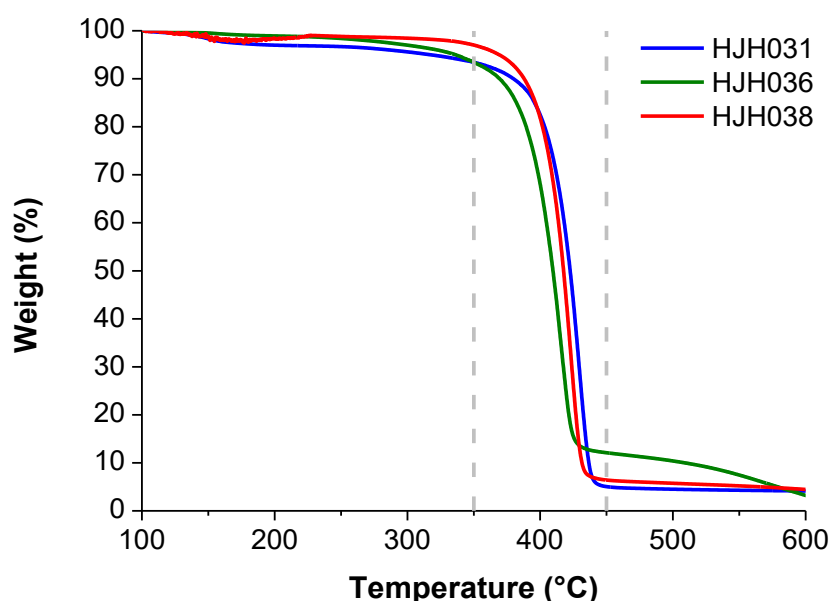


Figure 3.30. TGA degradation profile for PDMA macro-initiators (synthesised in water at larger scale) to be used in block copolymer reactions.

The purpose of this characterisation was to confirm that the thermal properties of the macro-initiators were consistent with those reported in the literature and the small scale kinetic studies, for later comparison to any PDMA-*b*-PNIPAM copolymers that may be produced.

### 3.8 Conclusions

This chapter describes the synthesis of poly(*N,N*-dimethylacrylamide) using bromoform-assisted polymerisation and has been discussed in detail. Multiple studies investigating varying bromoform content, solvent, bromoform as a potential photoinitiator, and the effect of oxygen on the reaction system have been explored.

Initially, the study focusing on the effect of increasing bromoform content, from 0 - 2.0 mol % (relative to monomer), highlighted that bromoform was not behaving as a CTA under the described conditions (in water). This was evidenced by the lack of relationship between bromoform concentration and molar mass from the near-identical GPC traces. If bromoform was behaving as a CTA the molar mass would be expected to decrease significantly with increasing bromoform content. These outcomes contradict the previous work of Thananukul

*et al.*<sup>212</sup>, where it was demonstrated that bromoform exhibits successful chain transfer capabilities during the polymerisation of acrylamide. However, there is no evidence of thermal control during the course of the reaction in the Thananukul *et al.* studies and the effects of bromoform as a CTA could be linked to the high temperatures (up to 50 °C) likely achieved during the prolonged UV irradiation times. Overall, in this study, the rate of the reaction was not altered with increasing bromoform content and all polymerisations (including repeats) achieved high monomer conversions ( $\geq 93\%$ ). Notably, the molar mass dispersity of the final polymers was high ( $\bar{D} = 2.8 - 3.4$ ), with no suggested relationship between molar mass dispersity and bromoform content.

Changing the solvent to DMF demonstrated considerable differences in the kinetics of DMA polymerisation at varying bromoform concentration (0, 0.5, 1.0 and 2.0 mol % relative to monomer). Firstly, the required reaction time needed to be increased from 60 to 360 minutes to achieve reasonably high monomer conversions ( $\geq 77\%$ ), due to extensive induction periods followed by a slower rate of reaction in DMF. Similar to the water study, the change in molar mass of resulting PDMA was negligible and the GPC traces were near-identical at all bromoform concentrations investigated. There was also a negligible change in polymerisation rate between the reactions, with no clear trend between bromoform concentration and the rate of the reaction being observed. Similarly, the molar mass dispersity values of the final polymers remained high ( $\bar{D} = 2.7 - 2.9$ ), with no clear relationship between molar mass dispersity and bromoform content. The final molar masses obtained in the DMF system (22.2 - 23.1 kg mol<sup>-1</sup>) were considerably lower than those achieved when using water as the solvent (242.3 - 294.8 kg mol<sup>-1</sup>), which is attributed to the lower propagation rates in DMF.

In both kinetic studies, appropriate purification methods were developed and analytical techniques (<sup>1</sup>H NMR spectroscopy, GPC, DSC and TGA) were used to further confirm the characteristics of the final polymers. In all cases, including repeats, the experimentally determined data ( $T_g$  and degradation temperature range) were within the known literature values. As previously discussed, the polymerisations revealed a solvent effect on the

homopolymerisation of DMA at varied bromoform concentration when moving from water to DMF which was reflected in a significant decrease in the molar mass of the samples. The reactions in DMF were used as a tool to determine the solvent effect and provide further insight into the role of bromoform in these syntheses. However, with the goal being to develop a more environmentally friendly, inexpensive, industrially relevant polymerisation technique future reactions were conducted in water. This removes the need for toxic, harmful organic solvents during the synthesis, which is one of the overarching objectives of this project.

In another study, in the absence of ACPA photoinitiator, it was determined that whilst bromoform produces radicals when exposed to UV light, these radicals are incapable of initiating the polymerisation of *N,N*-dimethylacrylamide under the described conditions. This is contradictory to the previous findings of Dunn *et al.*<sup>209</sup>, Miller<sup>208</sup> and Wu *et al.*<sup>211</sup>. In each of these examples, it was claimed that bromine radicals (generated from bromoform, carbon tetrabromide, dibromomethane, monobromomethane or bromotrichloromethane) are capable of initiating the polymerisation of acrylonitrile, acrylic acid, AMPS and styrene. However, the lack of thermal control throughout these reactions could be the contributing factor that resulted in the success of these polymerisations; with the highest solution temperature being reported as 50 °C<sup>208</sup>. Conversely, this does concur with the more recent work of Thananukul *et al.*<sup>212</sup>. In this case, bromoform was also deemed incapable of initiating the polymerisation of acrylamide at varied bromoform concentration, even without thermal control of the system.

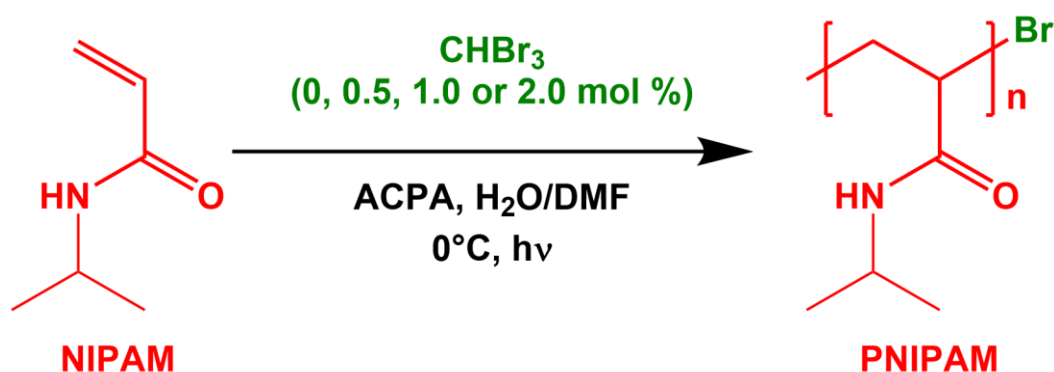
A study where oxygen was present in the reaction highlighted the importance of the degassing stage in the synthesis methodology. With oxygen present, a significant induction period was evident in all reactions ( $\geq 15$  minutes). Therefore, it was decided that degassing the reaction solution was important to maintain efficiency. Additionally, the reduced polymerisation time enables greater control over the temperature range at which the reaction is conducted. During the 60 minutes of UV irradiation, for the reactions in which no oxygen is present, the temperature only increased by a maximum of 4.9 °C.

Finally, the polymerisation of *N,N*-dimethylacrylamide at 2.0 mol % bromoform (relative to monomer), was scaled up to produce a suitable quantity of potentially bromine-terminated poly(*N,N*-dimethylacrylamide) macro-initiator (Section 3.7) for subsequent block copolymer syntheses (see Chapter 5). The PDMA-Br macro-initiator was synthesised to between 91 and 99 %, and then 70 %, monomer conversion in an attempt to increase the chain-end fidelity of the bromine-terminated polymer chains. Each macro-initiator synthesised in these studies exhibited similar properties to those synthesised at smaller scale (2 g), discussed in Section 3.3, including molar mass, molar mass dispersity,  $T_g$  and degradation profile. These macro-initiators were then used in further reactions in an attempt to synthesise PDMA-*b*-PNIPAM block copolymers (see Chapter 5).

# **Chapter 4. Bromoform-assisted polymerisation of *N*- isopropylacrylamide**

## 4.1 Homopolymerisation of *N*-isopropylacrylamide

This chapter describes the synthesis of poly(*N*-isopropylacrylamide) [PNIPAM] via bromoform-assisted polymerisation (Scheme 4.1). Multiple investigations were undertaken to determine the most appropriate synthesis route of a PNIPAM macro-initiator for use in further polymerisation reactions; to form block copolymers. As demonstrated in Scheme 4.1, due to the primary dissociation pathway of bromoform, it is predicted that the polymerisations will produce PNIPAM with a reversibly capped bromine chain end.



Scheme 4.1. Synthesis of PNIPAM via bromoform-assisted polymerisation at varied bromoform concentrations.

The main part of this study focuses on the synthesis of PNIPAM with varied bromoform content to provide insight into the role of increasing bromoform content on the overall polymerisation and determine the optimum route to synthesise a PNIPAM macro-initiator for future block copolymer synthesis. Moreover, these reactions were conducted in both high performance liquid chromatography (HPLC)-grade water and dimethylformamide (DMF) to determine the effect of solvent on the production of PNIPAM using this bromoform-assisted synthetic route. In addition to this research, two supplementary studies were conducted; an investigation in the absence of photoinitiator [namely 4,4-azobiscyanovaleric acid (ACPA)], and a study to determine the role of oxygen in the polymerisation system. The investigation in the absence of ACPA was designed to highlight the potential of bromoform to behave as a photoinitiator as implied in the earlier work of Miller<sup>208</sup>, Dunn *et al.*<sup>209</sup> and Wu *et al.*<sup>211</sup> (during the polymerisation



of acrylonitrile and acrylic acid, styrene and methyl methacrylate, and acrylic acid and 2-acrylamido-2-methylpropanesulfonic acid (AMPS), respectively), in addition to its potential chain transfer agent (CTA) capabilities (as suggested by Thananukul *et al.*<sup>212</sup>). The final investigation, whereby oxygen was not removed from the reaction flask, was used to further develop the synthesis methodology; determining whether there was a need for a degassing stage for the reaction to be successful under the described conditions.

## **4.2 Development of the *N*-isopropylacrylamide polymerisation procedure**

Chapter 3 highlights the development of the experimental set up including; ultraviolet (UV) source, metal box, use of borosilicate glass, stirrer plate and ACPA photoinitiator selection. Trial reactions conducted identified that the heat produced from the UV light source and the reaction was significant enough to increase the reaction temperature from 25 °C up to 45 °C (after 2 hours of UV irradiation). This was a problem for the synthesis of PNIPAM due to the lower critical solution temperature (LCST) that PNIPAM exhibits at approximately 32 °C<sup>1</sup> in water. In the trial reactions, without any means of temperature control, the PNIPAM could be seen precipitating out of solution very early on. Therefore, an ice bath was introduced to provide temperature control throughout the course of the reaction. Like in the poly(*N,N*-dimethylacrylamide) [PDMA] study (see Chapter 3), the ice did not cover the top of the vessel to allow sufficient UV irradiation from above and the reaction solution was stirred in the ice bath for 20 minutes to allow a homogenous solution to be formed and the temperature to stabilise. A temperature *versus* time study of the reaction solution concluded that the temperature increased by 1.1 °C over a 30 minute period of UV irradiation (Figure 4.1). The ice bath provided control of the temperature of the solution, significantly reducing thermal effects on the precipitation of PNIPAM, the dissociation of ACPA or bromoform and the overall rate of the polymerisation.

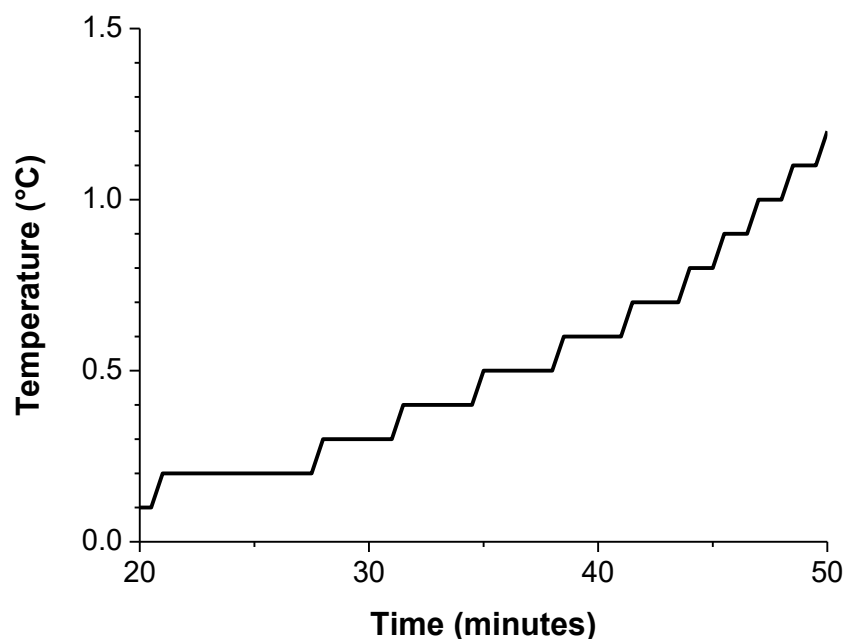


Figure 4.1. Temperature *versus* time plot for the trial synthesis of PNIPAM using an ice bath to provide temperature control.

### 4.3 Bromoform-assisted synthesis of poly(*N*-isopropylacrylamide) in HPLC-grade water

The focus of this research was to successfully synthesise amphiphilic block copolymers from macro-initiators with a labile C-Br bond; formed from the use of bromoform in the homopolymerisation reaction. Therefore, a detailed study was required focused on the synthesis of the macro-initiator. This section describes the synthesis of PNIPAM macro-initiators, formed at varied bromoform concentrations (0.0, 0.5, 1.0 and 2.0 mol% relative to monomer) and fixed ACPA concentration (1.0 mol% with respect to *N*-isopropylacrylamide) in water. Experiments were conducted in an ice bath and, in all cases, experiments were repeated in triplicate to eliminate potential anomalies within the data and highlight patterns and processes that were occurring. The effect of the addition of bromoform on the homopolymerisation was studied by monitoring monomer conversion and molar mass ( $M_n$ ) using  $^1\text{H}$  nuclear magnetic resonance (NMR) spectroscopy (Figure 4.2 and Appendices 7 - 9)

and gel permeation chromatography (GPC, using poly(methyl methacrylate) [PMMA] standards) (Figure 4.3), respectively.

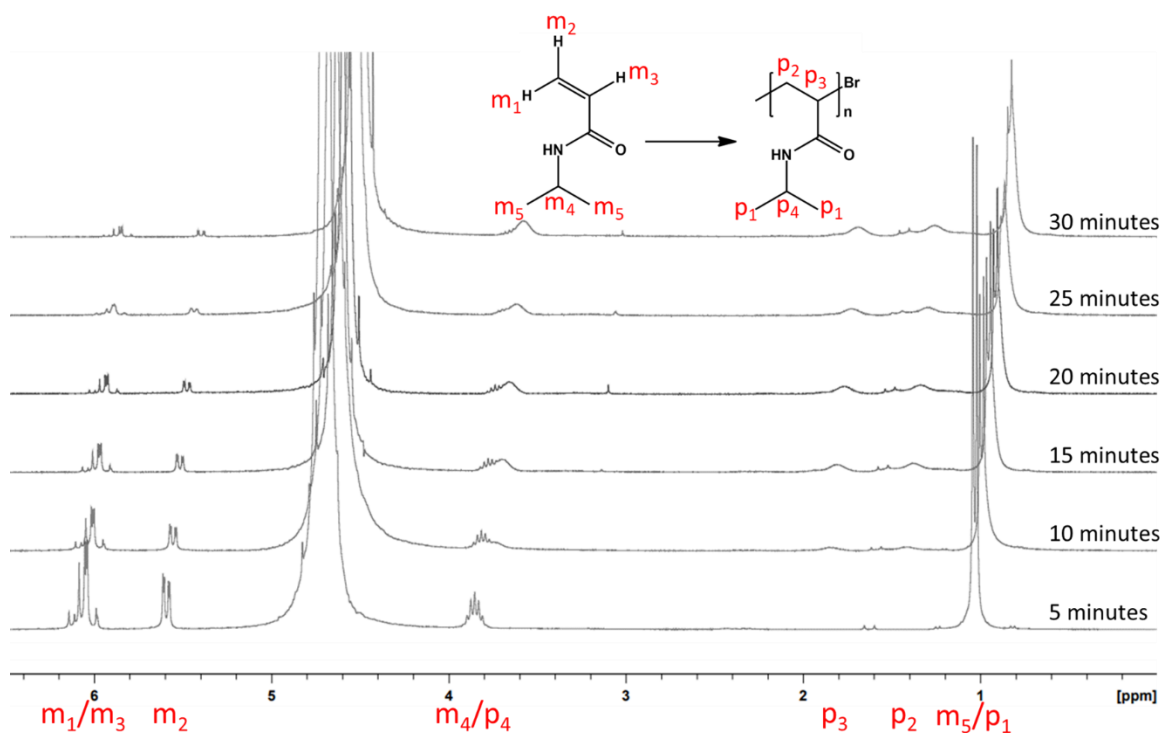


Figure 4.2. Exemplar  $^1\text{H}$  NMR kinetic overlay for the synthesis of PNIPAM in water at 2.0 mol % bromoform showing the disappearance of monomer and broadening of polymer peaks throughout the course of the reaction.

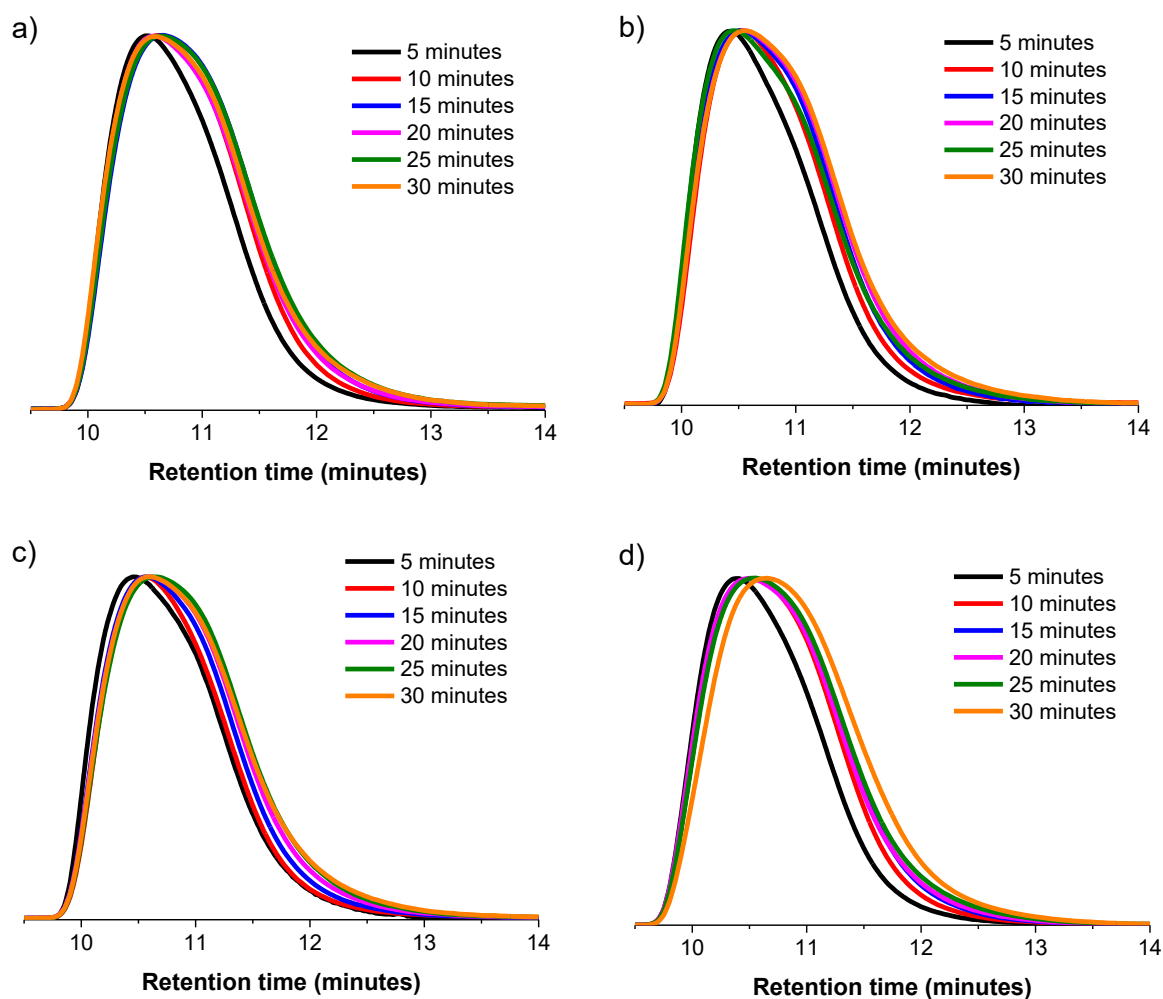


Figure 4.3. Kinetic GPC traces for the synthesis of PNIPAM in water at a) 0, b) 0.5, c) 1.0 and d) 2.0 mol % bromoform concentrations (relative to monomer).

High monomer conversions ( $\geq 88\%$ ) were achieved in each case, and the  $M_n$  of the resulting PNIPAM initially increases upon addition of bromoform (see data summarised in Table 4.1), however, there is then no identifiable relationship between bromoform concentration and molar mass. The resulting PNIPAM, in each case, was isolated by precipitation before residual water was removed via lyophilisation until constant weight was achieved. Excess unreacted monomer was confirmed to be removed via  $^1\text{H}$  NMR (Figure 4.4). Finally, the GPC traces of the precipitates at each bromoform concentration demonstrate that there is good reproducibility between the results (Figure 4.5).

Table 4.1. Summary of final conversion, molar mass, molar mass dispersity and apparent rate constant data for the polymerisation of *N*-isopropylacrylamide at varied bromoform concentrations in water.

Experiment series	Bromoform content (mol %) <sup>a</sup>	Final monomer conversion (%) <sup>b</sup>	$M_n$ (kg mol <sup>-1</sup> ) <sup>c</sup>	$\mathcal{D}$ ( $M_w/M_n$ ) <sup>c</sup>	$k_{app}$ (min <sup>-1</sup> )
HJH013	0	92	521.1	2.4	0.10
HJH014	0.5	88	532.6	2.2	0.09
HJH015	1.0	92	535.2	2.2	0.11
HJH016	2.0	91	530.2	2.2	0.12

a) Relative to monomer

b) Calculated using <sup>1</sup>H NMR spectroscopy and Equation 2.2

c) Determined using DMF GPC with PMMA standards

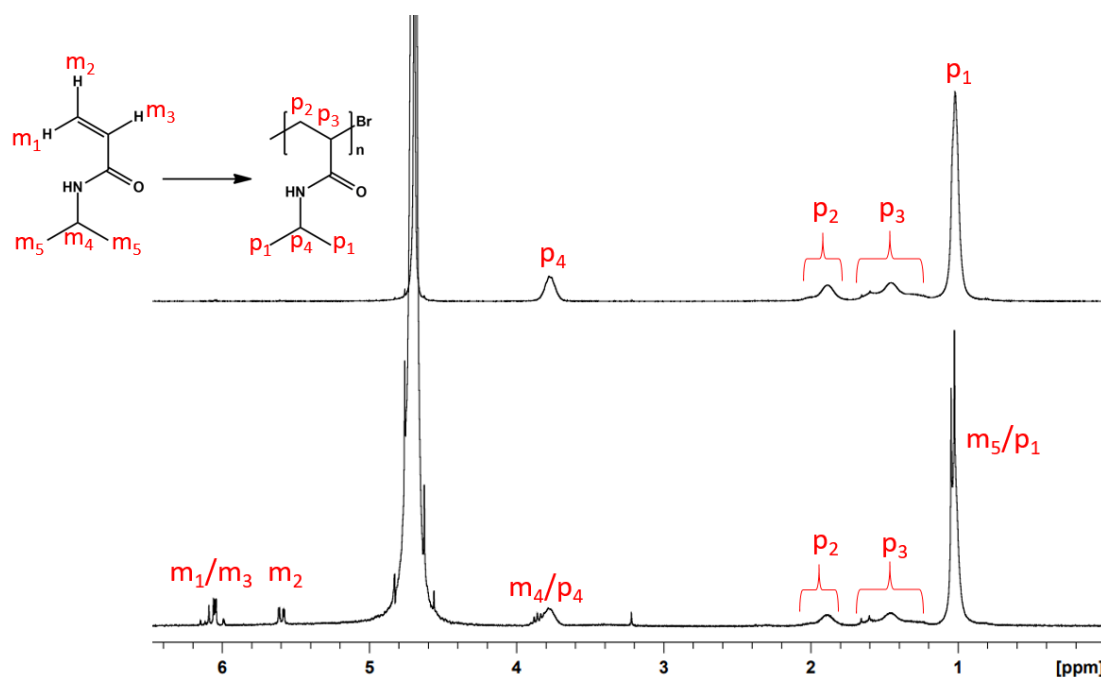


Figure 4.4. Comparative <sup>1</sup>H NMR spectra (in D<sub>2</sub>O) showing the disappearance of the monomer vinyl protons (5.6 and 6.1 ppm) between crude (bottom) and precipitated (top) PNIPAM (2 mol % bromoform, relative to monomer).

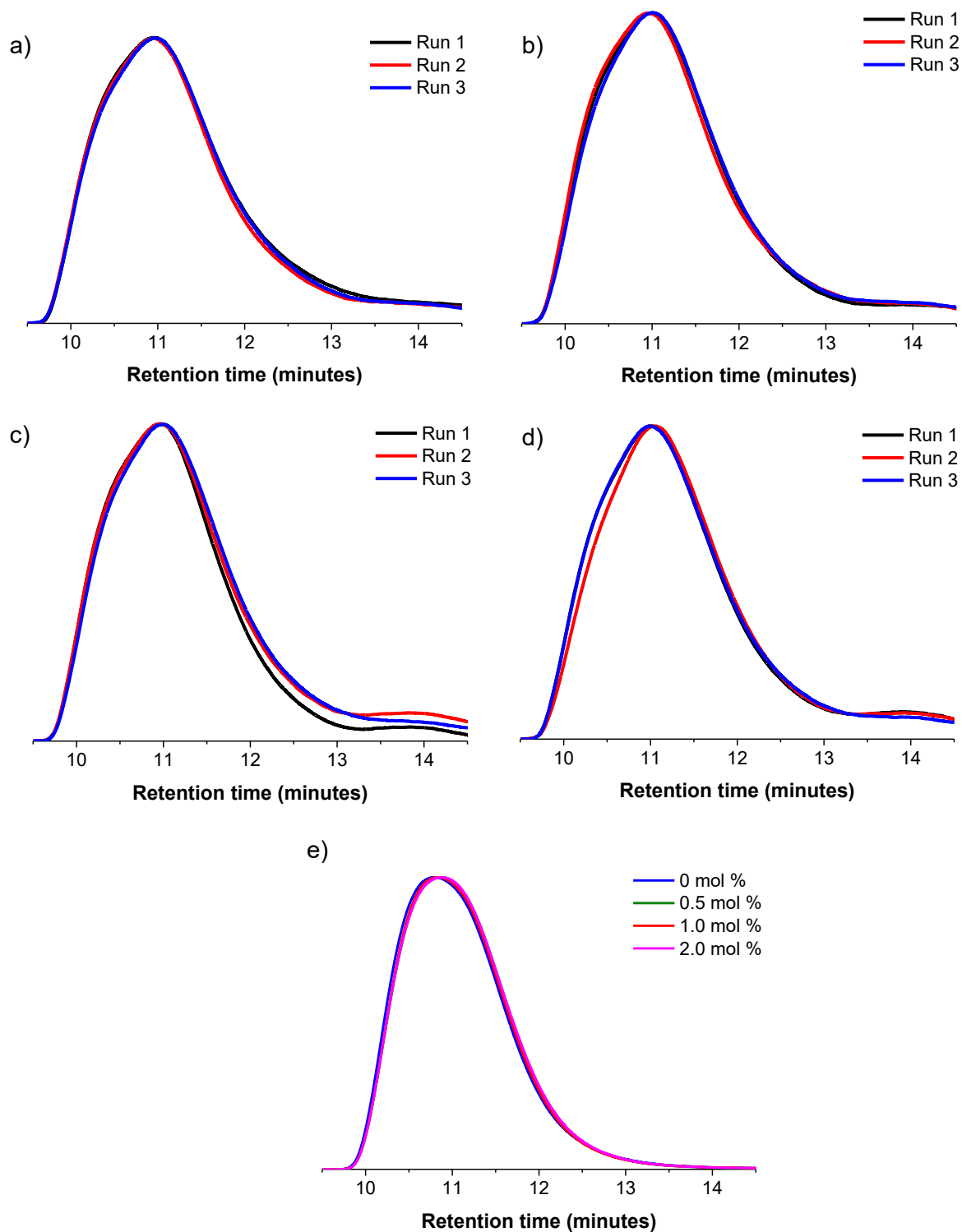


Figure 4.5. GPC traces of PNIPAM final precipitates at a) 0, b) 0.5, c) 1.0 and d) 2.0 mol % bromoform (relative to monomer, synthesised in water) demonstrating good reproducibility between runs and e) near-identical GPC traces of the final precipitate at each bromoform concentration.

Closer inspection of the GPC curves in this study (Figure 4.5) show that the reactions with bromoform are near-identical and the apparent increase in molar mass upon addition of bromoform is attributed to the change in molar mass dispersity ( $\bar{D} = 2.4 - 2.2$ ) and limits of the GPC calibration. The lack of relationship between bromoform concentration and molar mass is similar to the previous findings for the polymerisation of *N,N*-dimethylacrylamide (DMA) discussed in Chapter 3. Even with the presence of lithium bromide in the GPC eluent, to suppress hydrogen bonding between the PNIPAM and DMF, there is still some distortion observed in the shape of the GPC traces between the kinetic studies (Figure 4.3) and final precipitates (Figure 4.5).

Under the described conditions bromoform is not demonstrating chain transfer capabilities as the molar mass would be expected to decrease when increasing the bromoform content. Additionally, these findings oppose the observations made in the previous work conducted by Thananukul *et al.*<sup>212</sup>, where it was demonstrated that bromoform exhibits successful chain transfer capabilities during the polymerisation of acrylamide, highlighted through the apparent regulation of molar mass with increasing bromoform content. However, the system discussed herein differs to the Thananukul *et al.* study as an ice bath has been used to provide control over the temperature of the reaction. In the Thananukul *et al.* study, temperatures of up to 50 °C are reported during the 60 minutes of UV irradiation that the reaction solutions are exposed to. Therefore significant thermal effects could be the reason that bromoform exhibited CTA capabilities in their work. Furthermore, the bromoform-assisted polymerisation of NIPAM reached high conversion ( $\geq 88\%$ ) after only 30 minutes of UV irradiation; half the exposure time used in the polymerisation of DMA.

Further analysis of the kinetic data collected (Table 4.1, Figure 4.6 and Figure 4.7) demonstrate little to no difference in polymerisation rate observed for all bromoform concentrations studied. This is similar to the synthesis of PDMA (see Chapter 3) and the previous work of Thananukul *et al.*<sup>212</sup>, where it was reported that the addition of bromoform to the polymerisation system did not significantly affect the rate of polymerisation. Finally, the

molar mass dispersity of the final polymers was high ( $\bar{M}_w = 2.2 - 2.4$ ), with no apparent relationship between molar mass dispersity and bromoform content. The kinetic study shows that the PNIPAM molar mass decreases as the polymerisation proceeds at all bromoform concentrations (Figure 4.8). This is a typical observation in free radical polymerisations due to high initial rates of propagation leading to the formation of high molar mass chains, before the monomer concentration is reduced and thus shorter polymer chains are synthesised, resulting in a reduction in the average molar mass in the system<sup>294–296</sup>.

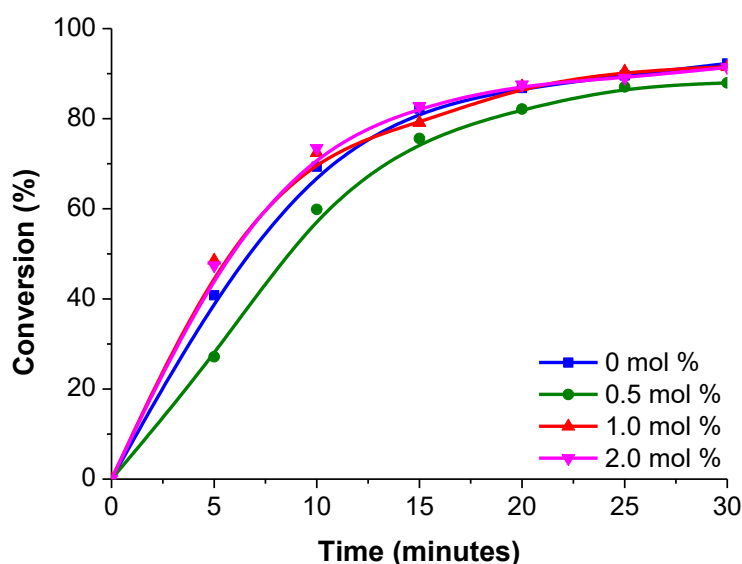


Figure 4.6. Monomer conversion *versus* time for the synthesis of PNIPAM at varying bromoform concentrations in water.



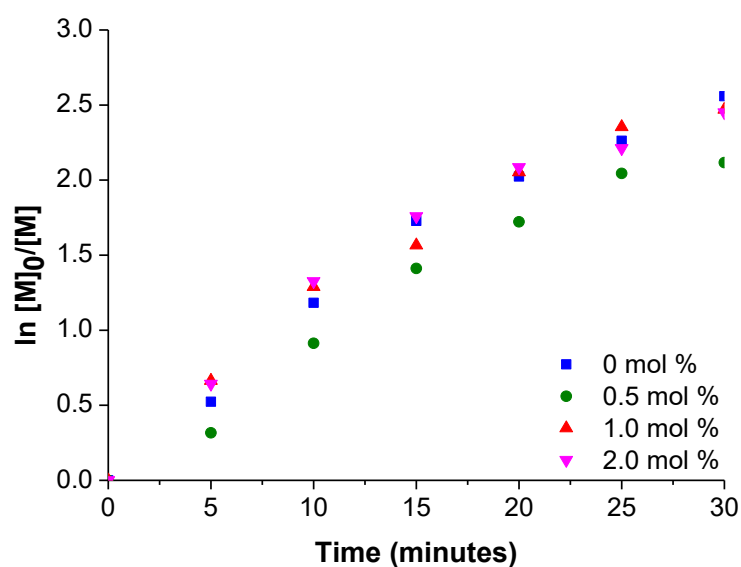


Figure 4.7. Semi-logarithmic plot for the synthesis of PNIPAM at varying bromoform concentration in water.

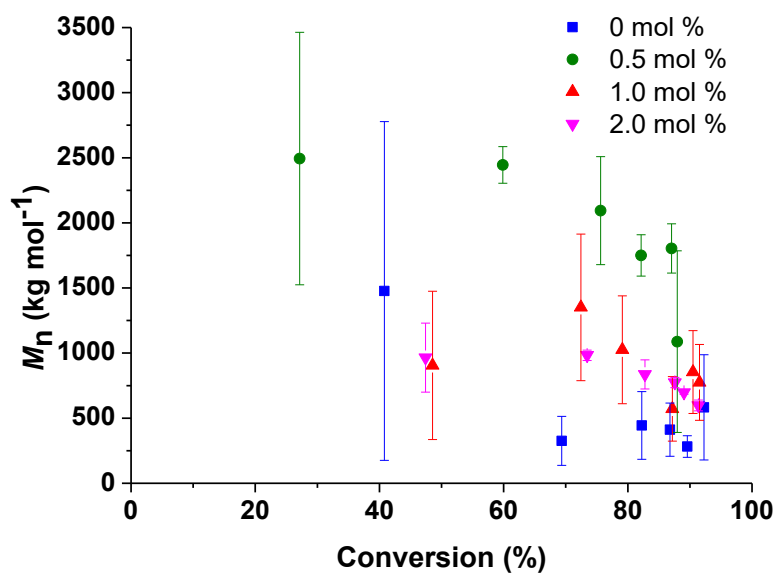


Figure 4.8. Molar mass *versus* monomer conversion for the synthesis of PNIPAM at varying bromoform concentrations in water (error bars represent the standard deviation of the triplicate data).

### 4.3.1 Thermal properties

In preparation for the synthesis of block copolymers, the resulting PNIPAM was purified by precipitation and further characterised via differential scanning calorimetry (DSC), thermal gravimetric analysis (TGA) and dynamic light scattering (DLS) to determine the glass transition temperature ( $T_g$ ), degradation profile and LCST, respectively. As described in Chapter 3, the results, regarding the thermal properties of the homopolymer, are collated for later comparison to subsequent block copolymers that may be synthesised. The purpose of which is to identify any changes between the properties of the homopolymers and the block copolymers.

For all samples, the  $T_g$  was determined to be between 138.5 - 140.0 °C (

Table 4.2 and Figure 4.9) which is within the expected range according to the literature (135 - 142 °C<sup>326–328</sup>). Similarly to PDMA, the available literature data indicate that PNIPAM also degrades between 350 - 450 °C<sup>329</sup>, via a one-step degradation profile, forming volatile, small molecules. This is evidenced in Figure 4.10, for the samples synthesised herein, which shows the degradation profile of PNIPAM at all bromoform concentrations.

Table 4.2. Summary of the glass transition temperatures of PNIPAM (synthesised in water) at varying bromoform concentration (0, 0.5, 1.0 and 2.0 mol % relative to monomer).

Experiment series	Bromoform (mol %) <sup>a</sup>	Onset of $T_g$ (°C)	Endset of $T_g$ (°C)	Midpoint of $T_g$ (°C)
HJH013	0	134	144	139.0
HJH014	0.5	135	145	140.0
HJH015	1.0	136	144	140.0
HJH016	2.0	134	143	138.5

a) Relative to monomer

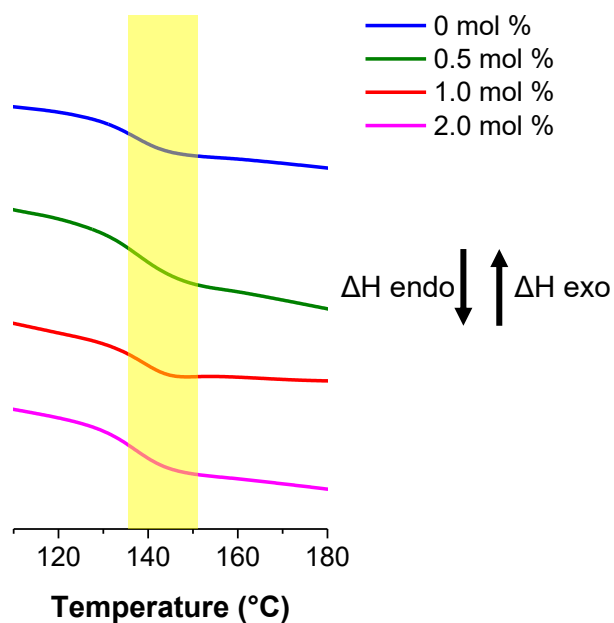


Figure 4.9. DSC thermograms (second heating cycle) for PNIPAM (synthesised in water) at varying bromoform concentration, highlighting the feature corresponding to the glass transition temperature for each sample.

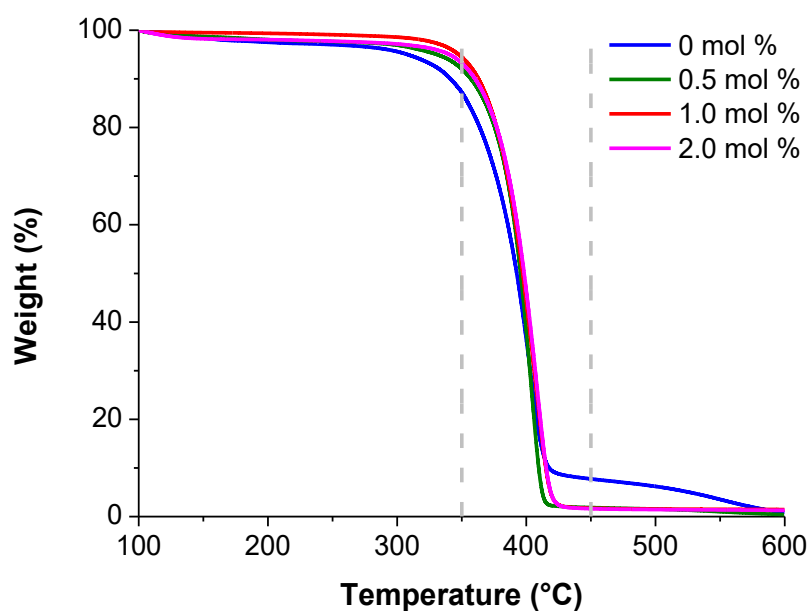


Figure 4.10. TGA degradation profiles of PNIPAM (synthesised in water) at varying bromoform concentration.

Finally, DLS was used to determine the LCST of the PNIPAM samples synthesised at each bromoform concentration. Below the LCST the water molecules are physically bound to the hydrophilic amide groups and arranged in such a way that they form a shield around the hydrophobic groups throughout the polymer<sup>254</sup>. This shield is often referred to as a hydrophobic hydration shell and is enthalpically favoured (whilst being entropically disfavoured) due to the water molecules forming stronger and longer-lived hydrogen bonds in this arrangement compared to the bulk<sup>255–258</sup>. The polymer structure goes from a state of well-solvated, randomly distributed polymer at low temperature to a state of highly packed chains at high temperature<sup>330</sup> and results in the polymer precipitating out of solution. Above the LCST the hydrophobic hydration shell is lost and the polymer aggregates and phase separates<sup>331–335</sup>. This transition from soluble to insoluble is known as the coil-to-globule transition and occurs due to the entropy gain from the release of the water molecules from the hydration shell outweighing the now smaller enthalpic contribution of water-polymer binding<sup>255,331,333,336–341</sup>. As previously mentioned PNIPAM typically has an LCST of 32 °C<sup>342,343</sup>, however, the available literature demonstrates that this transition can be between 30 - 35 °C<sup>1,339,344–346</sup>. Figure 4.11 shows that the PNIPAM samples synthesised herein exhibit an LCST between 34 and 35 °C; which is within the given literature range. This information will be used alongside the results discussed in Chapter 5 to highlight any changes in the LCST when forming block copolymers.

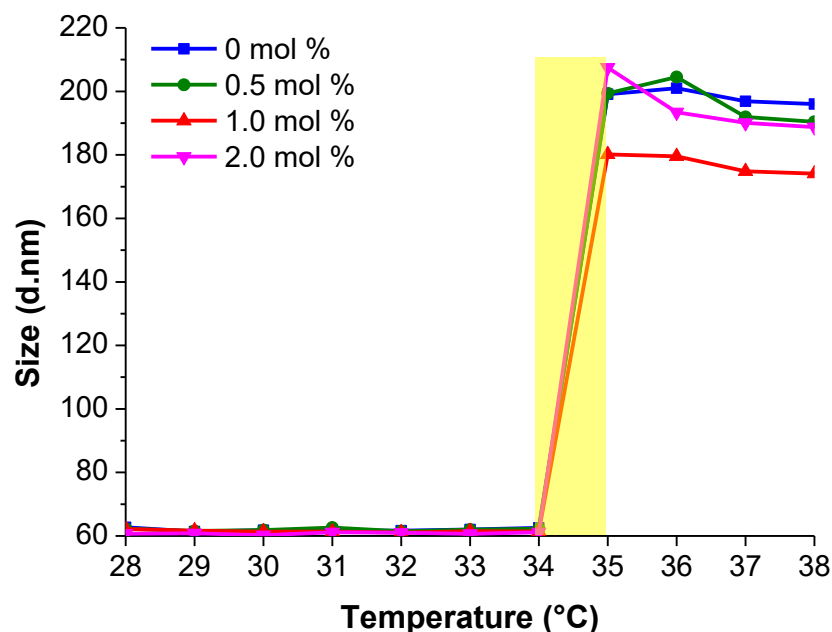


Figure 4.11. Size *versus* temperature of PNIPAM (synthesised in water) at varying bromoform concentrations highlighting the LCST (or coil-to-globule transition).

In this study, PNIPAM has been successfully synthesised at varying bromoform concentration in water. These results suggest that the molar mass of the samples is not controlled with increasing bromoform concentration (0 - 2 mol % relative to monomer). Eliminating the role of bromoform as a CTA for the synthesis of PNIPAM under the described conditions. This is similar to the results described in Chapter 3 regarding the synthesis of PDMA at varied bromoform concentration under the same conditions. Additionally, the rate of the polymerisation is negligibly changed at each bromoform concentration, with no apparent trend observed. Moreover, the molar mass dispersities of the final PNIPAM samples are relatively high ( $\bar{D} = 2.2 - 2.4$ ), however, there is good reproducibility observed for syntheses conducted at each bromoform concentration.

#### 4.4 Bromoform-assisted synthesis of poly(*N*-isopropylacrylamide) in DMF

To further build on the work conducted in Section 4.3, another series of PNIPAM syntheses were conducted at varying bromoform concentration (0, 0.5, 1.0 and 2.0 mol % relative to

monomer) and fixed ACPA concentration (1.0 mol % with respect to *N*-isopropylacrylamide); this time in DMF. To allow for direct comparison, ACPA concentration, volume of solvent, initial concentration of monomer and initial temperature (use of ice bath) were identical to those used in the investigation described in Section 4.3. In all cases, experiments were repeated in triplicate. The effect of bromoform on the homopolymerisation was studied by monitoring monomer conversion and molar mass using  $^1\text{H}$  NMR spectroscopy (Figure 4.12 and Appendices 10 - 12) and GPC (Figure 4.13), respectively.

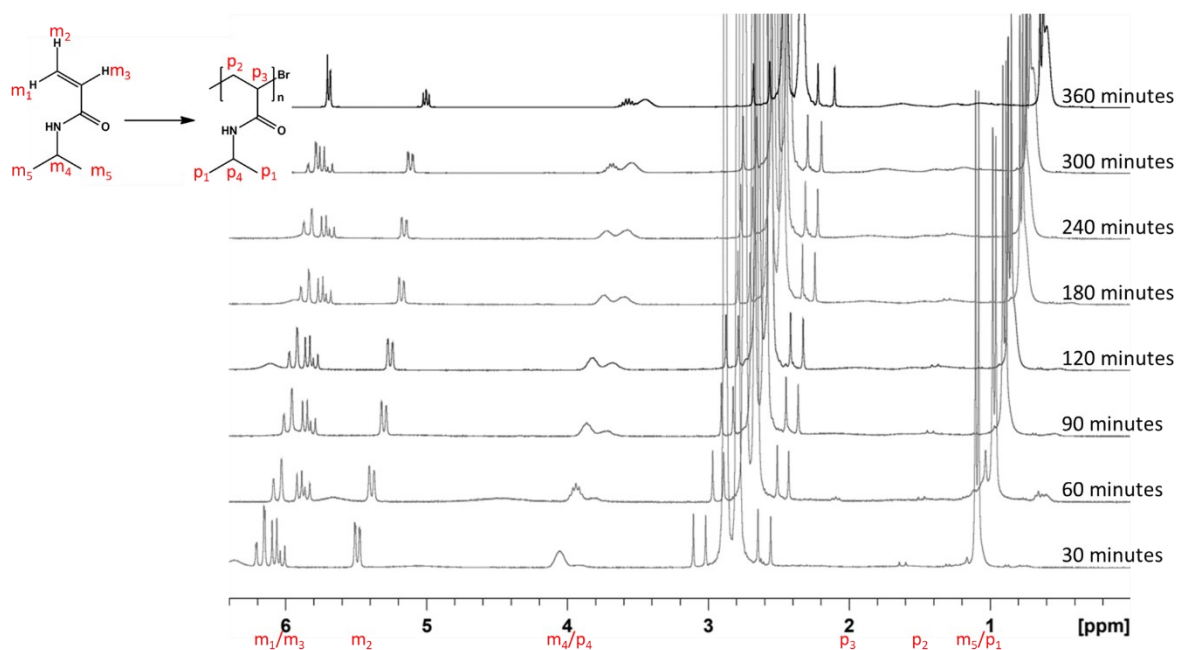


Figure 4.12. Exemplar  $^1\text{H}$  NMR kinetic overlay for the synthesis of PNIPAM in DMF at 2.0 mol % bromoform showing the disappearance of monomer and broadening of polymer peaks throughout the course of the reaction.

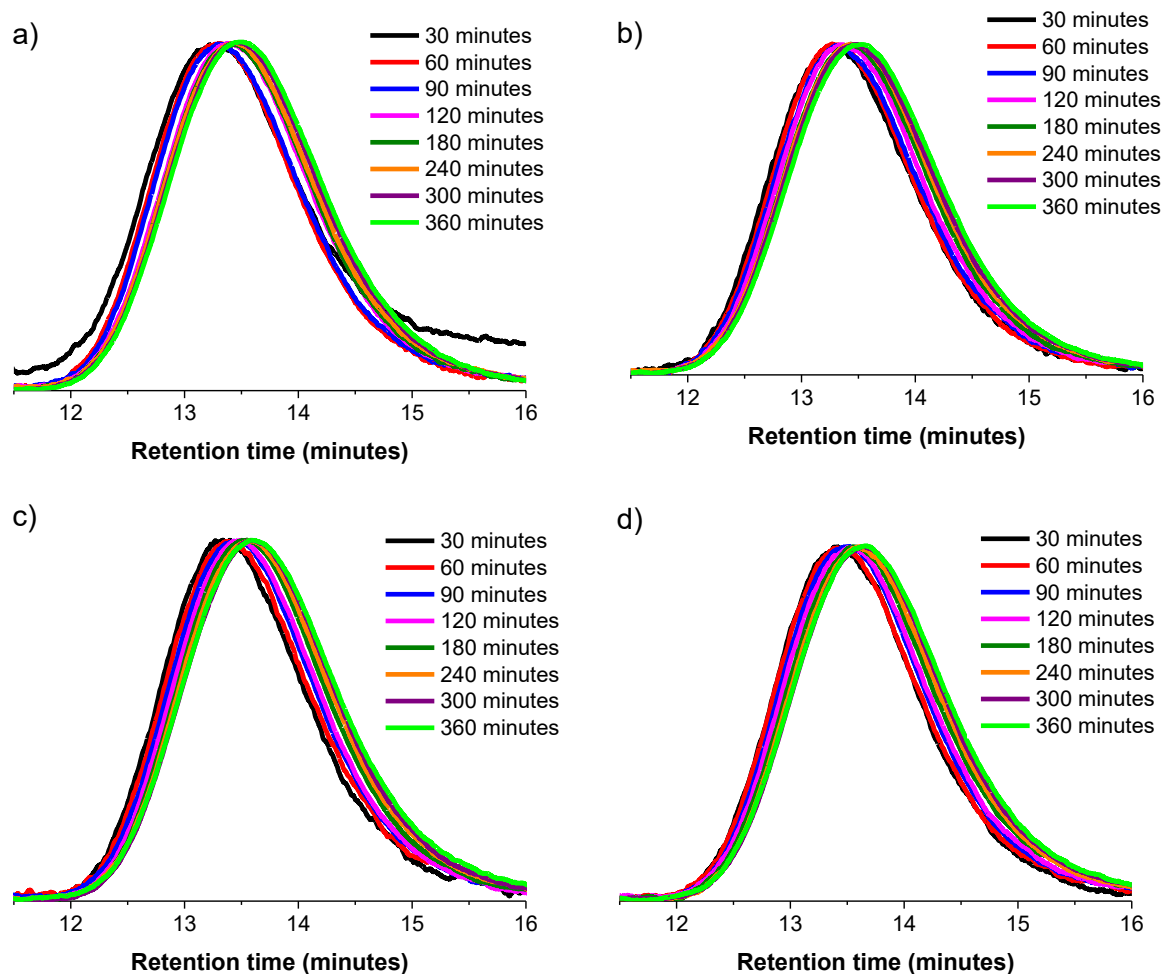


Figure 4.13. Kinetic GPC traces for the synthesis of PNIPAM in DMF at a) 0, b) 0.5, c) 1.0 and d) 2.0 mol % bromoform concentrations (relative to monomer).

Compared to the equivalent synthesis in water, lower final monomer conversions ( $\geq 64\%$ ) were achieved in each case, even with extended UV exposure times (from 30 to 360 minutes). However, in this case the molar mass of the resulting PNIPAM appears to decrease slightly with increasing bromoform concentration (see data summarised in Table 4.3). The resulting PNIPAM, in each case, was isolated by precipitation before residual water was removed via lyophilisation until constant weight was achieved. Excess unreacted monomer was confirmed to be removed via  $^1\text{H}$  NMR spectroscopy (Figure 4.14). As previously discussed in Chapter 3, the peak at 0.8 ppm (labelled with an asterisk (\*), Figure 4.14) is thought to be contributed to by the methyl groups of the ACPA initiator fragment at the  $\alpha$  chain end, from the initiation step

in the reaction. Upon further investigation of the PNIPAM samples produced in the water studies, a similar peak was also identified (Figure 4.15). The intensity of this peak is reduced when compared to Figure 4.14 due to the significantly higher molar mass of the polymers produced in the water study. Finally, the GPC traces of the purified PNIPAM synthesised at each bromoform concentration demonstrate that there is good reproducibility between the results (Figure 4.16).

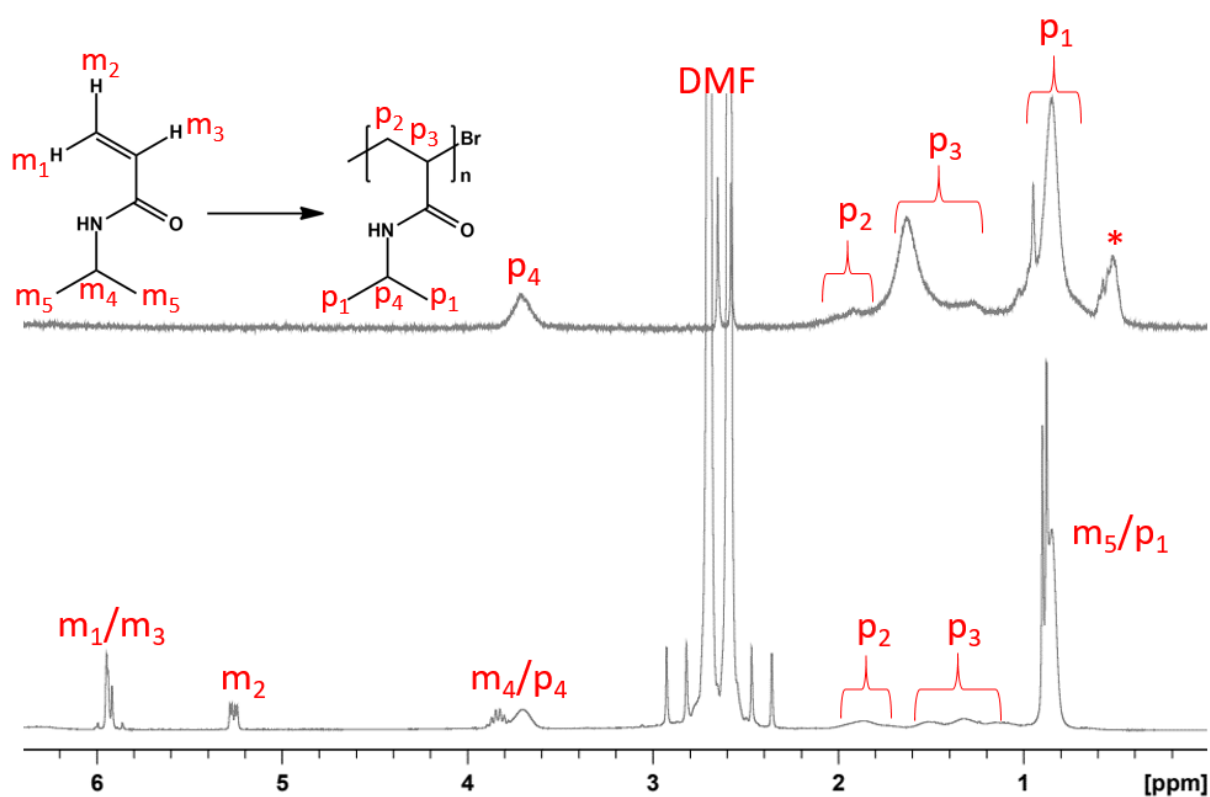


Figure 4.14. Comparative <sup>1</sup>H NMR spectra (in CDCl<sub>3</sub>) showing the disappearance of the monomer vinyl protons (5.3 and 5.9 ppm) between crude (bottom) and precipitated (top) PNIPAM (2 mol % bromoform, relative to monomer).



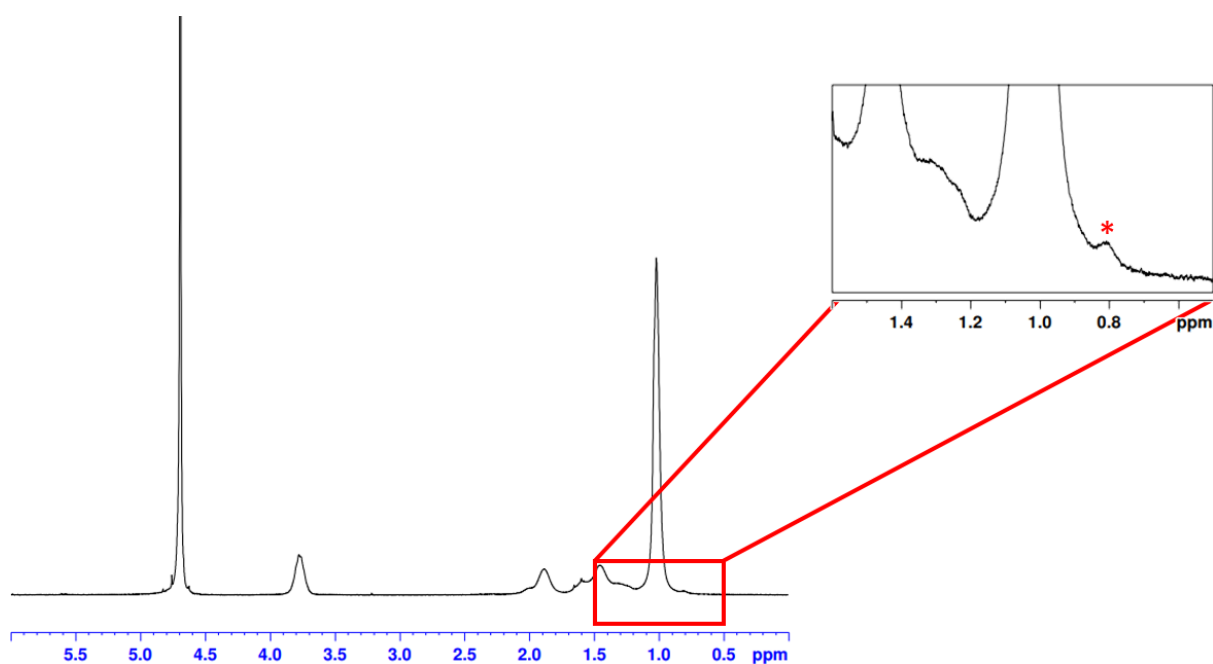


Figure 4.15. PNIPAM synthesised in HPLC-grade water highlighting the presence of a low intensity methyl group peak at approximately 0.8 ppm [labelled with an asterisk (\*)].

Table 4.3. Summary of final conversion, molar mass, molar mass dispersity and apparent rate constant data for the polymerisation of *N*-isopropylacrylamide at varied bromoform concentrations in DMF.

Experiment series	Bromoform content (mol %) <sup>a</sup>	Final monomer conversion (%) <sup>b</sup>	$M_n$ (kg mol <sup>-1</sup> ) <sup>c</sup>	$\bar{D}$ ( $M_w/M_n$ ) <sup>c</sup>	$k_{app}$ (min <sup>-1</sup> )
HJH039	0	64	27.2	2.2	0.0023
HJH040	0.5	64	26.3	2.2	0.0021
HJH041	1.0	64	25.7	2.2	0.0022
HJH042	2.0	66	23.8	2.3	0.0021

a) Relative to monomer

b) Calculated using <sup>1</sup>H NMR spectroscopy and Equation 2.1

c) Determined using DMF GPC with PMMA standards

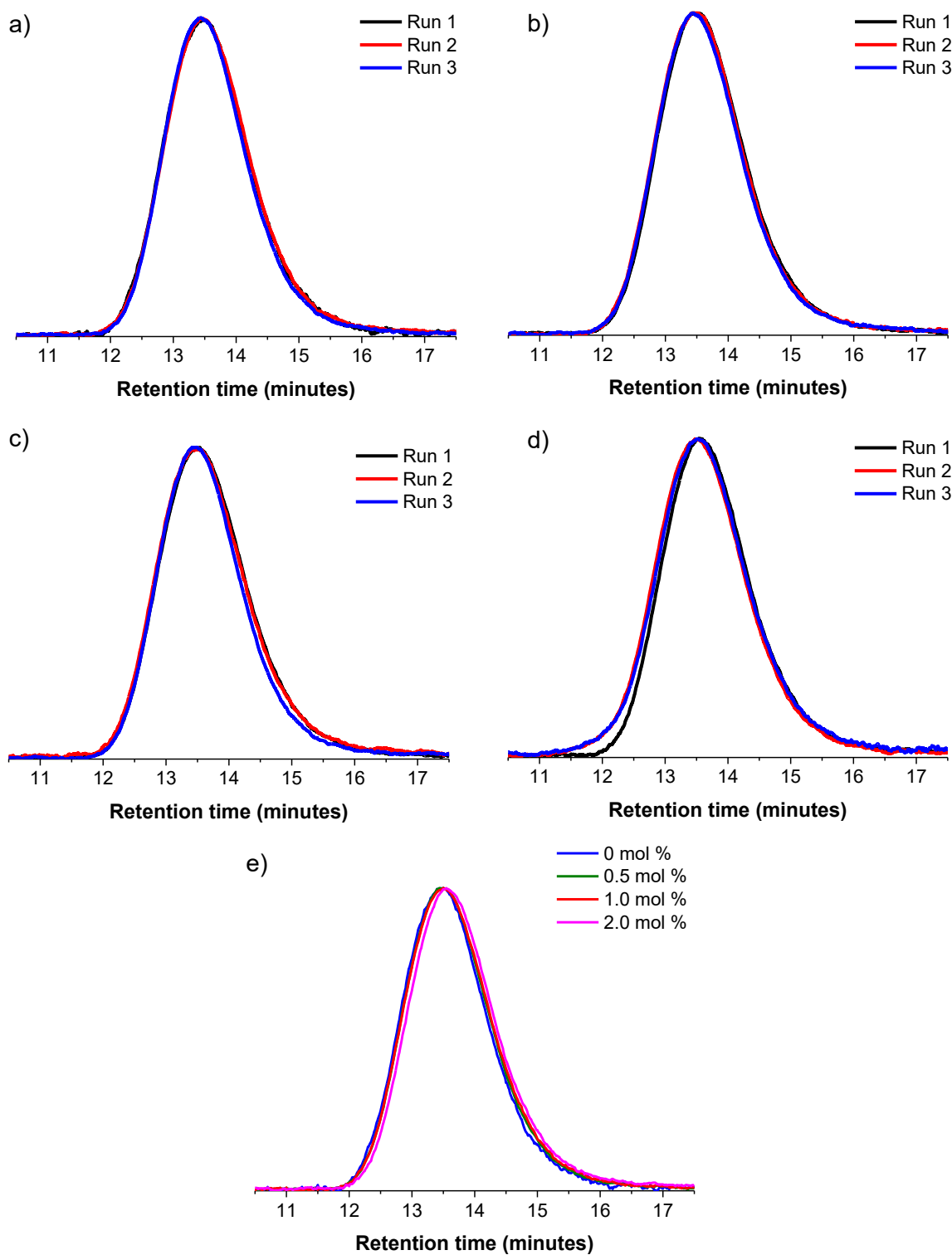


Figure 4.16. GPC traces of PNIPAM final precipitates at a) 0, b) 0.5, c) 1.0 and d) 2.0 mol % bromoform (relative to monomer, synthesised in DMF) demonstrating good reproducibility between runs and e) near-identical GPC traces of the final precipitate at each bromoform concentration.

The data summarised in Table 4.3 initially suggests that bromoform is exhibiting chain transfer capabilities under the described conditions; from the observed decrease in molar mass with increasing bromoform concentration between 0 - 2.0 mol % (relative to monomer). However, the decrease in molar mass could be considered negligible. Additionally, closer inspection of the broad GPC curves indicates that the molar mass profiles for the PNIPAM synthesised are near-identical for 0 - 1.0 mol % bromoform (Figure 4.16). This is similar to the findings from the previous study conducted in water (Section 4.3), and the investigation into the synthesis of PDMA (see Chapter 3), where no apparent relationship was identified between molar mass and bromoform concentration. In the same way as the previous studies described, these observations disagree with the previous work conducted by Thananukul *et al.*<sup>212</sup> where bromoform demonstrated successful chain transfer capabilities during the polymerisation of acrylamide; highlighted through the apparent regulation of molar mass with increasing bromoform content. However, as previously described, the system discussed herein differs to the Thananukul *et al.* study as an ice bath has been used to provide control over the temperature of the reaction. In the Thananukul *et al.*<sup>212</sup> study, temperatures of up to 50 °C are reported. Therefore significant thermal effects could be the reason that bromoform exhibited CTA capabilities in their work.

In the same way as the polymerisation studies in water, the kinetic studies performed in DMF (Table 4.3, Figure 4.17 and Figure 4.18) demonstrate that bromoform has little influence over the apparent rate constant for each reaction, with no observable relationship between bromoform content and rate of polymerisation. Additionally, the molar mass dispersity,  $\bar{D}$ , of the final polymers remains high ( $\bar{D} = 2.2 - 2.3$ ), with no suggested relationship between molar mass dispersity and bromoform content.

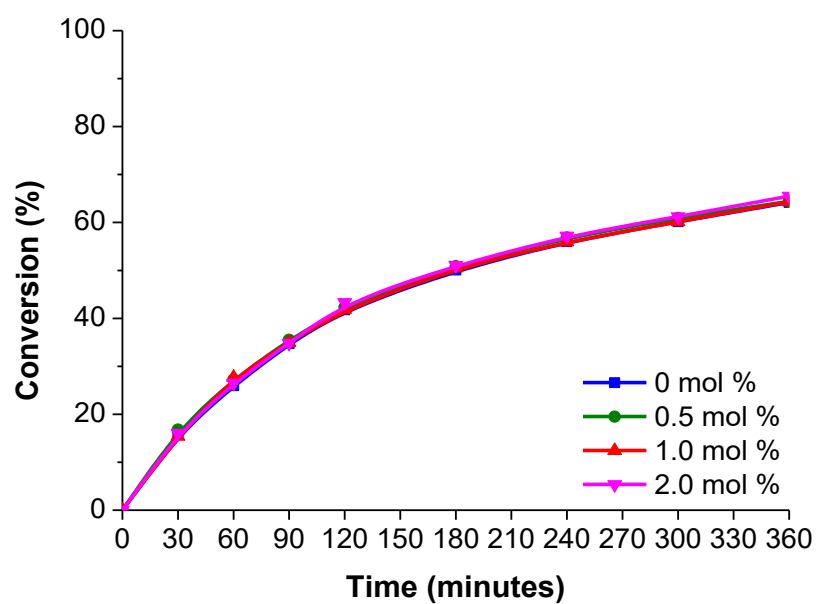


Figure 4.17. Monomer conversion *versus* time for the synthesis of PNIPAM at varying bromoform concentrations in DMF.

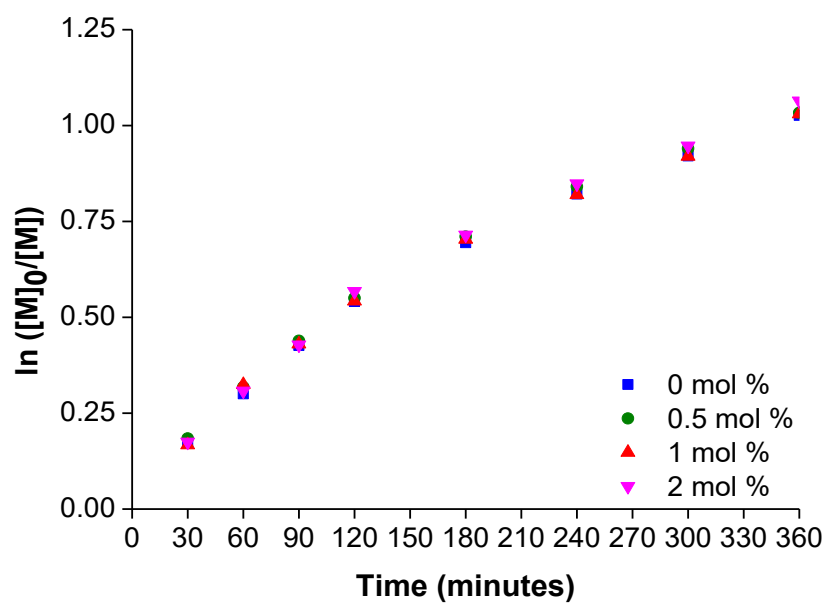


Figure 4.18. Semi-logarithmic plot for the synthesis of PNIPAM at varying bromoform concentration in DMF.

Figure 4.19 indicates that the molar mass of PNIPAM decreases as the polymerisation proceeds at all bromoform concentrations used. As previously discussed, this is a typical observation in free radical polymerisations<sup>294–296</sup>.

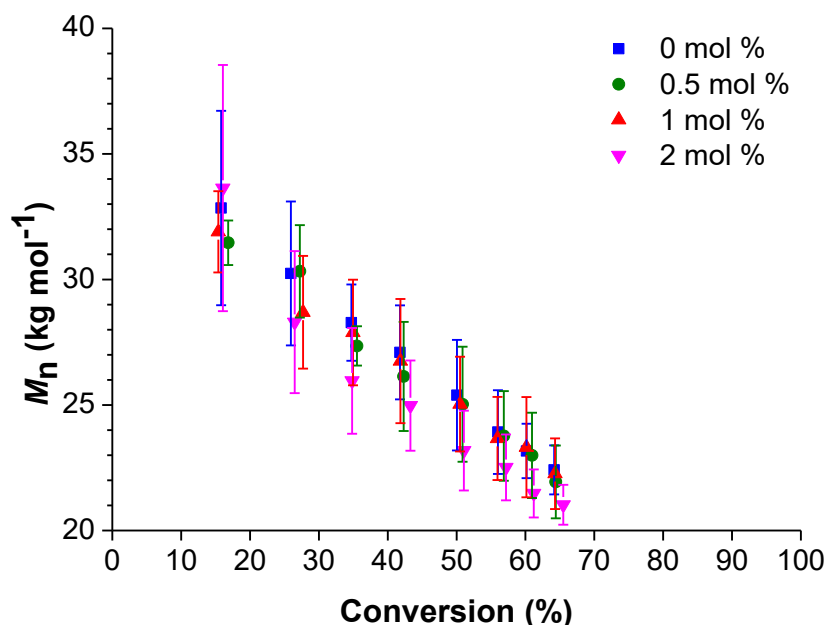


Figure 4.19.  $M_n$  versus monomer conversion for the synthesis of PNIPAM at varied bromoform concentrations in DMF (error bars represent the standard deviation of the triplicate data).

Notably, the final molar masses seen in the DMF formulation (23.8 - 27.2 kg mol<sup>-1</sup>) were considerably lower than those achieved when using water as the solvent (521.1 - 535.2 kg mol<sup>-1</sup>), even with the considerably extended UV irradiation period (increased from 60 to 360 minutes). As discussed in Chapter 3, solvent effects have been described in the literature for a number of acrylamide monomers and solvent systems<sup>273,303,308–310</sup>. It could be suggested that the extended reaction times required for the PDMA and PNIPAM DMF studies, and lower rate of reactions observed, are a result of the decreased reactivity of the monomer double bond<sup>304,305</sup>. This is due to the reduced hydrogen bonding interactions between the solvent and carbonyl group (on the amide) when moving from water to DMF. Additionally, the decrease in molar mass observed could be a result of reduced interactions between the bromoform and

solvent, again when moving from the water to DMF system<sup>273,311</sup>. Finally, the lower conversions achieved, in the DMF study, also contribute to the differences observed in the final molar masses.

#### 4.4.1 Thermal properties

As previously described, in preparation for the synthesis of poly(*N*-isopropylacrylamide)-*block*-poly(*N,N*-dimethylacrylamide) [PNIPAM-*b*-PDMA] copolymers, the PNIPAM was purified via precipitation and further characterised using DSC and TGA to determine the glass transition temperature ( $T_g$ ) and degradation profile, respectively. The results were then collated for future comparison with any block copolymers that may be synthesised.

Again, like the polymerisations conducted in water, the  $T_g$  was determined to be within the expected literature range (135 - 142 °C<sup>326–328</sup>); more specifically 136.0 - 136.5 °C (

Table 4.4 and Figure 4.20). Additionally, the degradation profiles, shown in Figure 4.21, are also near-identical to those produced in the water and PDMA studies; confirming that the samples degrade between 350 - 450 °C<sup>329</sup> as expected.

Table 4.4. Summary of the glass transition temperatures of PNIPAM (synthesised in DMF) at varying bromoform concentrations (0, 0.5, 1.0 and 2.0 mol % relative to monomer).

Experiment series	Bromoform (mol %) <sup>a</sup>	Onset of $T_g$ (°C)	Endset of $T_g$ (°C)	Midpoint of $T_g$ (°C)
HJH039	0	132	140	136.0
HJH040	0.5	132	140	136.0
HJH041	1.0	132	141	136.5
HJH042	2.0	132	140	136.0

a) Relative to monomer

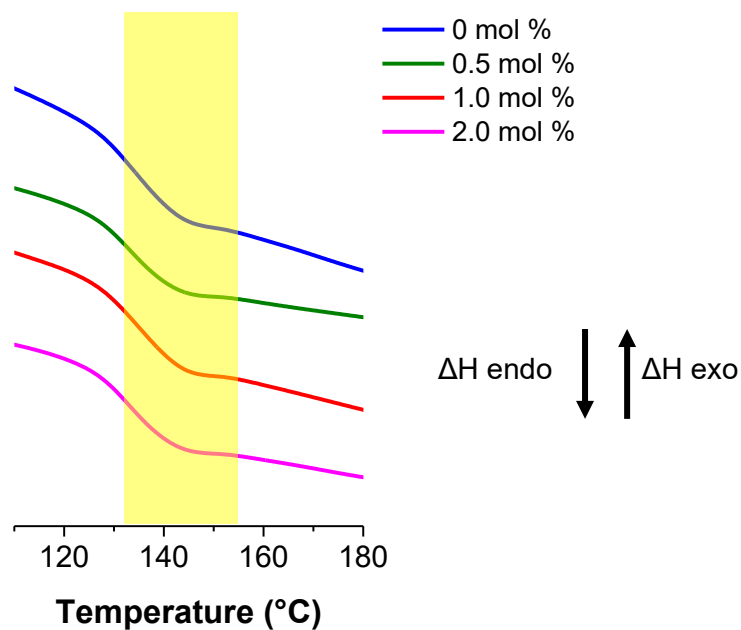


Figure 4.20. DSC thermograms (second heating cycle) for PNIPAM (synthesised in DMF) at varying bromoform concentrations; highlighting the feature corresponding to the glass transition temperature for each sample.

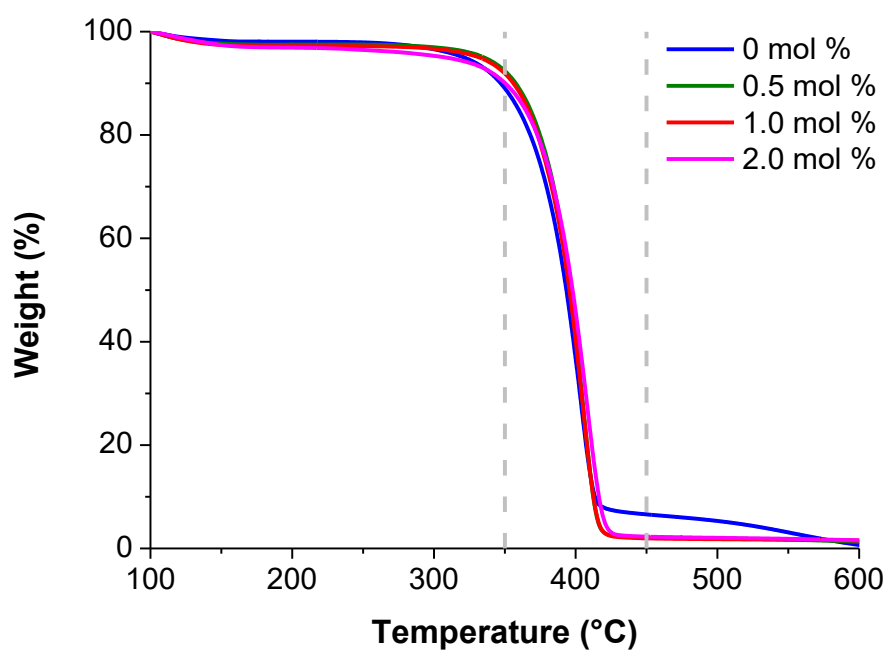


Figure 4.21. TGA degradation profile for PNIPAM (synthesised in DMF) at varying bromoform concentrations.

In the same way as the PDMA reactions (see Chapter 3), the NIPAM homopolymerisations at varying bromoform concentration also uncover a solvent effect, when moving from water to DMF. Significantly the rate of reaction is decreased when using DMF in both cases. Additionally, the reaction time had to be increased from 30 to 360 minutes, in the case of PNIPAM, in order to achieve significant monomer conversion ( $\geq 64\%$ ). Even with the extended UV irradiation time a significant decrease in the final molar mass was observed between the water and DMF studies. The final molar masses suggest that bromoform is not behaving as a CTA for the reactions described herein; as the molar mass would be expected to decrease with increasing bromoform content. However, in this study the final GPC traces are near-identical at all bromoform concentrations.

#### **4.5 Polymerisations conducted in the absence of photoinitiator (ACPA)**

As described in Sections 4.3 and 4.4, PNIPAM can be synthesised at varying bromoform concentration when the photoinitiator ACPA is also present in the system. The next stage of this investigation was to determine whether bromoform itself could also behave as a photoinitiator under these conditions. As previously discussed (see Chapter 3), the preliminary studies conducted by Miller<sup>208</sup>, Dunn *et al.*<sup>209</sup> and Wu *et al.*<sup>211</sup> claim that bromoform (amongst other similar bromine-containing compounds) can behave as a photoinitiator. However, in all three cases there is no evidence to suggest that the temperature of the reactions is controlled and temperatures of up to 50 °C<sup>208</sup> are described after prolonged periods of UV irradiation. Therefore, the heat contributions from the UV lamp could be providing enough energy to the system for initiation to occur using the bromine radicals produced and not the UV light alone. Additionally, these studies often describe the reactions of more reactive monomers (such as acrylamide and AMPS) which could also be a contributing factor to the apparent observed initiation using bromine-containing compounds.

A secondary study was therefore conducted whereby PNIPAM was targeted at varying bromoform concentrations (0, 0.5, 1.0 and 2.0 mol % relative to monomer) in the absence of ACPA photoinitiator. Water was used as the solvent and all other conditions, including volume



of water, initial concentration of monomer, temperature (use of ice bath) and UV exposure time were identical to those used in the investigation in Section 4.3. Figure 4.22 depicts the final  $^1\text{H}$  NMR at each bromoform concentration and shows that the reaction solution does not contain polymer after 30 minutes UV irradiation in each case. This is unlike the kinetic traces seen in Figure 4.2, where the intensity of the monomer peaks reduce, and the polymer peaks increase over time.

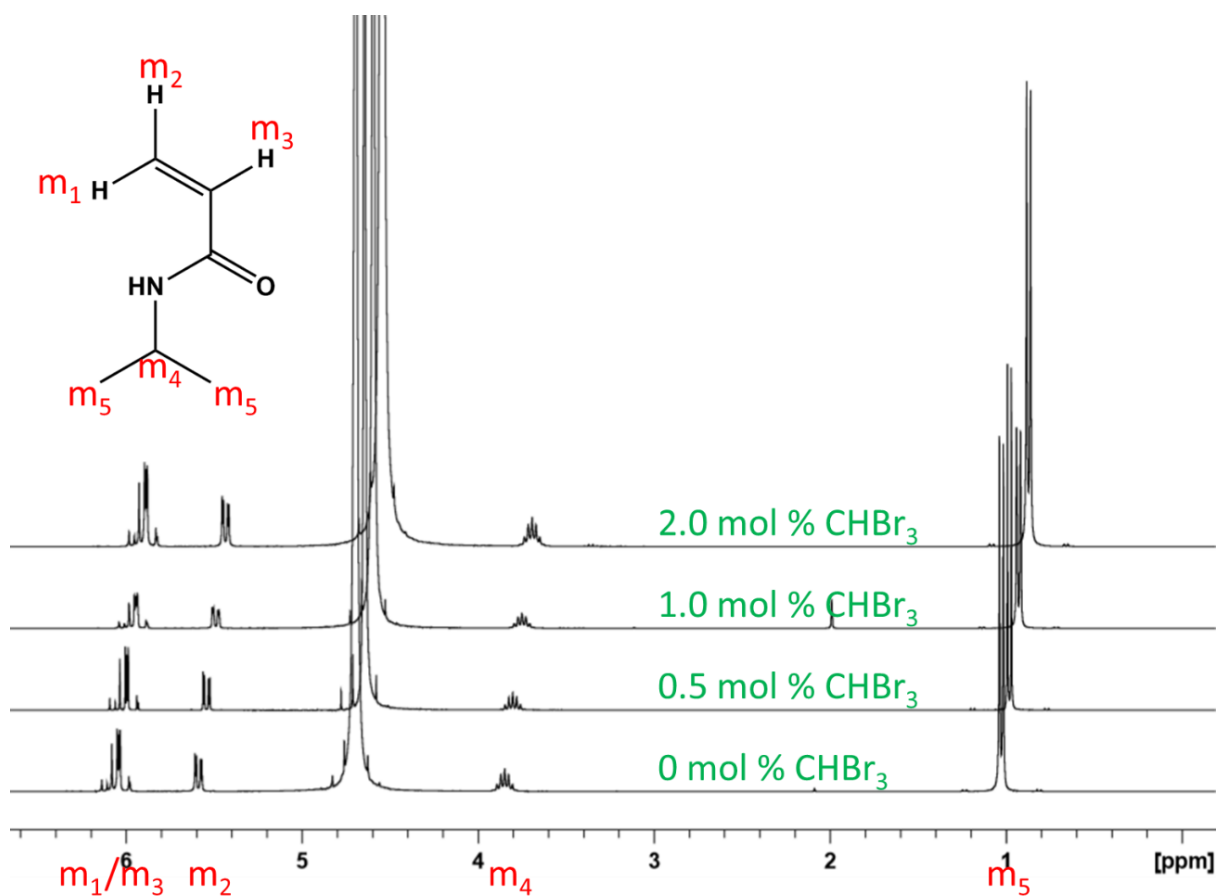


Figure 4.22. Final  $^1\text{H}$  NMR spectra for the attempted synthesis of PNIPAM in the absence of ACPA photoinitiator at varying bromoform concentrations (0, 0.5, 1.0 and 2.0 mol % relative to monomer) in water.

Like in the PDMA study (see Chapter 3), GPC data was collected and there was no peak present to indicate polymer formation had occurred. This evidence suggests that bromoform-derived radical species that are capable of initiating NIPAM polymerisation are not generated under the described conditions and thus the photopolymerisation of *N*-isopropylacrylamide

cannot proceed. Additionally, the reaction with no ACPA and 0 mol % bromoform indicates that *N*-isopropylacrylamide will not self-polymerise under the described conditions (Figure 4.22).

Whilst the observation that bromoform is incapable of initiating the polymerisation of *N*-isopropylacrylamide is not in agreement with some findings in the literature, it does corroborate the more recent work of Thananukul *et al.*<sup>212</sup>. Similarly, bromoform is deemed incapable of acting as a photoinitiator in the homopolymerisation of acrylamide at varied bromoform concentrations; even without the added thermal control provided in the experiments discussed herein. Interestingly, no evidence of temperature control is described in the Thananukul *et al.*<sup>212</sup> study. Finally, these findings support the work described in Chapter 3 that also established that bromoform will not produce radicals capable of initiating the polymerisation of DMA under the same conditions.

#### **4.6 Synthesis of PNIPAM in the presence of air**

Having determined that the polymerisation of *N*-isopropylacrylamide will not proceed in the absence of ACPA photoinitiator, under the conditions investigated herein, a final study was conducted to investigate the influence of oxygen on the polymerisations. As mentioned in Chapter 3, for PDMA synthesis, the purpose of this investigation was to determine the need of running the reactions under an inert atmosphere. As it is more beneficial and cost effective for industrial scale-up if the reactions can be completed in the presence of air. Four reaction formulations were set up using 0, 0.5, 1.0 and 2.0 mol % bromoform (relative to monomer) and whilst the flasks were sealed with a rubber septum, they were not subjected to oxygen removal via vacuum-nitrogen cycles. Water was used as the solvent and all other conditions, including ACPA concentration, volume of water, initial concentration of monomer, initial temperature (use of ice bath) and UV exposure time were identical to those used in the investigation in Section 4.3.

Figure 4.23 depicts the final  $^1\text{H}$  NMR at each bromoform concentration and shows that the reaction solution does not contain polymer after 30 minutes UV irradiation in each case. This evidence suggests that under the described conditions oxygen hinders the polymerisation of *N*-isopropylacrylamide. This is unlike that seen for the polymerisation of *N,N*-dimethylacrylamide (see Chapter 3), where instead an induction period of  $\geq 15$  minutes was present before the polymerisation then proceeded.

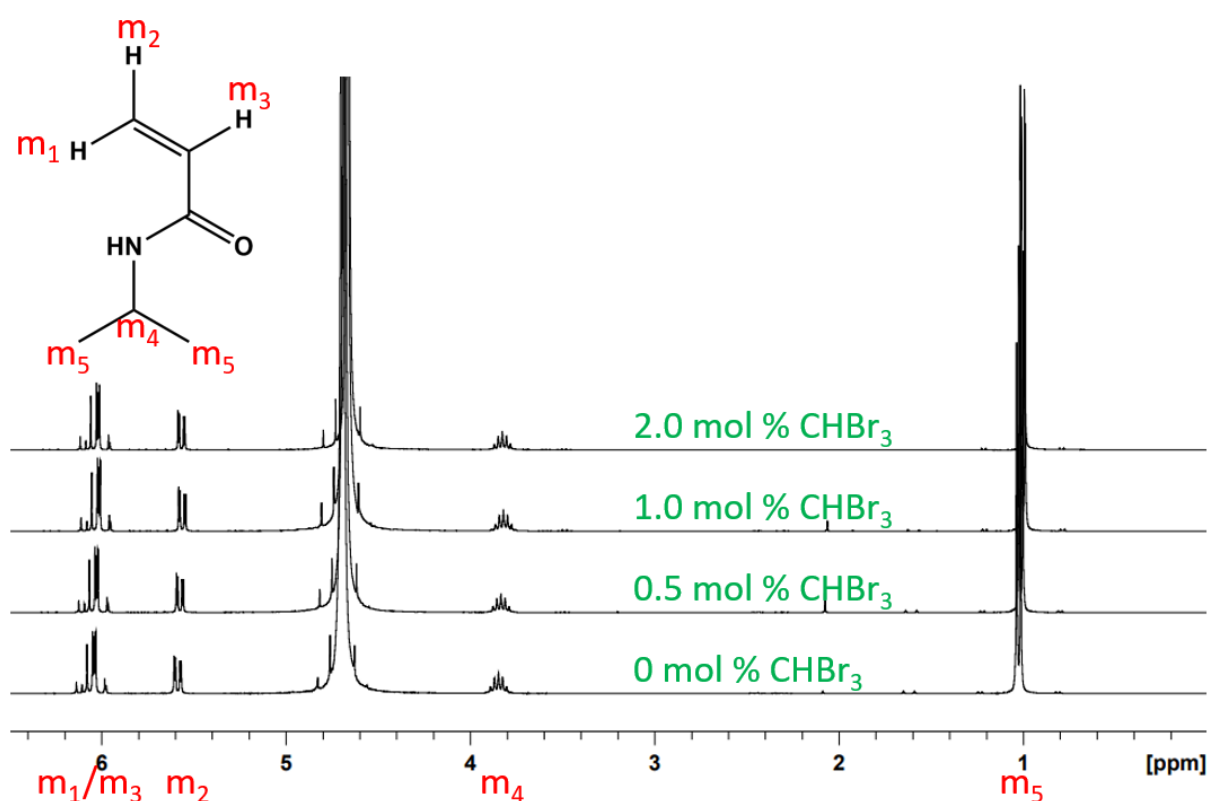


Figure 4.23. Final  $^1\text{H}$  NMR spectra for the attempted synthesis of PNIPAM in the presence of oxygen at varying bromoform concentrations (0, 0.5, 1.0 and 2.0 mol % relative to monomer) in water.

The effect of the presence of oxygen in free radical polymerisation formulations has been extensively discussed in the literature<sup>312–316</sup>. Oxygen is an excellent free radical scavenger<sup>266</sup> and can react with initiating or propagating radicals to form the typically unreactive peroxy radical<sup>314,316</sup>. This results in extended induction periods or termination of growing polymer chains within a polymerisation reaction<sup>314,316</sup>. In this example, one possibility could be that the

induction period exceeds the 30 minutes of UV irradiation that the solutions were exposed to and increased periods of UV irradiation could result in polymer formation.

ACPA (or possibly bromoform-derived) radicals that are generated during the reaction may interact with the oxygen present in the reaction flask. Bromoform is known to react with oxygen via several different mechanisms under varying conditions. Of particular relevance, reactions of the tribromomethyl ( $\text{Br}_3\text{C}^\bullet$ ) and dibromomethyl ( $\text{Br}_2\text{HC}^\bullet$ ) radicals can occur with molecular oxygen ( $\text{O}_2$ )<sup>317,318</sup>. As previously discussed, bromoform can undergo dissociation into  $\text{Br}_2\text{HC}^\bullet$  and  $\text{Br}^\bullet$  radicals upon UV irradiation, or hydrogen transfer, whereby  $\text{Br}_3\text{C}^\bullet$  and  $\text{H}^\bullet$  are produced, likely in competing pathways. It was already determined in Section 4.5 that these radicals ( $\text{Br}_2\text{HC}^\bullet$ ,  $\text{Br}^\bullet$ ,  $\text{Br}_3\text{C}^\bullet$  and  $\text{H}^\bullet$ ) are not capable of initiating the polymerisation of *N*-isopropylacrylamide under the described conditions. However, the  $\text{Br}_3\text{C}^\bullet$  and  $\text{Br}_2\text{HC}^\bullet$  radicals produced are known to react rapidly with  $\text{O}_2$  to form tribromomethyl and dibromomethyl peroxy radicals, respectively. These radicals are then known to decompose in water to form a combination of  $\text{H}^+$ ,  $\text{Br}^-$ ,  $\text{CO}$  and  $\text{CO}_2$ . Additionally, ACPA is also known to react with  $\text{O}_2$  to form unreactive peroxide radicals which can self-terminate through combination<sup>319</sup>, either between two ACPA peroxide radicals or the ACPA peroxide radical and another radical in the system. This second radical could be an ACPA-derived radical not involved in a reaction with  $\text{O}_2$  or one of the many radicals formed from UV-induced bromoform dissociation as previously described. The ACPA present could have been completely consumed by the oxygen, the peroxy radicals produced from the bromoform or one of the decomposition radicals present in the flask; resulting in no radicals capable of initiating the reaction being present.

These experiments highlighted how oxygen prevents the polymerisation of *N*-isopropylacrylamide under the described conditions. Therefore, it was decided that the degassing process (via vacuum-nitrogen cycles) is essential for these reactions.

## 4.7 Reaction scale-up

In order to obtain enough PNIPAM macro-initiator for future block copolymer studies, the homopolymerisation reaction was scaled up by a factor of ten to produce 20 g of polymer. Using the results obtained in Section 4.3, it was determined that the reaction with 2 mol % bromoform offered the opportunity for the highest proportion of potentially bromine-terminated chains to be formed within the usable bromoform miscibility range. Therefore, 2 mol % bromoform was used during the synthesis of 20 g PNIPAM macro-initiator for the purpose of synthesising PNIPAM-*b*-PDMA block copolymers.

$^1\text{H}$  NMR spectroscopy and GPC data were obtained for the PNIPAM macro-initiator produced and are summarised in Table 4.5. The overall conversion, molar mass and molar mass dispersity were all high. This is not dissimilar to the observations in the kinetic study (targeting 2 g of PNIPAM macro-initiator) as described in Section 4.2.

Table 4.5. Summary of final monomer conversion, molar mass and molar mass dispersity data for the polymerisation of *N*-isopropylacrylamide using 2 mol % bromoform targeting 20 g of macro-initiator (in water).

Experiment code	Final monomer conversion (%) <sup>a</sup>	$M_n$ (kg mol <sup>-1</sup> ) <sup>b</sup>	$\bar{D}$ <sup>b</sup>
HJH032	98	512.2	2.2

a) Calculated using  $^1\text{H}$  NMR spectroscopy and Equation 2.1

b) Determined using DMF GPC with PMMA standards

The  $T_g$  of the PNIPAM macro-initiator sample was determined using DSC (as described in Section 2.4.3). Table 4.6 demonstrates that the  $T_g$  is slightly above the literature range (135 - 142 °C<sup>326–328</sup>). Figure 4.24 shows the DSC thermogram of the PNIPAM macro-initiator, identifying the region in which the glass transition temperature occurs.

As previously described, PNIPAM degrades between 350 - 450 °C<sup>329</sup>, via a one-step degradation profile, forming volatile, small molecules. This is evidenced in Figure 4.25 which shows the degradation profile for the PNIPAM macro-initiator synthesised at the larger scale.

Table 4.6. Summary of the glass transition temperature for the PNIPAM macro-initiator synthesised at larger scale (water synthesis).

Experiment series	Onset of $T_g$ (°C)	Endset of $T_g$ (°C)	Midpoint of $T_g$ (°C)
HJH032	139	146	142.5

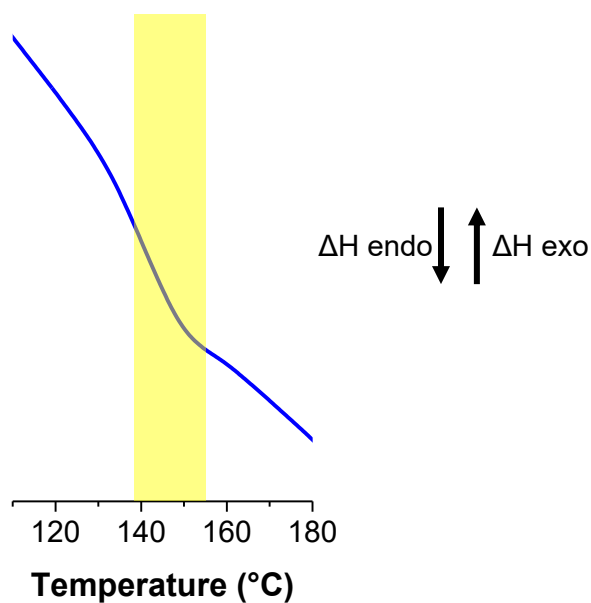


Figure 4.24. DSC thermograms of the PNIPAM macro-initiator (synthesised in water) to be used in future block copolymer reactions.

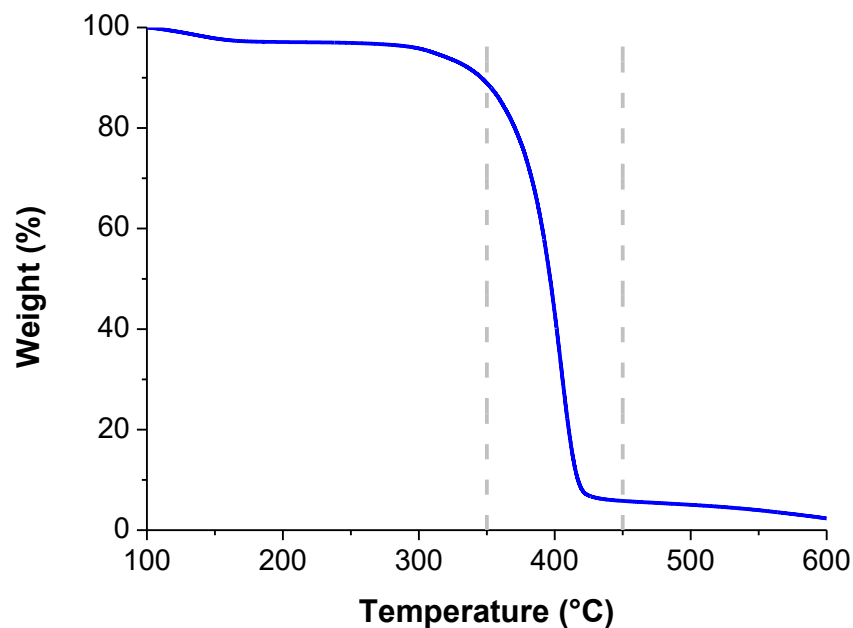


Figure 4.25. TGA degradation profile for the PNIPAM macro-initiator (synthesised in water at larger scale) to be used in block copolymer reactions.

Finally, DLS was used to determine the LCST of the PNIPAM macro-initiator synthesised at 2 mol % bromoform. As previously discussed, the polymer structure goes from a state of well-solvated, randomly distributed polymer at low temperature to a state of highly packed chains at high temperature<sup>330</sup> and results in the polymer precipitating out of solution. Figure 4.26 shows that the PNIPAM macro-initiator synthesised herein exhibits an LCST between 33 and 35 °C; within the given literature range (30 - 35 °C<sup>1,339,344–346</sup>). This information will be used alongside the results discussed in Chapter 5 to highlight any changes in the LCST when forming block copolymers.

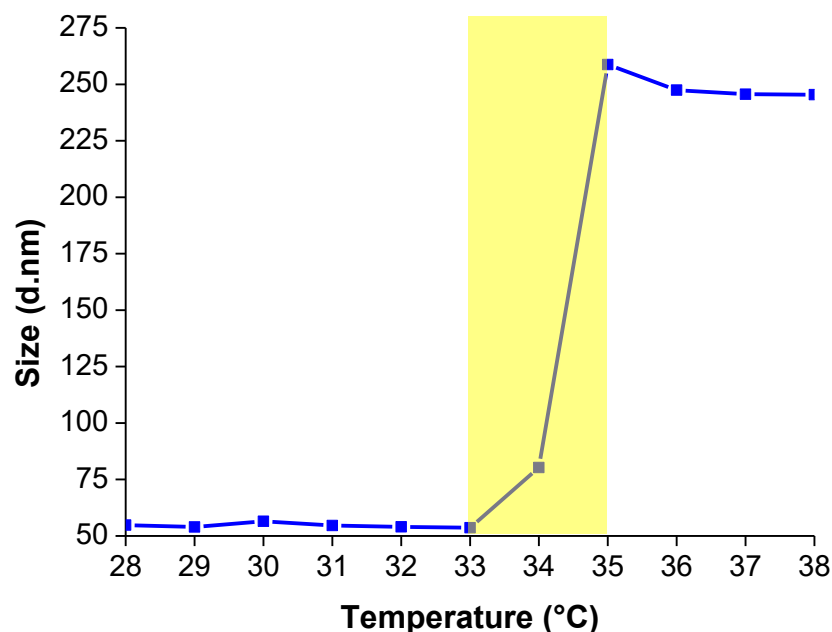


Figure 4.26. Size *versus* temperature of PNIPAM macro-initiator (synthesised in water) at varying bromoform concentrations highlighting the LCST (or coil-to-globule transition).

The purpose of this additional characterisation was to confirm that the thermal properties of the macro-initiators were consistent with those reported in the literature and the small scale kinetic studies, as described above. Additionally, this information will be used to compare the properties of any potential block copolymers to the individual homopolymers they are synthesised from.

## 4.8 Conclusions

This chapter describes the synthesis of poly(*N*-isopropylacrylamide) using bromoform-assisted polymerisation and has been discussed in detail. Multiple studies investigating varying bromoform content, solvent, bromoform as a potential photoinitiator, and the effect of oxygen on the reaction system have been explored.

Initially, the study focusing on the effect of increasing bromoform content, from 0 - 2.0 mol % (relative to monomer), highlighted that bromoform did not appear to exhibit chain transfer capabilities under the described conditions (in water). This was evidenced by the lack of



relationship between bromoform concentration and molar mass from the near-identical GPC traces. If bromoform was behaving as a CTA the molar mass would be expected to decrease significantly with increasing bromoform content. These outcomes contradict the previous work of Thananukul *et al.*<sup>212</sup>, where it was demonstrated that bromoform exhibits successful chain transfer capabilities during the polymerisation of acrylamide. However, there is no evidence of thermal control during the course of the reaction in the Thananukul *et al.* studies and the effects of bromoform as a CTA could be linked to the high temperatures (up to 50 °C) achieved during the prolonged UV irradiation times. Additionally, these findings are similar to the PDMA syntheses described in Chapter 3. Overall, the rate of the reaction, for the synthesis of PNIPAM, was not altered with increasing bromoform content and all reactions (including repeats) achieved high monomer conversions ( $\geq 88\%$ ). Notably, the molar mass dispersity of the final PNIPAM samples was high ( $\mathcal{D} = 2.2 - 2.4$ ), with no suggested relationship between molar mass dispersity and bromoform content.

Changing the solvent to DMF demonstrated considerable differences in the kinetics of NIPAM polymerisation at varying bromoform concentration (0, 0.5, 1.0 and 2.0 mol % relative to monomer). Firstly, the required reaction time needed to be increased from 30 to 360 minutes to achieve reasonably high monomer conversions ( $\geq 64\%$ ) due to the slower rate of reaction in DMF. Similar to the water study, the change in molar mass of resulting PNIPAM could be considered negligible and the GPC traces were near-identical at all bromoform concentrations investigated. There was also little to no change in the rate between the reactions, and no clear relationship between bromoform concentration and the rate of the reaction was observed. Similarly, the molar mass dispersity of the final polymers was high ( $\mathcal{D} = 2.2 - 2.3$ ), with no suggested relationship between molar mass dispersity and bromoform content. The final molar masses obtained in the DMF system (23.8 - 27.2 kg mol<sup>-1</sup>) were considerably lower than those achieved when using water as the solvent (521.1 - 535.6 kg mol<sup>-1</sup>), which is attributed to the lower propagation rates in DMF. Additionally, the results described for the synthesis of

PNIPAM in DMF are also similar to those for PDMA (see Chapter 3) under the same conditions.

In both the water and DMF kinetic studies appropriate purification methods were developed and analytical techniques ( $^1\text{H}$  NMR spectroscopy, GPC, DSC, TGA and DLS) were used to further confirm the characteristics of the final polymers. In all cases, including repeats, the experimentally determined data ( $T_g$ , degradation temperature range and LCST) were within the known literature values. This data will be useful when comparing the properties of the PNIPAM homopolymers to any block copolymers that may be synthesised. As previously discussed, the polymerisations revealed a solvent effect on the homopolymerisation of NIPAM at varied bromoform concentration when moving from water to DMF, which was reflected in a significant decrease in the molar mass of the samples. The reactions in DMF were used as a tool to determine the solvent effect and provide further insight into the role of bromoform in these syntheses. However, with the goal being to develop a more environmentally friendly, inexpensive, industrially relevant polymerisation technique future reactions were conducted in water. This removes the need for toxic, harmful organic solvents during the synthesis, which is one of the overarching objectives of this project.

In another study, in the absence of ACPA photoinitiator, it was determined that whilst bromoform produces radicals when exposed to UV light, these radicals are incapable of initiating the polymerisation of *N*-isopropylacrylamide under the studied conditions. This is contradictory to the previous findings of Dunn *et al.*<sup>209</sup>, Miller *et al.*<sup>208</sup> and Wu *et al.*<sup>211</sup>. In each of these examples, it is claimed that bromine radicals (generated from bromoform, carbon tetrabromide, dibromomethane, monobromomethane or bromotrichloromethane) are capable of initiating the polymerisation of acrylonitrile, acrylic acid, AMPS and styrene. However, the lack of thermal control throughout these reactions could be the contributing factor that resulted in the success of these polymerisations; with the highest solution temperature being reported as 50 °C<sup>208</sup>. Conversely, this does concur with the more recent work of Thananukul *et al.*<sup>212</sup>. In this case bromoform was also deemed incapable of initiating the polymerisation of

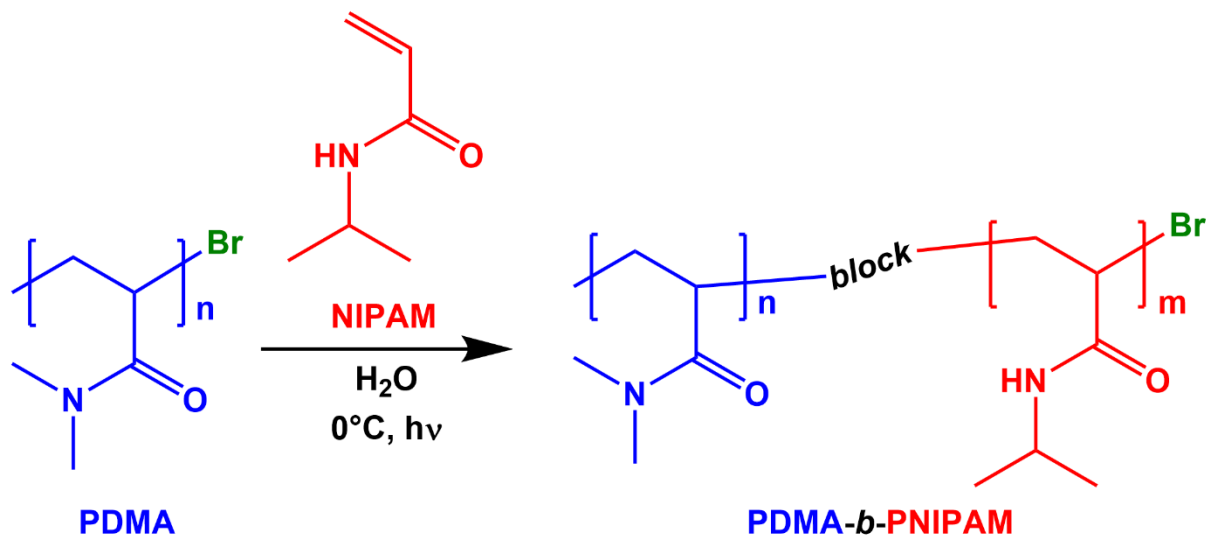
acrylamide at varied bromoform concentration, even without thermal control of the system. Additionally, these findings are analogous to those discussed in Chapter 3; similarly bromoform did not produce any radicals capable of initiating the polymerisation of DMA under the same conditions.

A study in which oxygen was present in the reaction highlighted the importance of the degassing stage in the methodology for these syntheses. With oxygen present, the reaction would not proceed at any bromoform concentration. This is unlike the synthesis of PDMA (see Chapter 3), where an induction period of  $\geq 15$  minutes was observed before the reaction ultimately proceeded. In the case of the attempted synthesis of PNIPAM in air, the ACPA present in each reaction solution could be being completely consumed by the oxygen, the peroxy radicals produced from the bromoform or one of the decomposition radicals present in the flask. In any case, this results in no radicals capable of initiating the reaction being present. Additionally, an induction period that exceeds the 30 minutes of UV irradiation time could also result in no polymer being formed. The hindrance of oxygen to these reactions has emphasised the need for the degassing stage within the methodology for all proceeding PNIPAM syntheses.

Finally, the polymerisation of *N*-isopropylacrylamide at 2.0 mol % bromoform (relative to monomer), was scaled up to produce a suitable quantity of a potentially bromine-terminated PNIPAM macro-initiator (Section 4.7) for subsequent block copolymer syntheses. The PNIPAM macro-initiator was synthesised to 98% conversion and exhibited similar properties to those synthesised at smaller scale (2 g), discussed in Section 4.3 including; high molar mass, high molar mass dispersity,  $T_g$ , degradation profile and LCST.

## **Chapter 5. Synthesis of poly(*N,N*-dimethylacrylamide)-*block*-poly(*N*-isopropylacrylamide) copolymers**

This chapter focuses on the synthesis of poly(*N,N*-dimethylacrylamide)-*block*-poly(*N*-isopropylacrylamide) [PDMA-*b*-PNIPAM] (Scheme 5.1) using suspected bromine-terminated poly(*N,N*-dimethylacrylamide) [PDMA] as a macro-initiator (see Chapter 3).



Scheme 5.1. Synthesis of poly(*N,N*-dimethylacrylamide)-*block*-poly(*N*-isopropylacrylamide) (PDMA-*b*-PNIPAM) using bromine-terminated *N,N*-dimethylacrylamide (PDMA).

One-pot and two-step syntheses were conducted to identify potential routes for the production of PDMA-*b*-PNIPAM block copolymers using PDMA that was synthesised with 2 mol % bromoform (relative to *N,N*-dimethylacrylamide monomer, see Chapter 3); in an attempt to maximise the number of bromine-terminated chains within the usable bromoform miscibility range. In addition, the two-step synthesis route was conducted using PDMA (2 mol % bromoform relative to monomer) that reached high conversion (91 %) and PDMA purposefully stopped at lower conversion (70 % conversion); again in an effort to further maximise the number of bromine-terminated chains. This approach was informed by the literature related to controlled radical polymerisation methods [such as reversible addition-fragmentation chain transfer (RAFT) polymerisation, atom transfer radical polymerisation (ATRP) and nitroxide-mediated polymerisation (NMP)], during which chain ends are often lost under monomer starved conditions (at high conversions, *i.e.*  $\geq 90$  %) to side reactions<sup>321–325</sup>.

*N,N*-Dimethylacrylamide (DMA) and *N*-isopropylacrylamide (NIPAM) were selected due to their desirable water solubility allowing the reaction to be conducted in HPLC-grade water. Similarly to the homopolymerisations of DMA and NIPAM the block copolymer reactions were completed in an ice bath to provide thermal control over the reaction conditions and prevent excessive heating during prolonged UV irradiation (2 hours). In all cases, no additional 4,4'-azobiscyanovaleric acid (ACPA) photoinitiator or bromoform was added to the system in the second step. Finally, a control reaction using a PDMA starting block synthesised without bromoform was conducted to determine whether bromoform was required to cap the polymer chain with a reversibly labile group for subsequent chain extension to occur.

## 5.1 One-pot method

Preliminary block copolymer studies were conducted using a crude (non-precipitated) PDMA starting block. Simply, NIPAM monomer was added to the reaction flask containing PDMA and water. However, as the PDMA had not been precipitated it is reasonable to assume that some unreacted ACPA photoinitiator, bromoform and DMA monomer were also present in the reaction solution.

PDMA-*b*-PNIPAM copolymers with a range of target DMA:NIPAM molar ratios were synthesised and are summarised in Table 5.1. The target degree of polymerisation (DP) was calculated using Equation 5.1. Dimethylformamide (DMF) gel permeation chromatography (GPC, using poly(methyl methacrylate) [PMMA] standards) was performed to determine the relative molar mass values for the PDMA macro-initiator and subsequent PDMA-*b*-PNIPAM block copolymers. The average experimental DPs of the PNIPAM block were determined using two methods; DMF GPC results alongside Equation 5.2 as well as NIPAM monomer conversions as judged by <sup>1</sup>H nuclear magnetic resonance (NMR) spectroscopy and Equation 5.3. In the discussion the average experimental DP of the PNIPAM block calculated from the <sup>1</sup>H NMR data and Equation 5.3 has been used due to the previously described limitations of the GPC data. The length of the PNIPAM block increased when targeting higher DPs; as expected. Furthermore, the monomer conversion was generally higher when longer PNIPAM

blocks were targeted, which is attributed to higher NIPAM concentrations during the polymerisation.

Table 5.1. Summary of  $M_n$ ,  $\bar{D}$  and the target and achieved PNIPAM DPs in PDMA-*b*-PNIPAM copolymers synthesised via the one-pot method, using 2 mol % bromoform and 1.0 mol % ACPA (relative to DMA monomer).

Target polymer <sup>a</sup>	NIPAM conversion <sup>b</sup> (%)	$M_n$ <sup>c</sup> (kg mol <sup>-1</sup> )	PNIPAM DP <sup>d</sup> (GPC)	PNIPAM DP <sup>e</sup> (NMR)	$\bar{D}$ <sup>c</sup> ( $M_w/M_n$ )
PDMA <sub>1450</sub> <sup>f</sup>	-	143.6	-	-	3.6
PDMA <sub>1450</sub> - <i>b</i> -PNIPAM <sub>160</sub>	62	145.3	15	100	4.2
PDMA <sub>1450</sub> - <i>b</i> -PNIPAM <sub>360</sub>	63	148.1	40	230	4.3
PDMA <sub>1450</sub> - <i>b</i> -PNIPAM <sub>620</sub>	88	145.9	20	550	3.4
PDMA <sub>1450</sub> - <i>b</i> -PNIPAM <sub>970</sub>	89	184.4	360	860	4.0
PDMA <sub>1450</sub> - <i>b</i> -PNIPAM <sub>1450</sub>	94	186.3	380	1360	5.0
PDMA <sub>1450</sub> - <i>b</i> -PNIPAM <sub>2180</sub>	90	259.1	1020	1960	5.3
PDMA <sub>1450</sub> - <i>b</i> -PNIPAM <sub>3380</sub>	96	233.2	790	3240	6.4
PDMA <sub>1450</sub> - <i>b</i> -PNIPAM <sub>5800</sub>	90	216.2	640	5220	8.4

a) Target PNIPAM DP calculated using GPC and Equation 5.1.

b) Calculated using <sup>1</sup>H NMR spectroscopy and Equation 2.1.

c) Determined by DMF GPC using PMMA standards.

d) Calculated using DMF GPC results and Equation 5.2 and values are rounded to the nearest ten.

e) Calculated using <sup>1</sup>H NMR spectroscopy and Equation 5.3. and values are rounded to the nearest ten.

f) PDMA macro-initiator achieving a final DMA monomer conversion of 99 %.

$$\frac{\text{DP of PDMA starting block}}{\text{DMA ratio in block copolymer}} \times \text{NIPAM target ratio in block copolymer} \quad \text{Equation 5.1.}$$

$$\frac{M_n \text{ of 'copolymer' } - M_n \text{ of PDMA macroinitiator}}{\text{molecular weight of single NIPAM unit}} \quad \text{Equation 5.2.}$$

$$\frac{\text{Conversion of NIPAM block}}{100} \times \text{target DP} \quad \text{Equation 5.3.}$$

The GPC traces of the PDMA-*b*-PNIPAM copolymers indicate successful chain extension of the PDMA macro-initiator with NIPAM before [Figure 5.1(a)] and after precipitation [Figure 5.1(b)]. A clear shift to shorter retention times was observed when extending PDMA with NIPAM monomer. However, the molar masses determined by GPC (see Table 5.1) do not reflect sufficiently increased molar mass values for block copolymers where the target PNIPAM DP was  $\leq 550$ . This is likely due to the already large size of the PDMA macro-initiators [ $M_n > 140.0 \text{ kg mol}^{-1}$ , relative to PMMA standards] and the limitations of the GPC. Additionally, there is significant broadening of the GPC traces or the presence of low molar mass shoulders (or tails) for block copolymers where the target PNIPAM DP was  $\geq 1360$  [Figure 5.1(b)]. This could be due to the presence of; unreacted PDMA macro-initiator, PNIPAM homopolymer and/or poly(*N,N*-dimethylacrylamide-*stat-N*-isopropylacrylamide) [PDMA-*st*-PNIPAM]. As previously discussed, bromoform can undergo dissociation into  $\text{Br}_2\text{HC}^\bullet$  and  $\text{Br}^\bullet$  radicals upon UV irradiation, or hydrogen transfer, whereby  $\text{Br}_3\text{C}^\bullet$  and  $\text{H}^\bullet$  are produced, likely in competing pathways. It was already determined in Chapters 3 and 4 that these radicals ( $\text{Br}_2\text{HC}^\bullet$ ,  $\text{Br}^\bullet$ ,  $\text{Br}_3\text{C}^\bullet$  and  $\text{H}^\bullet$ ) are not capable of initiating the polymerisation of DMA or NIPAM under the described conditions. However, the PDMA chains that have been capped by hydrogen (due to the aforementioned hydrogen transfer) would be irreversibly terminated and unable to react further to form block copolymers. Additionally, as aforementioned, the PDMA starting block has not been precipitated, so unreacted ACPA, bromoform and DMA monomer could be present in the reaction solution. Due to the presence of unreacted ACPA and DMA monomer in the system it is reasonable to assume that additional PDMA, as well as PNIPAM and PDMA-*st*-PNIPAM could be made during the reaction. Some of these products, including the



PNIPAM, could be formed at high molecular weights and be responsible for the apparent shift in the GPC traces observed [Figure 5.1]. The presence of one or more of these side products is also reflected in the significantly increased dispersities of the block copolymers (see Table 5.1) when compared to the PDMA macro-initiator and also contributes to the lack of linearity observed between average experimental DP and molar mass (Figure 5.2).

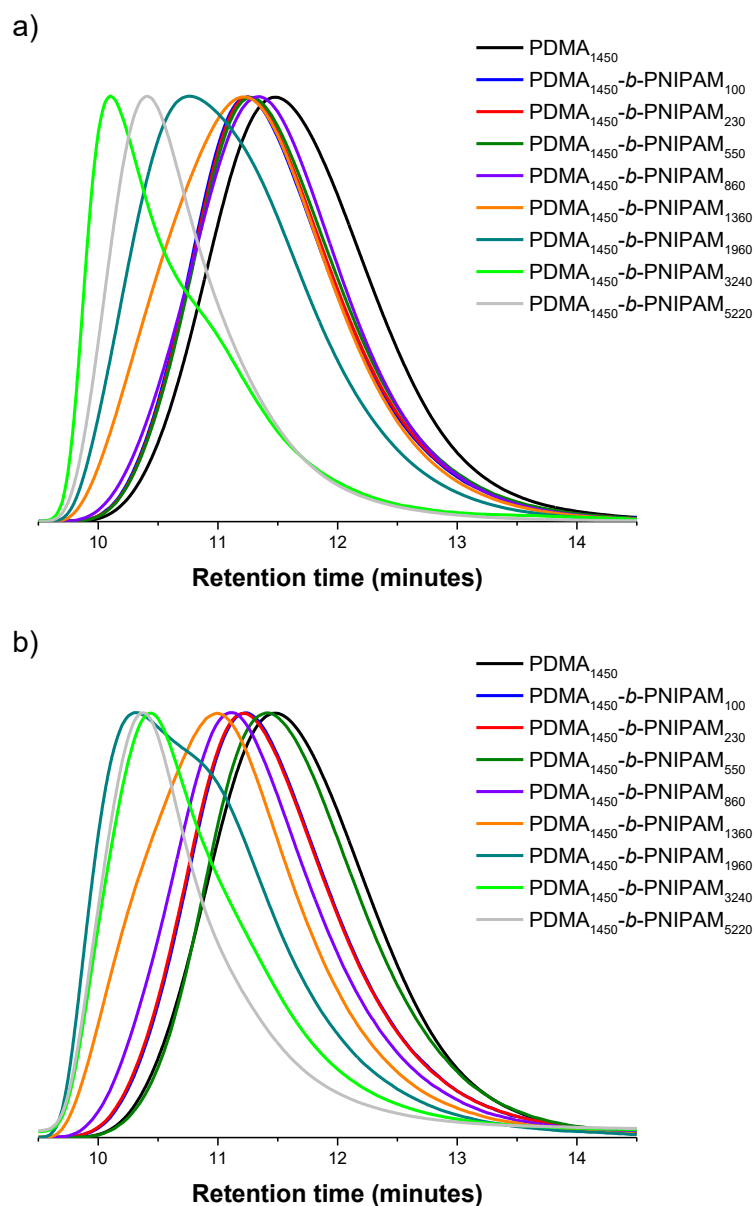


Figure 5.1. GPC traces of PDMA macro-initiator and PDMA-*b*-PNIPAM copolymers (one-pot) with target PNIPAM DPs ranging from 160 to 5800 (a) before precipitation and (b) after precipitation.

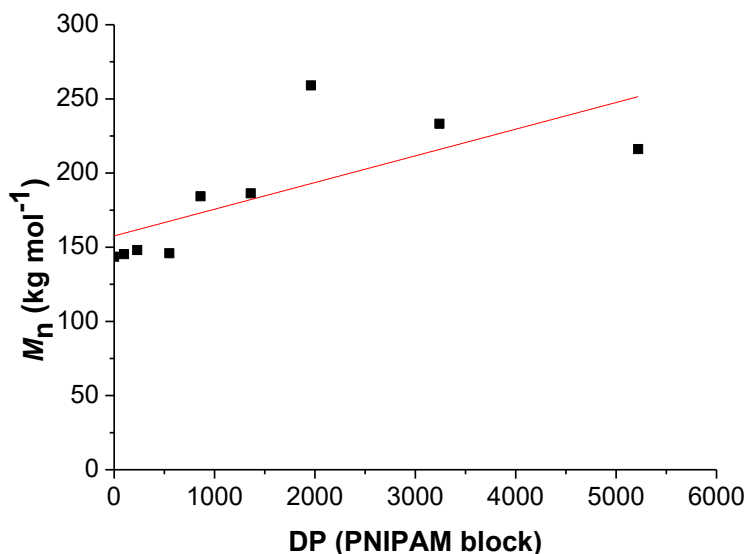


Figure 5.2. Achieved molar mass of the copolymer *versus* average experimental degree of polymerisation (determined using <sup>1</sup>H NMR spectroscopy and Equation 5.3.) of the PNIPAM block in the PDMA-*b*-PNIPAM block copolymers synthesised during the one-pot synthesis.

### 5.1.1 Thermal properties

The block copolymer samples were further characterised using differential scanning calorimetry (DSC), thermal gravimetric analysis (TGA) and dynamic light scattering (DLS). DSC (as described in Section 2.3.3) was used to determine the glass transition temperatures ( $T_g$ ) of the samples. As observed across the literature, it is common to identify two glass transitions for high molecular weight diblock and graft copolymers; one for each polymer phase present<sup>347</sup>. Table 5.2 summarises the two glass transition temperatures and Figure 5.3 shows the DSC thermograms in each of the copolymers except for PDMA<sub>1450</sub>-*b*-PNIPAM<sub>5220</sub>; which has the highest PNIPAM target block length and only a single transition. For the samples with two transitions, the first ( $T_{g1}$ ) is present between 74 - 90 °C. This transition appears lower than the available literature values (89 - 130 °C<sup>297–302</sup>) for PDMA homopolymer in most cases but is attributed to the PDMA block. The second transition ( $T_{g2}$ ) is present between 121 - 143 °C and is attributed to the PNIPAM block. Similarly, the samples with low PNIPAM DPs ( $\leq 230$ ) exhibit transitions lower than the literature range (135 - 142 °C<sup>326–328</sup>) for the homopolymer,

which is attributed to the oligomeric nature of the PNIPAM blocks. The decrease in the glass transition of the individual blocks is similar to other findings within the literature which have also demonstrated glass transitions below those of the individual homopolymers for other systems<sup>348</sup>.

Table 5.2. Summary of the glass transition temperatures for the PDMA macro-initiator, PDMA-*b*-PNIPAM copolymers (one-pot) and PNIPAM homopolymer synthesised using 2 mol % bromoform (relative to monomer).

Sample	$T_{g1}$ (°C)	$T_{g2}$ (°C)
PNIPAM (2 mol %)	-	143.0
PDMA <sub>1450</sub>	116.0	-
PDMA <sub>1450</sub> - <i>b</i> -PNIPAM <sub>100</sub>	80.0	121
PDMA <sub>1450</sub> - <i>b</i> -PNIPAM <sub>230</sub>	77.5	125.0
PDMA <sub>1450</sub> - <i>b</i> -PNIPAM <sub>550</sub>	74.0	142.0
PDMA <sub>1450</sub> - <i>b</i> -PNIPAM <sub>860</sub>	90.0	138.0
PDMA <sub>1450</sub> - <i>b</i> -PNIPAM <sub>1360</sub>	78.5	142.5
PDMA <sub>1450</sub> - <i>b</i> -PNIPAM <sub>1960</sub>	74.5	141.0
PDMA <sub>1450</sub> - <i>b</i> -PNIPAM <sub>3240</sub>	79.5	142.5
PDMA <sub>1450</sub> - <i>b</i> -PNIPAM <sub>5220</sub>	-	143.0

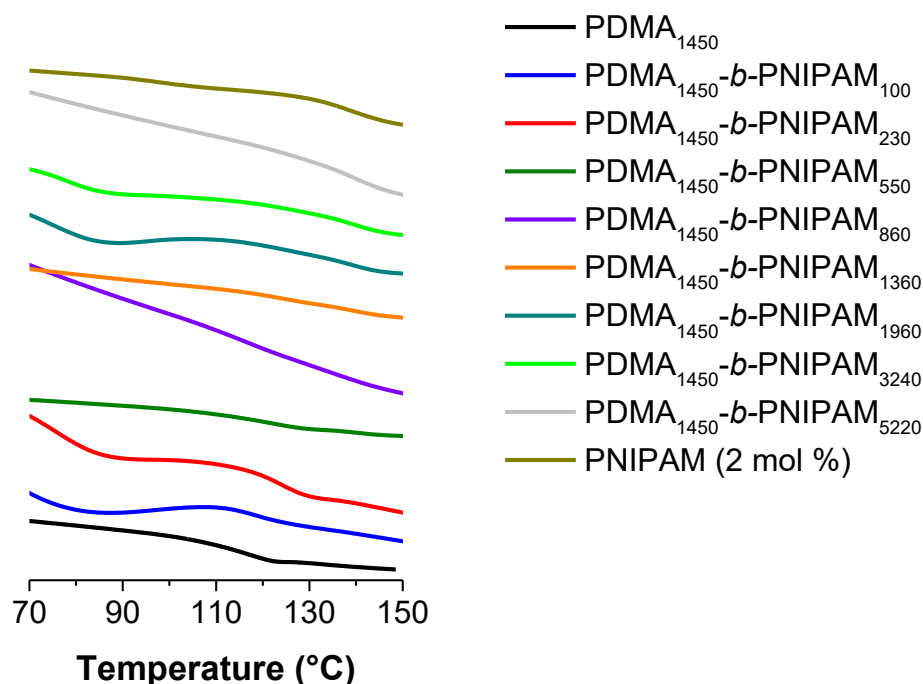


Figure 5.3. DSC thermograms of the PDMA macro-initiator, PDMA-*b*-PNIPAM copolymers (one-pot) and PNIPAM homopolymer synthesised using 2 mol % bromoform (relative to monomer).

TGA was used to determine the degradation profiles of the PDMA-*b*-PNIPAM copolymers. The available literature data indicate that both PDMA and PNIPAM homopolymers degrade between 350 and 450 °C<sup>302</sup> via a one-step degradation profile, forming volatile, small molecules. Therefore, it is unsurprising that each of the PDMA-*b*-PNIPAM copolymers also appear to degrade in this range (see Figure 5.4). Closer inspection of the degradation profiles shows that the copolymers with small quantities of PNIPAM more closely follow the profile of the PDMA homopolymer. Whilst the trend is not linear, the block copolymers that contain high quantities of PNIPAM more closely resemble the degradation profile of a PNIPAM homopolymer synthesised with 2 mol % bromoform (relative to monomer).

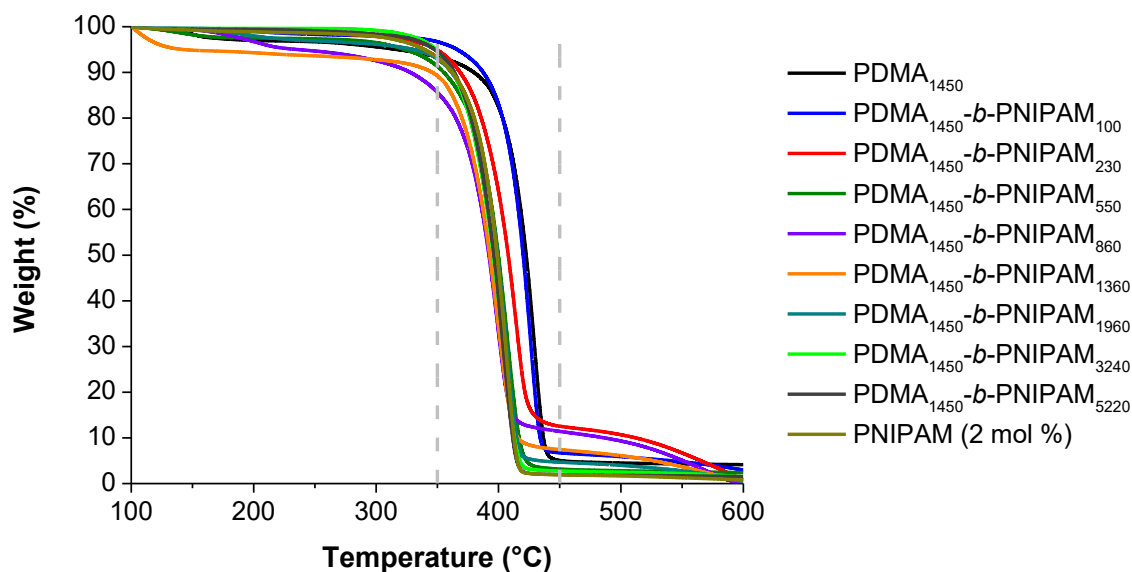


Figure 5.4. TGA degradation profiles for PDMA macro-initiator, PDMA-*b*-PNIPAM copolymers (one-pot) and PNIPAM homopolymer synthesised using 2 mol % bromoform (relative to monomer).

Finally, DLS was used to determine the lower critical solution temperature (LCST) of the block copolymers. There is varied information in the literature regarding the influence on the LCST when incorporating PNIPAM into block copolymers; in some cases a change (up to 44 °C) is reported<sup>279,345</sup>, in others, a negligible change is identified<sup>349,350</sup> and many show no change at all<sup>351–354</sup>. Herein, the samples with a DP  $\leq 230$  do not exhibit an LCST (between 25–50 °C) possibly due to the low quantities of PNIPAM in the copolymer structures and the dominance of PDMA. Additionally, the sample with a NIPAM DP of 550 exhibits an LCST slightly higher than that observed for the PNIPAM homopolymer; between 34 and 36 °C as opposed to 34 to 35 °C. All of the remaining samples exhibit a coil-to-globule transition between 34 and 35 °C, which is the same as that observed for the synthesis of PNIPAM homopolymers at varying bromoform concentrations (see Chapter 4). The coil-to-globule transition is highlighted by the change in size with temperature and in all cases, where a transition is present, the onset of the LCST (34 °C) is within the literature range for PNIPAM homopolymer<sup>1,339,344–346</sup>. However,

there is no apparent trend between size and PNIPAM block length in the copolymers after the transition has occurred.

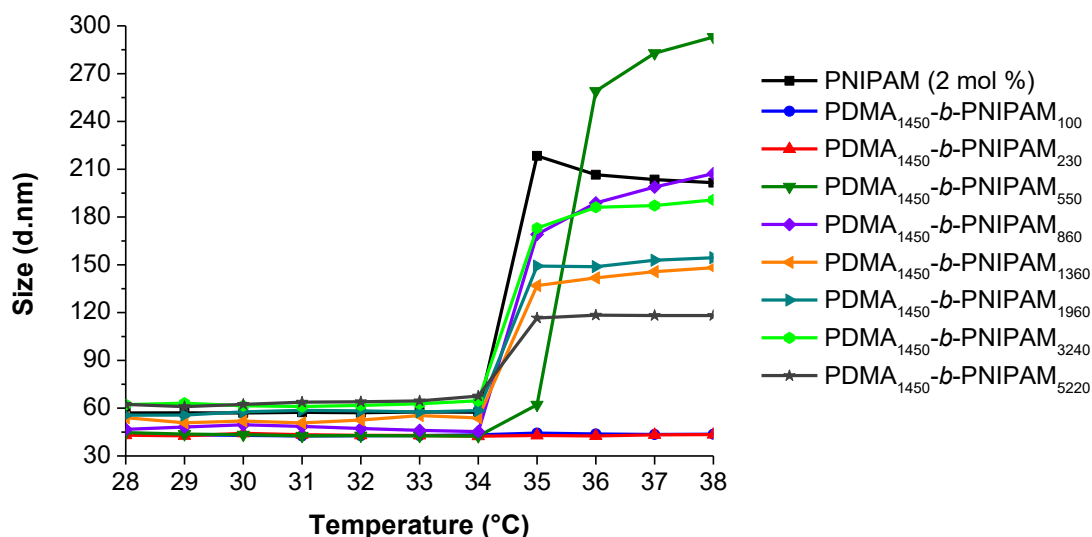


Figure 5.5. Size *versus* temperature of PNIPAM homopolymer (2 mol % bromoform relative to monomer) and PDMA-*b*-PNIPAM copolymers (one-pot) highlighting the LCST (or coil-to-globule transition).

In this study, PDMA-*b*-PNIPAM copolymers were synthesised via a one-pot method at varying PNIPAM block ratios in HPLC-grade water. The GPC traces of the PDMA-*b*-PNIPAM copolymers indicate successful chain extension of the PDMA macro-initiator as the traces shift to shorter retention times. However, the molar masses determined by GPC of these samples do not reflect the significant shifts observed in the traces. This is due to the already large size of the PDMA macro-initiators and the limits of the GPC. In addition, the traces exhibiting low molar mass shoulders (or tails) suggest that there are other species present in the final sample which also contributes to the large dispersities and inaccurate molar mass values obtained. As aforementioned, because the PDMA macro-initiator was not precipitated prior to these reactions, it is possible that PDMA (both non-reactive PDMA macro-initiator and newly created PDMA), PNIPAM and PDMA-*st*-PNIPAM contaminants could be formed due to the unreacted ACPA being present from the first stage of the reaction (used to produce the PDMA macro-

initiator). Additionally, the PNIPAM formed could have resulted in the apparent shift to shorter retention times that have been observed. Further characterisation in the form of DSC, TGA and DLS was completed to identify similarities between the potential PDMA-*b*-PNIPAM copolymers and the individual PDMA and PNIPAM homopolymers. Two glass transitions are identified in the block copolymers (excluding the PDMA<sub>1450</sub>-*b*-PNIPAM<sub>5220</sub> sample); each corresponding to the individual homopolymers which is common in block copolymers. The samples all degrade via a one-step degradation process between 350 and 450 °C; which is also seen for the individual homopolymers. Finally, the onset of the LCST of the block copolymers (at DP ≥ 550) is within the known literature range for PNIPAM and is not dissimilar to the PNIPAM synthesised at 2 mol % bromoform (relative to monomer). However, no LCST was observed for the copolymers with PNIPAM block lengths ≤ 230 likely due to the dominance of the PDMA portion of the block copolymers.

Using crude PDMA (*i.e.* non-precipitated) has resulted in the added difficulty of unwanted PDMA, PNIPAM and PDMA-*st*-PNIPAM potentially being present alongside the block copolymers that were targeted. Therefore, to remove this complication and delve deeper into understanding this system, a second series of reactions where the PDMA macro-initiator was suitably purified were conducted.

## 5.2 Two-step method

As identified in Section 5.1, using crude PDMA macro-initiator (in a one-pot synthesis route) leads to additional unwanted products being formed. Therefore, in this study precipitated PDMA macro-initiators have been used to remove unreacted ACPA, bromoform and DMA monomer and prevent the formation of unwanted PDMA and PNIPAM homopolymers and PDMA-*st*-PNIPAM copolymers. In this case, the reaction solutions in step two contain precipitated PDMA, NIPAM monomer and HPLC-grade water only. To further develop the synthetic methodology, two PDMA macro-initiators have been used in the two-step synthesis; namely a PDMA sample that reached high conversion (≥ 91 %) and PDMA purposefully

stopped at lower conversion (70 % conversion) in an effort to maximise the number of bromine-terminated chains.

### 5.2.1 Macro-initiator at high conversion

A PDMA macro-initiator was synthesised using 2 mol % bromoform (relative to DMA monomer) and allowed to proceed to high monomer conversion (91 % after 2 hours of UV irradiation, see Chapter 3). PDMA-*b*-PNIPAM copolymers with varying block molar ratios were subsequently targeted in a polymerisation formulation containing PDMA (see Figure 5.6), NIPAM monomer and water only. Importantly, the PDMA was purified to remove any unreacted monomer, initiator and bromoform impurities, and no additional ACPA or bromoform was used in this reaction. This purification step ensures that any subsequent polymerisation can only be initiated by the proposed PDMA macro-initiator (and not residual ACPA or bromoform), as the NIPAM does not self-polymerise under these conditions (*vide infra*).

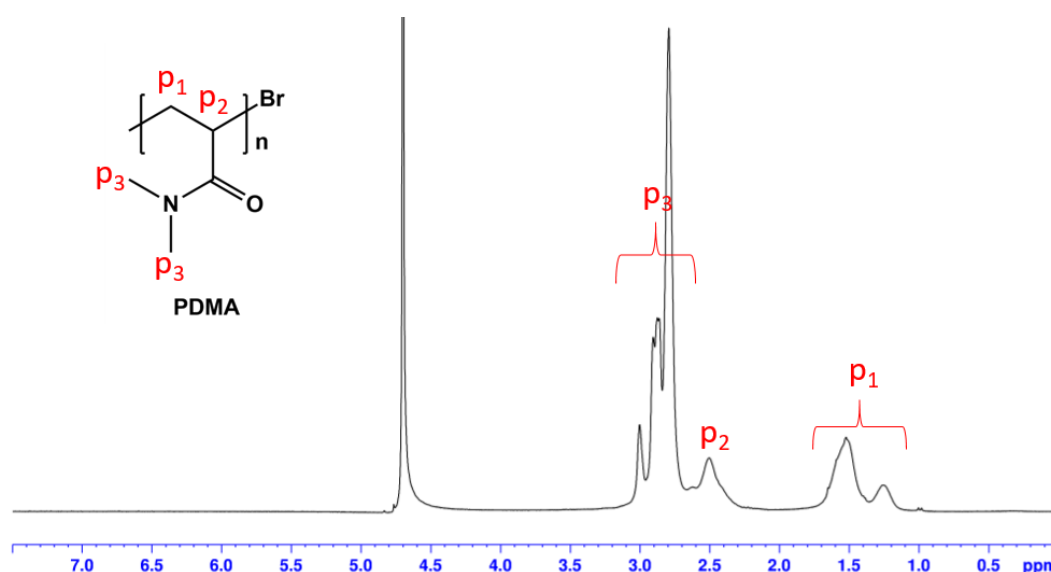


Figure 5.6. <sup>1</sup>H NMR spectrum of precipitated PDMA macro-initiator (synthesised to 91 % conversion) showing no residual monomer peaks present in the sample at 5.6, 6.0 and 6.6 ppm.



PDMA-*b*-PNIPAM copolymers with a range of target DMA:NIPAM molar ratios were synthesised as summarised in Table 5.3.

Table 5.3. Summary of  $M_n$ ,  $\bar{D}$  and the target and achieved PNIPAM DPs in PDMA-*b*-PNIPAM copolymers synthesised via the two-step method using PDMA that achieved high monomer conversion (91 %) in step one.

Target polymer <sup>a</sup>	NIPAM conversion <sup>b</sup> (%)	$M_n$ <sup>c</sup> (kg mol <sup>-1</sup> )	PNIPAM DP <sup>d</sup> (GPC)	PNIPAM DP <sup>e</sup> (NMR)	$\bar{D}$ <sup>c</sup> ( $M_w/M_n$ )
PDMA <sub>1500</sub> <sup>f</sup>	-	148.4	-	-	3.9
PDMA <sub>1500</sub> - <i>b</i> -PNIPAM <sub>170</sub>	66	163.6	130	110	3.4
PDMA <sub>1500</sub> - <i>b</i> -PNIPAM <sub>380</sub>	70	165.8	150	270	3.4
PDMA <sub>1500</sub> - <i>b</i> -PNIPAM <sub>640</sub>	65	196.3	420	420	3.2
PDMA <sub>1500</sub> - <i>b</i> -PNIPAM <sub>1000</sub>	75	164.4 <sup>g</sup>	140	750	5.3 <sup>g</sup>
PDMA <sub>1500</sub> - <i>b</i> -PNIPAM <sub>1500</sub>	87	264.8	1030	1310	4.1
PDMA <sub>1500</sub> - <i>b</i> -PNIPAM <sub>2300</sub>	89	392.6 <sup>h</sup>	2160	2050	4.1 <sup>h</sup>
PDMA <sub>1500</sub> - <i>b</i> -PNIPAM <sub>3500</sub>	95	463.6	2790	3330	3.9
PDMA <sub>1500</sub> - <i>b</i> -PNIPAM <sub>6000</sub>	85	603.7	4020	5100	3.4

a) Target PNIPAM DP calculated using GPC and Equation 5.1..

b) Calculated using <sup>1</sup>H NMR spectroscopy and Equation 2.1.

c) Determined by DMF GPC using PMMA standards.

d) Calculated using DMF GPC results and Equation 5.2 and values are rounded to the nearest ten.

e) Calculated using <sup>1</sup>H NMR spectroscopy and Equation 5.3. and values are rounded to the nearest ten.

f) PDMA macro-initiator synthesised using 2 mol % bromoform (relative to monomer), achieving a final DMA monomer conversion of 91 %.

g)  $M_n$  appears smaller than expected due to broadness of GPC trace, suggesting PDMA macro-initiator is still present. This is also reflected in the higher dispersity value.

h)  $M_n$  appears smaller than expected due to PDMA macro-initiator still present. This is also reflected in the higher dispersity value.

The target degree of polymerisation was calculated using Equation 5.1.. DMF GPC analysis was performed to determine the molar mass values for the PDMA macro-initiator and subsequent PDMA-*b*-PNIPAM block copolymers (relative to PMMA standards). The average experimental DPs of the PNIPAM block were determined using two methods; DMF GPC results alongside Equation 5.2 as well as NIPAM monomer conversions as judged by  $^1\text{H}$  nuclear magnetic resonance (NMR) spectroscopy and Equation 5.3. As previously described, the average experimental DP of the PNIPAM block calculated from the  $^1\text{H}$  NMR data and Equation 5.3 will be discussed due to the limitations of the GPC data.

As summarised in Table 5.3, the length of the PNIPAM block increased when targeting higher DPs, as expected. Furthermore, the monomer conversion was higher when longer PNIPAM blocks were targeted, which is attributed to higher NIPAM concentrations during the polymerisation. The GPC traces [Figure 5.7(b)] of the purified PDMA-*b*-PNIPAM copolymers indicate successful chain-extension of the PDMA macro-initiator with NIPAM for only the samples with an achieved PNIPAM DP  $\geq 420$ . A clear shift to shorter retention times was observed in these samples when extending PDMA with NIPAM monomer, before [Figure 5.7(a)] and after precipitation see [Figure 5.7(b)], which corresponds to a significant increase in  $M_n$  as summarised in Table 5.3. Notably, there is a clear formation of low molar mass species [Figure 5.7(a)] that is then removed from the final samples during precipitation [Figure 5.7(b)]. This is reflected in the traces shifting to shorter retention times after precipitation (Figure 5.7).

Encouragingly, there is a minimal low molar mass shoulder observed at retention times expected for the PDMA homopolymer alone in the final precipitated samples [Figure 5.7(b)], in many cases, and the  $M_n$  increases somewhat linearly when targeting larger PNIPAM DPs (Figure 5.8). On the other hand, Figure 5.7 suggests that little or no PDMA chain extension was achieved for block copolymers where the target PNIPAM DP was  $\leq 380$ . However,  $^1\text{H}$  NMR spectra confirm the presence of the PNIPAM block in both cases (Figure 5.9), suggesting block copolymers have been formed in all cases. These contrasting observations may allude

to the limitations of GPC when analysing the chain extension of the already high molar mass PDMA macro-initiator [ $M_n > 140.0 \text{ kg mol}^{-1}$ , relative to poly(methyl methacrylate) standards]. Additionally, GPC traces for purified PDMA<sub>1500</sub>-*b*-PNIPAM<sub>750</sub> and PDMA<sub>1500</sub>-*b*-PNIPAM<sub>2050</sub> block copolymers (target PDMA:PNIPAM molar ratios of 0.60:0.40 and 0.40:0.60, respectively) exhibit low molar mass shoulders (or tails) which are most likely due to unreacted PDMA macro-initiator. This is also reflected in the higher molar mass dispersity when compared to the other PDMA-*b*-PNIPAM block copolymers synthesised, and abnormally low  $M_n$  values as summarised in Table 5.3. This suggests that not all of the PDMA chains synthesised in the first step are capable of being chain-extended with NIPAM; likely due to the competing dissociation pathways of bromoform (between bromine and hydrogen transfer<sup>202–206</sup>). Additionally, this could be due to the presence of PDMA chains without the necessary bromine functionality for example, chains initiator-capped at both ends, most likely formed via termination events.

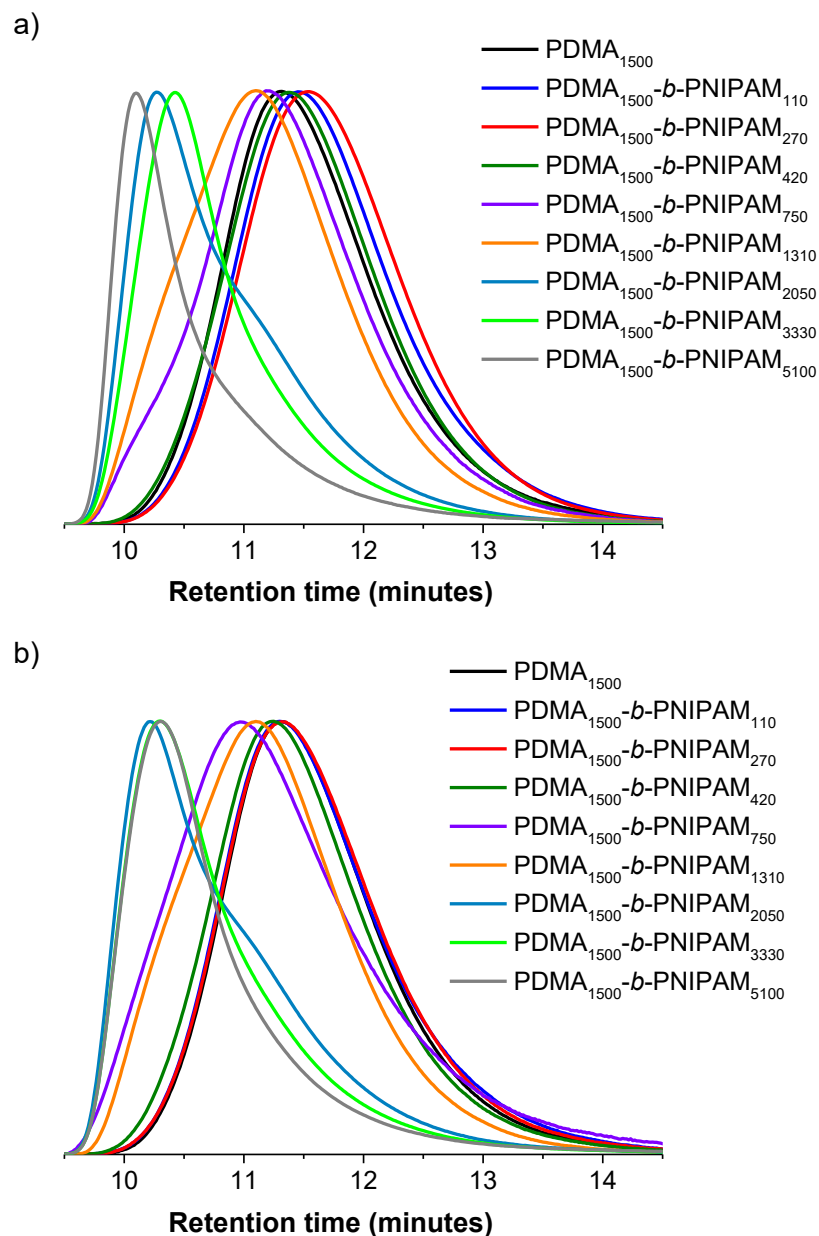


Figure 5.7. GPC traces of PDMA macro-initiator and PDMA-*b*-PNIPAM copolymers (two-step, PDMA macro-initiator 91 % conversion) with target PNIPAM DPs ranging from 170 to 6000 (a) before precipitation and (b) after precipitation.

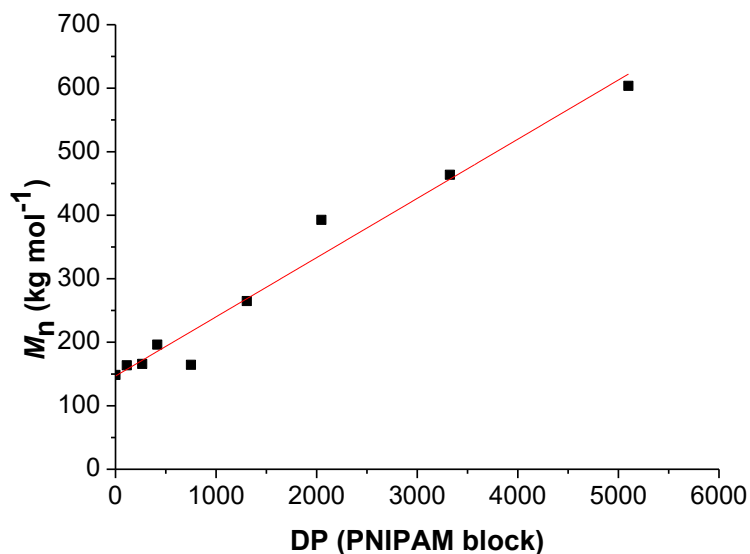


Figure 5.8. Achieved molar mass *versus* average experimental degree of polymerisation (determined using  $^1\text{H}$  NMR spectroscopy and Equation 5.3.) of the PNIPAM block in the PDMA-*b*-PNIPAM block copolymers synthesised during the two-step synthesis (using PDMA synthesised to 91 % conversion).

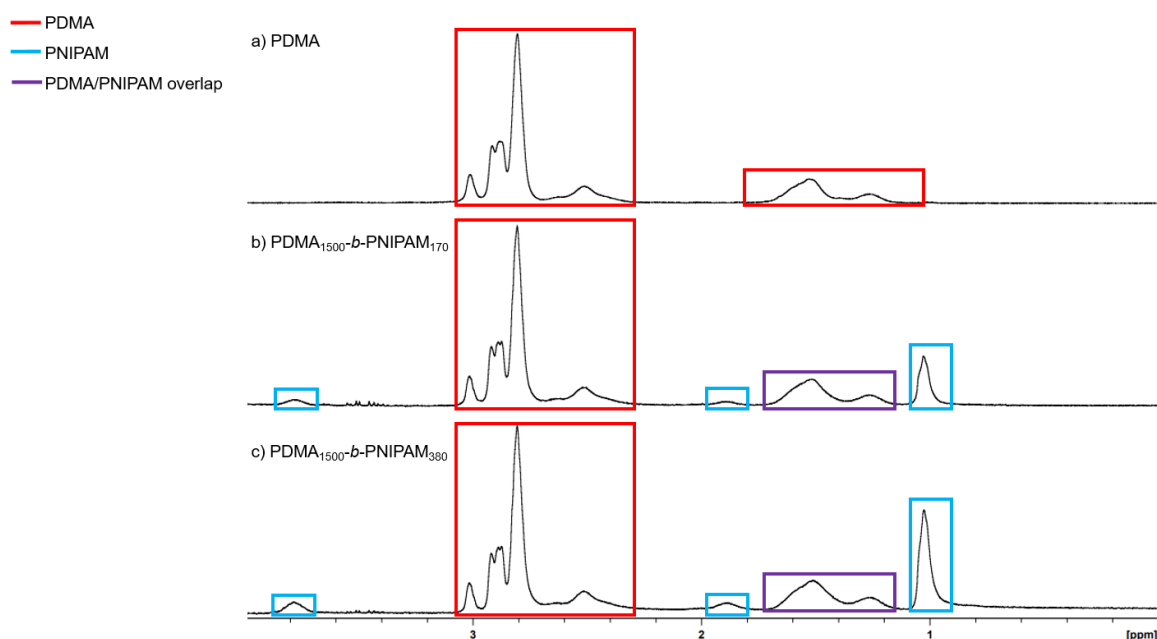


Figure 5.9.  $^1\text{H}$  NMR spectra showing (a) PDMA macro-initiator (91 % conversion), (b) PDMA<sub>1500</sub>-*b*-PNIPAM<sub>170</sub> and (c) PDMA<sub>1500</sub>-*b*-PNIPAM<sub>380</sub> all after precipitation; indicating the presence of PNIPAM in the block copolymers.

### 5.2.1.1 Thermal properties

As previously discussed, it is common for diblock copolymers to display individual glass transition temperatures ( $T_g$  values) corresponding to each constituent polymer block. Importantly, DSC analysis, as summarised in Table 5.4 and Figure 5.10, indicates the presence of two distinct  $T_g$  features for all PDMA-*b*-PNIPAM copolymers synthesised via the two-step method. In all cases, the first  $T_g$  ( $T_{g1}$ ) is observed between 65 - 97 °C, which is closest to the experimentally determined  $T_g$  value of the PDMA macro-initiator (121 °C). All  $T_{g1}$  values were either within or lower ( $\leq 25$  °C) than the reported literature range for PDMA homopolymer (89 - 130 °C)<sup>297–302</sup>. The second  $T_g$  ( $T_{g2}$ ) was observed between 125 - 143 °C for all copolymers. Again, all  $T_{g2}$  values were either within or slightly lower ( $\leq 10$  °C) than the available literature values for the  $T_g$  of PNIPAM homopolymer (135 - 142 °C)<sup>326–328</sup>. As aforementioned, the decrease in the glass transition of the individual blocks is similar to other findings within the literature<sup>348</sup>.

Table 5.4. Glass transition temperatures for PDMA macro-initiator, subsequent PDMA-*b*-PNIPAM block copolymers synthesised via the two-step method [using a macro-initiator synthesised to high conversion (91 %)] and a PNIPAM homopolymer (2 mol % bromoform).

Sample	$T_{g1}$ (°C)	$T_{g2}$ (°C)
PDMA <sub>1500</sub>	121	-
PNIPAM (2 mol % CHBr <sub>3</sub> )	-	143
PDMA <sub>1500</sub> - <i>b</i> -PNIPAM <sub>110</sub>	78	125
PDMA <sub>1500</sub> - <i>b</i> -PNIPAM <sub>270</sub>	73	126
PDMA <sub>1500</sub> - <i>b</i> -PNIPAM <sub>420</sub>	76	131
PDMA <sub>1500</sub> - <i>b</i> -PNIPAM <sub>750</sub>	70	132
PDMA <sub>1500</sub> - <i>b</i> -PNIPAM <sub>1310</sub>	69	125
PDMA <sub>1500</sub> - <i>b</i> -PNIPAM <sub>2050</sub>	65	138
PDMA <sub>1500</sub> - <i>b</i> -PNIPAM <sub>3330</sub>	71	138
PDMA <sub>1500</sub> - <i>b</i> -PNIPAM <sub>5100</sub>	74	133

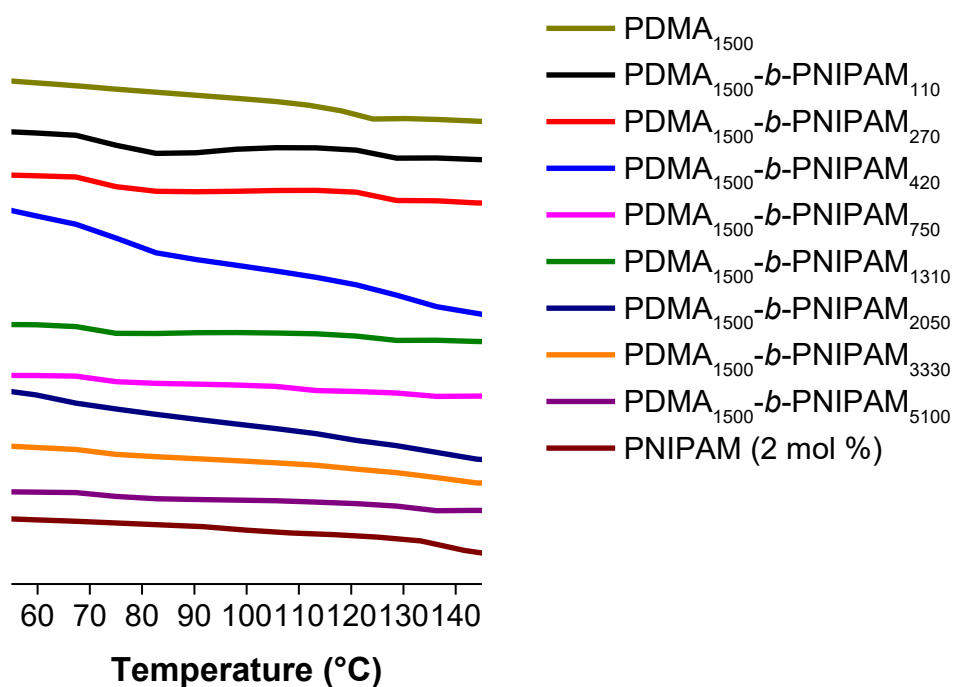


Figure 5.10. DSC thermograms of the PDMA macro-initiator (91 % conversion), subsequent PDMA-*b*-PNIPAM block copolymers (synthesised via the two-step route) and a PNIPAM homopolymer (2 mol % bromoform).

In addition, TGA analysis (Figure 5.11) shows that all homopolymers and block copolymers degrade in the known literature range (350 - 450 °C<sup>302,329</sup>) via a one-step degradation pathway, forming volatile, small molecules. Like the trend seen in the one-pot synthesis, the block copolymers (excluding the copolymer with PNIPAM DP ~ 110) appear to move between the degradation profile of PDMA to PNIPAM homopolymer with increasing PNIPAM block length.

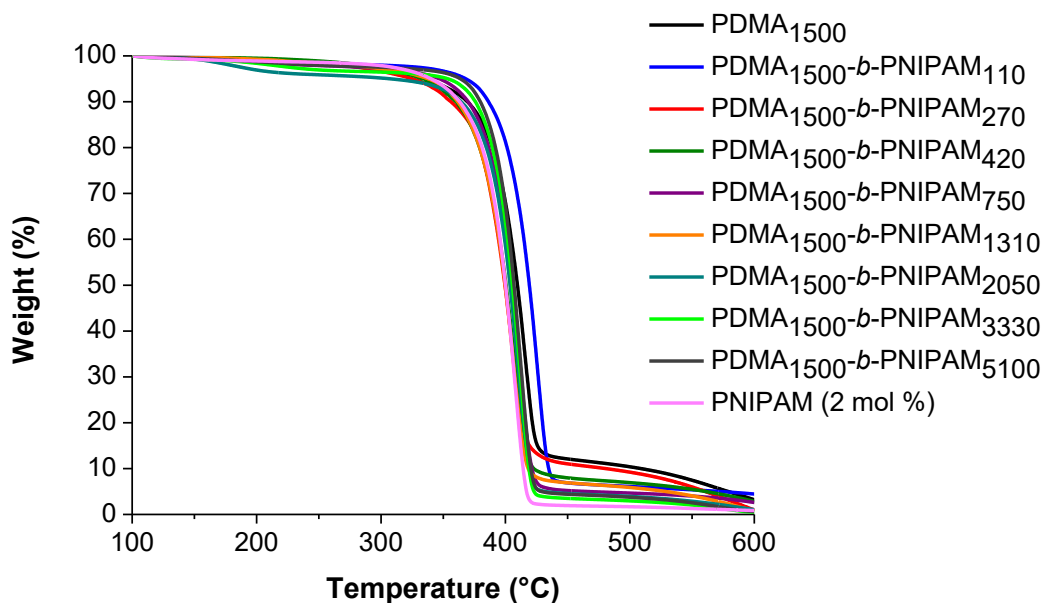


Figure 5.11. TGA degradation profile for the PDMA macro-initiator (91 % conversion), subsequent PDMA-*b*-PNIPAM block copolymers (synthesised via the two-step route) and a PNIPAM homopolymer (2.0 mol % bromoform).

Finally, DLS was used to determine the LCST of the block copolymers (see Figure 5.12). Similar to the one-pot method, the sample synthesised at a DP < 230 (*i.e.* DP ~ 110) for the PNIPAM block exhibited no LCST for the temperature range investigated, again, this is likely because of the dominance of the PDMA block. Additionally, the sample with DP equal to 270 exhibited a broader LCST range, namely 34 - 36 °C, when compared to the other block copolymers and PNIPAM homopolymer samples. All of the remaining samples exhibit a coil-to-globule transition between 34 - 35 °C which is the same as that observed for the PNIPAM homopolymers at all bromoform concentrations (see Chapter 4). The coil-to-globule transition is highlighted by the change in size with temperature and in all cases, where a transition is present, the onset of the LCST (34 °C) is within the literature range for PNIPAM homopolymer<sup>1,339,344–346</sup>. However, there is no apparent trend between size and PNIPAM block length in the copolymers after the transition has occurred.



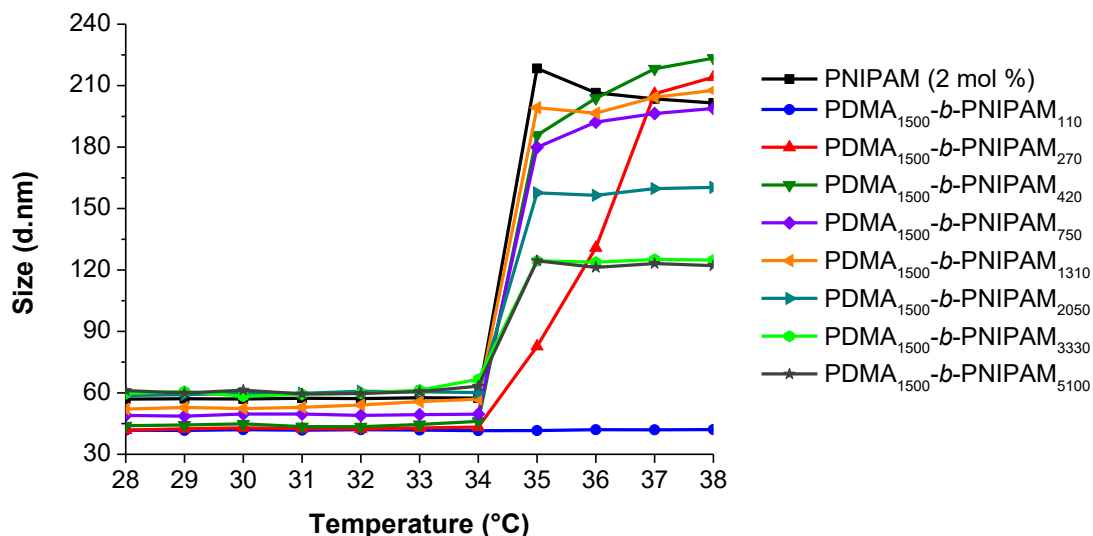


Figure 5.12. Size *versus* temperature of PNIPAM homopolymer (2 mol % bromoform relative to monomer) and PDMA-*b*-PNIPAM copolymers synthesised via the two-step method [using a PDMA macro-initiator synthesised to high conversion (91 %)] highlighting the LCST (or coil-to-globule transition).

In this study, PDMA-*b*-PNIPAM copolymers were synthesised using a two-step synthesis route. More specifically, a PDMA macro-initiator was synthesised to high final conversion (91 %) and was precipitated before being used in subsequent block copolymer reactions. The GPC traces of the PDMA-*b*-PNIPAM copolymers, before and after precipitation, indicate successful chain extension of the PDMA macro-initiator (in most cases) as the traces shift to shorter retention times. Additionally, the molar masses of all of the block copolymers increase somewhat linearly when targeting higher PNIPAM DPs. Similar to the one-pot synthesis route, the GPC traces of the final block copolymers still suggest that other species could be present in the final sample. However, as the PDMA macro-initiator was precipitated it is likely that the low molar mass shoulders (or tails) are only due to PDMA chains that have not been reversibly terminated with an appropriate chain end functionality required for block extension. The competition between bromine and hydrogen transfer from bromoform to the PDMA precursor block, in addition to the inherent termination and chain transfer events of free-radical

polymerisation, could result in PDMA chains being produced that are incapable of chain extension.

Further characterisation in the form of DSC, TGA and DLS was undertaken to compare the potential PDMA-*b*-PNIPAM copolymers and the individual PDMA and PNIPAM homopolymers. Two glass transitions are identified in the block copolymers; each corresponding to the individual homopolymers. Additionally, the samples all degrade via a one-step degradation process between 350 and 450 °C; which is also seen for the individual homopolymers. Finally, the onset of the LCST of the block copolymers ( $DP \geq 270$ ) is within the known literature range for PNIPAM and is not dissimilar to the PNIPAM synthesised at 2 mol % bromoform (relative to monomer). However, similar to the one-pot synthesis route, no LCST was observed for the copolymers with PNIPAM block lengths of  $\leq 230$  likely due to the dominance of the PDMA portion and oligomeric nature of the PNIPAM in the block copolymers.

The presence of PDMA chains without the required bromine chain end results in dead polymer chains incapable of chain extension for the production of block copolymers. Therefore, in an attempt to increase the number of bromine-terminated chains a final two-step synthesis was conducted. In this example the PDMA macro-initiator was synthesised and stopped at 70 % monomer conversion in an attempt to increase the chain end fidelity of the bromine. This synthetic route is informed by the literature related to controlled radical polymerisation methods during which chain ends are often lost under monomer starved conditions (*i.e.* at high conversions,  $\geq 90$  %) to side reactions<sup>321–325</sup>.

### 5.2.2 Macro-initiator at 70 % conversion

A PDMA macro-initiator was synthesised using 2 mol % bromoform (relative to monomer) and purposefully stopped at 70 % conversion in an attempt to increase the number of bromine-terminated chains present and subsequently the number of block copolymer chains formed in the second reaction. PDMA-*b*-PNIPAM copolymers with varying block molar ratios were targeted in a polymerisation formulation containing PDMA (see Figure 5.13), NIPAM monomer

and water only. As described in the previous two-step investigation, the PDMA was purified to remove any unreacted monomer, initiator and bromoform impurities, and no additional ACPA or bromoform was used in this reaction.

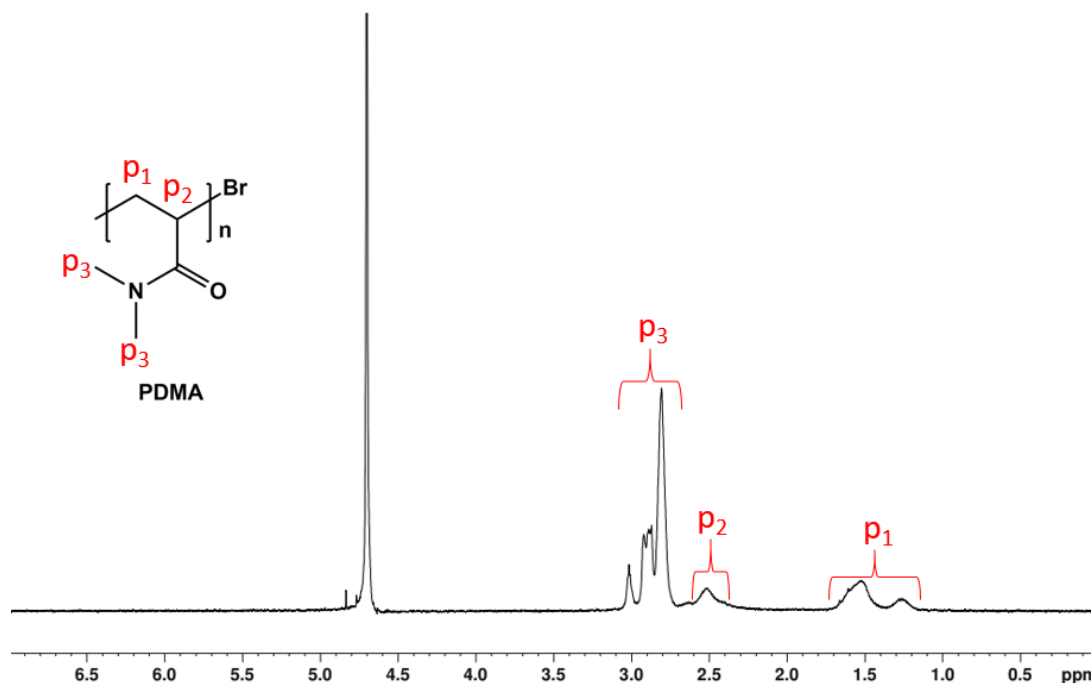


Figure 5.13.  $^1\text{H}$  NMR spectrum of precipitated PDMA macro-initiator (synthesised to 70 % conversion) showing no residual monomer peaks present in the sample at 5.6, 6.0 and 6.6 ppm.

PDMA-*b*-PNIPAM copolymers with a range of target DMA:NIPAM molar ratios were synthesised as summarised in Table 5.5. The target degree of polymerisation was calculated using Equation 5.1.. DMF GPC analysis was performed to determine the relative molar mass values for the PDMA macro-initiator and subsequent PDMA-*b*-PNIPAM block copolymers. The average experimental DPs of the PNIPAM block were determined using two methods; DMF GPC results alongside Equation 5.2 as well as NIPAM monomer conversions as judged by  $^1\text{H}$  nuclear magnetic resonance (NMR) spectroscopy and Equation 5.3. As previously described, the average experimental DP of the PNIPAM block calculated from the  $^1\text{H}$  NMR data and Equation 5.3 will be discussed due to the limitations of the GPC data.

Table 5.5. Summary of  $M_n$ ,  $\bar{D}$  and the target and achieved PNIPAM DP in PDMA-*b*-PNIPAM copolymers synthesised via the two-step method using PDMA that was stopped at 70 % conversion.

Target polymer <sup>a</sup>	NIPAM conversion <sup>b</sup> (%)	$M_n$ <sup>c</sup> (kg mol <sup>-1</sup> )	PNIPAM DP <sup>d</sup> (GPC)	PNIPAM DP <sup>e</sup> (NMR)	$\bar{D}$ <sup>c</sup> ( $M_w/M_n$ )
PDMA <sub>3280</sub> <sup>f</sup>	-	324.7	-	-	2.8
PDMA <sub>3280</sub> - <i>b</i> -PNIPAM <sub>360</sub>	81	259.1	g	300	3.3
PDMA <sub>3280</sub> - <i>b</i> -PNIPAM <sub>820</sub>	88	272.2	g	720	3.1
PDMA <sub>3280</sub> - <i>b</i> -PNIPAM <sub>1410</sub>	84	301.5	g	1180	3.1
PDMA <sub>3280</sub> - <i>b</i> -PNIPAM <sub>2190</sub>	89	255.2 <sup>h</sup>	g	1950	4.2 <sup>h</sup>
PDMA <sub>3280</sub> - <i>b</i> -PNIPAM <sub>3280</sub>	95	369.1 <sup>h</sup>	390	3120	3.5 <sup>h</sup>
PDMA <sub>3280</sub> - <i>b</i> -PNIPAM <sub>4920</sub>	90	325.8 <sup>h</sup>	10	4430	5.1 <sup>h</sup>
PDMA <sub>3280</sub> - <i>b</i> -PNIPAM <sub>7650</sub>	92	409.2 <sup>h</sup>	750	7040	4.4 <sup>h</sup>
PDMA <sub>3280</sub> - <i>b</i> -PNIPAM <sub>13,120</sub>	96	464.6 <sup>h</sup>	1240	12,600	4.4 <sup>h</sup>

a) Target PNIPAM DP calculated using GPC and Equation 5.1..

b) Calculated using <sup>1</sup>H NMR spectroscopy and Equation 2.1.

c) Determined by DMF GPC using PMMA standards.

d) Calculated using DMF GPC results and Equation 5.2 and values are rounded to the nearest ten.

e) Calculated using <sup>1</sup>H NMR spectroscopy and Equation 5.3. and values are rounded to the nearest ten.

f) PDMA macro-initiator synthesised using 2 mol % bromoform (relative to monomer), stopped at a final DMA monomer conversion of 70 %.

g) Not calculated as  $M_n$  of copolymer appears lower than PDMA macroinitiator.

h)  $M_n$  appears smaller than expected due to PDMA macro-initiator still present. This is also reflected in the higher dispersity value.

The length of the PNIPAM block increased when targeting higher DPs, as expected, and the NIPAM monomer conversion was high in all cases. Similar to the trend observed for the previous two-step synthesis (using PDMA synthesised to 91 % conversion, see Table 5.3),

the monomer conversion is higher when longer PNIPAM blocks are targeted, which is attributed to higher NIPAM concentrations during the polymerisation.

The GPC traces for the purified PDMA-*b*-PNIPAM copolymers indicate successful chain-extension of the PDMA macro-initiator with NIPAM clearly for the samples with an achieved PNIPAM DP  $\geq 1950$ . A clear shift to shorter retention times was observed when extending PDMA with NIPAM monomer, both before [Figure 5.14(a)] and after precipitation [Figure 5.14(b)], for these samples which corresponds to a significant increase in  $M_n$  as summarised in Table 5.5. The remaining samples show small shifts in the GPC traces only after precipitation [Figure 5.14(b)]. However, in all cases there is significant peak broadening and/or the presence of a low molar mass shoulder observed at retention times expected for the PDMA homopolymer alone [Figure 5.14(b)]. Additionally, the shift to shorter retention times, in these cases, is not reflected by a significant increase in average molar mass that would also be expected. This is likely due to the high dispersities (3.5-5.1) of the broad or bimodal peaks that result in inaccurate molar mass approximations; suggesting that not all of the PDMA chains synthesised in the first step are capable of being chain-extended with NIPAM. Qualitatively, this implies that the PDMA polymerisation at 70 % conversion (compared to the one at higher conversion of 91 %) does not increase the number of bromine-terminated PDMA chains to be used in the block copolymer reaction. Unlike the previous two-step synthesis, using PDMA synthesised to 91 % conversion, Figure 5.15 highlights that there is an unclear trend between final molar mass and DP of the PNIPAM block as some points appear below the molar mass of the macroinitiator.

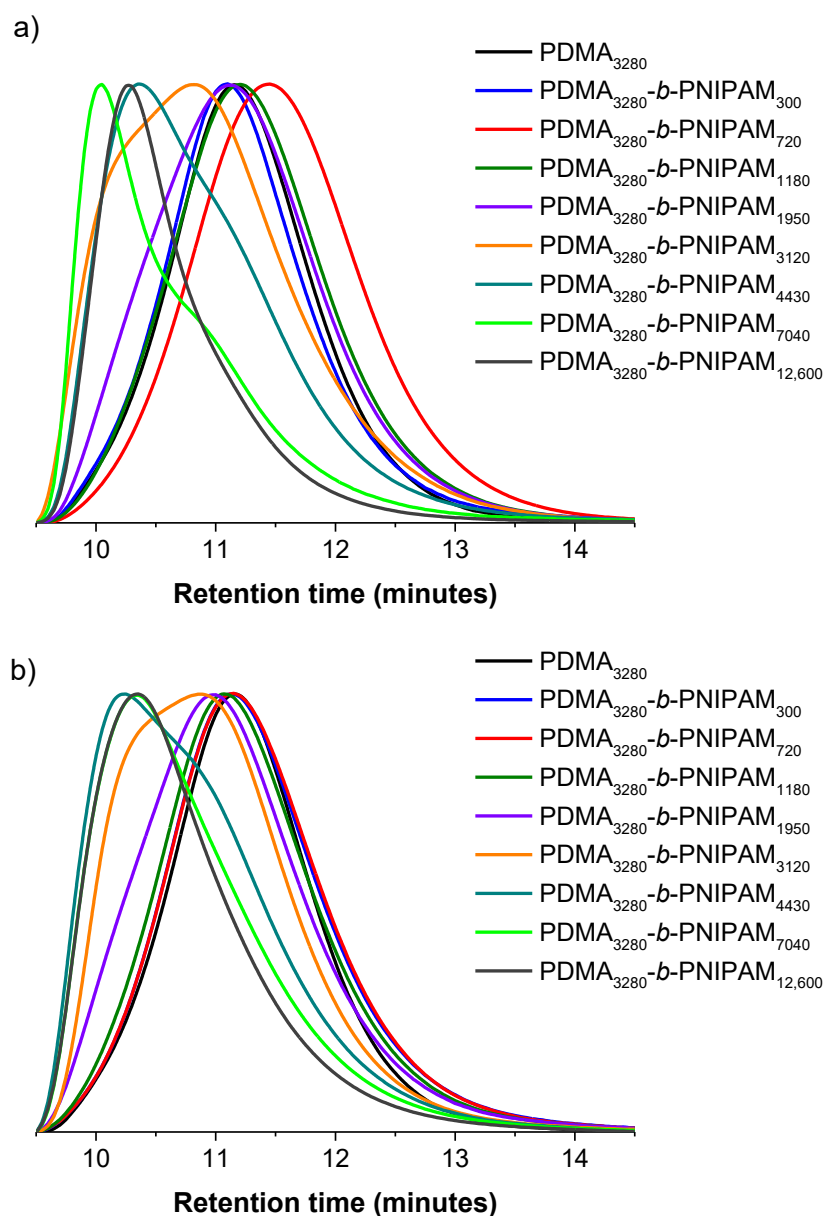


Figure 5.14. GPC traces of PDMA macro-initiator and PDMA-*b*-PNIPAM copolymers (two-step, PDMA macro-initiator 70 % conversion) with target PNIPAM DPs ranging from 300 to 13,120 (a) before precipitation and (b) after precipitation.

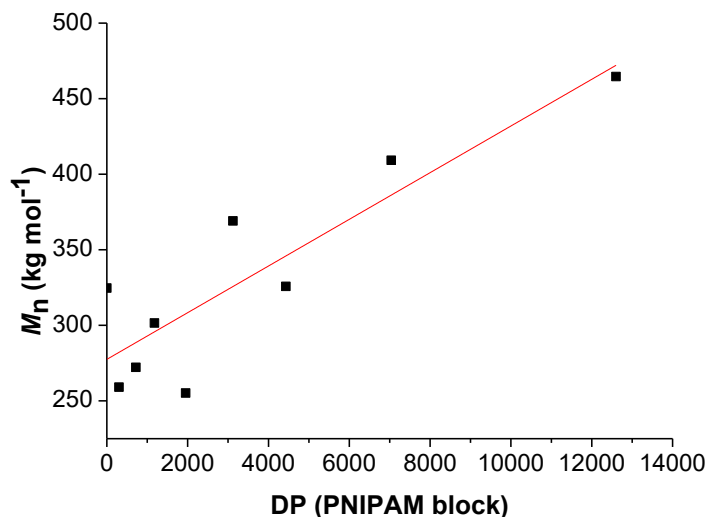


Figure 5.15. Achieved molar mass *versus* average experimental DP (determined via <sup>1</sup>H NMR spectroscopy and Equation 5.3.) of the PNIPAM block in the PDMA-*b*-PNIPAM block copolymers in the two-step synthesis (PDMA synthesised to 70 % conversion).

The PDMA synthesised to 70 % conversion is approximately double the molar mass of the PDMA that was synthesised to high conversion (91 %); this is a result of high initial rates of propagation leading to the formation of high molar mass chains when more monomer is present in the system (*i.e.* at lower conversions). For the PDMA synthesised to 91 % conversion, after the high initial rates of propagation, the monomer concentration is reduced and thus shorter polymer chains are synthesised, resulting in a reduction in the average molar mass in the system<sup>294–296</sup>. This has only amplified the limitations of GPC when analysing the chain extension of the already high molar mass PDMA macro-initiator [ $M_n > 320.0 \text{ kg mol}^{-1}$ , relative to PMMA standards]. Significantly, the PDMA-*b*-PNIPAM copolymers with achieved PNIPAM DPs  $\leq 1180$  are near-identical to the PDMA macro-initiator suggesting that chain extension with NIPAM was unsuccessful in these cases. However, <sup>1</sup>H NMR spectra does confirm the presence of PNIPAM in all cases (Figure 5.16).

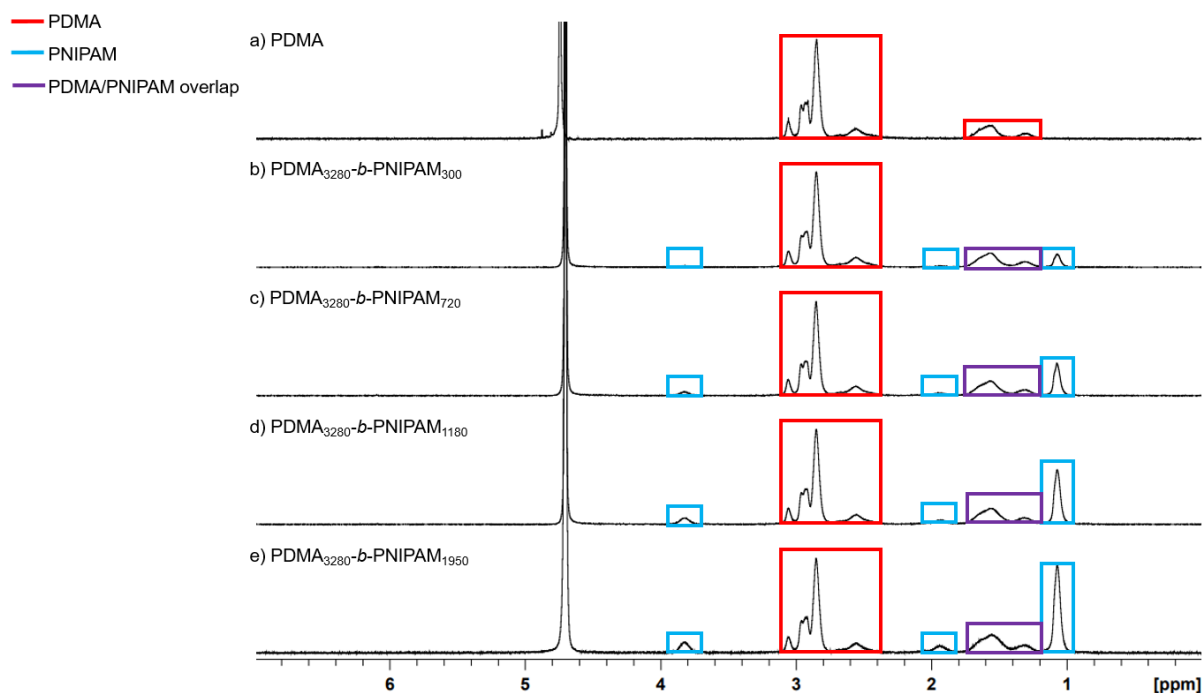


Figure 5.16.  $^1\text{H}$  NMR spectra showing (a) PDMA macro-initiator (70 % conversion), (b)  $\text{PDMA}_{3280}\text{-}b\text{-PNIPAM}_{300}$ , (c)  $\text{PDMA}_{3280}\text{-}b\text{-PNIPAM}_{720}$ , (d)  $\text{PDMA}_{3280}\text{-}b\text{-PNIPAM}_{1180}$  and (e)  $\text{PDMA}_{3280}\text{-}b\text{-PNIPAM}_{1950}$  all after precipitation; indicating the presence of PNIPAM in the block copolymers.

One possible reason for the PNIPAM block being present (as confirmed by  $^1\text{H}$  NMR) but no shift in the GPC trace is that the lower molar mass PDMA macro-initiator chains are the only ones being extended with NIPAM. This could be because of the increased probability of NIPAM monomer being able to find a reversibly capped chain end in the lower molar mass PDMA chains. The remaining higher molar mass PDMA chains are either not or negligibly chain extended. The significant quantity of high molar mass PDMA macro-initiator still present could be dominating the GPC traces making it appear as though no chain extension has occurred. Finally, Figure 5.14(b) shows a significant low molar mass tail in each sample which is likely the cause of the final molar mass values being lower than the PDMA macro initiator alone (Table 5.5).

In this study, PDMA-*b*-PNIPAM copolymers were synthesised using a two-step synthesis route from a PDMA macro-initiator purposefully synthesised to 70 % conversion. As previously



described, this approach was informed by the literature related to controlled radical polymerisation methods (including RAFT, NMP and ATRP) during which chain ends are often lost under monomer starved conditions (at high conversions, *i.e.*  $\geq 90\%$ ) to side reactions<sup>321–325</sup>. The PDMA macro-initiator was precipitated before being used in subsequent block copolymer reactions. The GPC traces of the PDMA-*b*-PNIPAM copolymers, before and after precipitation, indicate successful chain extension in a limited number of the samples. The GPC traces of the block copolymers with PNIPAM DPs  $\geq 1950$  shift to shorter retention times, however, contain significant tails or shoulders that indicate a high quantity of PDMA incapable of being chain extended is also present. The remaining samples with PNIPAM DP  $\leq 1180$  do not shift to shorter retention times and appear near-identical to the PDMA macro-initiator alone. Additionally, the molar mass data obtained from these GPC traces do not reflect significant chain extension of the PDMA even with  $^1\text{H}$  NMR confirming the presence of the PNIPAM block. However, this is likely a result of only the low molar mass PDMA macro-initiator chains being successfully chain extended in each reaction and the high molar mass PDMA, that were not chain extended, dominating the GPC trace. Shifts in the GPC traces are also difficult to identify due to the limitations of GPC alongside the broad dispersity of the PDMA macro-initiator used in these syntheses.

In all of the block copolymer studies described herein one common theme has been the discussion regarding the GPC data.  $^1\text{H}$  NMR successfully confirms the presence of the PNIPAM block in all cases (one-pot and both two-step synthetic routes), however, due to the already large size of the PDMA macro-initiators and the limits of the GPC, the molar mass data do not always reflect successful chain extension. Additionally, where the GPC traces shift to lower retention times and an increase in the molar mass is observed, this alone cannot be used as conclusive evidence of successful chain extension. It could simply represent the presence of another high molar mass species; such as PNIPAM homopolymer as opposed to PDMA-*b*-PNIPAM copolymers. Therefore, a series of control reactions were conducted to provide further indirect evidence of chain extension of the PDMA macro-initiator with NIPAM.

### 5.3 Control experiments

To further confirm that PDMA-*b*-PNIPAM block copolymers were successfully synthesised, and not simply a mixture of PDMA and PNIPAM homopolymers, important control experiments were conducted. Firstly, NIPAM homopolymerisations were attempted in the absence of ACPA photoinitiator (*i.e.* only NIPAM, bromoform and water present). Importantly, no polymerisation occurred after irradiation with UV light (Figure 5.17), which indicates that bromoform itself does not act as a photoinitiator under these conditions. This is contrary to previous reports by Miller<sup>208</sup> and Wu *et al.*<sup>211</sup>, who proposed the use of bromoform as a photoinitiator during the polymerisation of acrylamide, acrylonitrile, acrylic acid and 2-acrylamido-2-methylpropane sulfonic acid (AMPS). However, as previously discussed, these studies lack thermal control and temperatures of up to 50 °C, reached during the UV irradiation, could be causing bromoform to behave as a thermal initiator. Secondly, polymerisations without ACPA and bromoform (*i.e.* only NIPAM and water present) were attempted in order to determine whether NIPAM would self-polymerise. Using the previously described conditions and even extended UV exposure times, homopolymerisation of NIPAM did not take place (Figure 5.17). This further suggests that the shift to lower retention times, observed in both of the two-step synthetic routes, is not due to the production of PNIPAM homopolymer and can only have occurred due to the successful chain extension of the PDMA with NIPAM. Additionally, the block copolymer samples that did not show a shift in the GPC trace, or increase in molar mass, but did confirm the presence of PNIPAM by <sup>1</sup>H NMR could also have been successfully chain extended. However, it could be that only the lower molar mass PDMA chains are being predominantly chain extended with NIPAM in these cases. Additionally, the high proportion of PDMA not capped with bromine, still present in these samples, could be dominating the GPC traces making it appear as though no chain extension has occurred.

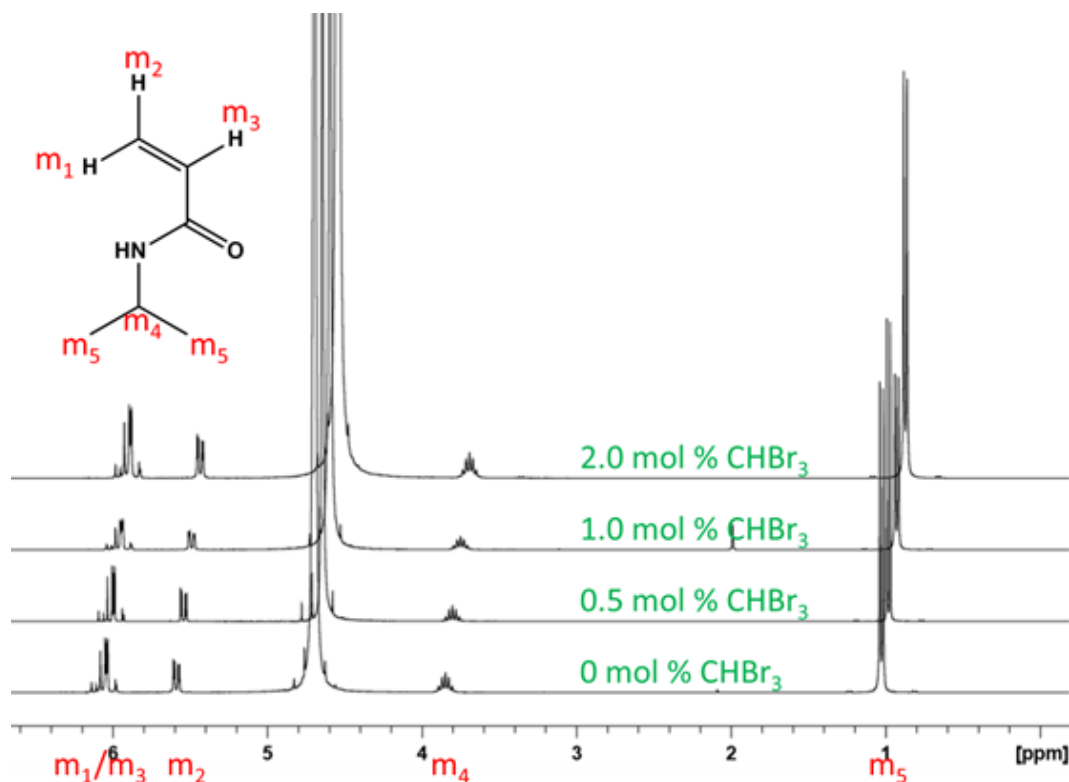


Figure 5.17.  $^1\text{H}$  NMR spectra showing only monomer peaks present for the attempted synthesis of PNIPAM in the absence of photoinitiator (namely ACPA) at varied bromoform (0, 0.5, 1.0 and 2.0 mol % relative to monomer) concentrations. All experiments were completed in 25 mL deionised water for 7 hours of UV irradiation (starting temperature 0 °C, ice bath replenished every 1 hour to maintain temperature control).

Thirdly, a control reaction using PDMA synthesised without bromoform was conducted. When targeting PDMA<sub>1500</sub>-*b*-PNIPAM<sub>3500</sub> under these conditions, no NIPAM polymerisation was observed (neither homopolymerisation nor PDMA chain-extension), indicating that bromoform is needed during the synthesis of the macro-initiator for the formation of the desired diblock copolymer (Figure 5.18 and Appendix 13). These control studies (summarised in Scheme 5.2) provide further evidence that bromoform is required to impart bromine functionality onto the PDMA chains to enable block copolymer synthesis.

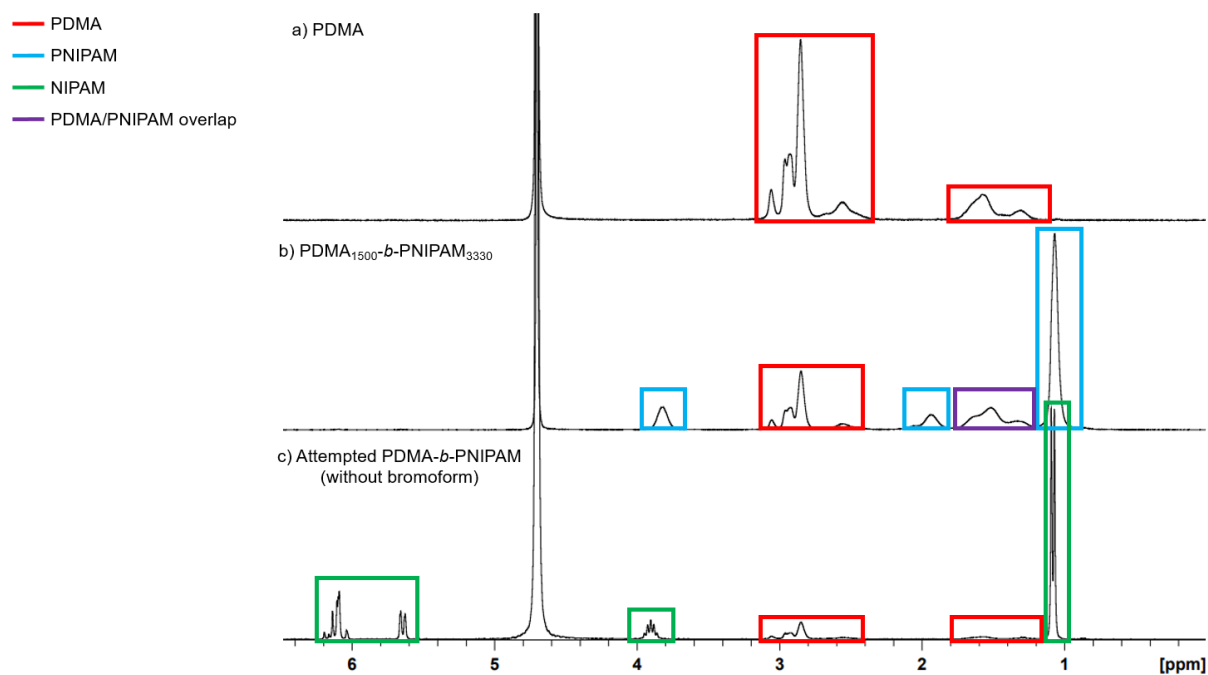
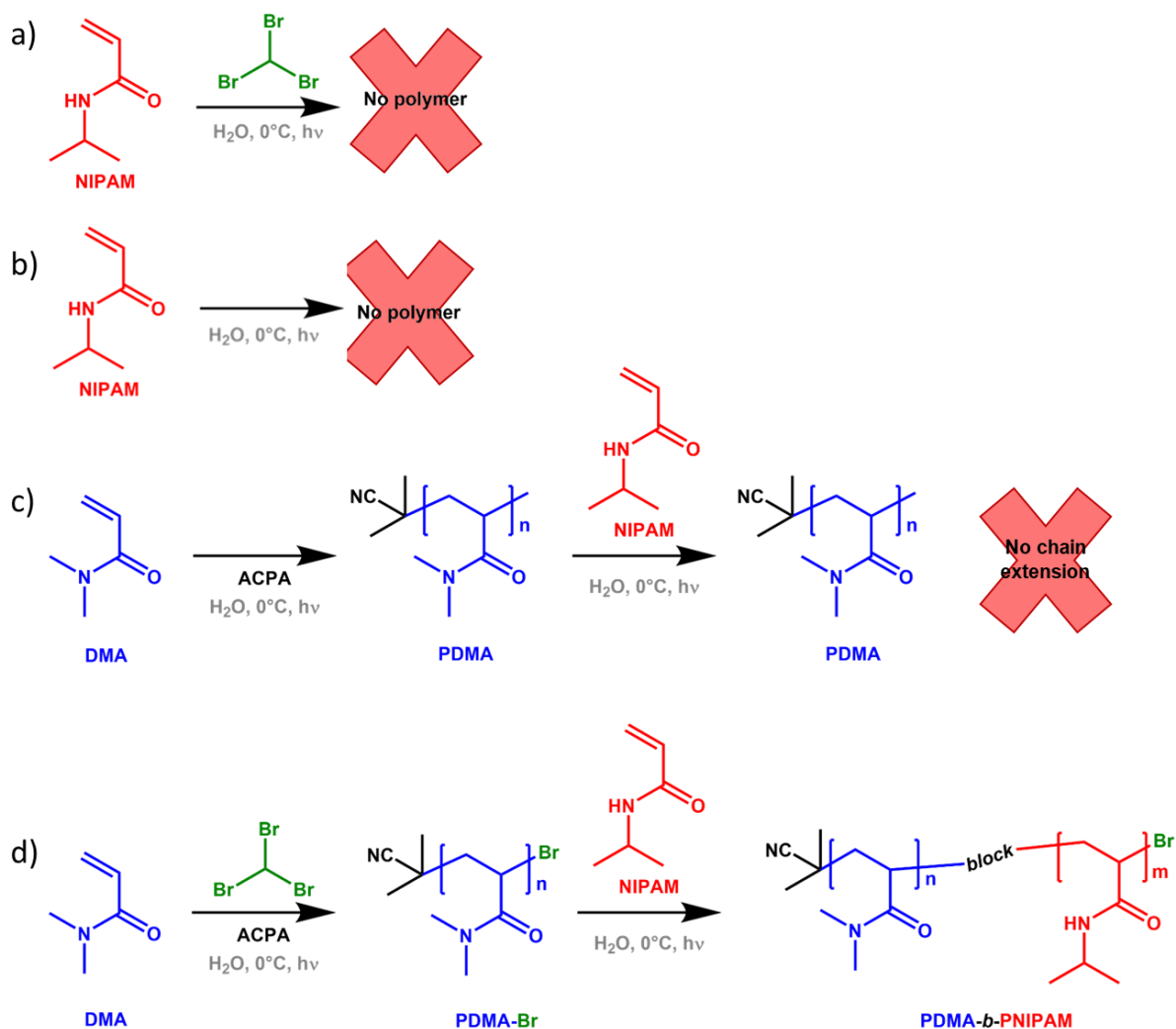


Figure 5.18.  $^1\text{H}$  NMR spectra showing (a) PDMA after precipitation, (b) PDMA<sub>1500</sub>-*b*-PNIPAM<sub>3330</sub> (using 2 mol % bromoform in step 1) after precipitation and (c) only NIPAM monomer peaks present for the attempted synthesis of PDMA-*b*-PNIPAM from PDMA (0 mol % bromoform).



Scheme 5.2. (a) Attempted synthesis of NIPAM homopolymer in the absence of ACPA photoinitiator. (b) Attempted synthesis of NIPAM homopolymer in the absence of bromoform and ACPA photoinitiator. (c). Attempted synthesis of PDMA-*b*-PNIPAM copolymers without bromoform in step 1. (d) Successful two-step synthesis of PDMA-*b*-PNIPAM copolymers using PDMA prepared using bromoform in step 1.

## 5.4 Conclusion

This chapter describes in detail the one- and two-step synthesis of PDMA-*b*-PNIPAM copolymers. Multiple studies using PDMA macro-initiators that were crude, precipitated and stopped at varied final conversions have been explored as potentially suitable precursors for effective block copolymer formation.

Initially, PDMA-*b*-PNIPAM copolymers were synthesised via a one-pot method at varying PDMA:PNIPAM block ratios in HPLC-grade water. The GPC traces of the PDMA-*b*-PNIPAM copolymers indicate successful chain extension of the PDMA macro-initiator as the traces shift to shorter retention times in all cases. However, the molar masses determined by GPC of these samples do not always reflect the shifts, this is due to some traces exhibiting low molar mass shoulders (or tails) indicating that there are other species present in the final sample. It is possible that PDMA, PNIPAM and PDMA-*st*-PNIPAM 'contaminants' could have been produced due to unreacted ACPA and DMA monomer still present from the PDMA macro-initiator synthesis. Additional analyses via DSC, TGA and DLS highlighted the thermal properties of the block copolymer samples. However, these results mimic those of the two homopolymers, or a homopolymer mixture and do not confirm whether block copolymer formation was successful.

To eliminate the potential of creating unwanted polymer products in the block copolymer synthesis, a second series of reactions was conducted; using a two-step synthetic route. This involved the precipitation of the PDMA macro-initiator to remove residual ACPA, bromoform and DMA monomer. Firstly, a series of reactions using a PDMA macro-initiator synthesised to high final conversion (91 %) was conducted. The GPC traces of the PDMA-*b*-PNIPAM copolymers produced indicate successful chain extension of the PDMA macro-initiator, in most cases, and the molar masses of the block copolymers increase somewhat linearly when targeting higher PNIPAM DPs. Similar to the one-pot synthesis route, the GPC results suggest that other species are present in the final sample. Hydrogen transfer, from the bromoform, in addition to termination events could result in PDMA chains that have not been terminated with the appropriate bromine chain end functionality required for block copolymer formation. Similarly, DSC, TGA and DLS analyses determine the thermal properties of the final samples to be similar to the two homopolymers, or a homopolymer mixture and do not confirm whether block copolymer formation had been successful.

In an attempt to increase the number of bromine-terminated chains in the macro-initiator sample a final PDMA synthesis was conducted and stopped at 70 % conversion. Similarly, the PDMA macro-initiator was precipitated before being used in subsequent block copolymer reactions to eliminate the formation of unwanted homo- or statistical copolymer species. The GPC traces of these PDMA-*b*-PNIPAM copolymers only suggest successful chain extension in the block copolymers with PNIPAM DP  $\geq 1950$ , however, they all contain significant shoulders (or tails) that indicate a high quantity of PDMA is present that is incapable of being chain extended. The remaining samples do not shift to shorter retention times and appear near-identical to the PDMA macro-initiator alone. The molar mass data obtained from these GPC traces do not reflect significant chain extension of the PDMA even with  $^1\text{H}$  NMR confirming the presence of the PNIPAM block in all cases. However, one possibility is that only the low molar mass PDMA chains are extended with NIPAM in these cases; due to the increased probability of NIPAM finding a reversibly capped PDMA chain end in this case. The remaining high molar mass PDMA, whilst still present, isn't or is negligibly chain extended and dominates the GPC trace; making it seem as though chain extension has been unsuccessful. Additionally, the limitations of GPC when analysing already high molar mass macro-initiators could also be causing inaccuracies in the data. The study described in Section 5.1.2, using a PDMA macro-initiator synthesised to 91 % conversion (with a significantly lower molar mass), demonstrates greater visual success (from the GPC traces) of the block copolymers at all molar ratios.

As previously mentioned, the one common problem highlighted in this work has been the limitations of the GPC data. Working with already high molar mass PDMA macro-initiator samples has led to questions being raised about the suitability of GPC for confirming successful block copolymer synthesis. To rectify this a series of control experiments were conducted to provide further evidence that successful chain extension of the PDMA with NIPAM had occurred; particularly for the two-step syntheses. These control reactions determined that bromoform will not behave as a photoinitiator for NIPAM under the present

conditions. Additionally, when no bromoform or ACPA are present, NIPAM will not homopolymerise; this is important for the two-step syntheses where significant increase in the molar masses was observed as this suggests it must be because of successful chain extension of PDMA with NIPAM to form PDMA-*b*-PNIPAM copolymers. Finally, a control reaction was used to determine whether bromoform is required in the macro-initiator synthesis for subsequent successful chain extension to occur. This reaction confirmed that bromoform is required to generate bromine-terminated PDMA chains that are capable of chain-extension with NIPAM. When bromoform is not used for the synthesis of PDMA, no PNIPAM-containing species were produced at all (*i.e.* no PNIPAM homopolymer or PDMA-*b*-PNIPAM block copolymers) under otherwise identical conditions.



# **Chapter 6. Conclusions and Future Work**

## 6.1 Conclusions

The development of synthetic techniques that eliminate the need for sulfur- or metal-containing compounds is of great interest for producing commercially-relevant block copolymers. Furthermore, replacing organic solvents with water significantly reduces the environmental impact of the process and opens the opportunity up for the production of biomedical block copolymers via this route.

With these goals in mind, bromoform-assisted free radical polymerisation, as a viable synthetic route to commercially-relevant block copolymers, has been explored. Initial exploration of the scope and limitations of this technique have been investigated regarding the production of poly(*N,N*-dimethylacrylamide)-*block*-poly(*N*-isopropylacrylamide) [PDMA-*b*-PNIPAM] copolymers. More specifically, multiple poly(*N,N*-dimethylacrylamide) [PDMA] macro-initiators were synthesised to determine the most appropriate route for successful block copolymer synthesis. After which, block copolymers at varying PDMA:poly(*N*-isopropylacrylamide) (PNIPAM) molar ratios were subsequently targeted.

Initially, homopolymerisations of *N,N*-dimethylacrylamide (DMA) and *N*-isopropylacrylamide (NIPAM) were conducted to determine the influence of bromoform on the rate, molar mass ( $M_n$ ) and dispersity ( $\mathcal{D}$ ) of the polymer produced. Additionally, the effect of solvent [high performance liquid chromatography (HPLC)-grade water and dimethylformamide (DMF)] were explored in an attempt to better understand the role of bromoform in these reactions. Notably, an ice bath was employed to offer thermal control over the course of the reaction; to eliminate any thermal effects from the UV lamp likely present in previously reported studies<sup>207–209,211,212</sup>.

The kinetic studies (0 - 2 mol % bromoform relative to monomer) in water, for both PDMA (Chapter 3) and PNIPAM (Chapter 4), demonstrate that the evolution of molar mass with monomer conversion is in line with conventional free radical polymerisation<sup>72–74</sup>, rather than RDRP<sup>75–79</sup>, where the relationship would be linear. Additionally, there is little to no difference in polymerisation rate observed for either PDMA or PNIPAM at all bromoform concentrations

studied herein. High monomer conversions ( $\geq 88\%$ ) and dispersities were achieved in all cases. Gel permeation chromatography (GPC) highlighted that there was good reproducibility of the syntheses conducted at all bromoform concentrations (three repeats of each polymer synthesis at each bromoform concentration).

For the studies conducted in DMF the key difference was the extended reaction time, from 60 to 360 and 30 to 360 minutes for PDMA and PNIPAM, respectively. The reaction time had to be increased to ensure sufficiently high conversions ( $\geq 77\%$  and  $\geq 64\%$  for PDMA and PNIPAM, respectively) were achieved in each reaction. Additionally, the final molar masses of the PDMA and PNIPAM were significantly lower than those achieved in the water study at all bromoform concentrations. Similarly, GPC confirmed good reproducibility between runs for both polymers at each bromoform concentration. The significant decrease in the rate of reaction and molar mass of the polymers, when moving from water to DMF, is attributed to a decrease in the reactivity of the monomer double bond. More specifically, in polar solvents (such as water) the rate of propagation has been shown to increase as a result of hydrogen bonding at the carbonyl group on the amide. This effect results in increased reactivity at the double bond of the monomer which in turn results in faster propagation rates. The hydrogen bonding effect, whilst still present, is significantly reduced in organic solvents. Additionally, the reduced conversion, even with extended polymerisation time, is also a contributing factor to the lower molar masses observed in the DMF studies.

For both PDMA and PNIPAM, in water and DMF, there was no apparent relationship observed between bromoform content and rate,  $M_n$  or dispersity  $\mathcal{D}$  of the reaction. This suggests that, under the described conditions, bromoform is not behaving as a conventional chain transfer agent (CTA) as indicated in previous work by Thananukul *et al.*<sup>212</sup> for the polymerisation of acrylamide. Therefore, further reactions were conducted in an attempt to determine the role of bromoform in the system. Significantly, water was used as the solvent in all subsequent reactions to develop a greener synthetic route to block copolymers.

Bromoform was investigated for its initiating capabilities under the same reaction conditions. In this case the photo initiator, 4,4'-azobis(4-cyanovaleric acid) [ACPA], was not included in the reaction mixture so that only monomer, bromoform and water were present. Significantly, bromoform did not behave as a photoinitiator at any bromoform concentration (0 - 2 mol %) for either PDMA or PNIPAM homopolymerisation under the conditions used ( $\sim 4^\circ\text{C}$ ); signifying that photoinitiator is needed to create a radical source for polymerisation to occur. Importantly, the control reactions with no bromoform or ACPA, for DMA and NIPAM, did not produce polymer. Confirming that DMA and NIPAM do not self-polymerise under the described conditions.

To further improve the synthetic methodology, a final series of homopolymerisation reactions in the presence of oxygen were investigated. However, this introduced a lengthy induction period for the synthesis of PDMA and hindered the PNIPAM reaction altogether (for the reaction times studied). Therefore, the degassing stage was determined to be essential for efficient homopolymer synthesis in both cases.

Refinement of the homopolymerisation studies then led to an optimal route for the synthesis of PDMA and PNIPAM macro-initiators. Each homopolymerisation reaction was scaled up (to 20 g) using 2 mol % bromoform (relative to monomer) in an attempt to maximise the proportion of potentially bromine-terminated PDMA or PNIPAM chains within the usable bromoform miscibility range. The macro-initiators synthesised in these studies exhibited similar properties to those synthesised during the corresponding kinetic (2 g) reactions previously described.

At all stages the thermal properties of the PDMA and PNIPAM samples were analysed. More specifically, the glass transition ( $T_g$ ) temperature, degradation range and, where appropriate, lower critical solution temperature (LCST) were determined. In all cases, including the reaction scale up, the observations were as expected. The  $T_g$  values of the final polymers were within the known literature ranges of  $89 - 130^\circ\text{C}^{297-302}$  and  $135 - 142^\circ\text{C}^{326-328}$  for PDMA and PNIPAM, respectively. Both homopolymers exhibited a single step thermal degradation

between 350 - 450 °C<sup>302,329</sup> and the PNIPAM samples all demonstrated a LCST transition between 30 - 35 °C<sup>1,339,344–346</sup> as expected.

A further in-depth investigation was then undertaken to determine the potential of PDMA macro-initiators to successfully reinitiate under further UV irradiation for subsequent block copolymer synthesis to occur (Chapter 5). Initially, a one-pot investigation was completed as the simplest, quickest way to determine whether block copolymers could be formed from a PDMA macro-initiator. A variety of PDMA:PNIPAM block ratios were targeted and the GPC traces indicated significant chain extension in all cases from the observed shift to lower retention times. However, the molar masses determined by GPC were deemed inaccurate in some cases due to the presence of a low molar mass shoulder (or tail) from potential 'contaminants' in the final sample. As the PDMA macro-initiator, for the one-pot synthesis, was not precipitated it was assumed that unreacted ACPA, bromoform and DMA monomer were also present in the reaction solution. Therefore poly(*N,N*-dimethylacrylamide-*stat-N*-isopropylacrylamide) [PDMA-*st*-PNIPAM], PDMA and PNIPAM homopolymer 'contaminants' could be present in the final samples; resulting in the inaccurate molar mass data obtained from GPC analysis. Significantly, due to the presence of unreacted ACPA, high molar mass PNIPAM homopolymer could also have been produced which could be the cause of the shift in the GPC traces to lower retention times. Hence, a two-step synthetic route in which unreacted ACPA, bromoform and DMA monomer were removed via precipitation, was then explored to eliminate unwanted 'contaminants' being produced and provide further evidence as to whether block copolymers could be formed via this route.

The two-step synthetic route was further divided into two studies; one using a PDMA macro-initiator synthesised to high (91 %) conversion and another using a PDMA macro-initiator purposefully stopped at 70 % conversion. In the first example, the GPC traces indicate successful chain extension of the PDMA macro-initiator (synthesised to 91 % conversion) from the apparent shift to lower retention times. Whilst there were low mass shoulders (or tails) present in some of the samples, overall the molar masses of the PDMA-*b*-PNIPAM

copolymers increased somewhat linearly with increasing PNIPAM target degree of polymerisations (DP). The presence of the low molar mass shoulders (or tails) was attributed to PDMA chains that were not bromine-terminated. The PDMA without the bromine chain end is likely formed due to the competing pathways of hydrogen and bromine transfer, from the bromoform, in addition to termination events typical in free radical polymerisation.

In an attempt to increase the number of bromine-terminated chains present in the macro-initiator a sample of PDMA was synthesised and purposefully stopped at 70 % conversion. This method was informed by the literature related to controlled radical polymerisation methods during which chain ends are often lost under monomer starved conditions (*i.e.* at high conversions,  $\geq 90\%$ ) to side reactions<sup>321–325</sup>. As previously mentioned, the PDMA macro-initiator was precipitated to remove any unreacted ACPA, bromoform or DMA monomer to prevent unwanted ‘contaminants’ being synthesised alongside the block copolymers targeted. Significantly, chain extension was only observed via GPC for the PDMA-*b*-PNIPAM copolymers with PNIPAM DP  $\geq 1950$ . Even then, all of these block copolymer samples contained significant shoulders (or tails) indicating that a high quantity of PDMA is present that is incapable of being chain extended. The remaining samples, with a PNIPAM DP  $\leq 1180$ , did not shift to shorter retention times and appear near-identical to the PDMA macro-initiator, however,  $^1\text{H}$  nuclear magnetic resonance (NMR) spectroscopy confirmed the presence of a PNIPAM species in all cases. There is the possibility that only the short chains of the PDMA macro-initiator were extended and due to the overwhelming quantity of large PDMA chains [present at significantly higher molar mass ( $324.7\text{ kg mol}^{-1}$ ) than those produced to high conversion in the previous study ( $148.4\text{ kg mol}^{-1}$ )] this was not translated in the GPC curves of the final block copolymer samples. This study suggests that using a PDMA macro-initiator synthesised to 70 % conversion (as opposed to higher conversions of  $\geq 91\%$ ) does not result in an increase in the number of bromine-terminated chains required for block copolymer synthesis.

One significant issue highlighted in the block copolymer studies has been the limitations of GPC as an analytical tool for confirming the presence of block copolymers<sup>355</sup>. Working with already high molar mass macro-initiators ( $\geq 143.6 \text{ kg mol}^{-1}$ ) in all cases highlighted the need for further investigation to provide more conclusive evidence of successful chain extension in all cases. Therefore, a final series of control reactions were conducted to provide further evidence that the PDMA macro-initiators discussed, particularly for the two-step syntheses, were chain extended with NIPAM to produce PDMA-*b*-PNIPAM copolymers.

The first series of control reactions determined that bromoform will not behave as a photoinitiator for NIPAM under the described conditions. Additionally, NIPAM will not self-polymerise when no ACPA or bromoform are present, like the conditions in the two-step synthesis route. These results establish that the presence of PNIPAM (confirmed in all cases by  $^1\text{H}$  NMR spectroscopy) and the significant increase in the molar mass observed can only have been due to the successful chain extension of the PDMA macro-initiator with NIPAM. Finally, a control reaction was used to determine whether bromoform was required to impart bromine functionality onto the PDMA chains for successful chain extension to occur. When bromoform was not used for the synthesis of PDMA, no PNIPAM-containing species were produced at all (*i.e.* no PDMA-*b*-PNIPAM block copolymers) under otherwise identical conditions. Therefore, this control reaction provides strong evidence that bromoform is required to generate PDMA chains that are capable of chain-extension with NIPAM.

## 6.2 Future Work

During this project it has been shown that amphiphilic block copolymers can be synthesised via a metal and sulfur-free, bromoform-assisted, aqueous free-radical polymerisation technique. Initial focus of the influence of bromoform on the synthesis of PDMA and PNIPAM macro-initiators was described, under UV conditions, and determined that bromoform was not behaving as a CTA; as implied in previous work by Thananukul *et al.*<sup>212</sup> (for the synthesis of polyacrylamide). Subsequent studies then identified that bromoform is not a photoinitiator for the synthesis of PDMA or PNIPAM under the described conditions. The main goal for future

work is to continue to elucidate the mechanism of the bromoform-assisted synthesis technique.

The syntheses conducted herein describe thermally controlled conditions, a development from the previous studies<sup>207–209,211,212</sup>. Therefore, it would be advantageous to investigate the role of bromoform under thermal conditions to elucidate whether bromoform can be used as a simple, readily available, inexpensive, stable (easily stored), water-miscible CTA or thermal initiator. This is based on the hypothesis of bromoform having thermally cleavable C-Br bonds that have the potential to create reactive radical sites in their own right. However, as PNIPAM exhibits an LCST (30–35 °C<sup>1,339,344–346</sup>) in water, an alternative water soluble comonomer would need to be selected. Alternatively, the thermal effect of bromoform could be studied for the current monomer combination in organic solvents; such as DMF. The study in organic solvents could also open up the opportunity to synthesise commercially-relevant block copolymers from hydrophobic monomers using this bromoform-assisted technique.

To further amplify the effect of bromoform on the kinetics of the reactions discussed herein, and the thermal studies to be completed, a range of initiator (namely ACPA) concentrations should also be investigated. Decreasing the ACPA concentration (from the 1.0 mol % used herein) would slow down the reactions and could allow the interaction of bromoform on the system to dominate. Additionally, the monomer concentration could also be reduced to result in the same effect. Both series of investigations could provide more significant insights regarding the role of bromoform in these studies. This could also result in a decrease in the dispersity of the macro-initiator and subsequent block copolymers formed.

Additionally, the PDMA macro-initiators described herein were synthesised using 2 mol % bromoform (within the miscibility range). Further studies could be undertaken to investigate the effect of bromoform concentration on the performance of the PDMA macro-initiators in terms of blocking efficacy. Therefore, PDMA macro-initiators could be produced at 0.5 and 1.0 mol % bromoform to further uncover the most effective route to block copolymer synthesis.



In order to provide more conclusive evidence that block copolymers have been formed other analytical techniques could be explored. More specifically, diffusion-ordered spectroscopy (DOSY) which evaluates the movement of molecules; specifically, how they diffuse through a known medium<sup>356–360</sup>. This technique has been particularly useful in identifying which small molecules are present in a given mixture<sup>356</sup>. Whilst the literature is dominated by non-polymer applications of DOSY it is becoming an increasingly popular tool in copolymer analysis<sup>355,358–361</sup>. Regarding this work, DOSY could be used to determine whether block copolymers or a mixture of homopolymers are present in the sample. This is due to the fact that the homopolymers, with their lower individual molecular weights, will diffuse at a faster rate than the corresponding copolymer<sup>357,358,360</sup>. To confirm successful copolymer synthesis, it is expected that both polymer blocks in the sample will diffuse at the same rate.

In addition, to the synthetic and analytical avenues that could be explored, the precipitation method for isolating the block copolymers should also be developed. The block copolymer studies described in Chapter 5 highlight the presence of impurities in the final products regardless of whether the one or two-step synthetic route is used. Developing a method that would isolate the block copolymers and eliminate any unreacted PDMA, PNIPAM or potential PDMA-*st*-PNIPAM is vitally important if DOSY NMR (*vide supra*) is to be used to confirm the presence of the block copolymers.

Finally, to advance this technique even further the ability to synthesise block copolymers of reversed monomer order, like that seen in photoiniferter polymerisation described in Chapter 1, could be investigated. This could open up the opportunity to synthesise poly(*N*-isopropylacrylamide)-*block*-poly(*N,N*-dimethylacrylamide) [PNIPAM-*b*-PNIPAM] copolymers as well as many other monomer combinations that could be investigated using this technique. The ability to synthesise block copolymers with indiscriminate sequencing is of great importance as it could allow access to materials that present techniques (such as RAFT<sup>277,362</sup>) cannot readily produce. This bromoform-assisted technique could provide an opportunity to

synthesise industrially-relevant block copolymers that are currently not possible; generating a new library of materials for use in a range of applications.

## References

- 1 K. Jain, R. Vedarajan, M. Watanabe, M. Ishikiriya and N. Matsumi, Tunable LCST Behavior of Poly(*N*-isopropylacrylamide/ionic liquid) Copolymers, *Polym. Chem.*, 2015, **6**, 6819–6825.
- 2 International Agency for Research on Cancer, *Chlorinated Drinking-water; Chlorination By-products; Some Other Halogenated Compounds; Cobalt and Cobalt Compounds*, 1991, vol. 52.
- 3 S. H. Yalkowsky, Y. He and P. Jain, *Handbook of Aqueous Solubility Data*, CRC Press, USA, Second Edition, 2016, 1-3.
- 4 W. M. Haynes, *CRC Handbook of Chemistry and Physics*, CRC Press, Boca Raton, 92<sup>nd</sup> Edition, 2011, 5-87.
- 5 J. M. G. Cowie, *Polymers: Chemistry and Physics of Modern Materials*, Stanley Thornes, Cheltenham, 2nd Edition, 1998, 1-10.
- 6 H. Staudinger, About Polymerization, *Eur. J. Inorg. Chem.*, 1920, **53**, 1073–1085.
- 7 J. A. Brydson and Marianne Gilbert, *Brydson's Plastics Materials*, Elsevier, London, 8th Edition, 2017, 1-13.
- 8 H. Staudinger, About the Constitution of Rubber, *Eur. J. Inorg. Chem.*, 1924, **57**, 1203–1208.
- 9 M. A. C. Stuart, W. T. S. Huck, J. Genzer, M. Müller, C. Ober, M. Stamm, G. B. Sukhorukov, I. Szleifer, V. V. Tsukruk, M. Urban, F. Winnik, S. Zauscher, I. Luzinov and S. Minko, Emerging Applications of Stimuli-Responsive Polymer Materials, *Nat. Mater.*, 2010, **9**, 101–113.
- 10 L. Wang, M. Wang, P. D. Topham and Y. Huang, Fabrication of Magnetic Drug-Loaded Polymeric Composite Nanofibres and their Drug Release Characteristics, *RSC Adv.*,

2012, **2**, 2433–2438.

- 11 P. A. Gunatillake and R. Adhikari, Biodegradable Synthetic Polymers for Tissue Engineering., *Eur. Cell. Mater.*, 2003, **5**, 1–16.
- 12 P. Mikes, J. Horakova, A. Saman, L. Vejsadova, P. Topham, W. Punyodom, M. Dumklang and V. Jencova, Comparison and Characterization of Different Polyester Nano/Micro Fibres for use in Tissue Engineering Applications, *J. Ind. Text.*, 2021, **50**, 870–890.
- 13 N. Tuancharoensri, G. M. Ross, S. Mahasaranon, P. D. Topham and S. Ross, Ternary Blend Nanofibres of Poly(lactic acid), Polycaprolactone and Cellulose Acetate Butyrate for Skin Tissue Scaffolds: Influence of Blend Ratio and Polycaprolactone Molecular Mass on Miscibility, Morphology, Crystallinity and Thermal Properties, *Polym. Int.*, 2017, **66**, 1463–1472.
- 14 P. H. Corkhill, C. J. Hamilton and B. J. Tighe, Synthetic Hydrogels. VI. Hydrogel Composites as Wound Dressings and Implant Materials, *Biomaterials*, 1989, **10**, 3–10.
- 15 W. Li, Q. Yu, H. Yao, Y. Zhu, P. D. Topham, K. Yue, L. Ren and L. Wang, Superhydrophobic Hierarchical Fiber/Bead Composite Membranes for Efficient Treatment of Burns, *Acta Biomater.*, 2019, **92**, 60–70.
- 16 B. J. Tighe and A. Mann, in *Contact Lenses*, Elsevier, London, 6th Edition, 2018, 18–19.
- 17 V. Saez-Martinez, A. Mann, F. Lydon, F. Molock, S. A. Layton, D. T. W. Toolan, J. R. Howse, P. D. Topham and B. J. Tighe, The Influence of Structure and Morphology on Ion Permeation in Commercial Silicone Hydrogel Contact Lenses, *J. Biomed. Mater. Res. - Part B Appl. Biomater.*, 2021, **109**, 137–148.
- 18 J. F. Lutz, Polymerization of Oligo(ethylene glycol) (meth)acrylates: Toward New Generations of Smart Biocompatible Materials, *J. Polym. Sci. Part A Polym. Chem.*,

- 2008, **46**, 3459–3470.
- 19 J. M. G. G. Swann and P. D. Topham, Design and Application of Nanoscale Actuators Using Block-Copolymers, *Polymers*, 2010, **2**, 454–469.
  - 20 P. D. Topham, A. Glidle, D. T. W. Toolan, M. P. Weir, M. W. A. Skoda, R. Barker and J. R. Howse, The Relationship Between Charge Density and Polyelectrolyte Brush Profile Using Simultaneous Neutron Reflectivity and In Situ Attenuated Total Internal Reflection FTIR, *Langmuir*, 2013, **29**, 6068–6076.
  - 21 P. D. Topham, J. R. Howse, C. J. Crook, A. J. Parnell, M. Geoghegan, R. A. L. Jones and A. J. Ryan, Controlled Growth of Poly(2-(diethylamino)ethyl methacrylate) Brushes via Atom Transfer Radical Polymerisation on Planar Silicon Surfaces, *Polym. Int.*, 2006, **55**, 808–815.
  - 22 P. D. Topham, J. R. Howse, C. J. Crook, A. J. Gleeson, W. Bras, S. P. Armes, R. A. L. Jones and A. J. Ryan, Autonomous Volume Transitions of a Polybase Triblock Copolymer Gel in a Chemically Driven pH-Oscillator, *Macromol. Symp.*, 2007, **256**, 95–104.
  - 23 P. D. Topham, J. R. Howse, C. M. Fernyhough and A. J. Ryan, The Performance of Poly(styrene)-block-poly(2-vinyl pyridine)-block-poly(styrene) Triblock Copolymers as pH-Driven Actuators, *Soft Matter*, 2007, **3**, 1506–1512.
  - 24 J. D. Willott, T. J. Murdoch, B. A. Humphreys, S. Edmondson, G. B. Webber and E. J. Wanless, Critical Salt Effects in the Swelling Behavior of a Weak Polybasic Brush, *Langmuir*, 2014, **30**, 1827–1836.
  - 25 L. A. Fielding, S. Edmondson and S. P. Armes, Synthesis of pH-Responsive Tertiary Amine Methacrylate Polymer brushes and their Response to Acidic Vapour, *J. Mater. Chem.*, 2011, **21**, 11773–11780.
  - 26 T. Haino, Designer Supramolecular Polymers with Specific Molecular Recognitions,

- Polym. J.*, 2019, **51**, 303–318.
- 27 M. F. Maitz, Applications of Synthetic Polymers in Clinical Medicine, *Biosurface and Biotribology*, 2015, **1**, 161–176.
  - 28 S. K. Gill, N. Roohpour, P. D. Topham and B. J. Tighe, Tuneable Denture Adhesives using Biomimetic Principles for Enhanced Tissue Adhesion in Moist Environments, *Acta Biomater.*, 2017, **63**, 326–335.
  - 29 C. Sanson, C. Schatz, J. F. Le Meins, A. Br, A. Soum and S. Ebastien Lecommandoux, Biocompatible and Biodegradable Poly(trimethylene carbonate)-b-poly(L-glutamic acid) Polymersomes: Size Control and Stability, *Langmuir*, 2010, **26**, 2751–2760.
  - 30 I. Engelberg and J. Kohn, Physico-Mechanical Properties of Degradable Polymers used in Medical Applications: A Comparative Study, *Biomaterials*, 1991, **12**, 292–304.
  - 31 S. Phetsuk, R. Molloy, K. Nalampang, P. Meepowpan, P. D. Topham, B. J. Tighe and W. Punyodom, Physical and Thermal Properties of L-lactide/ε-caprolactone Copolymers: The Role of Microstructural Design, *Polym. Int.*, 2020, **69**, 248–256.
  - 32 K. Suthapakti, R. Molloy, W. Punyodom, K. Nalampang, T. Leejarkpai, P. D. Topham and B. J. Tighe, Biodegradable Compatibilized Poly(l-lactide)/Thermoplastic Polyurethane Blends: Design, Preparation and Property Testing, *J. Polym. Environ.*, 2018, **26**, 1818–1830.
  - 33 S. Ruengde, J. Siripitayananon, R. Molloy, R. Somsunan, P. D. Topham and B. J. Tighe, Preparation of a Poly(L-lactide-co -caprolactone) Copolymer using a Novel Tin(II) alkoxide Initiator and its Fiber Processing for Potential use as an Absorbable Monofilament Surgical Suture, *Int. J. Polym. Mater. Polym. Biomater.*, 2016, **65**, 277–284.
  - 34 E. S. Gil and S. M. Hudson, Stimuli-Reponsive Polymers and their Bioconjugates, *Prog. Polym. Sci.*, 2004, **29**, 1173–1222.

- 35 C. H. Alarcón, S. Pennadam and C. Alexander, Stimuli Responsive Polymers for Biomedical Applications, *Chem. Soc. Rev.*, 2005, **34**, 276–285.
- 36 K. Harrison, in *Biomedical Polymers*, Elsevier Inc., 2007, 1–32.
- 37 D. Colombani and P. Chaumont, Addition-Fragmentation Processes in Free Radical Polymerization, *Prog. Polym. Sci.*, 1996, **21**, 439–503.
- 38 R. F. T. Stepto, Dispersity in Polymer Science (IUPAC Recommendations 2009), *Pure Appl. Chem.*, 2009, **81**, 351–353.
- 39 A. Ravve, in *Principles of Polymer Chemistry*, Springer US, Boston, 2<sup>nd</sup> Edition, 2000, 327–448.
- 40 J. K. Stille, Step-Growth Polymerization, *J. Chem. Educ.*, 1981, **58**, 862.
- 41 W. F. Su, in *Principles of Polymer Design and Synthesis*, Springer, Berlin, Heidelberg, 2013, vol. 82, 111–136.
- 42 T. Otsu, M. Yoshida and T. Tazaki, A Model for Living Radical Polymerization, *Die Makromol. Chemie, Rapid Commun.*, 1982, **3**, 133–140.
- 43 E. Rizzardo and D. H. Solomon, On the Origins of Nitroxide Mediated Polymerization (NMP) and Reversible Addition–Fragmentation Chain Transfer (RAFT), *Aust. J. Chem.*, 2012, **65**, 945.
- 44 W. F. Su, in *Principles of Polymer Design and Synthesis*, Springer, Berlin, 2013, 137–183.
- 45 H. K. Reimschuessel, General Aspects in Polymer Synthesis., *Environ. Health Perspect.*, 1975, **11**, 9–20.
- 46 M. Chen, M. Zhong and J. A. Johnson, Light-Controlled Radical Polymerization: Mechanisms, Methods and Applications, *Chem. Rev.*, 2016, **116**, 10167–10211.
- 47 M. M. Ghobashy, in *Ionizing Radiation Effects and Applications*, InTech, Egypt, 2018,

113–134.

- 48 P. E. M. Allen and A. G. Moody, Polymerisation of Methylmethacrylate Initiated by Organometallic Compounds. II. The Effects of Temperature, *Die Makromol. Chemie*, 1965, **83**, 220–225.
- 49 R. C. Schulz, H. W. Eifel, T. Perner and K. Mühlbach, Some New Examples of Cationic Polymerization, *Makromol. Chemie. Macromol. Symp.*, 1986, **3**, 163–178.
- 50 M. Frankel, A. Ottolenghi, M. Albeck and A. Zilkha, Anionic Polymerisation of Vinyl Monomers with Butyl-lithium, *J. Chem. Soc.*, 1959, 3858.
- 51 W. A. Braunecker, Controlled/Living Radical Polymerization: Features, Developments and Perspectives, *Prog. Polym. Sci.*, 2007, **32**, 93–146.
- 52 J. C. Bevington, H. W. Melville and R. P. Taylor, The Termination Reaction in Radical Polymerizations. II. Polymerizations of Styrene at 60° and of Methyl Methacrylate at 0 and 60°, and the Copolymerization of These Monomers at 60°, *J. Polym. Sci.*, 1954, **14**, 463–476.
- 53 A. Takuzo, B. Coutin, J. Crivello, C. D. Eisenbach, H. Gorrissen, S. Inoue, Z. J. Jedlinski, W. Kaminsky, H. R. Kricheldorf, G. Lattermann, H. Nefzger, O. Nuyken, H. Sekiguchi and D. A. Tomalia, *Handbook of Polymer Synthesis*, CRC Press, New York, 2<sup>nd</sup> Edition, 1992, vol. 24, 4-5.
- 54 J. Collins, Z. Xiao, A. Espinosa-Gomez, B. P. Fors and L. A. Connal, Extremely Rapid and Versatile Synthesis of High Molecular Weight Step Growth Polymers via Oxime Click Chemistry, *Polym. Chem.*, 2016, **7**, 2581–2588.
- 55 S. K. Gupta and A. Kumar, *Reaction Engineering of Step Growth*, Springer Science & Business Media, London, 2012.
- 56 M. B. Hocking, in *Handbook of Chemical Technology and Pollution Control*, Elsevier, Canada, 3<sup>rd</sup> Edition, 2005, 669–688.



- 57 Q. Gao, N. X. Huang, Z. L. Tang and L. Gerking, Modelling of Solid State Polycondensation of Poly(ethylene terephthalate), *Chem. Eng. Sci.*, 1997, **52**, 371–376.
- 58 G. Moad and D. H. Solomon, *The Chemistry of Radical Polymerization*, Elsevier, 2006, 233-278.
- 59 A. Yokoyama and T. Yokozawa, Converting Step-Growth to Chain-Growth Condensation Polymerization, *Macromolecules*, 2007, **40**, 4093–4101.
- 60 M. A. Al-Nasassrah, F. Podczeczek and J. M. Newton, The Effect of an Increase in Chain Length on the Mechanical Properties of Polyethylene glycols, *Eur. J. Pharm. Biopharm.*, 1998, **46**, 31–38.
- 61 K. Vats, G. Marsh, K. Harding, I. Zampetakis, R. E. Waugh and D. S. W. Benoit, Nanoscale Physicochemical Properties of Chain- and Step-Growth Polymerized PEG Hydrogels Affect Cell-Material Interactions, *J. Biomed. Mater. Res. - Part A*, 2017, **105**, 1112–1122.
- 62 C. W. Bunn, The Melting Points of Chain Polymers, *J. Polym. Sci. Part B Polym. Phys.*, 1996, **34**, 799–819.
- 63 A. L. Agapov and A. P. Sokolov, Does the Molecular Weight Dependence of  $T_g$  Correlate to  $M_e$ ?, *Macromolecules*, 2009, **42**, 2877–2878.
- 64 K. Balani, V. Verma, A. Agarwal and R. Narayan, in *Biosurfaces: A Materials Science and Engineering Perspective*, John Wiley & Sons, New Jersey, 2015, 329–344.
- 65 K. Matyjaszewski and J. Spanswick, Controlled/Living Radical Polymerization, *Mater. Today*, 2005, **8**, 26–33.
- 66 M. Szwarc, 'Living' polymers, *Nature*, 1956, **178**, 1168–1169.
- 67 S. Penczek and J. B. Pretula, in *Polymer Science: A Comprehensive Reference*,

Elsevier, 2012, vol. 3, 3–38.

- 68 R. Sáez, C. McArdle, F. Salhi, J. Marquet and R. M. Sebastián, Controlled Living Anionic Polymerization of Cyanoacrylates by Frustrated Lewis Pair Based Initiators, *Chem. Sci.*, 2019, **10**, 3295–3299.
- 69 M. U. Kahveci, Y. Yagci, A. Avgeropoulos and C. Tsitsilianis, in *Polymer Science: A Comprehensive Reference*, Elsevier, 2012, vol. 6, 455–509.
- 70 T. Ishizone and R. Goseki, in *Encyclopedia of Polymeric Nanomaterials*, Springer Berlin Heidelberg, 2014, 1–18.
- 71 S. Bywater and D. J. Worsfold, Alkylolithium Anionic Polymerization Initiators in Hydrocarbon Solvents, *J. Organomet. Chem.*, 1967, **10**, 1–6.
- 72 H. Kokubo and M. Watanabe, Anionic Polymerization of Methyl Methacrylate in an Ionic Liquid, *Polym. Adv. Technol.*, 2008, **19**, 1441–1444.
- 73 T. Ishizone and R. Goseki, in *Encyclopedia of Polymeric Nanomaterials*, Springer Berlin Heidelberg, 2014, 1–11.
- 74 M. Szwarc, M. Levy and R. Milkovich, Polymerization Initiated by Electron Transfer to Monomer. A New Method of Formation of Block Polymers, *J. Am. Chem. Soc.*, 1956, **78**, 2656–2657.
- 75 E. M. W. Tsang and S. Holdcroft, in *Polymer Science: A Comprehensive Reference*, Elsevier, London, 2012, vol. 10, 651–689.
- 76 J. Morsbach, A. H. E. Müller, E. Berger-Nicoletti and H. Frey, Living Polymer Chains with Predictable Molecular Weight and Dispersity via Carbanionic Polymerization in Continuous Flow: Mixing Rate as a Key Parameter, *Macromolecules*, 2016, **49**, 5043–5050.
- 77 R. P. Quirk, Q. Zhuo, S. H. Jang, Y. Lee and G. Lizarraga, Principles of Anionic

Polymerization: An Introduction, *ACS Symp. Ser.*, 1998, **696**, 2–27.

- 78 H. Frey and T. Ishizone, Living Anionic Polymerization - Part II: Further Expanding the Synthetic Versatility for Novel Polymer Architectures, *Macromol. Chem. Phys.*, 2018, **219**, 1700567.
- 79 M. J. Kim, Y. G. Yu, N. G. Kang, B. G. Kang and J. S. Lee, Precise Synthesis of Functional Block Copolymers by Living Anionic Polymerization of Vinyl Monomers Bearing Nitrogen Atoms in the Side Chain, *Macromol. Chem. Phys.*, 2017, **218**, 1600445.
- 80 N. Hadjichristidis, H. Iatrou, S. Pispas and M. Pitsikalis, Anionic Polymerization: High Vacuum Techniques, *J. Polym. Sci. Part A Polym. Chem.*, 2000, **38**, 3211–3234.
- 81 L. J. Fetters, Procedures for Homogeneous Anionic Polymerization, *J. Res. Natl. Bur. Stand. Sect. A Phys. Chem.*, 1966, **70A**, 428.
- 82 F. Le Dévédec, L. Houdaihed and C. Allen, Anionic Polymerization of an Amphiphilic Copolymer for Preparation of Block Copolymer Micelles Stabilized by  $\pi$ - $\pi$  Stacking Interactions, *J. Vis. Exp.*, 2016, **2016**, 54422.
- 83 W. F. Su, in *Principles of Polymer Design and Synthesis*, Springer, Berlin, Heidelberg, Berlin, 2013, 185–218.
- 84 L. Hu, W. Zhao, J. He and Y. Zhang, Silyl Ketene Acetals/ $\text{B}(\text{C}_6\text{F}_5)_3$  Lewis Pair-Catalyzed Living Group Transfer Polymerization of Renewable Cyclic Acrylic Monomers, *Molecules*, 2018, **23**, 1–19.
- 85 J. Chen, R. R. Gowda, J. He, Y. Zhang and E. Y. X. Chen, Controlled or High-Speed Group Transfer Polymerization by Silyl Ketene Acetals Without Catalyst, *Macromolecules*, 2016, **49**, 8075–8087.
- 86 O. W. Webster, W. R. Hertler, D. Y. Sogah, W. B. Farnham and T. V. Rajan-Babu, Group-Transfer Polymerization. 1. A New Concept for Addition Polymerization with H.J.Hutchins, PhD Thesis, Aston University, 2021.

- Organosilicon Initiators, *J. Am. Chem. Soc.*, 1983, **105**, 5706–5708.
- 87 W. J. Brittain and I. B. Dicker, Isomerization of Silyl Ketene Acetals: Models for the Propagating Chain End in Group Transfer Polymerization, *Polym. Int.*, 1993, **30**, 101–107.
  - 88 T. Kitaura and T. Kitayama, Anionic Polymerization of Methyl Methacrylate by Difunctional Lithium Amide Initiators with Trialkylsilyl Protection, *Polym. J.*, 2013, **45**, 1013–1018.
  - 89 K. Fuchise, Y. Chen, T. Satoh and T. Kakuchi, Recent Progress in Organocatalytic Group Transfer Polymerization, *Polym. Chem.*, 2013, **4**, 4278–4291.
  - 90 M. Baško and P. Kubisa, Mechanism of Propagation in the Cationic Polymerization of L,L-lactide, *J. Polym. Sci. Part A Polym. Chem.*, 2008, **46**, 7919–7923.
  - 91 S. Aoshima and S. Kanaoka, A Renaissance in Living Cationic Polymerization, *Chem. Rev.*, 2009, **109**, 5245–5287.
  - 92 M. Basko, Activated Monomer Mechanism in the Cationic Polymerization of L,L-lactide, *Pure Appl. Chem.*, 2012, **84**, 2081–2088.
  - 93 A. Rudin and P. Choi, in *The Elements of Polymer Science & Engineering*, Elsevier, London, 3<sup>rd</sup> Edition, 2013, 449–493.
  - 94 J. S. Wang and K. Matyjaszewski, ‘Living’/Controlled Radical Polymerization. Transition-Metal-Catalyzed Atom Transfer Radical Polymerization in the Presence of a Conventional Radical Initiator, *J. Am. Chem. Soc.*, 1995, **28**, 7572–7573.
  - 95 L. Hutson, J. Krstina, C. L. Moad, G. Moad, G. R. Morrow, A. Postma, E. Rizzardo and S. H. Thang, Chain Transfer Activity of  $\omega$ -Unsaturated Methacrylic Oligomers in Polymerizations of Methacrylic Monomers, *Macromolecules*, 2004, **37**, 4441–4452.
  - 96 G. Moad, Y. K. Chong, A. Postma, E. Rizzardo and S. H. Thang, Advances in RAFT

- Polymerization: The Synthesis of Polymers with Defined End-Groups, *Polymer*, 2005, **46**, 8458–8468.
- 97 R. T. A. Mayadunne, J. Jeffery, G. Moad and E. Rizzardo, Living Free Radical Polymerization with Reversible Addition-Fragmentation Chain Transfer (RAFT Polymerization): Approaches to Star Polymers, *Macromolecules*, 2003, **36**, 1505–1513.
  - 98 H. Fischer, The Persistent Radical Effect: A Principle for Selective Radical Reactions and Living Radical Polymerizations, *Chem. Rev.*, 2001, **101**, 3581–3610.
  - 99 Y. Nakamura, Y. Kitada, Y. Kobayashi, B. Ray and S. Yamago, Quantitative Analysis of the Effect of Azo Initiators on the Structure of  $\alpha$ -Polymer Chain Ends in Degenerative Chain-Transfer-Mediated Living Radical Polymerization Reactions, *Macromolecules*, 2011, **44**, 8388–8397.
  - 100 X. Guo, B. Choi, A. Feng and S. H. Thang, Polymer Synthesis with More Than One Form of Living Polymerization Method, *Macromol. Rapid Commun.*, 2018, **39**, 1800479.
  - 101 C. H. Peng, J. Kong, F. Seeliger and K. Matyjaszewski, Mechanism of Halogen Exchange in ATRP, *Macromolecules*, 2011, **44**, 7546–7557.
  - 102 B. T. Cheesman, J. D. Willott, G. B. Webber, S. Edmondson and E. J. Wanless, pH-Responsive Brush-Modified Silica Hybrids Synthesized by Surface-Initiated ARGET ATRP, *ACS Macro Lett.*, 2012, **1**, 1161–1165.
  - 103 F. Di Lena and K. Matyjaszewski, Transition Metal Catalysts for Controlled Radical Polymerization, *Prog. Polym. Sci.*, 2010, **35**, 959–1021.
  - 104 D. J. Siegwart, J. K. Oh and K. Matyjaszewski, ATRP in the Design of Functional Materials for Biomedical Applications, *Prog. Polym. Sci.*, 2012, **37**, 18–37.
  - 105 K. Matyjaszewski, Atom Transfer Radical Polymerization (ATRP): Current Status and Future Perspectives, *Macromolecules*, 2012, **45**, 4015–4039.

- 106 V. Yadav, N. Hashmi, W. Ding, T. H. Li, M. K. Mahanthappa, J. C. Conrad and M. L. Robertson, Dispersity Control in Atom Transfer Radical Polymerizations through Addition of Phenylhydrazine, *Polym. Chem.*, 2018, **9**, 4332–4342.
- 107 R. Whitfield, N. P. Truong, D. Messmer, K. Parkatzidis, M. Rolland and A. Anastasaki, Tailoring Polymer Dispersity and Shape of Molecular Weight Distributions: Methods and Applications, *Chem. Sci.*, 2019, **10**, 8724–8734.
- 108 Y. Miura, K. Hirota, H. Moto and B. Yamada, High-Yield Synthesis of Functionalized Alkoxyamine Initiators and Approach to Well-Controlled Block Copolymers using them, *Macromolecules*, 1999, **32**, 8356–8362.
- 109 T. Kothe, S. Marque, R. Martschke, M. Popov and H. Fischer, Radical Reaction Kinetics During Homolysis of *N*-Alkoxyamines: Verification of the Persistent Radical Effect, *J. Chem. Soc.*, 1998, 1553–1559.
- 110 C. J. Hawker, A. W. Bosman and E. Harth, New Polymer Synthesis by Nitroxide Mediated Living Radical Polymerizations, *Chem. Rev.*, 2001, **101**, 3661–3688.
- 111 J. Nicolas and Y. Guillaneuf, in *Encyclopedia of Polymeric Nanomaterials*, Editors: S. Kobayashi and K. Mullen, Springer, Berlin, 2014, 1–16.
- 112 C. Barner-Kowollik and S. Perrier, The Future of Reversible Addition Fragmentation Chain Transfer Polymerization, *J. Polym. Sci. Part A Polym. Chem.*, 2008, **46**, 5715–5723.
- 113 G. Moad, J. Chiefari, Y. K. Chong, J. Krstina, R. T. A. Mayadunne, A. Postma, E. Rizzardo and S. H. Thang, Living Free-Radical Polymerization by Reversible Addition–Fragmentation Chain Transfer: The RAFT Process, *Macromolecules*, 1998, **31**, 5559–5562.
- 114 H. Willcock and R. K. O'Reilly, End Group Removal and Modification of RAFT Polymers, *Polym. Chem.*, 2010, **1**, 149–157.

- 115 G. Moad, J. Chiefari, Y. K. Chong, J. Krstina, R. T. Mayadunne, A. Postma, E. Rizzardo and S. H. Thang, Living Free Radical Polymerization with Reversible Addition-Fragmentation Chain Transfer (The Life of RAFT), *Polym. Int.*, 2000, **49**, 993–1001.
- 116 S. Perrier, P. Takolpuckdee, J. Westwood and D. M. Lewis, Versatile Chain Transfer Agents for Reversible Addition Fragmentation Chain Transfer (RAFT) Polymerization to Synthesize Functional Polymeric Architectures, *Macromolecules*, 2004, **37**, 2709–2717.
- 117 J. F. Baussard, J. L. Habib-Jiwan, A. Laschewsky, M. Mertoglu and J. Storsberg, New Chain Transfer Agents for Reversible Addition-Fragmentation Chain Transfer (RAFT) Polymerisation in Aqueous Solution, *Polymer (Guildf)*., 2004, **45**, 3615–3626.
- 118 M. F. Cunningham, Controlled/Living Radical Polymerization in Aqueous Dispersed Systems, *Prog. Polym. Sci.*, 2008, **33**, 365–398.
- 119 J. Qiu, B. Charleux and K. Matyjaszewski, Controlled/Living Radical Polymerization in Aqueous Media: Homogeneous and Heterogeneous Systems, *Prog. Polym. Sci.*, 2001, **26**, 2083–2134.
- 120 S. Perrier, 50th Anniversary Perspective: RAFT Polymerization - A User Guide, *Macromolecules*, 2017, **50**, 7433–7447.
- 121 G. Hawkins, P. B. Zetterlund and F. Aldabbagh, RAFT polymerization in supercritical carbon dioxide based on an induced precipitation approach: Synthesis of 2-ethoxyethyl methacrylate/acrylamide block copolymers, *J. Polym. Sci. Part A Polym. Chem.*, 2015, **53**, 2351–2356.
- 122 I. Fraga Domínguez, J. Kolomanska, P. Johnston, A. Rivaton and P. D. Topham, Controlled Synthesis of Poly(neopentyl p -styrene sulfonate) via Reversible Addition-Fragmentation Chain Transfer Polymerisation, *Polym. Int.*, 2015, **64**, 621–630.
- 123 A. Isakova, C. Burton, D. J. Nowakowski and P. D. Topham, Diels-Alder Cycloaddition

- and RAFT Chain End Functionality: An Elegant Route to Fullerene End-Capped Polymers with Control over Molecular Mass and Architecture, *Polym. Chem.*, 2017, **8**, 2796–2805.
- 124 A. Isakova, O. Efremova, N. Pullan, L. L  er and P. D. Topham, Design, Synthesis and RAFT Polymerisation of a Quinoline-Based Monomer for use in Metal-Binding Composite Microfibers, *RSC Adv.*, 2016, **6**, 6598–6606.
  - 125 E. Hancox, E. Liarou, J. S. Town, G. R. Jones, S. A. Layton, S. Huband, M. J. Greenall, P. D. Topham and D. M. Haddleton, Microphase Separation of Highly Amphiphilic, Low N polymers by Photoinduced Copper-Mediated Polymerization, Achieving Sub-2 nm Domains at Half-Pitch, *Polym. Chem.*, 2019, **10**, 6254–6259.
  - 126 J. Nicolas, Y. Guillaneuf, C. Lefay, D. Bertin, D. Gigmes and B. Charleux, Nitroxide-Mediated Polymerization, *Prog. Polym. Sci.*, 2013, **38**, 63–235.
  - 127 G. Moad, E. Rizzardo and S. H. Thang, Living Radical Polymerization by the RAFT Process - A Second Update, *Aust. J. Chem.*, 2009, **62**, 1402.
  - 128 D. R. Robello, A. Andr  , T. A. Mccovick, A. Kraus and T. H. Mourey, Synthesis and Characterization of Star Polymers Made from Simple, Multifunctional Initiators, *Macromolecules*, 2002, **35**, 9334–9344.
  - 129 M. S. Donovan, T. A. Sanford, A. B. Lowe, B. S. Sumerlin, Y. Mitsukami and C. L. McCormick, RAFT Polymerization of *N,N*-Dimethylacrylamide in Water, *Macromolecules*, 2002, **35**, 4570–4572.
  - 130 A. Narumi, Y. Chen, M. Sone, K. Fuchise, R. Sakai, T. Satoh, Q. Duan, S. Kawaguchi and T. Kakuchi, Poly( *N* -hydroxyethylacrylamide) Prepared by Atom Transfer Radical Polymerization as a Nonionic, Water-Soluble, and Hydrolysis-Resistant Polymer and/or Segment of Block Copolymer with a Well-Defined Molecular Weight, *Macromol. Chem. Phys.*, 2009, **210**, 349–358.



- 131 A. Isakova, P. D. Topham and A. J. Sutherland, Controlled RAFT Polymerization and Zinc Binding Performance of Catechol-Inspired Homopolymers, *Macromolecules*, 2014, **47**, 2561–2568.
- 132 N. Pullan, M. Liu and P. D. Topham, Reversible Addition-Fragmentation Chain Transfer Polymerization of 2-Chloro-1,3-butadiene, *Polym. Chem.*, 2013, **4**, 2272–2277.
- 133 J. Kolomanska, P. Johnston, A. Gregori, I. Fraga Domínguez, H. J. Egelhaaf, S. Perrier, A. A. Rivaton, C. Dagron-Lartigau and P. D. Topham, Design, Synthesis and Thermal Behaviour of a Series of Well-Defined Clickable and Triggerable Sulfonate Polymers, *RSC Adv.*, 2015, **5**, 66554–66562.
- 134 B. Klumperman, in *Encyclopedia of Polymer Science and Technology*, Wiley, 2015, 1–27.
- 135 K. E. B. Doncom, L. D. Blackman, D. B. Wright, M. I. Gibson and R. K. O'Reilly, Dispersity Effects in Polymer Self-Assemblies: A Matter of Hierarchical Control, *Chem. Soc. Rev.*, 2017, **46**, 4119–4134.
- 136 R. Whitfield, K. Parkatzidis, N. P. Truong, T. Junkers and A. Anastasaki, Tailoring Polymer Dispersity by RAFT Polymerization: A Versatile Approach, *Chem*, 2020, **6**, 1340–1352.
- 137 D. T. Gentekos and B. P. Fors, Molecular Weight Distribution Shape as a Versatile Approach to Tailoring Block Copolymer Phase Behavior, *ACS Macro Lett.*, 2018, **7**, 677–682.
- 138 S. I. Rosenbloom and B. P. Fors, Shifting Boundaries: Controlling Molecular Weight Distribution Shape for Mechanically Enhanced Thermoplastic Elastomers, *Macromolecules*, 2020, **53**, 7479–7486.
- 139 D. T. Gentekos, L. N. Dupuis and B. P. Fors, Beyond Dispersity: Deterministic Control of Polymer Molecular Weight Distribution, *J. Am. Chem. Soc.*, 2016, **138**, 1848–1851.

- 140 S. Han, J. Wu, Y. Zhang, J. Lai, Y. Chen, L. Zhang and J. Tan, Utilization of Poor RAFT Control in Heterogeneous RAFT Polymerization, *Macromolecules*, 2021, 1–13.
- 141 B. R. Parker, M. J. Derry, Y. Ning and S. P. Armes, Exploring the Upper Size Limit for Sterically Stabilized Diblock Copolymer Nanoparticles Prepared by Polymerization-Induced Self-Assembly in Non-Polar Media, *Langmuir*, 2020, **36**, 3730–3736.
- 142 M. J. Derry, T. Smith, P. S. O’Hora and S. P. Armes, Block Copolymer Nanoparticles Prepared via Polymerization-Induced Self-Assembly Provide Excellent Boundary Lubrication Performance for Next-Generation Ultralow-Viscosity Automotive Engine Oils, *ACS Appl. Mater. Interfaces*, 2019, **11**, 33364–33369.
- 143 S. I. Rosenbloom, R. J. Sifri and B. P. Fors, Achieving Molecular Weight Distribution Shape Control and Broad Dispersities using RAFT Polymerizations, *Polym. Chem.*, 2021, 1–6.
- 144 G. F. Meijs, E. Rizzardo and P. T. Le, New Chain Transfer Agents for Free Radical Polymerizations, *Polym. Int.*, 1991, **26**, 239–244.
- 145 G. Moad, E. Rizzardo and S. H. Thang, Radical Addition Fragmentation Chemistry in Polymer Synthesis, *Polymer*, 2008, **49**, 1079–1131.
- 146 S. Fakirov, in *Fundamentals of Polymer Science for Engineers*, Wiley-VCH, Weinheim, 1<sup>st</sup> Edition, 2017, 241–277.
- 147 D. Kukulj, A. Thomas P. Davis and R. G. Gilbert, Chain Transfer to Monomer in the Free-Radical Polymerizations of Methyl Methacrylate, Styrene, and  $\alpha$ -Methylstyrene, *Macromolecules*, 1998, **31**, 994–999.
- 148 E. Rizzardo, Y. K. Chong, R. A. Evans, G. Moad and S. H. Thang, Control of Polymer Structure by Chain Transfer Processes, *Macromol. Symp.*, 1996, **111**, 1–11.
- 149 T. Otsu and M. Yoshida, Role of Initiator-Transfer Agent-Terminator (Iniferter) in Radical Polymerizations: Polymer Design by Organic Disulfides as Iniferters, H.J.Hutchins, PhD Thesis, Aston University, 2021.

*Macromolecular*, 1982, **3**, 127–132.

- 150 T. R. Nogueira, M. C. Gonçalves, L. M. Ferrareso Lona, E. Vivaldo-Lima, N. McManus and A. Penlidis, Effect of Initiator Type and Concentration on Polymerization Rate and Molecular Weight in the Bimolecular Nitroxide-Mediated Radical Polymerization of Styrene, *Adv. Polym. Technol.*, 2010, **29**, 11–19.
- 151 T. Junkers and C. Barner-Kowollik, The Role of Mid-Chain Radicals in Acrylate Free Radical Polymerization: Branching and Scission, *J. Polym. Sci. Part A Polym. Chem.*, 2008, **46**, 7585–7605.
- 152 C. Plessis, G. Arzamendi, J. M. Alberdi, Mathias Agnely, J. R. and Leiza and J. M. Asua, Intramolecular Chain Transfer to Polymer in the Emulsion Polymerization of 2-Ethylhexyl Acrylate, *Macromolecules*, 2001, **34**, 6138–6143.
- 153 M. J. Roedel, The Molecular Structure of Polyethylene. I. Chain Branching in Polyethylene during Polymerization, *J. Am. Chem. Soc.*, 1953, **75**, 6110–6112.
- 154 D. E. Kline, J. A. Sauer and A. E. Woodward, Effect of Branching on Dynamic Mechanical Properties of Polyethylene, *J. Polym. Sci.*, 1956, **22**, 455–462.
- 155 N. Moghadam, S. Srinivasan, M. C. Grady, A. M. Rappe and M. Soroush, Theoretical Study of Chain Transfer to Solvent Reactions of Alkyl Acrylates, *J. Phys. Chem. A*, 2014, **118**, 5474–5487.
- 156 S. R. Palit, U. S. Nandi and N. G. Saha, Studies in Chain Transfer. III. Determination of Chain Transfer Coefficients from Catalyzed Polymerization Data, *J. Polym. Sci.*, 1954, **14**, 295–304.
- 157 Y. Sugihara, P. O’connor, P. B. Zetterlund and F. Aldabbagh, Chain Transfer to Solvent in the Radical Polymerization of *N*-Isopropylacrylamide, *J. Polym. Sci. Part A Polym. Chem.*, 2011, **49**, 1856–1864.
- 158 C. Magee, Y. Sugihara, P. B. Zetterlund and F. Aldabbagh, Chain Transfer to Solvent  
H.J.Hutchins, PhD Thesis, Aston University, 2021.

- in the Radical Polymerization of Structurally Diverse Acrylamide Monomers using Straight-Chain and Branched Alcohols as Solvents, *Polym. Chem.*, 2014, **5**, 2259–2265.
- 159 T. Furuncuoğlu, I. Uğur, I. Değirmenci and V. Aviyente, Role of Chain Transfer Agents in Free Radical Polymerization Kinetics, *Macromolecules*, 2010, **43**, 1823–1835.
- 160 C. Schilli, M. G. and Lanzendörfer and A. H. E. Müller, Benzyl and Cumyl Dithiocarbamates as Chain Transfer Agents in the RAFT Polymerization of N-Isopropylacrylamide. In Situ FT-NIR and MALDI-TOF MS Investigation, *Macromolecules*, 2002, **35**, 6819–6827.
- 161 S. Perrier and P. Takolpuckdee, Macromolecular Design via Reversible Addition-Fragmentation Chain Transfer (RAFT)/Xanthates (MADIX) Polymerization, *J. Polym. Sci. Part A Polym. Chem.*, 2005, **43**, 5347–5393.
- 162 D. Neugebauer, in *Encyclopedia of Polymer Science and Technology*, John Wiley & Sons, New Jersey, 2016, 1–42.
- 163 J. Vandenberg and T. Junkers, Alpha and Omega: Importance of the Nonliving Chain End in RAFT Multiblock Copolymerization, *Macromolecules*, 2014, **47**, 5051–5059.
- 164 S. Perrier, 50th Anniversary Perspective: RAFT Polymerization—A User Guide, *Macromolecules*, 2017, **50**, 7433–7447.
- 165 M. Farina, Chemistry and Kinetics of the Chain Transfer Reaction, *Macromol. Symp.*, 1987, **10–11**, 255–272.
- 166 G. Moad, E. Rizzardo and S. H. Thang, Radical Addition–Fragmentation Chemistry in Polymer Synthesis, *Polymer*, 2008, **49**, 1079–1131.
- 167 M. S. Donovan, A. B. Lowe, B. S. Sumerlin and C. L. McCormick, Raft Polymerization of *N,N*-dimethylacrylamide Utilizing Novel Chain Transfer Agents Tailored for High Reinitiation Efficiency and Structural Control, *Macromolecules*, 2002, **35**, 4123–4132.

- 168 D. B. Thomas, A. J. Convertine, R. D. Hester, A. B. Lowe and C. L. McCormick, Hydrolytic Susceptibility of Dithioester Chain Transfer Agents and Implications in Aqueous RAFT Polymerizations, *Macromolecules*, 2004, **37**, 1735–1741.
- 169 Y. K. Chong, J. Krstina, T. P. T. T. Le, G. Moad, A. Postma, E. Rizzardo, S. H. Thang, B. Y. K. Chong, J. Krstina, T. P. T. T. Le, G. Moad, A. Postma, E. Rizzardo and S. H. Thang, Thiocarbonylthio Compounds [SC(Ph)S-R] in Free Radical Polymerization with Reversible Addition-Fragmentation Chain Transfer (RAFT Polymerization). Role of the Free-Radical Leaving Group (R), *Macromolecules*, 2003, **36**, 2256–2272.
- 170 M. Destarac, D. Charmot, X. Franck and S. Z. Zard, Dithiocarbamates as Universal Reversible Addition-Fragmentation Chain Transfer Agents, *Macromol. Rapid Commun.*, 2000, **21**, 1035–1039.
- 171 A. V. Fuchs and K. J. Thurecht, Stability of Trithiocarbonate RAFT Agents Containing Both a Cyano and a Carboxylic Acid Functional Group, *ACS Macro Lett.*, 2017, **6**, 287–291.
- 172 V. K. Patel, N. K. Vishwakarma, A. K. Mishra, C. S. Biswas, P. Maiti and B. Ray, Synthesis of Alkyne-Terminated Xanthate RAFT Agents and Their Uses for the Controlled Radical Polymerization of *N*-Vinylpyrrolidone and the Synthesis of its Block Copolymer Using Click Chemistry, *J. Appl. Polym. Sci.*, 2013, **127**, 4305–4317.
- 173 B. N. Patra, D. Rayeroux and P. Lacroix-Desmazes, Synthesis of Cationic Amphiphilic Diblock Copolymers of Poly(vinylbenzyl triethylammonium chloride) and Polystyrene by Reverse Iodine Transfer Polymerization (RITP), *React. Funct. Polym.*, 2010, **70**, 408–413.
- 174 D. J. Keddie, G. Moad, E. Rizzardo and S. H. Thang, RAFT Agent Design and Synthesis, *Macromolecules*, 2012, **45**, 5321–5342.
- 175 C. Y. Lin, M. L. Coote, A. Gennaro and K. Matyjaszewski, Ab Initio Evaluation of the

- Thermodynamic and Electrochemical Properties of Alkyl Halides and Radicals and their Mechanistic Implications for Atom Transfer Radical Polymerization, *J. Am. Chem. Soc.*, 2008, **130**, 12762–12774.
- 176 N. Guo, R. Maurice, D. Teze, J. Graton, J. Champion, G. Montavon and N. Galland, Experimental and Computational Evidence of Halogen Bonds Involving Astatine, *Nat. Chem.*, 2018, **10**, 1–7.
- 177 J. Tonnar and P. Lacroix-Desmazes, Controlled Radical Polymerization of Styrene by Iodine Transfer Polymerization (ITP) in ab Initio Emulsion Polymerization, *Polymer*, 2016, **106**, 267–274.
- 178 J. Jennings, G. He, S. M. Howdle and P. B. Zetterlund, Block Copolymer Synthesis by Controlled/Living Radical Polymerisation in Heterogeneous Systems, *Chem. Soc. Rev.*, 2016, **45**, 5055–5084.
- 179 K. Matyjaszewski, S. Gaynor and J. S. Wang, Controlled Radical Polymerizations: The Use of Alkyl Iodides in Degenerative Transfer, *Macromolecules*, 1995, **28**, 2093–2095.
- 180 C. Farcet, M. Lansalot, R. Pirri, J. P. Vairon and B. Charleux, Polystyrene-block-poly(butyl acrylate) and Polystyrene-block-poly[(butyl acrylate)-co-styrene] Block Copolymers Prepared via Controlled Free-Radical Miniemulsion Polymerization Using Degenerative Iodine Transfer, *Macromol. Rapid Commun.*, 2000, **21**, 921–926.
- 181 K. Koumura, K. Satoh, M. Kamigaito and Y. Okamoto, Iodine Transfer Radical Polymerization of Vinyl Acetate in Fluoroalcohols for Simultaneous Control of Molecular Weight, Stereospecificity and Regiospecificity, *Macromolecules*, 2006, **39**, 4054–4061.
- 182 M. Tatemoto, in *Polymeric Materials Encyclopedia*, Elsevier Science, Amsterdam, 1996, 3847–3862.
- 183 V. Percec, A. V. Popov, E. Ramirez-Castillo, J. F. J. Coelho and L. A. Hinojosa-Falcon, Non-transition Metal-Catalyzed Living Radical Polymerization of Vinyl Chloride Initiated

- with Iodoform in Water at 25 °C, *J. Polym. Sci. Part A Polym. Chem.*, 2004, **42**, 6267–6282.
- 184 P. Lacroix-Desmazes, R. Severac and B. Boutevin, in *Advances in Controlled/Living Polymerization*, American Chemical Society, Michigan, 2003, 570–585.
- 185 C. Boyer, D. Valade, L. Sauguet, B. and Ameduri and B. Boutevin, Iodine Transfer Polymerization (ITP) of Vinylidene Fluoride (VDF). Influence of the Defect of VDF Chaining on the Control of ITP, *Macromolecules*, 2005, **38**, 10353–10362.
- 186 K. Koumura, K. Satoh, M. Kamigaito and Y. Okamoto, Iodine Transfer Radical Polymerization of Vinyl Acetate in Fluoroalcohols for Simultaneous Control of Molecular Weight, Stereospecificity and Regiospecificity, *Macromolecules*, 2006, **39**, 4054–4061.
- 187 B. Li, Y. Shi, W. Zhu, Z. Fu and W. Yang, Synthesis of Amphiphilic Polystyrene-*b*-poly(acrylic acid) Diblock Copolymers by Iodide-Mediated Radical Polymerization, *Polym. J.*, 2006, **38**, 387–394.
- 188 United States Patent Office, US2647107A, 1953, 1–3.
- 189 J. Hui, Y. Shi, T. Li, J. Wu and Z. Fu, Reverse Iodine Transfer Polymerization (RITP) of Chloroprene, *RSC Adv.*, 2015, **5**, 44326–44335.
- 190 D. Rayeroux, B. N. Patra and P. Lacroix-Desmazes, Synthesis of Anionic Amphiphilic Diblock Copolymers of Poly(styrene)and Poly(acrylic acid) by Reverse Iodine Transfer Polymerization (RITP) in Solution and Emulsion, *J. Polym. Sci. Part A Polym. Chem.*, 2013, **51**, 4389–4398.
- 191 X. Liu, Q. Xu, L. Zhang, Z. Cheng and X. Zhu, Visible-Light-Induced Living Radical Polymerization Using *in situ* Bromine-Iodine Transformation as an Internal Boost, *Polym. Chem.*, 2017, **8**, 2538–2551.
- 192 L. Xiao, K. Sakakibara, Y. Tsujii and A. Goto, Organocatalyzed Living Radical Polymerization via *in situ* Halogen Exchange of Alkyl Bromides to Alkyl Iodides, H.J.Hutchins, PhD Thesis, Aston University, 2021.

*Macromolecules*, 2017, **50**, 1882–1891.

- 193 H. Li, Q. Xu, X. Xu, L. Zhang, Z. Cheng and X. Zhu, One-Step Photocontrolled Polymerization-Induced Self-Assembly (Photo-PISA) by Using *in situ* Bromine-Iodine Transformation Reversible-Deactivation Radical Polymerization, *Polymers*, 2020, **12**, 1–10.
- 194 H. Li, H. Zhao, L. Yao, L. Zhang, Z. Cheng and X. Zhu, Photocontrolled Bromine–Iodine Transformation Reversible-Deactivation Radical Polymerization: Facile Synthesis of Star Copolymers and Unimolecular Micelles, *Polym. Chem.*, 2021, 1–11.
- 195 A. Burrows, J. Holman, A. Parsons, G. Pilling and G. Price, *Chemistry<sup>3</sup>: Introducing Inorganic, Organic and Physical Chemistry*, Oxford University Press, London, 2<sup>nd</sup> Edition, 2013.
- 196 T. Ando, M. Kamigaito and M. Sawamoto, Reversible Activation of Carbon–Halogen Bonds by  $\text{RuCl}_2(\text{PPh}_3)_3$ : Halogen Exchange Reactions in Living Radical Polymerization, *Macromolecules*, 2000, **33**, 2819–2824.
- 197 K. Adachi and Y. Tsukahara, in *Encyclopedia of Polymeric Nanomaterials*, Springer Berlin Heidelberg, 2015, 1167–1175.
- 198 G. Cankaya and N. Bicak, Zinc Powder-Alkyl Halide: A Radical Initiation System for Living/Controlled Polymerization of Vinyl Monomers, *Des. Monomers Polym.*, 2015, **18**, 27–34.
- 199 T. Furuncuoğlu, I. Uğur, I. Değirmenci and V. Aviyente, Role of Chain Transfer Agents in Free Radical Polymerization Kinetics, *Macromolecules*, 2010, **43**, 1823–1835.
- 200 B. C. Y. Whang, G. Lichti, R. G. Gilbert, D. H. Napper and D. F. Sangster, The Effects of a Chain Transfer Agent on the Kinetics of the Emulsion Polymerization of Styrene, *J. Polym. Sci. Polym. Lett. Ed.*, 1980, **18**, 711–716.
- 201 P. J. Flory, *Principles of Polymer Chemistry*, Cornell University Press, New York, 1953, H.J.Hutchins, PhD Thesis, Aston University, 2021.



143-144.

- 202 W. Scan McGivern, O. Sorkhabi, A. G. Suits, A. Derecskei-Kovacs and S. W. North, Primary and Secondary Processes in the Photodissociation of  $\text{CHBr}_3$ , *J. Phys. Chem. A*, 2000, **104**, 10085–10091.
- 203 T. Ying, J. Lei, T. Bi-Feng, Z. Rong-Shu, Z. Song and Z. Bing, Photodissociation of Alkyl Bromides at UV Scope, *Acta Physico-Chimica Sin.*, 2004, **20**, 344–349.
- 204 P. Zou, J. Shu, T. J. Sears, G. E. Hall and S. W. North, Photodissociation of Bromoform at 248 nm: Single and Multiphoton Processes, *J. Phys. Chem. A*, 2004, **108**, 1482–1488.
- 205 S. X. Yang, G. Y. Hou, J. H. Dai, C. H. Chang and B. C. Chang, Spectroscopic Investigation of the Multiphoton Photolysis Reactions of Bromomethanes ( $\text{CHBr}_3$ ,  $\text{CHBr}_2\text{Cl}$ ,  $\text{CHBrCl}_2$ , and  $\text{CH}_2\text{Br}_2$ ) at Near-Ultraviolet Wavelengths, *J. Phys. Chem. A*, 2010, **114**, 4785–4790.
- 206 K. D. Bayes, R. R. Friedl, S. P. Sander and D. W. Toohey, Measurements of Quantum Yields of Bromine Atoms in the Photolysis of Bromoform from 266 to 324 nm, *J. Geophys. Res. Atmos.*, 2003, **108**, 1–6.
- 207 M. L. Miller, Block and Graft Polymers: I. Graft Polymers from Acrylamide and Acrylonitrile, *Can. J. Chem.*, 1958, **36**, 303–308.
- 208 M. L. Miller, Block and Graft Polymers II. Block Polymers from Acrylamide and Acrylonitrile and Acrylamide and Acrylic Acid, *Can. J. Chem.*, 1958, **36**, 309–315.
- 209 A. S. Dunn, B. D. Stead and H. W. Melville, The Synthesis of Block Copolymers of Styrene and Methyl Methacrylate, *Trans. Faraday Soc.*, 1954, **50**, 279.
- 210 G. Odian, in *Principles of Polymerization*, John Wiley & Sons, New Jersey, 4th Edition, 2004, 619–728.

- 211 European Patent Office, 4540498, 1983, 1–5.
- 212 K. Thananukul, J. Porkaew, P. Punyamoonwongsa, R. Molloy and B. J. Tighe, Kinetic Studies of the Photopolymerisation of Acrylamide in Aqueous Solution: Effects of Bromoform as a Chain Transfer Agent, *Chiang Mai J. Sci.*, 2014, **41**, 1352–1360.
- 213 J. S. Wang and K. Matyjaszewski, Controlled/"Living" Radical Polymerization. Atom Transfer Radical Polymerization in the Presence of Transition-Metal Complexes, *J. Am. Chem. Soc.*, 1995, **117**, 5614–5615.
- 214 J. S. Wang and K. Matyjaszewski, Controlled/"Living" Radical Polymerization. Halogen Atom Transfer Radical Polymerization Promoted by a Cu(I)/Cu(II) Redox Process, *Macromolecules*, 1995, **28**, 7901–7910.
- 215 C. H. Wang, R. McNair and P. Levins, Generation of Free Radicals through Organic Oxidation—Reduction Systems, *J. Org. Chem.*, 1965, **30**, 3817–3819.
- 216 A. S. Sarac, Redox Polymerization, *Prog. Polym. Sci.*, 1999, **24**, 1149–1204.
- 217 J. Tonnar, P. Lacroix-Desmazes and B. Boutevin, Controlled Radical ab Initio Emulsion Polymerization of N-Butyl Acrylate by Reverse Iodine Transfer Polymerization (RITP): Effect of the Hydrolytic Disproportionation of Iodine, *Macromol. Rapid Commun.*, 2006, **27**, 1733–1738.
- 218 J. Krstina, C. L. Moad, G. Moad, E. Rizzardo, C. T. Berge and M. Fryd, A New Form of Controlled Growth Free Radical Polymerization, *Macromol. Symp.*, 1996, **111**, 13–23.
- 219 I. Chaduc, A. Crepet, O. Boyron, B. Charleux, F. D'Agosto and M. Lansalot, Effect of the pH on the RAFT Polymerization of Acrylic Acid in Water. Application to the Synthesis of Poly(acrylic acid)-Stabilized Polystyrene Particles by RAFT Emulsion Polymerization, *Macromolecules*, 2013, **46**, 6013–6023.
- 220 J. Zhou, H. Yao and R. He, Synthesis of Fluorinated Polyacrylate Surfactant-Free Core-Shell Latex by RAFT-Mediated Polymerization-Induced Self-Assembly: Effects of the H.J.Hutchins, PhD Thesis, Aston University, 2021.

- Concentration of Hexafluorobutyl Acrylate, *Adv. Polym. Technol.*, 2018, **37**, 3804–3812.
- 221 T. Cheikhalard, L. Tighzert and J. P. Pascault, Thermal Decomposition of some Azo Initiators: Influence of Chemical Structure, *Macromol. Mater. Eng.*, 1998, **256**, 49–59.
- 222 S. A. Seabrook and R. G. Gilbert, Photo-Initiated Polymerization of Acrylamide in Water, *Polymer*, 2007, **48**, 4733–4741.
- 223 K. Kishore and K. N. Santhanalakshmi, Thermal Polymerization of Acrylamide by Differential Scanning Calorimetry, *J. Polym. Sci. Polym. Chem. Ed.*, 1981, **19**, 2367–2375.
- 224 B. Hassen and R. Narain, Reversible Addition–Fragmentation Chain Transfer Polymerization of *N*-Isopropylacrylamide: A Comparison between a Conventional and a Fast Initiator, *J. Phys. Chem.*, 2007, **111**, 11120–11126.
- 225 P. Datta, K. Efimenko and J. Genzer, Thermally Driven Directional Free-Radical Polymerization in Confined Channels, *Polym. Chem.*, 2019, **10**, 920–925.
- 226 C. Erbil, C. Cin, A. B. Soydan and A. S. Sarac, Polyaminocarboxylic Acids-Ce ( IV) Redox Systems as an Initiator in Acrylamide Polymerization, *J. Appl. Polym. Sci.*, 1993, **47**, 1643–1648.
- 227 F. Martellini, L. H. I. Mei, J. L. Baliño and M. Carenza, Water and Drug Transport in Radiation-Crosslinked Poly(2-methoxyethylacrylate-co-dimethyl acrylamide) and Poly(2-methoxyethylacrylate-co-acrylamide) Hydrogels, *Radiat. Phys. Chem.*, 2003, **66**, 155–159.
- 228 S. B. Patil, S. Z. Inamdar, K. R. Reddy, A. V. Raghu, S. K. Soni and R. V. Kulkarni, Novel Biocompatible Poly(acrylamide)-grafted-dextran Hydrogels: Synthesis, Characterization and Biomedical Applications, *J. Microbiol. Methods*, 2019, **159**, 200–210.

- 229 Z. Bai, W. Dan, G. Yu, Y. Wang, Y. Chen, Y. Huang, C. Yang and N. Dan, Tough and Tissue-Adhesive Polyacrylamide/Collagen Hydrogel with Dopamine-Grafted Oxidized Sodium Alginate as Crosslinker for Cutaneous Wound Healing, *RSC Adv.*, 2018, **8**, 42123–42132.
- 230 A. Arora, *Aromatic Organic Chemistry*, Discovery Publishing House, New Delhi, 2006, 75.
- 231 R. J. LaPorte, in *Hydrophilic Polymer Coatings for Medical Devices*, CRC Press, New York, 1997, 199.
- 232 E. Patyukova, T. Rottreau, R. Evans, P. D. Topham and M. J. Greenall, Hydrogen Bonding Aggregation in Acrylamide: Theory and Experiment, *Macromolecules*, 2018, **51**, 7032–7043.
- 233 E. Caló and V. V. Khutoryanskiy, Biomedical Applications of Hydrogels: A Review of Patents and Commercial Products, *Eur. Polym. J.*, 2015, **65**, 252–267.
- 234 J. Schrooten, I. Lacík, M. Stach, P. Hesse and M. Buback, Propagation Kinetics of the Radical Polymerization of Methylated Acrylamides in Aqueous Solution, *Macromol. Chem. Phys.*, 2013, **214**, 2283–2294.
- 235 I. Lacík, A. Chovancová, L. Uhelská, C. Preusser, R. A. Hutchinson and M. Buback, PLP-SEC Studies into the Propagation Rate Coefficient of Acrylamide Radical Polymerization in Aqueous Solution, *Macromolecules*, 2016, **49**, 3244–3253.
- 236 F. S. Dainton and M. Tordoff, The Polymerization of Acrylamide in Aqueous Solution: Part 3. - The Hydrogen Peroxide Photosensitized Reaction at 25°C, *Trans. Faraday Soc.*, 1957, **53**, 499–511.
- 237 S. Zhou, S. Fan, S. C. F. Au-Yeung and C. Wu, Light-Scattering Studies of Poly(*N*-isopropylacrylamide) in Tetrahydrofuran and Aqueous Solution, *Polymer*, 1995, **36**, 1341–1346.

- 238 G. Conzatti, S. Cavalie, C. Combes, J. Torrisani, N. Carrere and A. Tourrette, PNIPAM Grafted Surfaces through ATRP and RAFT Polymerization: Chemistry and Bioadhesion, *Colloids Surfaces B Biointerfaces*, 2017, **151**, 143–155.
- 239 X. Lu, L. Zhang, L. Meng and Y. Liu, Synthesis of Poly(*N*-isopropylacrylamide) by ATRP using a Fluorescein-Based Initiator, *Polym. Bull.*, 2007, **59**, 195–206.
- 240 T. Schulte, K. O. Siegenthaler, H. Luftmann, M. Letzel and A. Studer, Nitroxide-Mediated Polymerization of *N*-isopropylacrylamide: Electrospray Ionization Mass Spectrometry, Matrix-Assisted Laser Desorption Ionization Mass Spectrometry, and Multiple-Angle Laser Light Scattering studies on Nitroxide-Terminated Poly-*N*-isopropyl, *Macromolecules*, 2005, **38**, 6833–6840.
- 241 W. H. Binder, D. Gloger, H. Weinstabl, G. Allmaier and E. Pittenauer, Telechelic Poly(*N*-isopropylacrylamides) via Nitroxide-Mediated Controlled Polymerization and “Click” Chemistry: Livingness and “Grafting-from” Methodology, *Macromolecules*, 2007, **40**, 3097–3107.
- 242 X. Wang, S. Li, Y. Su, F. Huo and W. Zhang, Aqueous RAFT Polymerization of *N*-Isopropylacrylamide-Mediated with Hydrophilic Macro-RAFT Agent: Homogeneous or Heterogeneous Polymerization?, *J. Polym. Sci. Part A Polym. Chem.*, 2013, **51**, 2188–2198.
- 243 J. Park, H. Kim, K. C. Da Silveira, Q. Sheng, A. Postma, C. D. Wood and Y. Seo, Experimental Evaluation of RAFT-Based Poly(*N*-isopropylacrylamide) (PNIPAM) Kinetic Hydrate Inhibitors, *Fuel*, 2019, **235**, 1266–1274.
- 244 L. Wang, Y. Li, L. Chen, C. Ban, G. Li and J. Ni, Fabrication of Honeycomb-Patterned Porous Films from PS-*b*-PNIPAM Amphiphilic Diblock Copolymers Synthesized via RITP, *J. Colloid Interface Sci.*, 2014, **420**, 112–118.
- 245 J. Chen, M. Liu, H. Gong, Y. Huang and C. Chen, Synthesis and Self-Assembly of

- Thermoresponsive PEG-b-PNIPAM-b-PCL ABC Triblock Copolymer through the Combination of Atom Transfer Radical Polymerization, Ring-Opening Polymerization, and Click Chemistry, *J. Phys. Chem. B*, 2011, **115**, 14947–14955.
- 246 L. Ahmadkhani, M. Abbasian and A. Akbarzadeh, Synthesis of Sharply Thermo and pH Responsive PMA-b-PNIPAM-b-PEG-b-PNIPAM-b-PMA by RAFT Radical Polymerization and its Schizophrenic Micellization in Aqueous Solutions, *Des. Monomers Polym.*, 2017, **20**, 406–418.
- 247 H. Chen, J. Li, Y. Ding, G. Zhang, Q. Zhang and C. Wu, Folding and Unfolding of Individual PNIPAM-g-PEO Copolymer Chains in Dilute Aqueous Solutions, *Macromolecules*, 2005, **38**, 4403–4408.
- 248 P. Chmielarz, P. Kryszewski, S. Park and K. Matyjaszewski, PEO-b-PNIPAM Copolymers via SARA ATRP and eATRP in Aqueous Media, *Polymer*, 2015, **71**, 143–147.
- 249 Y. Z. You, Q. H. Zhou, D. S. Manickam, L. Wan, G. Z. Mao and D. Oupický, Dually Responsive Multiblock Copolymers via Reversible Addition–Fragmentation Chain Transfer Polymerization: Synthesis of Temperature- and Redox-Responsive Copolymers of Poly(*N*-isopropylacrylamide) and Poly(2-(dimethylamino)ethyl methacrylate), *Macromolecules*, 2007, **40**, 8617–8624.
- 250 X. X. Ke, L. Wang, J. T. Xu, B. Y. Du, Y. F. Tu and Z. Q. Fan, Effect of Local Chain Deformability on the Temperature-Induced Morphological Transitions of Polystyrene-*b*-poly(*N*-isopropylacrylamide) Micelles in Aqueous Solution, *Soft Matter*, 2014, **10**, 5201–5211.
- 251 M. Heskins and J. E. Guillet, Solution Properties of Poly(*N*-isopropylacrylamide), *J. Macromol. Sci. Part A - Chem.*, 1968, **2**, 1441–1455.
- 252 M. A. Ward and T. K. Georgiou, Thermoresponsive Polymers for Biomedical Applications, *Polymer*, 2011, **3**, 1215–1242.

- 253 A. S. Hoffman, Stimuli-Responsive Polymers: Biomedical Applications and Challenges for Clinical Translation, *Adv. Drug Deliv. Rev.*, 2013, **65**, 10–16.
- 254 W. Leobandung, H. Ichikawa, Y. Fukumori and N. A. Peppas, Monodisperse Nanoparticles of Poly(ethylene glycol) Macromers and *N*-Isopropyl Acrylamide for Biomedical Applications, *J. Appl. Polym. Sci.*, 2003, **87**, 1678–1684.
- 255 I. Bischofberger, D. C. E. Calzolari, P. De Los Rios, I. Jelezarov and V. Trappe, Hydrophobic Hydration of Poly-*N*-isopropyl acrylamide: A Matter of the Mean Energetic State of Water, *Sci. Rep.*, 2014, **4**, 1–7.
- 256 F. H. Stillinger, Water Revisited, *Science*, 1980, **209**, 451–457.
- 257 T. M. Raschke and M. Levitt, Nonpolar Solutes Enhance Water Structure within Hydration Shells while Reducing Interactions Between them, *Proc. Natl. Acad. Sci. U. S. A.*, 2005, **102**, 6777–6782.
- 258 B. Widom, P. Bhimalapuram and K. Koga, The Hydrophobic Effect, *Phys. Chem. Chem. Phys.*, 2003, **5**, 3085–3093.
- 259 F. Candau and J. Selb, Hydrophobically-Modified Polyacrylamides Prepared by Micellar Polymerization, *Adv. Colloid Interface Sci.*, 1999, **79**, 149–172.
- 260 P. A. Lovell and F. J. Schork, Fundamentals of Emulsion Polymerization, *Biomacromolecules*, 2020, **21**, 4396–4441.
- 261 C. S. Chern, Emulsion Polymerization Mechanisms and Kinetics, *Prog. Polym. Sci.*, 2006, **31**, 443–486.
- 262 S. W. Prescott, M. J. Ballard, E. Rizzardo and R. G. Gilbert, RAFT in Emulsion Polymerization: What Makes it Different?, *Aust. J. Chem.*, 2002, **55**, 415–424.
- 263 D. Neugebauer, Atom Transfer Radical Copolymerization of *N,N'*-Dimethylacrylamide with Methacrylate-Functionalized Poly(ethylene oxide), *React. Funct. Polym.*, 2008, **68**,

535–543.

- 264 L. Yan and T. Wei, Graft Copolymerization of *N,N*-Dimethylacrylamide to Cellulose in Homogeneous Media Using Atom Transfer Radical Polymerization for Hemocompatibility, *J. Biomed. Sci. Eng.*, 2008, **1**, 37–43.
- 265 K. Schierholz, M. Givéchi, P. Fabre, F. Nallet, E. Papon, O. Guerret and Y. Gnanou, Acrylamide-Based Amphiphilic Block Copolymers via Nitroxide-Mediated Radical Polymerization, *Macromolecules*, 2003, **36**, 5995–5999.
- 266 T. Kitayama and K. I. Katsukawa, Living Anionic Polymerization of *N,N*-Dimethylacrylamide and Copolymerization with Methyl Methacrylate in the presence of Bulky Aluminum Phenoxide, *Polym. Bull.*, 2004, **52**, 117–124.
- 267 K. Inui, H. Okumura, T. Miyata and T. Uragami, Characteristics of Permeation and Separation of Dimethyl acrylamide-methyl methacrylate Random and Graft Copolymer Membranes for a Benzene/Cyclohexane Mixture, *Polym. Bull.*, 1997, **39**, 733–740.
- 268 C. Fang, Y. Jing, Y. Zong and Z. Lin, Effect of *N,N*-Dimethylacrylamide (DMA) on the Comprehensive Properties of Acrylic Latex Pressure Sensitive Adhesives, *Int. J. Adhes. Adhes.*, 2016, **71**, 105–111.
- 269 B. I. Nakhmanovich, T. N. Prudskova, A. A. Arest-Yakubovich and A. H. E. Muller, Copolymerization of *N,N*-Dimethylacrylamide with Styrene and Butadiene: The First Example of Polar Growing Chain End/Nonpolar Monomer Cross-Initiation, *Macromol. Rapid Commun.*, 2001, **22**, 1243–1248.
- 270 A. Y. Sung and T. H. Kim, Optical Application of Poly(HEMA-co-MMA) Containing Silver Nanoparticles and *N,N*-Dimethylacrylamide, *Korean J. Chem. Eng.*, 2012, **29**, 686–691.
- 271 V. Bekiari, M. Sotiropoulou, G. Bokias and P. Lianos, Use of Poly(*N,N*-dimethylacrylamide-co-sodium acrylate) Hydrogel to Extract Cationic Dyes and Metals from Water, *Colloids Surfaces A Physicochem. Eng. Asp.*, 2008, **312**, 214–218.



- 272 F. Wang, X. Yong, J. Deng and Y. Wu, Poly(*N,N*-dimethylacrylamide-octadecyl acrylate)-Clay Hydrogels with High Mechanical Properties and Shape Memory Ability, *RSC Adv.*, 2018, **8**, 16773–16780.
- 273 A. Valdebenito and M. V. Encinas, Effect of Solvent on the Free Radical Polymerization of *N,N*-dimethylacrylamide, *Polym. Int.*, 2010, **59**, 1246–1251.
- 274 G. Sun, Y. Huang, D. Li, E. Chen, Y. Zhong, Q. Fan and J. Shao, Blue Light Initiated Photopolymerization: Kinetics and Synthesis of Superabsorbent and Robust Poly(*N, N'*-dimethylacrylamide/sodium acrylate) Hydrogels, *Ind. Eng. Chem. Res.*, 2019, **58**, 9266–9275.
- 275 Y. Nakayama, T. Matsuda and M. Irie, A Novel Surface Photo-Graft Polymerization Method for Fabricated Devices, *Am. Soc. Artif. Intern. Organs*, 1993, **39**, 542–544.
- 276 A. Rudin, in *The Elements of Polymer Science & Engineering*, Academic Press, London, 2<sup>nd</sup> Edition, 1999, 241–276.
- 277 C. P. Easterling, Y. Xia, J. Zhao, G. E. Fanucci and B. S. Sumerlin, Block Copolymer Sequence Inversion through Photoiniferter Polymerization, *ACS Macro Lett.*, 2019, **8**, 1461–1466.
- 278 F. R. Mayo and F. M. Lewis, Copolymerization. I. A Basis for Comparing the Behavior of Monomers in Copolymerization: The Copolymerization of Styrene and Methyl Methacrylate, *J. Am. Chem. Soc.*, 1944, **66**, 1594–1601.
- 279 A. J. Convertine, B. S. Lokitz, Y. Vasileva, L. J. Myrick, C. W. Scales, A. B. Lowe and C. L. McCormick, Direct Synthesis of Thermally Responsive DMA/NIPAM Diblock and DMA/NIPAM/DMA Triblock Copolymers via Aqueous, Room Temperature RAFT Polymerization, *Macromolecules*, 2006, **39**, 1724–1730.
- 280 A. Van Herk, in *Synthesis and Applications of Copolymers*, Editor: A. Parthiban, John Wiley & Sons, New Jersey, 1<sup>st</sup> Edition, 2014, 54–66.

- 281 K. Bauri, S. G. Roy, S. Arora, R. K. Dey, A. Goswami, G. Madras and P. De, Thermal Degradation Kinetics of Thermoresponsive Poly(*N*-isopropylacrylamide-*co*-*N,N*-dimethylacrylamide) Copolymers Prepared via RAFT Polymerization, *J. Therm. Anal. Calorim.*, 2013, **111**, 753–761.
- 282 K. F. O'Driscoll, T. P. Davis, B. Klumperman and E. L. Madruga, Solvent Effects in Copolymerization, *Macromol. Rapid Commun.*, 1995, **16**, 207–210.
- 283 A. M. Chatterjee and C. M. Burns, Solvent Effects in Free Radical Copolymerization, *Can. J. Chem.*, 1971, **49**, 3251.
- 284 M. Rubens, P. Latsrisaeng and T. Junkers, Visible Light-Induced Iniferter Polymerization of Methacrylates Enhanced by Continuous Flow, *Polym. Chem.*, 2017, **8**, 6496–6505.
- 285 T. G. McKenzie, Q. Fu, E. H. H. Wong, D. E. Dunstan and G. G. Qiao, Visible Light Mediated Controlled Radical Polymerization in the Absence of Exogenous Radical Sources or Catalysts, *Macromolecules*, 2015, **48**, 3864–3872.
- 286 T. Otsu, Iniferter Concept and Living Radical Polymerization, *J. Polym. Sci. Part A*, 2000, **38**, 2121–2136.
- 287 J. F. Quinn, L. Barner, C. Barner-Kowollik, E. Rizzardo and T. P. Davis, Reversible Addition–Fragmentation Chain Transfer Polymerization Initiated with Ultraviolet Radiation, *Macromolecules*, 2002, **35**, 7620–7627.
- 288 R. N. Carmean, C. A. Figg, T. E. Becker and B. S. Sumerlin, Closed-System One-Pot Block Copolymerization by Temperature-Modulated Monomer Segregation, *Angew. Chemie Int. Ed.*, 2016, **55**, 8624–8629.
- 289 H. E. Gottlieb, V. Kotlyar and A. Nudelman, NMR Chemical Shifts of Common Laboratory Solvents as Trace Impurities, *J. Org. Chem.*, 1997, **62**, 7512–7515.
- 290 Special fluorescent lamps CLEO Compact, <http://www.twlp.com.tw/pdf/17582.pdf>, H.J.Hutchins, PhD Thesis, Aston University, 2021.

(accessed 27 May 2021).

- 291 T. A. McMurray, J. A. Byrne, P. S. M. Dunlop and E. T. McAdams, Photocatalytic and Electrochemically Assisted Photocatalytic Oxidation of Formic Acid on TiO<sub>2</sub> Films Under UVA and UVB Irradiation, *J. Appl. Electrochem.*, 2005, **35**, 723–731.
- 292 C. G. Overberger and D. A. Labianca, Azo Compounds. Investigation of Optically Active Azonitriles, *J. Org. Chem.*, 1970, **35**, 1762–1770.
- 293 Y. Zhou, Z. Zhang, A. Postma and G. Moad, Kinetics and Mechanism for Thermal and Photochemical Decomposition of 4,4'-Azobis(4-cyanopentanoic acid) in Aqueous Media, *Polym. Chem.*, 2019, **10**, 3284–3287.
- 294 K. Matyjaszewski, in *Controlled/Living Radical Polymerization*, Oxford University Press, Washington, 2000, 2–26.
- 295 Marianne Gilbert, *Brydson's Plastic Materials*, Elsevier, London, 8<sup>th</sup> Edition, 2017, 1-32.
- 296 P. L. Silveston and R. R. Hudgins, *Periodic Operation of Chemical Reactors*, Butterworth-Heinemann, London, 2012.
- 297 T. N. T. Phan, S. Maiez-Tribut, J. P. Pascault, A. Bonnet, P. Gerard, O. Guerret and D. Bertin, Synthesis and Characterizations of Block Copolymer of Poly(n-butyl acrylate) and Gradient Poly(methyl methacrylate-co-N,N-dimethyl acrylamide) made via Nitroxide-Mediated Controlled Radical Polymerization, *Macromolecules*, 2007, **40**, 4516–4523.
- 298 K. Haraguchi, R. Farnworth, A. Ohbayashi and T. Takehisa, Compositional Effects on Mechanical Properties of Nanocomposite Hydrogels Composed of Poly(N,N-dimethylacrylamide) and Clay, *Macromolecules*, 2003, **36**, 5732–5741.
- 299 E. Meaurio, J. L. Velada, L. C. Cesteros and I. Katime, Blends and Complexes of Poly(monomethyl itaconate) with Polybases Poly(N,N-dimethylacrylamide) and Poly(ethyloxazoline). Association and Thermal Behavior, *Macromolecules*, 1996, **29**, 239.
- H.J.Hutchins, PhD Thesis, Aston University, 2021.

4598–4604.

- 300 M. E. S. Ribeiro E Silva, J. C. Machado, V. Mano and G. G. Silva, Positron Annihilation and Differential Scanning Calorimetry Studies of Polyacrylamide and Poly(dimethylacrylamide)/Poly(ethylene glycol) Blends, *J. Polym. Sci. Part B Polym. Phys.*, 2003, **41**, 1493–1500.
- 301 Y. Mohajer, G. L. Wilkes and J. E. McGrath, Influence of Tacticity and Sorbed Water on the Material Properties of Poly(N,N'-dimethylacrylamide), *J. Appl. Polym. Sci.*, 1981, **26**, 2827–2839.
- 302 S. Bennour and F. Louzri, Study of Swelling Properties and Thermal Behavior of Poly(N,N-dimethylacrylamide-co-maleic acid) Based Hydrogels, *Adv. Chem.*, 2014, 1–10.
- 303 S. Beuermann, Solvent Influence on Propagation Kinetics in Radical Polymerizations Studied by Pulsed Laser Initiated Polymerizations, *Macromol. Rapid Commun.*, 2009, **30**, 1066–1088.
- 304 Y. Katsumoto, T. Tanaka, H. Sato and Y. Ozaki, Conformational Change of Poly(N-isopropylacrylamide) during the Coil–Globule Transition Investigated by Attenuated Total Reflection/Infrared Spectroscopy and Density Functional Theory Calculation, *J. Phys. Chem. A*, 2002, **106**, 3429–3435.
- 305 Y. Katsumoto, T. Tanaka, K. Ihara, M. Koyama and Y. Ozaki, Contribution of Intramolecular CO···H–N Hydrogen Bonding to the Solvent-Induced Reentrant Phase Separation of Poly(N-isopropylacrylamide), *J. Phys. Chem. B*, 2007, **111**, 12730–12737.
- 306 M. J. Deetz, J. E. Fahey and B. D. Smith, NMR Studies of Hydrogen Bonding Interactions with Secondary Amide and Urea Groups, *J. Phys. Org. Chem.*, 2001, **14**, 463–467.

- 307 G. Eaton, M. C. R. Symons and P. P. Rastogi, Spectroscopic Studies of the Solvation of Amides with N-H Groups. Part 1. - The Carbonyl Group, *J. Chem. Soc. Faraday Trans. 1 Phys. Chem. Condens. Phases*, 1989, **85**, 3257–3271.
- 308 B. De Sterck, R. Vaneerdeweg, F. Du Prez, M. Waroquier and V. Van Speybroeck, Solvent Effects on Free Radical Polymerization Reactions: The Influence of Water on the Propagation Rate of Acrylamide and Methacrylamide, *Macromolecules*, 2010, **43**, 827–836.
- 309 G. Saini, A. Leoni and S. Franco, Solvent Effects in Radical Copolymerization. I. Acrylamide, *Die Makromol. Chemie*, 1971, **144**, 235–244.
- 310 S. Beuermann and N. García, A Novel Approach to the Understanding of the Solvent Effects in Radical Polymerization Propagation Kinetics, *Macromolecules*, 2004, **37**, 3018–3025.
- 311 C. Henríquez, C. Bueno, E. A. Lissi and M. V. Encinas, Thiols as Chain Transfer Agents in Free Radical Polymerization in Aqueous Solution, *Polymer*, 2003, **44**, 5559–5561.
- 312 A. Ghosh and M. H. George, Comparative Rates of Radical Autoxidation of Acrylamide, Methacrylamide and Styrene, *Polymer*, 1978, **19**, 1057–1062.
- 313 J. Xu, K. Jung and C. Boyer, Oxygen Tolerance Study of Photoinduced Electron Transfer-Reversible Addition-Fragmentation Chain Transfer (PET-RAFT) Polymerization Mediated by Ru(bpy)<sub>3</sub>Cl<sub>2</sub>, *Macromolecules*, 2014, **47**, 4217–4229.
- 314 J. Yeow, R. Chapman, A. J. Gormley and C. Boyer, *Chem. Soc. Rev.*, 2018, **47**, 4357–4387.
- 315 S. K. Ghosh, M. Nazimuddin and B. M. Mandal, Water-soluble Triplet Radical Generators as Photoinitiators in Inverse Emulsion Polymerization of Acrylamide, *Die Makromol. Chemie, Rapid Commun.*, 1992, **13**, 583–586.
- 316 B. Husár, S. C. Ligon, H. Wutzel, H. Hoffmann and R. Liska, The Formulator's Guide to H.J.Hutchins, PhD Thesis, Aston University, 2021.

Anti-Oxygen Inhibition Additives, *Prog. Org. Coatings*, 2014, **77**, 1789–1798.

- 317 W. S. McGivern, J. S. Francisco and S. W. North, Investigation of the Atmospheric Oxidation Pathways of Bromoform: Initiation via OH/Cl Reactions, *J. Phys. Chem. A*, 2002, **106**, 6395–6400.
- 318 H. S. Lal, Manohar, Mahal, Free Radical Reactions of Bromoform (BF) in Air Free and Air Saturated Aqueous Solutions. Effect of pH, *Int. J. Radiat. Appl. Instrumentation. Part C. Radiat. Phys. Chem.*, 1988, **32**, 599–603.
- 319 M. H. George and A. Ghosh, Effect of Oxygen on the Radical Polymerization of Acrylamide in Ethanol and Water, *J. Polym. Sci. Polym. Chem. Ed.*, 1978, **16**, 981–995.
- 320 D. Greszta, D. Mardare and K. Matyjaszewski, “Living” Radical Polymerization. 1. Possibilities and Limitations, *Macromolecules*, 1994, **27**, 638–644.
- 321 C. György, S. J. Hunter, C. Girou, M. J. Derry and S. P. Armes, Synthesis of Poly(stearyl methacrylate)-poly(2-hydroxypropyl methacrylate) Diblock Copolymer Nanoparticles: Via RAFT Dispersion Polymerization of 2-Hydroxypropyl methacrylate in Mineral Oil, *Polym. Chem.*, 2020, **11**, 4579–4590.
- 322 E. J. Cornel, S. Van Meurs, T. Smith, P. S. O’Hora and S. P. Armes, *In situ* Spectroscopic Studies of Highly Transparent Nanoparticle Dispersions Enable Assessment of Trithiocarbonate Chain-End Fidelity during RAFT Dispersion Polymerization in Nonpolar Media, *J. Am. Chem. Soc.*, 2018, **140**, 12980–12988.
- 323 M. Semsarilar, E. R. Jones and S. P. Armes, Comparison of Pseudo-Living Character of RAFT Polymerizations Conducted under Homogeneous and Heterogeneous Conditions, *Polym. Chem.*, 2014, **5**, 195–203.
- 324 G. C. Huang and S. X. Ji, Effect of Halogen Chain End Fidelity on the Synthesis of Poly(methyl methacrylate-*b*-styrene) by ATRP, *Chinese J. Polym. Sci. (English Ed.)*, 2018, **36**, 1217–1224.

- 325 M. Rodlert, E. Harth, I. Rees and C. J. Hawker, End-Group Fidelity in Nitroxide-Mediated Living Free-Radical Polymerizations, *J Polym Sci A Polym Chem*, 2000, **38**, 4749–4763.
- 326 C. S. Biswas, V. K. Patel, N. K. Vishwakarma, V. K. Tiwari, B. Maiti, P. Maiti, M. Kamigaito, Y. Okamoto and B. Ray, Effects of Tacticity and Molecular Weight of Poly(*N*-isopropylacrylamide) on its Glass Transition Temperature, *Macromolecules*, 2011, **44**, 5822–5824.
- 327 R. G. Sousa, W. F. Magalhães and R. F. S. Freitas, Glass Transition and Thermal Stability of Poly(*N*-isopropylacrylamide) Gels and some of their Copolymers with Acrylamide, *Polym. Degrad. Stab.*, 1998, **61**, 275–281.
- 328 W. Yin, H. Yang and R. Cheng, Glass transition of the Two Distinct Single-Chain Particles of Poly(*N*-isopropylacrylamide), *Eur. Phys. J. E*, 2005, **17**, 1–5.
- 329 M. Teresa Garay, M. Cristina Llamas and E. Iglesias, Study of Polymer-Polymer Complexes and Blends of Poly(*N*-isopropylacrylamide) with Poly(carboxylic acid): 1. Poly(acrylic acid) and Poly(methacrylic acid), *Polymer*, 1997, **38**, 5091–5096.
- 330 S. Fujishige, K. Kubota and I. Ando, Phase Transition of Aqueous Solutions of Poly(*N*-isopropylacrylamide) and Poly(*N*-isopropylmethacrylamide), *J. Phys. Chem.*, 1989, **93**, 3311–3313.
- 331 M. Podewitz, Y. Wang, P. K. Quoika, J. R. Loeffler, M. Schauperl and K. R. Liedl, Coil-Globule Transition Thermodynamics of Poly(*N*-isopropylacrylamide), *J. Phys. Chem. B*, 2019, **123**, 8838–8847.
- 332 K. Shiraga, H. Naito, T. Suzuki, N. Kondo and Y. Ogawa, Hydration and Hydrogen Bond Network of Water during the Coil-to-Globule Transition in Poly(*N*-isopropylacrylamide) Aqueous Solution at Cloud Point Temperature, *J. Phys. Chem. B*, 2015, **119**, 5576–5587.

- 333 I. Juurinen, S. Galambosi, A. G. Anghelescu-Hakala, J. Koskelo, V. Honkimäki, K. Hämäläinen, S. Huotari and M. Hakala, Molecular-Level Changes of Aqueous Poly(*N*-isopropylacrylamide) in Phase Transition, *J. Phys. Chem. B*, 2014, **118**, 5518–5523.
- 334 S. A. Deshmukh, S. K. R. S. Sankaranarayanan and D. C. Mancini, Vibrational Spectra of Proximal Water in a Thermo-Sensitive Polymer Undergoing Conformational Transition Across the Lower Critical Solution Temperature, *J. Phys. Chem. B*, 2012, **116**, 5501–5515.
- 335 L. Tavagnacco, E. Zaccarelli and E. Chiessi, On the Molecular Origin of the Cooperative Coil-to-Globule Transition of Poly(*N*-isopropylacrylamide) in Water, *Phys. Chem. Chem. Phys.*, 2018, **20**, 9997–10010.
- 336 S. Moelbert and P. De Los Rios, Hydrophobic Interaction Model for Upper and Lower Critical Solution Temperatures, *Macromolecules*, 2003, **36**, 5845–5853.
- 337 D. Paschek, Heat Capacity Effects Associated with the Hydrophobic Hydration and Interaction of Simple Solutes: A Detailed Structural and Energetical Analysis based on Molecular Dynamics Simulations, *J. Chem. Phys.*, 2004, **120**, 10605–10617.
- 338 K. A. T. Silverstein, A. D. J. Haymet and K. A. Dill, The Strength of Hydrogen Bonds in Liquid Water and Around Nonpolar Solutes, *J. Am. Chem. Soc.*, 2000, **122**, 8037–8041.
- 339 Z. Ahmed, E. A. Gooding, K. V. Pimenov, L. Wang and S. A. Asher, UV Resonance Raman Determination of Molecular Mechanism of Poly(*n*-isopropylacrylamide) Volume Phase Transition, *J. Phys. Chem. B*, 2009, **113**, 4248–4256.
- 340 S. A. Deshmukh, S. K. R. S. Sankaranarayanan, K. Suthar and D. C. Mancini, Role of Solvation Dynamics and Local Ordering of Water in Inducing Conformational Transitions in Poly(*N*-isopropylacrylamide) Oligomers through the LCST, *J. Phys. Chem. B*, 2012, **116**, 2651–2663.
- 341 L. J. Abbott, A. K. Tucker and M. J. Stevens, Single Chain Structure of a Poly(*N*-

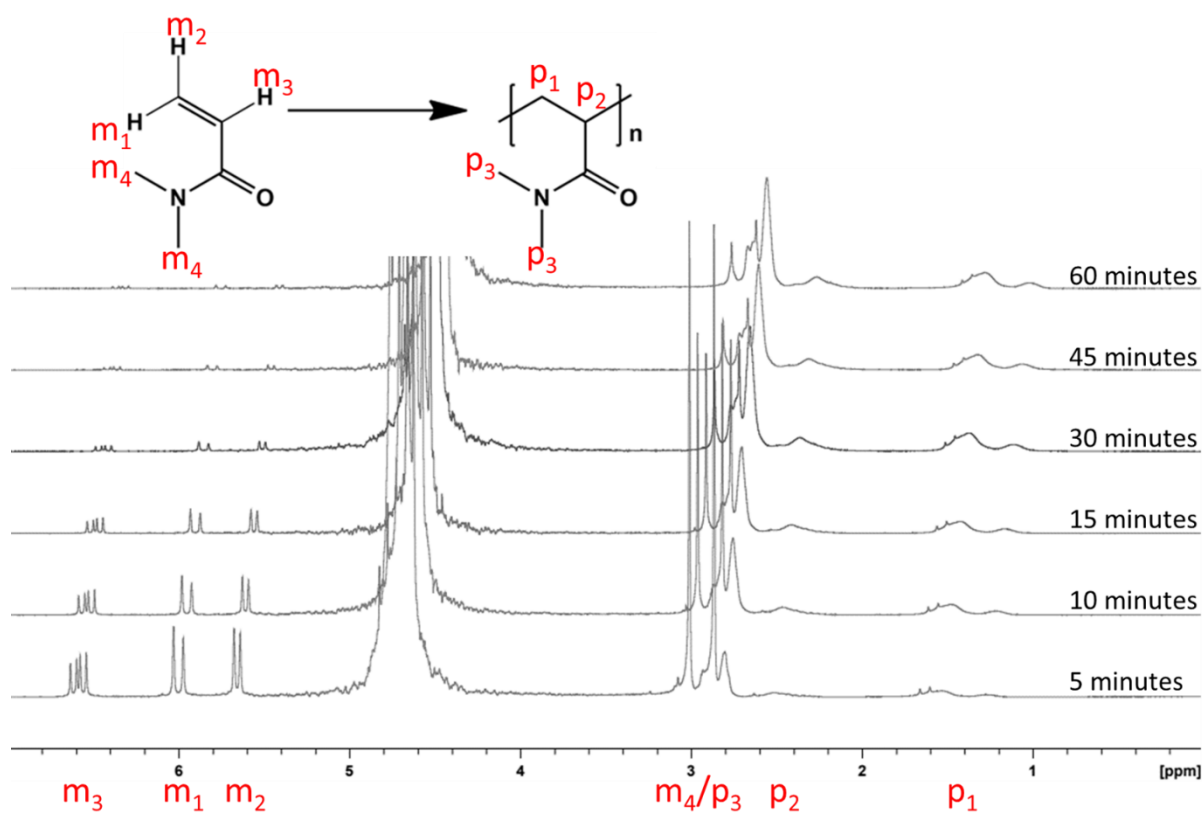


- isopropylacrylamide) Surfactant in Water, *J. Phys. Chem. B*, 2015, **119**, 3837–3845.
- 342 M. H. Futscher, M. Philipp, P. Müller-Buschbaum and A. Schulte, The Role of Backbone Hydration of Poly(*N*-isopropyl acrylamide) Across the Volume Phase Transition Compared to its Monomer, *Sci. Rep.*, 2017, **7**, 1–10.
- 343 G. Kamath, S. A. Deshmukh, G. A. Baker, D. C. Mancini and S. K. R. S. Sankaranarayanan, Thermodynamic Considerations for Solubility and Conformational Transitions of Poly-*N*-isopropyl-acrylamide, *Phys. Chem. Chem. Phys.*, 2013, **15**, 12667–12673.
- 344 R. Plummer, D. J. T. Hill and A. K. Whittaker, Solution Properties of Star and Linear Poly(*N*-isopropylacrylamide), *Macromolecules*, 2006, **39**, 8379–8388.
- 345 S. I. Yusa, Y. Shimada, Y. Mitsukami, T. Yamamoto and Y. Morishima, Heat-Induced Association and Dissociation Behavior of Amphiphilic Diblock Copolymers Synthesized via Reversible Addition-Fragmentation Chain Transfer Radical Polymerization, *Macromolecules*, 2004, **37**, 7507–7513.
- 346 A. Gandhi, A. Paul, S. O. Sen and K. K. Sen, Studies on Thermoresponsive Polymers: Phase Behaviour, Drug Delivery and Biomedical Applications, *Asian J. Pharm. Sci.*, 2015, **10**, 99–107.
- 347 R. J. Angelo, R. M. Ikeda and M. L. Wallach, Multiple Glass Transitions of Block Polymers, *Polymer*, 1965, **6**, 141–156.
- 348 W. W. Wang, L. Jiang, W. Y. Ren, C. M. Zhang, C. Z. Man, T. P. Nguyen and Y. Dan, The Crystallinity, Thermal Properties and Microscopic Morphology of Di-block Copolymers of L-lactide and Several Acrylates, *RSC Adv.*, 2016, **6**, 31934–31946.
- 349 C. M. Schilli, M. Zhang, E. Rizzardo, S. H. Thang, Y. K. Chong, K. Edwards, G. Karlsson and A. H. E. Müller, A New Double-Responsive Block Copolymer Synthesized via RAFT Polymerization: Poly(*N*-isopropylacrylamide)-block-poly(acrylic acid), *Macromolecules*,

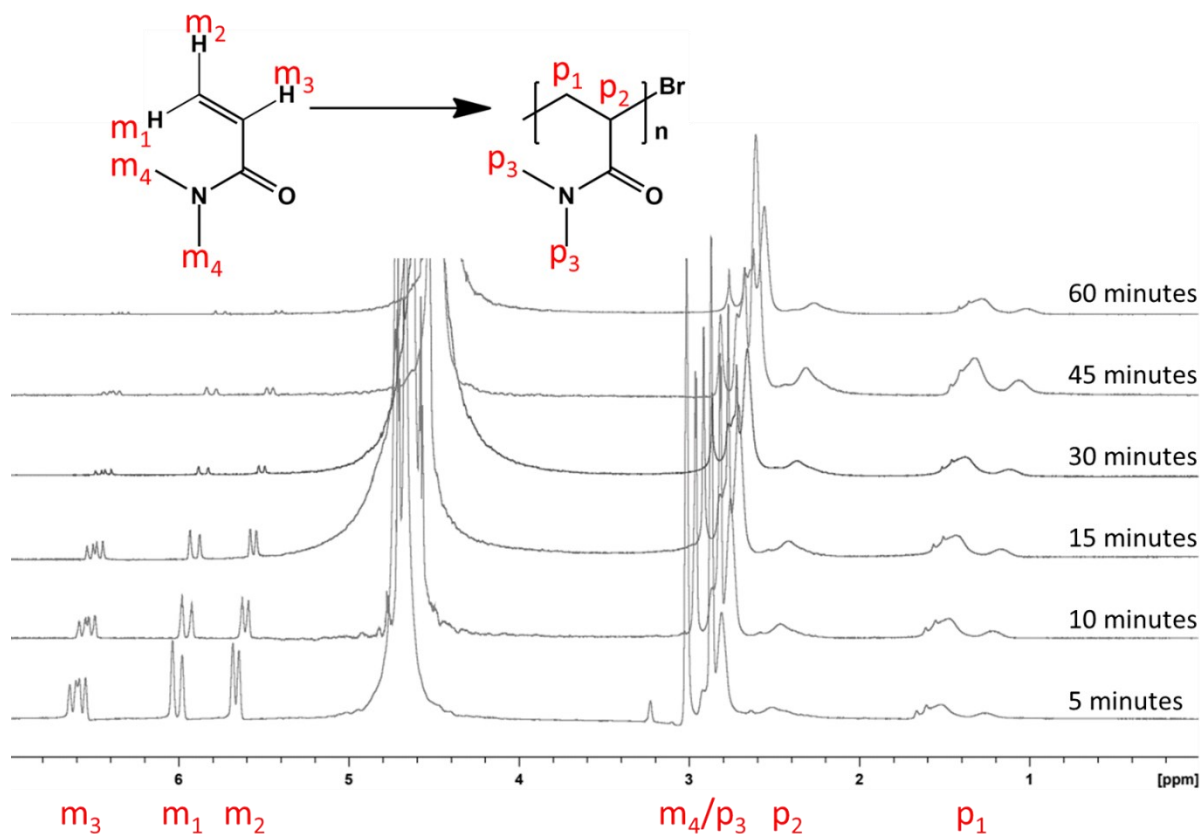
- 2004, **37**, 7861–7866.
- 350 J. Virtanen, S. Holappa, H. Lemmetyinen and H. Tenhu, Aggregation in Aqueous Poly(*N*-isopropylacrylamide)-block-poly(ethylene oxide) Solutions Studied by Fluorescence Spectroscopy and Light Scattering, *Macromolecules*, 2002, **35**, 4763–4769.
- 351 D. Roy, J. N. Cambre and B. S. Sumerlin, Triply-Responsive Boronic Acid Block Copolymers: Solution Self-Assembly Induced by Changes in Temperature, pH, or Sugar Concentration, *Chem. Commun.*, 2009, **0**, 2106–2108.
- 352 C. Zhao, X. Zhuang, C. He, X. Chen and X. Jing, Synthesis of Novel Thermo- and pH-Responsive Poly(L-lysine)-Based Copolymer and its Micellization in Water, *Macromol. Rapid Commun.*, 2008, **29**, 1810–1816.
- 353 L. A. Picos-Corrales, A. Licea-Claverie, J. M. Cornejo-Bravo, S. Schwarz and K. F. Arndt, Well-defined *N*-Isopropylacrylamide Dual-Sensitive Copolymers with LCST  $\approx 38$  °C in Different Architectures: Linear, Block and Star Polymers, *Macromol. Chem. Phys.*, 2012, **213**, 301–314.
- 354 Y. You, C. Hong, W. Wang, W. Lu and C. Pan, Preparation and Characterization of Thermally Responsive and Biodegradable Block Copolymer Comprised of PNIPAAm and PLA by Combination of ROP and RAFT Methods, *Macromolecules*, 2004, **37**, 9761–9767.
- 355 K. Philipps, T. Junkers and J. J. Michels, The Block Copolymer Shuffle in Size Exclusion Chromatography: The Intrinsic Problem with using Elugrams to Determine Chain Extension Success, *Polym. Chem.*, 2021, **12**, 2522–2531.
- 356 G. Pagès, V. Gilard, R. Martino and M. Malet-Martino, Pulsed-Field Gradient Nuclear Magnetic Resonance Measurements (PFG NMR) for Diffusion Ordered Spectroscopy (DOSY) Mapping, *Analyst*, 2017, **142**, 3771–3796.

- 357 S. Viel, M. Mazarin, R. Giordanengo, T. N. T. Phan, L. Charles, S. Caldarelli and D. Bertin, Improved Compositional Analysis of Block Copolymers using Diffusion Ordered NMR Spectroscopy, *Anal. Chim. Acta*, 2009, **654**, 45–48.
- 358 Y. Bakkour, V. Darcos, S. Li and J. Coudane, Diffusion Ordered Spectroscopy (DOSY) as a Powerful Tool for Amphiphilic Block Copolymer Characterization and for Critical Micelle Concentration (CMC) Determination, *Polym. Chem.*, 2012, **3**, 2006–2010.
- 359 W. Li, H. Chung, C. Daeffler, J. A. Johnson and R. H. Grubbs, Application of  $^1\text{H}$  DOSY for Facile Measurement of Polymer Molecular Weights, *Macromolecules*, 2012, **45**, 9595–9603.
- 360 P. Groves, Diffusion Ordered Spectroscopy (DOSY) as Applied to Polymers, *Polym. Chem.*, 2017, **8**, 6700–6708.
- 361 G. Patias, A. M. Wemyss, S. Efstathiou, J. S. Town, C. J. Atkins, A. Shegiwal, R. Whitfield and D. M. Haddleton, Controlled Synthesis of Methacrylate and Acrylate Diblock Copolymers via End-Capping using CCTP and FRP, *Polym. Chem*, 2019, **10**, 6447–6455.
- 362 B. M. Peterson, V. Kottisch, M. J. Supej and B. P. Fors, On Demand Switching of Polymerization Mechanism and Monomer Selectivity with Orthogonal Stimuli, *ACS Cent. Sci.*, 2018, **4**, 1228–1234.

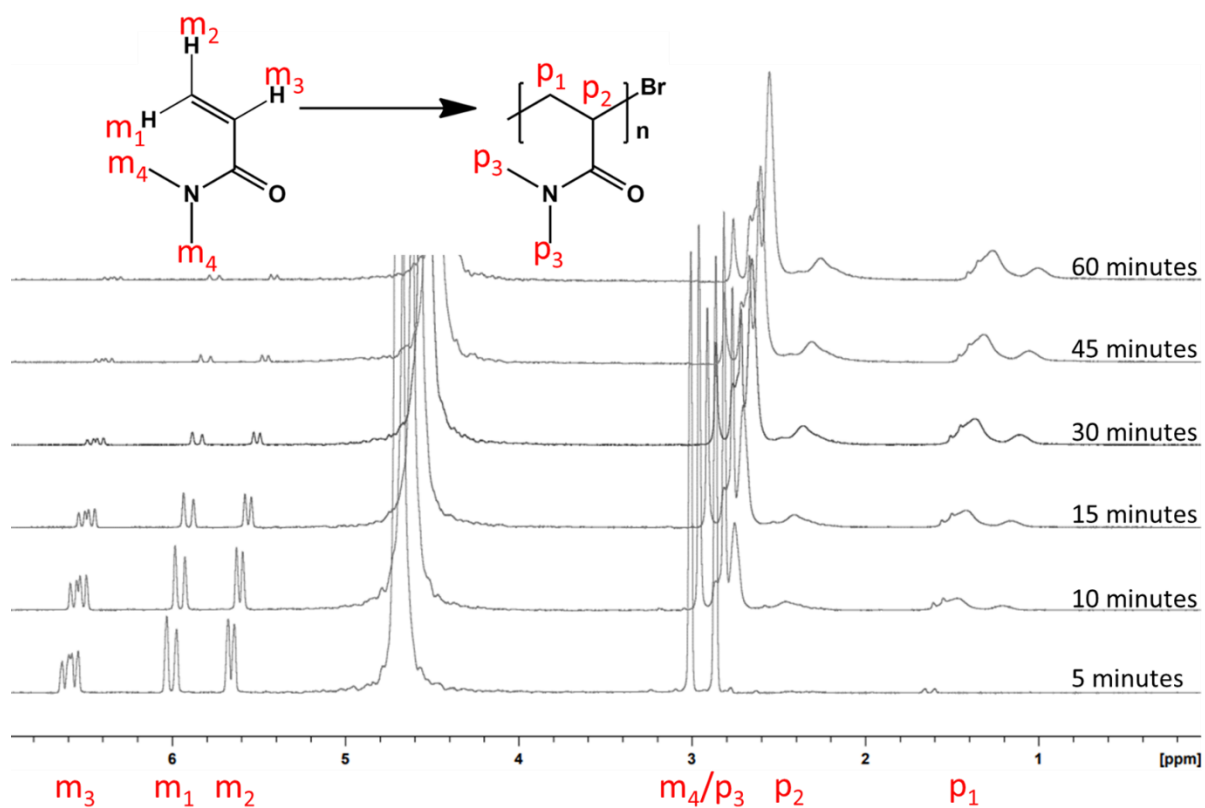
## Appendix



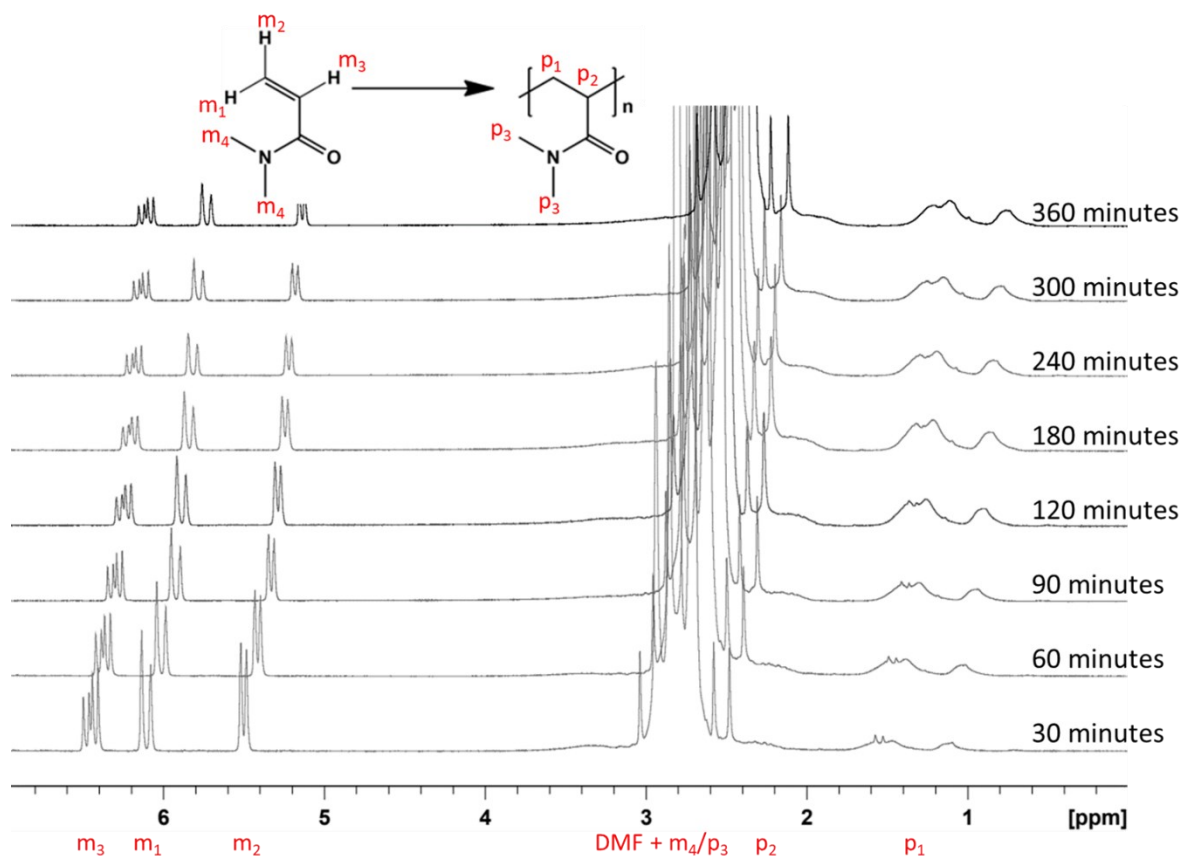
Appendix 1.  $^1\text{H}$  NMR kinetic overlay for the synthesis of PDMA in HPLC-grade water at 0 mol % bromoform showing the disappearance of monomer and broadening of polymer peaks throughout the course of the reaction.



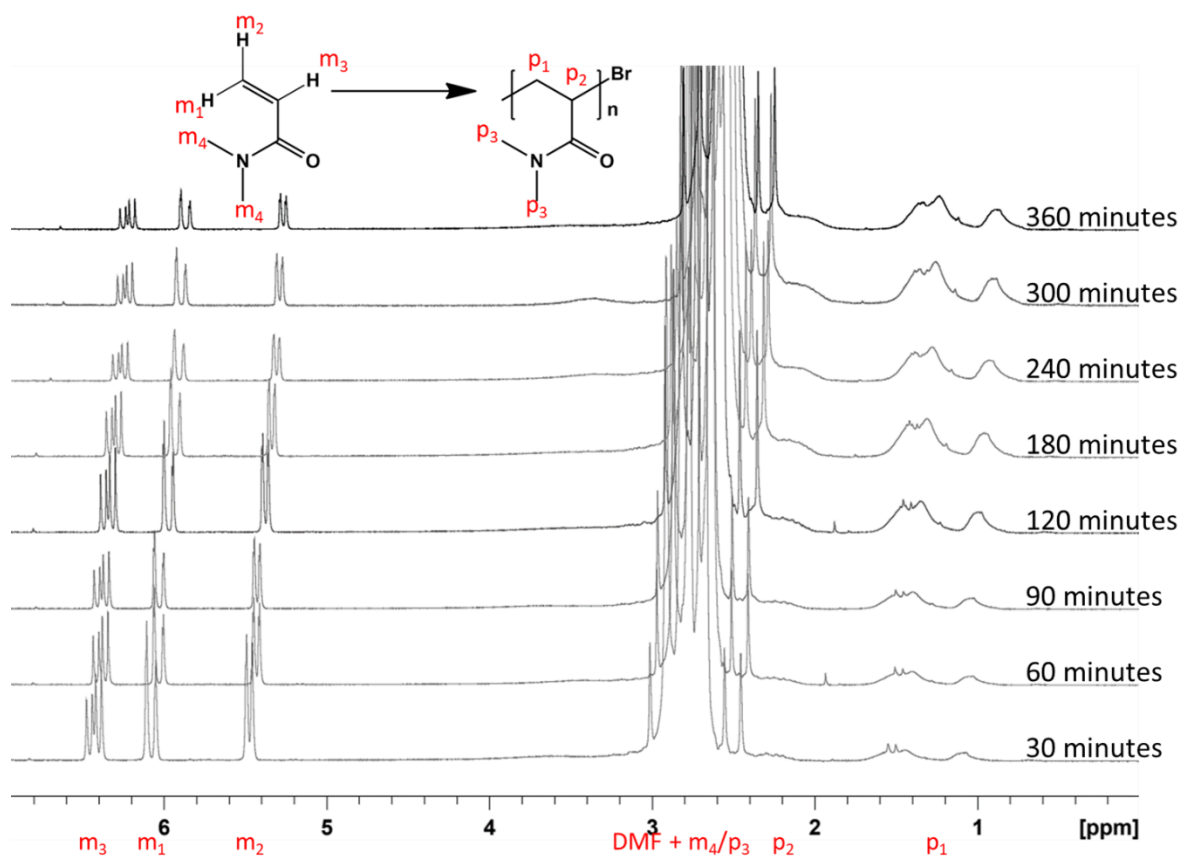
Appendix 2.  $^1\text{H}$  NMR kinetic overlay for the synthesis of PDMA in HPLC-grade water at 0.5 mol % bromoform showing the disappearance of monomer and broadening of polymer peaks throughout the course of the reaction.



Appendix 3.  $^1\text{H}$  NMR kinetic overlay for the synthesis of PDMA in HPLC-grade water at 1.0 mol % bromoform showing the disappearance of monomer and broadening of polymer peaks throughout the course of the reaction.

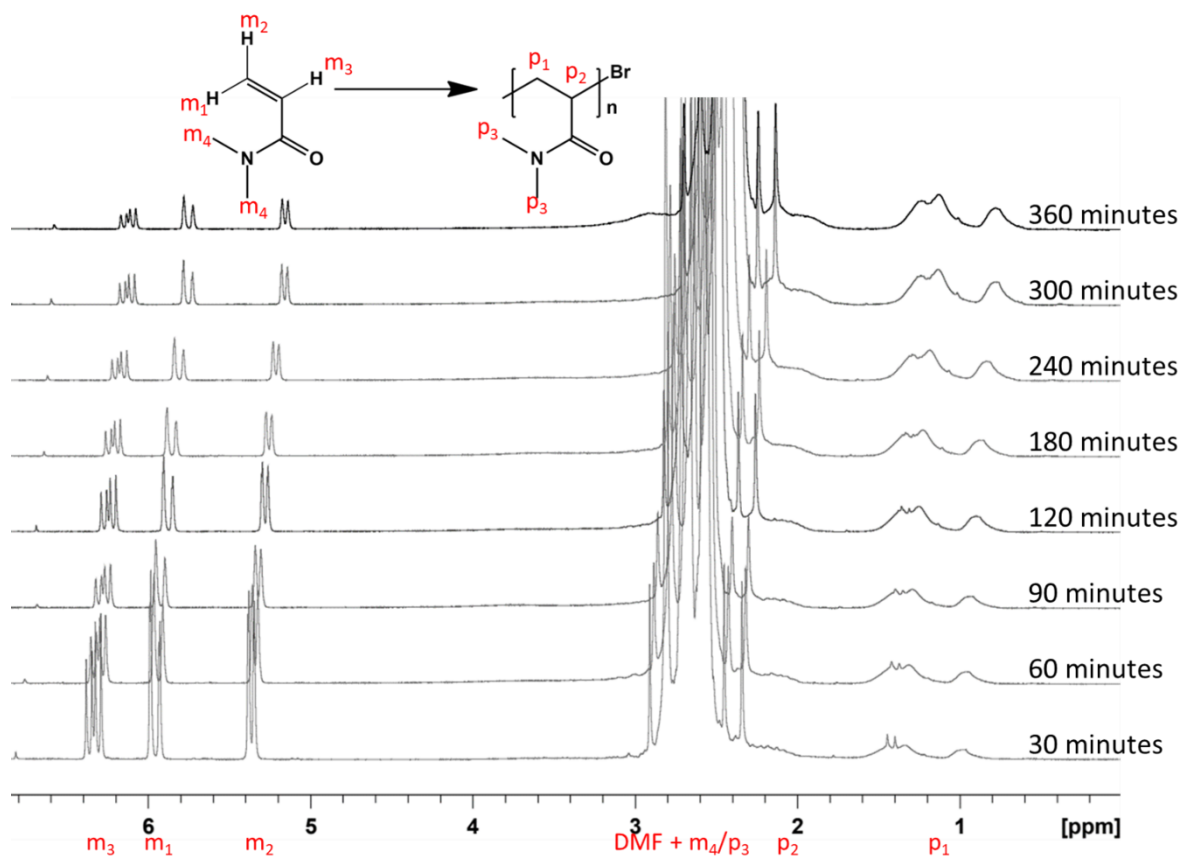


Appendix 4.  $^1\text{H}$  NMR kinetic overlay for the synthesis of PDMA in DMF at 0 mol % bromoform showing the disappearance of monomer and broadening of polymer peaks throughout the course of the reaction.

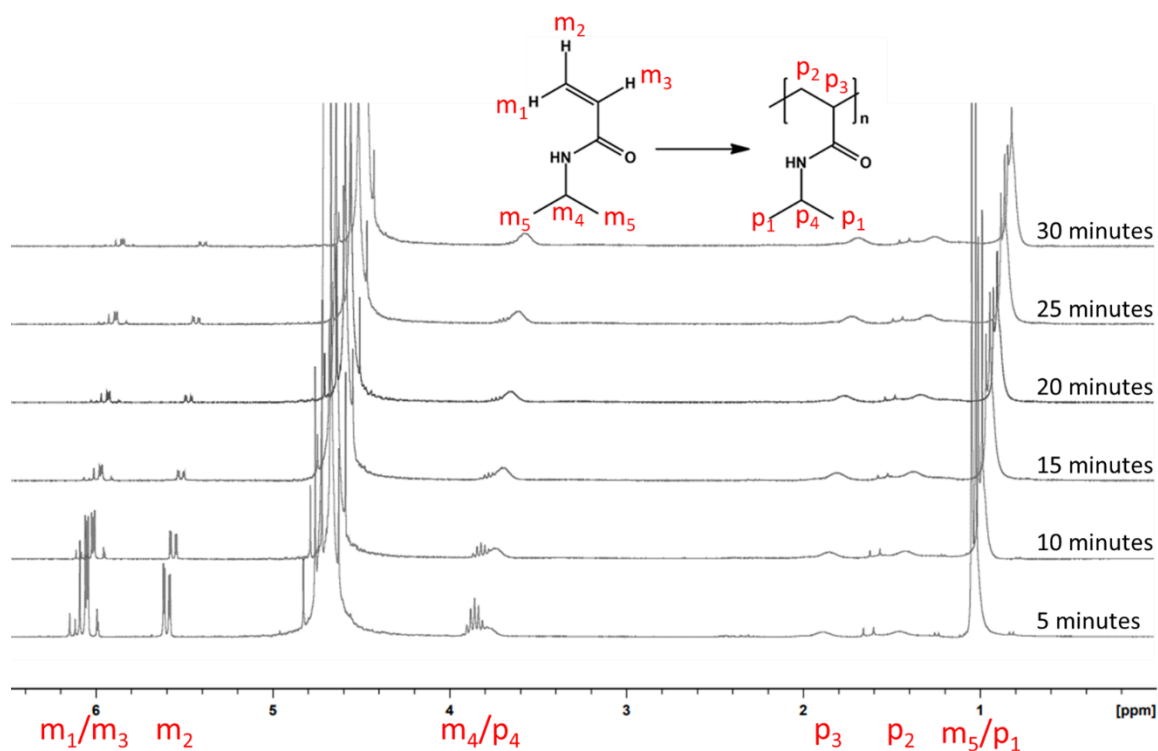


Appendix 5.  $^1H$  NMR kinetic overlay for the synthesis of PDMA in DMF at 0.5 mol % bromoform showing the disappearance of monomer and broadening of polymer peaks throughout the course of the reaction.

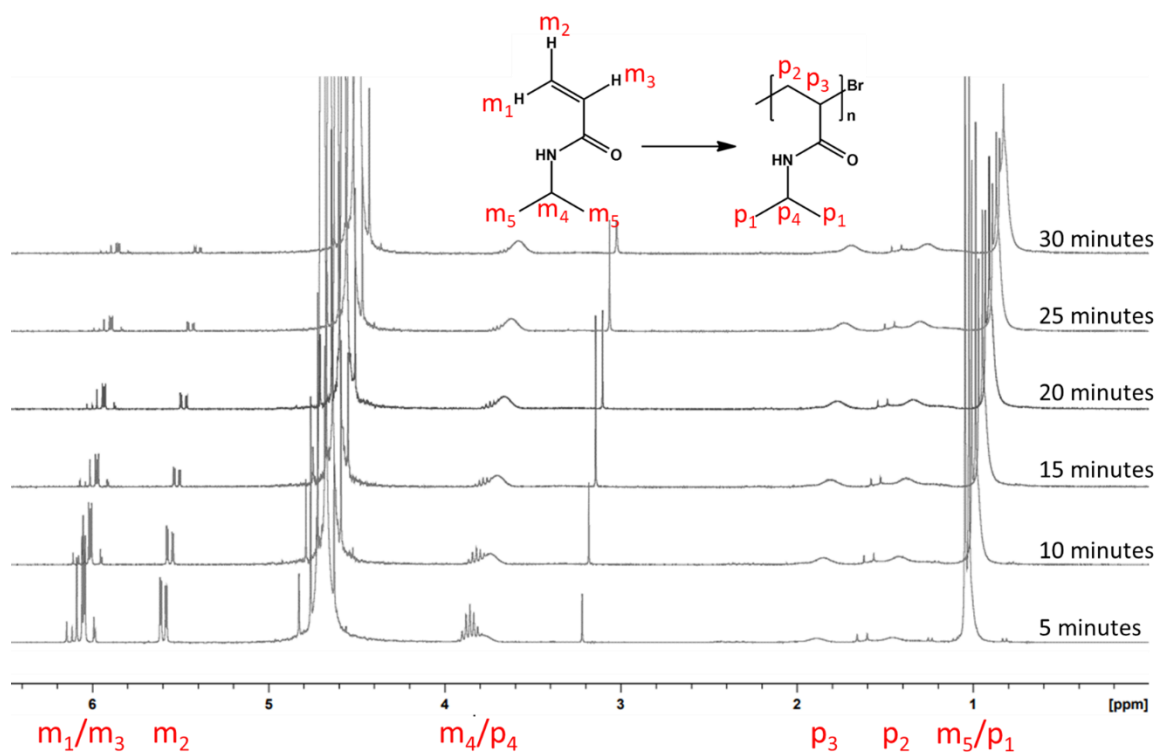




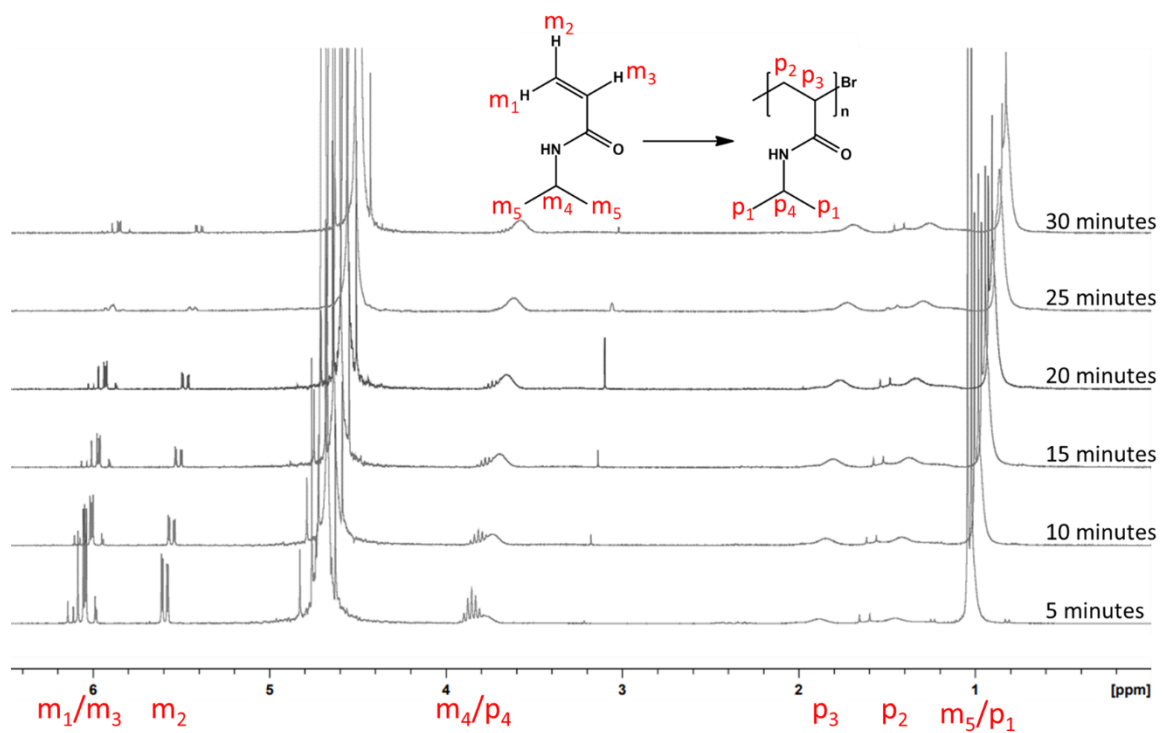
Appendix 6.  $^1\text{H}$  NMR kinetic overlay for the synthesis of PDMA in DMF at 1.0 mol % bromoform showing the disappearance of monomer and broadening of polymer peaks throughout the course of the reaction.



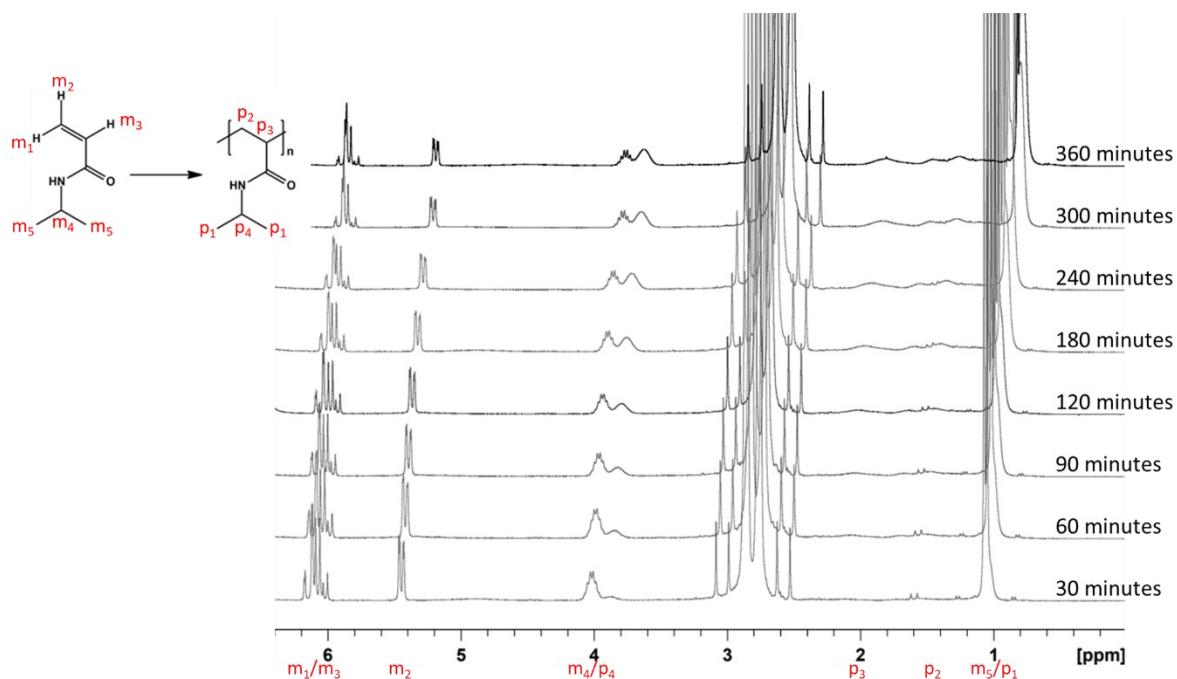
Appendix 7.  $^1\text{H}$  NMR kinetic overlay for the synthesis of PNIPAM in HPLC-grade water at 0 mol % bromoform showing the disappearance of monomer and broadening of polymer peaks throughout the course of the reaction.



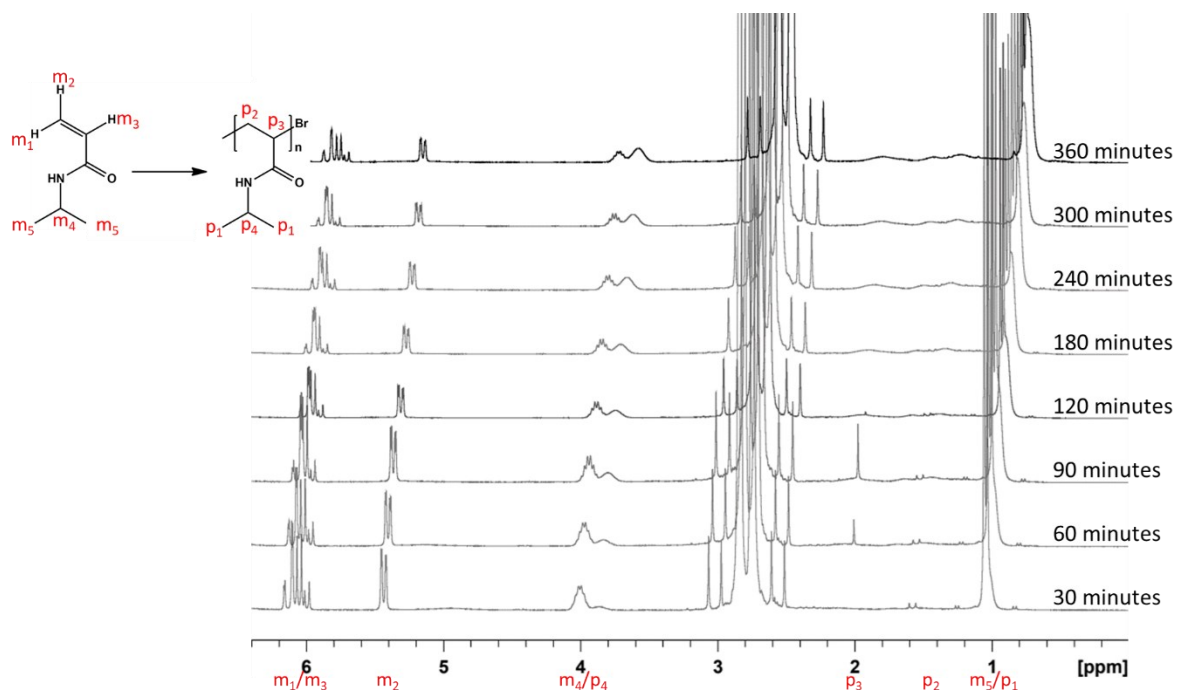
Appendix 8.  $^1\text{H}$  NMR kinetic overlay for the synthesis of PNIPAM in HPLC-grade water at 0.5 mol % bromoform showing the disappearance of monomer and broadening of polymer peaks throughout the course of the reaction.



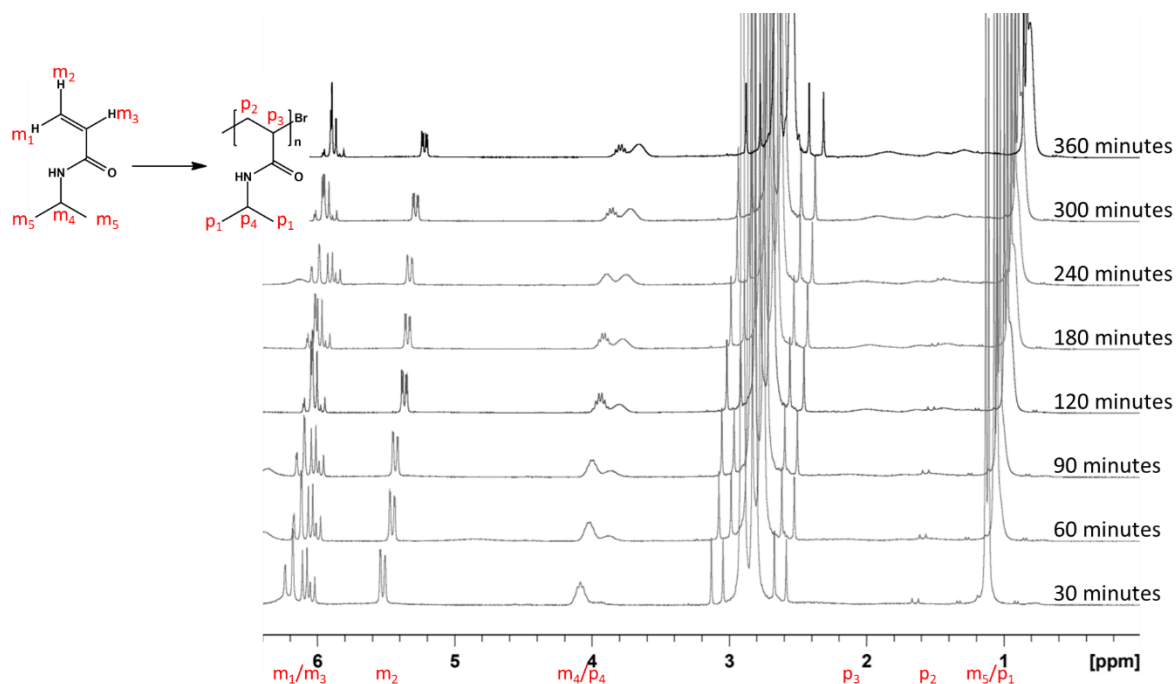
Appendix 9.  $^1\text{H}$  NMR kinetic overlay for the synthesis of PNIPAM in HPLC-grade water at 1.0 mol % bromoform showing the disappearance of monomer and broadening of polymer peaks throughout the course of the reaction.



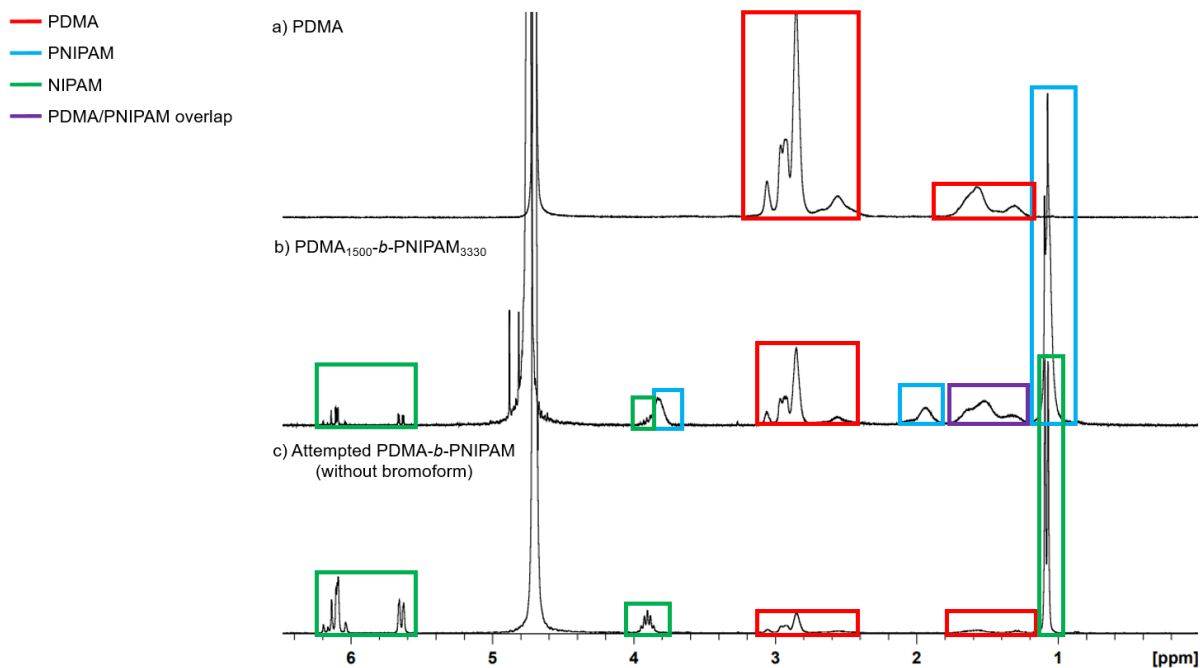
Appendix 10.  $^1\text{H}$  NMR kinetic overlay for the synthesis of PNIPAM in DMF at 0 mol % bromoform showing the disappearance of monomer and broadening of polymer peaks throughout the course of the reaction.



Appendix 11.  $^1\text{H}$  NMR kinetic overlay for the synthesis of PNIPAM in DMF at 0.5 mol % bromoform showing the disappearance of monomer and broadening of polymer peaks throughout the course of the reaction.



Appendix 12.  $^1\text{H}$  NMR kinetic overlay for the synthesis of PNIPAM in DMF at 1.0 mol % bromoform showing the disappearance of monomer and broadening of polymer peaks throughout the course of the reaction.



Appendix 13.  $^1\text{H}$  NMR spectrum showing (a) PDMA after precipitation, (b) PDMA<sub>1500</sub>-*b*-PNIPAM<sub>3330</sub> before precipitation and (c) only NIPAM monomer peaks present for the attempted synthesis of PDMA<sub>1500</sub>-*b*-PNIPAM<sub>3500</sub> from PDMA (0 mol % bromoform).